JCDCG^3 2019

The 22nd Japan Conference on Discrete and Computational Geometry, Graphs, and Games

6th September – 8th September 2019

Tokyo University of Science

The 22nd Japan Conference on Discrete and Computational Geometry, Graphs, and Games

Conference date
September 6 – 8, 2019
Venue
Tokyo University of Science
(Kagurazaka Campus)

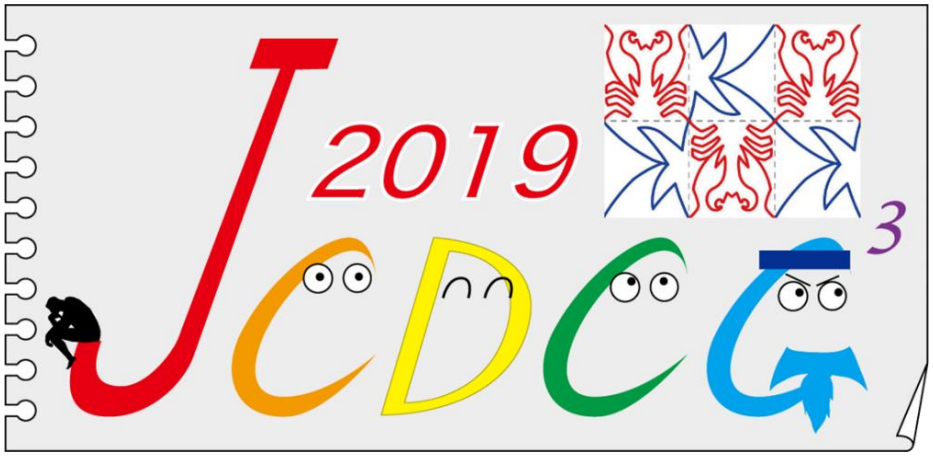

Invited Plenary Speakers

Takao Asano	(Chuo University, Japan)
Erik Demaine	(MIT, USA)
Stefan Langerman	(ULB, Belgium)
János Pach	(EPFL, Switzerland and Rényi Institute, Hungary)
Akira Saito	(Nihon University, Japan)
Géza Tóth	(Alfréd Rényi Institute of Mathematics, Hungary)

Conference Chair

Jin Akiyama	(Tokyo University of Science, Japan)

Program Committee

Jean Cardinal	(ULB, Belgium)
Ruy Fabila-Monroy	(Cinvestav, Mexico)
Takashi Horiyama	(Saitama University, Japan)
Hiro Ito	(UEC, Japan; Chair)
Chie Nara	(Meiji University, Japan)
Yoshio Okamoto	(UEC, Japan)
Hirotaka Ono	(Nagoya University, Japan)
Kenta Ozeki	(Yokohama National University, Japan)
Vera Sacristan	(UPC, Spain)
Toshinori Sakai	(Tokai University, Japan)
Ryuhei Uehara	(JAIST, Japan)
Yushi Uno	(Osaka Prefecture University, Japan)
Aaron Williams	(Bard College at Simon's Rock, USA)

Organizing Committee

Hiro Ito	(UEC, Japan)
Takako Kodate	(Tokyo Woman's Christian University, Japan)
Keiko Kotani	(Tokyo University of Science, Japan; Co-chair)
Yasuko Matsui	(Tokai University, Japan)
Atsuki Nagao	(Ochanomizu University, Japan)
Shunsuke Nakamura	(Tokyo University of Science, Japan)
Toshinori Sakai	(Tokai University, Japan; Co-chair)
Akifumi Sako	(Tokyo University of Science, Japan)
Xuehou Tan	(Tokai University, Japan)
Shin-ichi Tokunaga	(Tokyo Medical and Dental University, Japan)

Sponsored by

Tokyo University of Science

In cooperation with

JST CREST: Foundations of Innovative Algorithms for Big Data (ABD14)

Tokai University

Table of Contents

Invited Talks

Contributed Talks

Outline of Program

6th Sep. (Fri.)

09:00 Registration Desk Open.
10:20-10:30 Opening Address
10:30-11:20 Invited Talk 1 by Erik Demaine
11:35-12:25 Invited Talk 2 by Takao Asano
12:25-14:00 Lunch Break
14:00-15:20 Contributed Talks
15:20-15:50 Coffee Break
15:50-17:30 Contributed Talks

7th Sep. (Sat.)

09:00-09:50 Invited Talk 3 by Janos Pach
10:00-10:50 Invited Talk 4 by Geza Toth
11:05-12:05 Contributed Talks
12:05-12:15 Group Photo
12:15-13:50 Lunch Break
13:50-15:10 Contributed Talks
15:10-15:40 Coffee Break
15:40-17:20 Contributed Talks
18:00-20:00 Banquet

8th Sep. (Sun.)

09:00-09:50 Invited Talk 5 by Stefan Langerman
10:00-10:50 Invited Talk 6 by Akira Saito
11:05-12:05 Contributed Talks
12:05-13:40 Lunch Break
13:40-14:40 Contributed Talks
14:40-15:10 Coffee Break
15:10-16:10 Contributed Talks
16:10-16:15 Closing Address

Geometry, Graphs, Games and Optimization

Takao Asano

Chuo University, Bunkyo-ku, Tokyo 112-8551, Japan
asano@ise.chuo-u.ac.jp

Abstract. In this talk, I discuss envy-free mechanisms for the cake cutting and pie cutting problems. Specifically, based on envy-free and truthful mechanisms for the cake cutting problem by M. Seddighin et al. [1], I present an envy-free and truthful mechanism for the pie cutting problem, which is a kind of generalizations of the cake cutting problem. I also present my representative results in computational geometry, graphs, games, and combinatorial optimization during 45 years research jointly done with my colleagues.

1 Pie cutting

M. Seddighin, M. Farhadi, M. Ghodsi, R. Alijani, and A.S. Tajik [1] considered the following cake cutting problem. Given a divisible heterogeneous cake $(0, 1]$ and n strategic players with valuation $V_i = (a_i, b_i] = \{x \mid 0 \leq a_i < x \leq b_i \leq 1\}$ for each player i, find a mechanism for dividing the cake and allocating pieces of the cake to n players to meet the following conditions:

(i) the mechanism is envy-free, i.e., each player (weakly) prefers his/her allocated cake to any other player's allocated cake,
(ii) the mechanism is strategy-proof (truthful), i.e., each player's dominant strategy is to reveal his/her own true valuation over the cake, and
(iii) the number of cuts made on the cake is small.

They proposed a polynomial time algorithm (mechanism) for this cake cutting problem.

H. Umeda and T. Asano [2] considered the following pie cutting problem. Given a divisible heterogeneous pie $(0, 2\pi]$ and n strategic players with valuation $V_i = (a_i, b_i]$ $(0 \leq a_i \neq b_i \leq 2\pi)$ for each player i where $V_i = \{x \mid a_i < x \leq b_i\}$ if $a_i < b_i$ and $V_i = \{x \mid a_i < x \leq 2\pi\} \cup \{x \mid 0 < x \leq b_i\}$ if $a_i > b_i$, divide the pie and allocate sectors of the pie to n players to meet the following conditions:

(i) the mechanism is envy-free, i.e., each player (weakly) prefers his/her allocated sectors of the pie to any other player's allocated sectors of the pie,
(ii) the mechanism is strategy-proof (truthful), i.e., each player's dominant strategy is to reveal his/her own true valuation over the pie, and
(iii) the number of cuts made on the pie is small.

They proposed a polynomial time algorithm (mechanism) for this pie cutting problem. Note that, if we consider problems on interval graphs and circular-arc graphs, the problem of M. Seddighin et al. corresponds to one on interval graphs and problem of Umeda and Asano corresponds to one on circular-arc graphs. In this talk, I present the algorithm proposed by Umeda and Asano [2].

2 Works jointly done with my colleagues

I also present brief overviews of the following works in computational geometry, graphs, games, and combinatorial optimization jointly done with my colleagues.

(a) General results on tour lengths in machines and digraphs, *SIAM Journal on Computing*, 5 (1976) (with I. Takanami)
(b) An upper bound on the length of a hamiltonian walk of a maximal planar graph, *Journal of Graph Theory*, 4 (1980) (with T. Nishizeki, T. Watanabe)
(c) Edge-deletion and edge-contraction problems, *14th ACM STOC*, 1982 (with T. Hirata)
(d) Finding the connected components and a maximal clique of an intersection graph of rectangles in the plane, *Journal of Algorithms*, 4 (1983) (with H. Imai)
(e) A note on nongraphic matroids, *Journal of Combinatorial Theory*, B, 37 (1984) (with T. Nishizeki, P.D. Seymour)
(f) A new point-location algorithm and its practical efficiency - comparison with existing algorithms, *ACM Transactions on Graphics*, 3 (1984) (with M. Edahiro, I. Kokubo)
(g) Dynamic segment intersection search with applications, *25th IEEE FOCS*, 1984 (with H. Imai)
(h) Visibility polygon search and Euclidean shortest paths, *26th IEEE FOCS*, 1985 (with Tetsuo Asano, L. Guibas, J. Hershberger, H. Imai)
(i) Partitioning a polygonal region into trapezoids, *Journal of ACM*, 33 (1986) (with Tetsuo Asano, H. Imai) (A preliminary version: Minimum partition of polygonal regions into trapezoids, *24th IEEE FOCS*, 1983 (with Tetsuo Asano))
(j) A bucketing algorithm for the orthogonal segment intersection search problem and its practical efficiency, *3rd ACM Symposium on Computational Geometry*, 1987, (with M. Edahiro, K. Tanaka, T. Hoshino)
(k) Improved approximation algorithms for MAX SAT, *11th ACM-SIAM SODA*, 2000 (with D.P. Williamson)
(l) Nash equilibria in combinatorial auctions with item bidding and subadditive symmetric valuations, *IEICE Transactions on Fundamentals*, 2018 (with H. Umeda)
(m) The dial-a-ride problem with fairness, *Bulletin of the JSME*, 2018 (with M. Miyaoka, N. Sukegawa)

References

1. M. Seddighin, M. Farhadi, M. Ghodsi, R. Alijani, and A.S. Tajik, Expand the shares together: envy-free mechanisms with a small number of cuts, *Algorithmica*, 81(2019), pp. 1728–1755 (A preliminary version: R. Alijani, M. Farhadi, M. Ghodsi, M. Seddighin, and A.S. Tajik, Envy-free mechanisms with minimum number of cuts, *Proc. of 31st AAAI Conference on Artificial Intelligence*, pp. 312–318, 2017).
2. H. Umeda and T. Asano, An envy-free mechanism with minimum number of cuts for the pie-cutting problem (in Japanese), *FIT (Forum on Information Technology) 2018*, A-023.

New Results in Computational Origami

Erik D. Demaine
Massachusetts Institute of Technology

Abstract

Computational origami has proved itself an exciting field, providing beautiful mathematical and algorithmic challenges, and enabling many exciting applications in robotics, 3D manufacturing, architecture, deployable structures, and self-assembly. I will describe several recent results and applications in this field. For example:

- The Origamizer algorithm (Demaine and Tachi 2017) finds an efficient "watertight" folding of a square piece of paper into any 3D polyhedron.
- The Origami Simulator software (Ghassaei, Demaine, Gershenfeld 2018) lets you test out a crease pattern and visualize its folding without having to pick up a piece of paper. See Figure 1.
- The FOLD format (Demaine, Ku, Lang 2016) enables this software to interoperate with other origami software, such as the excellent Freeform Origami (Tachi 2010).
- We now understand the fundamental conditions that make curved crease patterns fold (Demaine, Demaine, Huffman, Koschitz, Tachi 2018).
- We have more efficient ways to fold certain 2.5D structures (Biswas, Demaine, Ku 2018; Demaine, Ku, Yoder 2018).

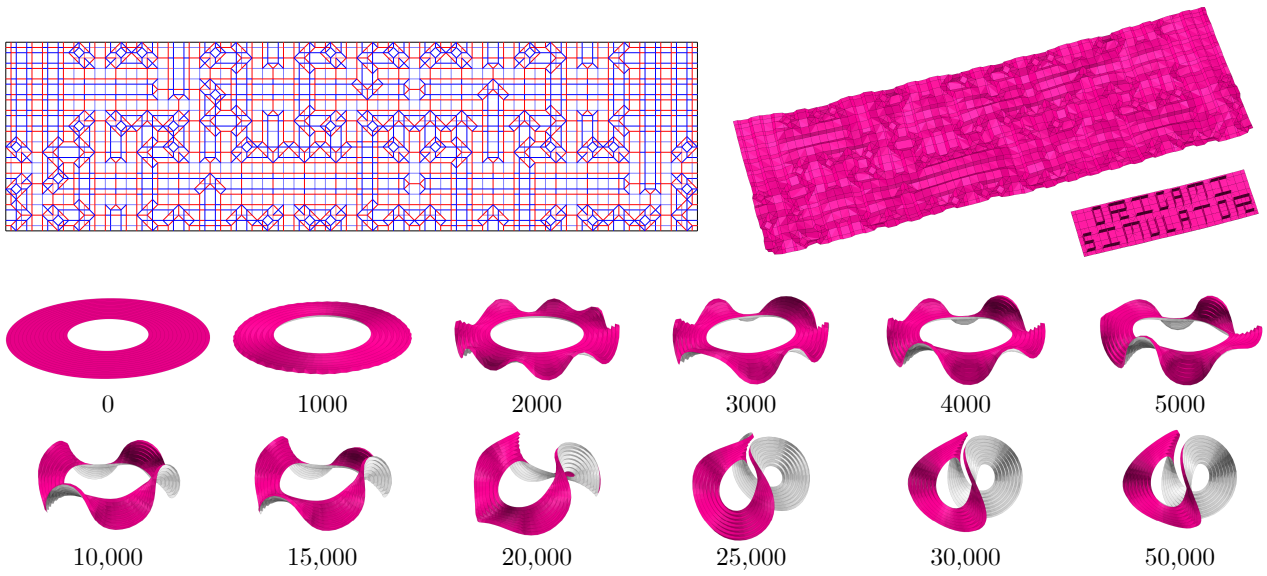

Figure 1: Two examples of interactive origami folding using the Origami Simulator by Ghassaei, Demaine, and Gershenfeld (2018). [http://origamisimulator.org/]

The Geometry of Diamonds

Stefan Langerman*

Département d'Informatique
Université Libre de Bruxelles
stefan.langerman@ulb.ac.be

In 1919, Marcel Tolkowsky published his book *Diamond Design* [1] providing for the first time a mathematical study on how to design a diamond and tune its proportions so as to optimize its brilliance and fire. His computations were the basis of the modern round brilliant cut which is still, a hundred years later, the most popular way to cut a diamond. Today, his round brilliant cut might very well be one of the smallest, priciest and yet most common man-made polyhedra.

In this talk, I will go over different physical and geometric characteristics of the diamond material, and the many different facets of the design and manufacture of a polished diamond, highlighting geometric and computational open problems and challenges along the way.

References

[1] Marcel Tolkowsky. *Diamond Design*. Spon & Chamberlain, New York, 1919. 104 pp.

*Directeur de recherches du F.R.S.-FNRS

Small triangular containers for triangles

Gergely Kiss and János Pach*

To find a minimum area ellipse (Löwner-John ellipse), triangle, rectangle, or convex k-gon enclosing a given point set are classical problems in geometry with interesting applications in packing and covering, approximation, convexity, computational geometry, robotics, and elsewhere [2], [6], [3], [1]. Unaware of many old results and recent developments in this field, R. Nandakumar, a gifted computer programmer and college teacher from Kochi, India, raised an interesting special instance of this problem, which is not trivial even if we want to enclose a triangle by a triangle [5]: *Determine the smallest area isosceles triangle containing a given triangle ABC.*

Nandakumar defined three special isosceles triangles associated with a triangle ABC, as follows. Denote the lengths of the sides by $a = |BC|$, $b = |AC|$, and $c = |AB|$. If two sides coincide, then ABC is is the smallest enclosing isosceles triangle of itself. In the sequel, we assume without loss of generality that $a < b < c$. Let B' denote the point on the ray $\vec{BC}$, for which $|B'C| = b$. See Fig. 1. Analogously, let C' (and C'') denote the points on $\vec{AC}$ (resp., $\vec{BC}$) with $|AC'| = c$ (resp., $|BC''| = c$). Obviously, the triangles $AB'C$, ABC', and ABC'' are *isosceles*. We call them *special containers* associated with ABC. All of them share an angle with ABC. Nandakumar suggested that for every triangle ABC, one of the three special containers associated with it is a smallest area isosceles triangle. If this were true, it would be very easy to find a smallest "container", that is, a smallest area isosceles triangle containing ABC. (It turns out that for "most" triangles ABC, apart from a set of measure 0, the smallest container is uniquely determined.)

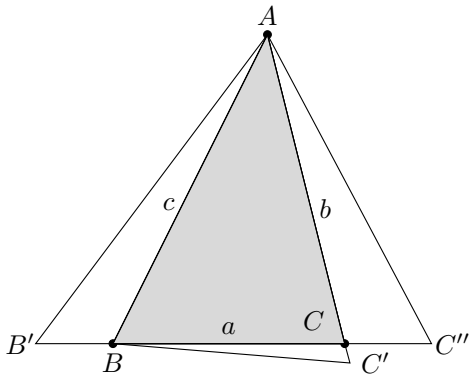

Figure 1: Special containers $AB'C$, ABC', and ABC''.

Here, we show that the situation is more delicate.

Proposition 1. *For every $\gamma > \pi/2$, there exists a triangle ABC with largest angle γ such that none of the special containers is a smallest area isosceles container for ABC.*

Proof. Let $\gamma > \pi/2$ and, using the above notation, consider an "almost isosceles" triangle ABC, such that its largest angle (at C) is γ and b is only slightly larger than a. Let R be the unique point on the line BC such that $|AR| = |BR|$ (see Fig. 2). If $b - a$ is sufficiently small, then $\sphericalangle ARB > \pi/2$. Let $AB'C$ denote the special container defined above. We have $|AR| = |BR| < |AC| = |B'C|$. The altitudes of the triangles $AB'C$ and ABR belonging to the sides $B'C$ and BR, respectively, are the same. Therefore, the area of ABR is strictly smaller than the area of $AB'C$, showing that $AB'C$ cannot be a smallest area isosceles container. On the other hand, if $b - a$ was small enough, the areas of the other two special containers, ABC' and ABC'', are even larger than the area of $AB'C$. This means that none of the special containers are minimal. □

*Rényi Institute of the Hungarian Academy of Sciences, Budapest.

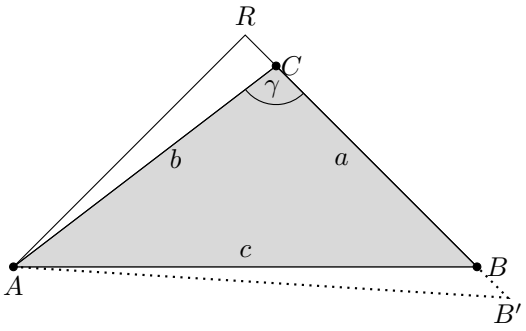

Figure 2: Obtuse triangle whose smallest area isosceles container is not special.

Clearly, all special containers of an acute triangle are acute. Next, we show that in some cases none of these special containers can be minimal.

Proposition 2. *There exists an acute triangle ABC contained in an obtuse isosceles triangle whose area is smaller than the area of any special container associated with ABC.*

Proof. Start with an almost isosceles triangle ABC such that b is only slightly larger than a, and the angle at C is $\pi/2$. Then c is close to $\sqrt{2}b$. Let D denote the point on the ray $\vec{AB}$, different from A, at distance b from C; see Fig. 3. As before, let $AB'C$ be the special container with $|B'C| = b$.

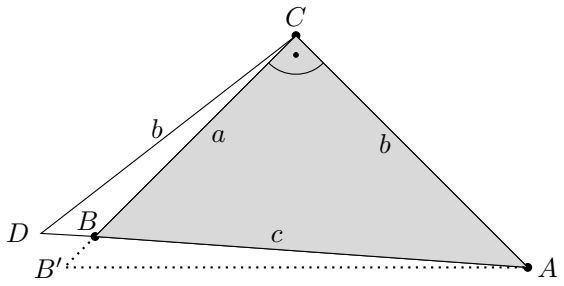

Figure 3: Acute triangle with an obtuse container smaller than the special containers.

Since $\sphericalangle ACD > \sphericalangle ACB' = \pi/2$ and $|CD| = |CB'| = b$, the area of the special container $AB'C$ is slightly larger than the area of the triangle ACD. The areas of the other two special containers, ABC' and ABC'', are even larger (roughly $\sqrt{2}$ times larger).

Keep A and B fixed, and continuously move C away from A without changing the direction of AC. Then ABC becomes an acute triangle, and the point D at distance b from C continuously moves away from B. At the beginning of the motion, $\sphericalangle ACD > \pi/2$ and the area of the isosceles triangle ACD is still smaller than the area of the special containers associated with ABC. Thus, ABC meets the requirements of the Proposition. □

However, in a forthcoming paper [4], under an additional assumption, we shall verify Nandakumar's conjecture.

Theorem 3. [4] *Suppose that a triangle ABC has an acute smallest area isosceles container. Then this container must be identical with one of the special containers associated to ABC.*

Consider now a triangle ABC with an obtuse isosceles container that satisfies the conditions in Proposition 2. It follows immediately from Theorem 3 that all smallest area isosceles containers of ABC must be obtuse or right-angled.

Although, it might happen that none of the special containers is a minimal one, a slightly weaker conjecture of Nandakumar is still true.

Theorem 4. [4] *Any triangle and any of its smallest area isosceles containers share a vertex and the angle at this vertex.*

The proof of this fact requires a surprising amount of work.

It is not difficult to construct triangles for which the *smallest area* and the *smallest perimeter* isosceles containers are not the same [5]. Nevertheless, an analogue of Theorem 4 may well be true for smallest perimeter containers.

Conjucture 5 (Nandakumar)**.** *Any triangle and any of its smallest perimeter isosceles containers share a vertex and the angle at this vertex.*

We do not know if the analogue of Theorem 3 is true for smallest perimeter containers.

Question 6. Is it true that if a triangle ABC has a smallest perimeter isosceles container which is acute, then this container must be identical to one of the special containers associated to ABC?

References

[1] J. E. Boyce, D. P. Dobkin, R. L. Drysdale, and L. J. Guibas, Finding extremal polygons, *SIAM J. Computing* **14** (1985), 134–147.

[2] L. Fejes Tóth, *Lagerungen in der Ebene, auf der Kugel und im Raum, Die Grundlehren der Mathematischen Wissenschaften (in German)*, **LXV**, Springer-Verlag, Berlin, 1953.

[3] F. John, Extremum problems with inequalities as subsidiary conditions. In: *Studies and Essays presented to R. Courant on his 60th Birthday*, Interscience Publishers, NY, 1948, 187–204.

[4] G. Kiss, J. Pach, and G. Somlai, Smallest area isosceles containers of triangles, manuscript, 2019.

[5] R. Nandakumar, Oriented convex container of polygons, https://arxiv.org/ftp/arxiv/papers/1802/1802.10447.pdf

[6] J. O'Rourke, Finding minimal enclosing boxes, *Internat. J. Computer and Information Sc.* **14** (3) (1985), 183–199.

Spanning bipartite graphs in graphs with large degree sum

Akira Saito, Nihon University

This talk is based on the joint researches with Guantao Chen (Georgia State University, USA), Shuya Chiba (Kumamoto University, Japan), Ronald J. Gould (Emory University, USA), Xiaofeng Gu (University of West Georgia, USA), Masao Tsugaki (Tokyo Medical and Dental University, Japan) and Tomoki Yamashita (Kindai University, Japan).

Degree sum is a topic which has been studied actively in the theory of hamiltonicity. It deals with the minimum sum of degrees of vertices in certain independent sets and relates it with hamiltonian properties of graphs. One of the most well-known results in this topic is Ore's Theorem. For a non-complete graph G, we define $\sigma_2(G)$ by

$$\sigma_2(G) = \min\{d_G(x) + d_G(y) \colon x, y \in V(G), x \neq y, xy \notin E(G)\},$$

where $d_G(v)$ is the degree of a vertex v in G. If G is a complete graph, we define $\sigma_2(G) = +\infty$.

Theorem A (Ore's Theorem [3]). *For $n \geq 3$, every graph G of order n with $\sigma_2(G) \geq n$ is hamiltonian.*

Moon and Moser [2] investigated a degree sum condition for hamiltonicity in bipartite graphs. Trivially, a bipartite graph contains a hamiltonian cycle only if it is balanced. Also, in the spirit of Ore's Theorem, it may not be appropriate to incorporate the degree sum of vertices chosen from the same partite set. For this reason, a slightly different type of degree sum is often used. Let G be a bipartite graph with partite sets X and Y. If G is not a complete bipartite graph, we define $\sigma_{1,1}(G)$ by

$$\sigma_{1,1}(G) = \min\{d_G(x) + d_G(y) \colon x \in X, y \in Y, xy \notin E(G)\}.$$

If G is a complete bipartite graph, we define $\sigma_{1,1}(G) = +\infty$.

Moon and Moser gave a sufficient condition for a balanced bipartite graph G to contain a hamiltonian cycle in terms of $\sigma_{1,1}(G)$.

Theorem B (Moon–Moser Theorem [2]). *For $n \geq 2$, every balanced bipartite graph G of order $2n$ with $\sigma_{1,1}(G) \geq n+1$ is hamiltonian.*

The degree sum condition in Theorem B is sharp. For integers n and t with $n \geq 2$ and $1 \leq t \leq n-1$, define $H_{t,n-t}$ to be the graph formed from $K_{t,t} \cup K_{n-t,n-t}$ by selecting one partite set of each component and adding all possible edges between them. Then every graph G with $K_{t,t} \cup K_{n-t,n-t} \subseteq G \subseteq H_{t,n-t}$ is a balanced bipartite graph of order $2n$ and satisfies $\sigma_{1,1}(G) = n$, but it is not hamiltonian. Also, The graphs G_1 and G_2 depicted in Figure 1 are balanced bipartite graphs of order 8 and satisfy $\sigma_{1,1}(G_i) = 4$ $(i = 1, 2)$, but they are not hamiltonian.

The above examples act as exceptions if we relax the hypothesis of $\sigma_{1,1}(G) \geq n+1$ in Theorem B to $\sigma_{1,1}(G) \geq n$. However, Ferrara, Jacobson and Powell [1] proved that no other exception arises.

Theorem C ([1]). *Let n be an integer with $n \geq 2$ and let G be a balanced bipartite graph of order $2n$ with $\sigma_{1,1}(G) \geq n$. Then*

(1) G is hamiltonian,

(2) $K_{t,t} \cup K_{n-t,n-t} \subseteq G \subseteq H_{t,n-t}$ for some t with $1 \leq t \leq n-1$, or

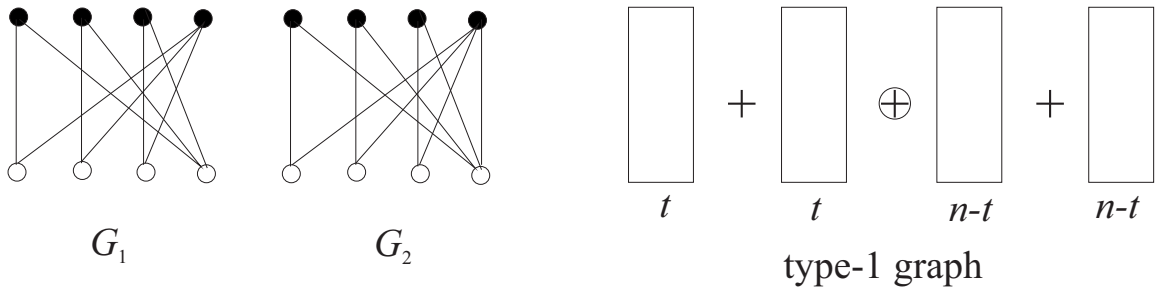

Figure 1: type-1 and type-2 graphs

(3) $n = 4$ *and* G *is isomorphic to* G_1 *or* G_2*.*

Theorem C only deals with bipartite graphs, while Ore's Theorem handles both bipartite and non-bipartite graphs. Apparently, Ore's Theorem concerns a broader class of graphs. However, we report that Theorem C implies Ore's Theorem. We say that a graph G is a type-1 graph if $K_{t,t} \cup K_{n-t,n-t} \subseteq G \subseteq H_{t,n-t}$ for some t with $1 \leq t \leq n-1$, and that it is a type-2 graph if G is isomorphic to G_1 or G_2.

Theorem 1. *Let* n *be an integer with* $n \geq 2$ *and let* G *be a graph of order* $2n$*. If* $\sigma_2(G) \geq 2n$*, then* G *contains a spanning balanced bipartite graph* H *such that*

(1) $\sigma_{1,1}(H) \geq n$*, and*

(2) H *is neither a type-1 nor a type-2 graph.*

For graphs of even order satisfying Ore's condition, Theorem 1 gives more detailed information than the existence of a hamiltonian cycle.

While Theorem 1 says that a refinement of Moon–Moser Theorem implies Ore's Theorem, we suspect that Moon–Moser Theorem itself does not imply Ore's Theorem. However, our attempt to construct an example to show it has so far failed.

If G is a graph of odd order, we cannot obtain a spanning balanced bipartite subgraph of G. However, we can still relate Ore' Theorem with hamiltonian properties of dense bipartite graphs. We will discuss the detail in the talk.

References

[1] M.J. Ferrara, M.S. Jacobson and J. Powell, Characterizing degree-sum maximal nonhamiltonian bipartite graphs, Discrete Math. **312** (2012) 459–461.

[2] J.W. Moon and L. Moser, On hamiltonian bipartite graphs, Israel J. Math. **1** (1963) 163–165.

[3] O. Ore, Note on Hamilton circuits, Amer. Math. Monthly **67** (1960) 55.

Dense point sets with many halving lines

Géza Tóth
Rényi Institute, Hungarian Academy of Sciences, Budapest

Suppose that we have a set P of n points in the plane in general position. A line, determined by two points of P, is a *halving line* if it has the same number of points of P on both sides. Determining the maximum number of halving lines $f(n)$ of a set of n points turned out to be very important in the analysis of geometric algorithms. We are still very far from the solution, the best bounds are $ne^{c\sqrt{\log n}} \leq f(n) \leq cn^{4/3}$.

A planar point set of n points is called γ-*dense* if the ratio of the largest and smallest distances among the points is at most $\gamma\sqrt{n}$. We construct dense point sets with $ne^{c\sqrt{\log n}}$ halving lines. This improves the bound $cn \log n$ of Edelsbrunner, Valtr and Welzl from 1997. Our construction can be generalized to higher dimensions.

Joint work with István Kovács (Technical University, Budapest).

On the convex crossing number

B. M. Ábrego*, S. Fernández-Merchant*†

Abstract

We improve the bounds for the minimum number $\mathrm{bkcr}_1(n,m)$ of crossings among convex drawings of graphs with n vertices and m edges. We show that $\frac{1}{3.9551} \leq \mathrm{bkcr}_1(n,m)n^2/m^3 \leq \frac{1}{3}$, whenever $n \ll m \ll n^2$. We also present conjectures about the precise and asymptotic value of $\mathrm{bkcr}_1(n,m)$.

1 Convex geometric graphs

A *convex drawing* of a graph is a drawing of a graph where the vertices are located on a convex closed curve and the edges are closed curves that lie entirely within that curve. The goal of this paper is to bound the number of crossings in such drawings depending on its number of vertices and edges, n and m, respectively. In 1982, Ajtai, Chvátal, Newborn, and Szemerédi [1], and independently Leighton [2], proved the so called *Crossing Lemma*. It states that any drawing of any graph with n vertices and $m > 4n$ edges has at least $c \cdot m^3/n^2$ edge-crossings, where c is a universal constant.

This result was refined for convex drawings by Shahrokhi et al. [6]. Specifically, for any graph G, if $\mathrm{bkcr}_1(G)$ denotes the minimum number of crossings over all convex drawings of G, then $\mathrm{bkcr}_1(G) \geq \frac{1}{27}m^3/n^2$ for any graph G with n vertices and $m \geq 3n$ edges. (The notation $\mathrm{bkcr}_1(G)$ follows [5] because the convex crossing number is equivalent to the book crossing number of graphs drawn in a single page)

In this paper we improve Shahrokhi et al. result as follows

Theorem 1. *If G is a graph with n vertices and $m \geq (61/16)n$ edges, then*

$$\mathrm{bkcr}_1(G) \geq \frac{512}{2025}\frac{(m-n)^3}{n^2} > \frac{1}{3.9551}\frac{(m-n)^3}{n^2}$$

To complement this result, we exhibit drawings of graphs with n vertices, m edges, and few crossings.

Theorem 2. *For every $n \geq 3$ and $m \geq n-3$, there are graphs G on n vertices and m edges such that*

$$\mathrm{bkcr}_1(G) \leq \frac{1}{3}\frac{(m+1)^3}{(n-2)^3}.$$

2 Crossing inequalities

The proof of the main theorem is based on a technique developed by Pach et al. [4, 3] for general graphs: the idea is to prove tight inequalities for the crossing number of sparse graphs, and then use the probabilistic method to establish a general result. These inequalities are interesting on their own as they settle the minimum value of $\mathrm{bkcr}_1(G)$ for some classes of sparse graphs.

Because the edges joining consecutive vertices in the boundary do not have any crossings, from now on we consider only drawings with no edges among consecutive vertices. We call these drawings *strictly convex* (this only affects m by at most n, which is negligible when $m \gg n$).

Theorem 3. *If D is a strictly convex drawing of a graph on n vertices and m edges, then*

1. $\mathrm{cr}(D) \geq (m+1) - (n-2)$,
2. $\mathrm{cr}(D) \geq \frac{7}{3}(m+1) - 3(n-2)$,
3. $\mathrm{cr}(D) \geq \frac{25}{6}(m+1) - \frac{20}{3}(n-2)$,
4. $\mathrm{cr}(D) \geq 6(m+1) - \frac{45}{4}(n-2)$.

The first three inequalities are tight for $n-2 \leq m+1 \leq \frac{3}{2}(n-2)$, $\frac{3}{2}(n-2) \leq m+1 \leq 2(n-2)$, and $2(n-2) \leq m+1 \leq \frac{5}{2}(n-2)$; respectively.

The proof is omitted due to space limitations.

3 Proof of Theorem 1

Consider an arbitrary convex drawing D on n vertices and m edges. Remove the $b \leq n$ edges in

*California State Univ., Northridge, [bernardo.abrego, silvia.fernandez]@csun.edu.

†Supported by the NSF grant DMS-1400653.

the boundary. Then consider a random induced subgraph H obtained by selecting each vertex independently with probability p. If $n(H)$, $m(H)$, and $\mathrm{cr}(H)$ denote the number of vertices, edges, and crossings of H, respectively; then by Theorem 3(4), it follows that $\mathrm{cr}(H)+\frac{33}{2} \geq 6m(H)-\frac{45}{4}n(H)$. Furthermore, the expected value preserves this inequality and $\mathbb{E}(n(H)) = pn$, $\mathbb{E}(m(H)) = p^2(m-b)$, and $\mathbb{E}(\mathrm{cr}(H)) = p^4\,\mathrm{cr}(D)$. Thus

$$\mathrm{cr}(D) \geq 6(m-b)p^{-2} - \frac{45}{4}np^{-3} - \frac{33}{2}p^{-4}.$$

Letting $p = 45n/(16(m-b))$, it follows that

$$\mathrm{cr}(D) \geq \frac{512}{2025}\frac{(m-n)^3}{n^2} + o(m^3/n^2).$$

4 Constructions

Theorem 4. *There exist strictly convex drawings D on n vertices and m edges such that*

$$\mathrm{cr}(D) \leq \frac{1}{3}\frac{(m+1)^3}{(n-2)^2}.$$

Proof. Let m and n be positive integers. Let D_j denote a strictly convex drawing of the complete graph on j vertices minus its j boundary edges. The constructions are obtained by connecting copies of D_k and D_{k+1} by an edge (between any 2 copies, see Figure 1). If there are a copies of D_k and b copies of D_{k+1}, then the resulting drawing has $n = a(k-2)+b(k-1)+2$ vertices, $m = a\binom{k}{2} - k + 1) + b(\binom{k+1}{2} - k) - 1$ edges, and $cr = a\binom{k}{4} + b\binom{k+1}{4}$ crossings. This implies that

$$cr = \frac{k(3k-5)}{12}(m+1) - \frac{k(k-1)^2}{12}(n-2).$$

This shows the tightness of the first three inequalities in Theorem 3. If $k = \lceil 2(m+1)/(n-2)\rceil$, then it can be verified that

$$\frac{k(3k-5)}{12}(m+1) - \frac{k(k-1)^2}{12}(n-2) \leq \frac{(m+1)^3}{(n-2)^2}.$$

□

5 Conjectures

Conjecture 5. *For any integer $k \geq 3$, and any strictly convex drawing D of a graph on n vertices and m edges*

$$\mathrm{cr}(D) \geq \frac{k(3k-5)}{12}(m+1) - \frac{k(k-1)^2}{12}(n-2).$$

This conjecture was proved for $k \in \{3,4,5\}$ in Theorem 3. If this conjecture is true, then by the proof of Theorem 4, the inequality would be tight when $(k-1)(n-2)/2 \leq (m+1) \leq k(n-2)$. Furthermore, the validity of this conjecture would provide the exact minimum number of crossings of an arbitrary strictly convex drawing.

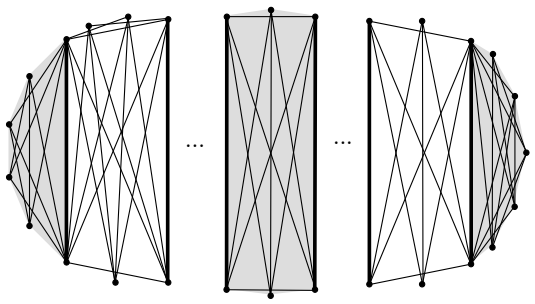

Figure 1: A construction illustrating Theorem 4 for $k = 6$. This construction is obtained by attaching copies of D_k and D_{k+1}.

Conjecture 6. *For any strictly convex drawing D of a graph on n vertices and m edges let $k = \lceil 2(m+1)/(n-2)\rceil$. We have that*

$$\mathrm{cr}(D) \geq \frac{k(3k-5)}{12}(m+1) - \frac{k(k-1)^2}{12}(n-2),$$

and this inequality is tight for some D.

Finally, this last conjecture would further imply the value of the mid-range crossing constant for convex graphs.

Conjecture 7. *If $\mathrm{bkcr}_1(n,m)$ denotes the minimum number of crossings among all convex drawings on n vertices and m edges, and if $n \ll m \ll n^2$, then*

$$\lim_{n\to\infty} \mathrm{bkcr}_1(n,m)\frac{n^2}{m^3} = \frac{1}{3}.$$

References

[1] M. Ajtai, V. Chvátal, M. Newborn, and A. Szemerédi. Crossing-free subgraphs, *Ann. Discrete Mathematics*, **12** (1982), 9-12.

[2] T. Leighton. *Complexity Issues in VLSI, Foundations of Computing Series*, MIT Press, Cambridge, MA, 1983.

[3] J. Pach, R. Radoičić, G. Tardos, and G. Tóth. Improving the crossing lemma by finding more crossings in sparse graphs. *Discrete Comput. Geom.* **36** (2006), 527-552.

[4] J. Pach and G. Tóth. Graphs drawn with few crossings per edge. *Combinatorica* **17** (1997) no. 3, 427–439.

[5] Schaefer, M.: The Graph Crossing Number and its Variants: A Survey, *E. J. Combinatorics* DS21 (2014).

[6] F. Shahrokhi, O. Sýkora, L. Székely, and I. Vrt'o, Book embeddings and crossing numbers. In *Graph-theoretic concepts in computer science*, Lecture Notes in Comput. Sci. **903**, Springer-Berlin (1995) 256–268.

Crossings in twisted graphs

B. M. Ábrego*, S. Fernández-Merchant*A. P. Figueroa†,
J. J. Montellano-Ballesteros‡, E. Rivera-Campo§

Abstract

We consider twisted graphs, that is, topological graphs that are weakly isomorphic to subgraphs of the complete twisted graph. We determine the exact minimum number of crossings of edges among the set of twisted graphs with n vertices and m edges; state a version of the crossing lemma for twisted graphs and conclude that the mid-range crossing constant for twisted graphs is 1/6.

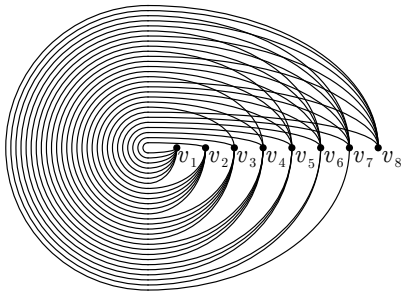

Figure 1: The complete twisted graph T_8.

1 Introduction

A *simple topological graph* is a drawing of a graph in the plane where the vertices are points, and the edges are simple continuous arcs satisfying that any two arcs have at most one point in common, which is either a common endpoint or a proper crossing, and no arc passes through any other vertex different from its endpoints. If all edges of a simple topological graph are straight-line segments, then it is called a *geometric graph*. A geometric graph whose vertices are in convex position, is called a *convex graph*. Two simple topological graphs G and G' are *weakly isomorphic* if there exists an isomorphism between G and G' such that two edges of G' cross if and only if the corresponding edges of G do.

The *complete twisted graph* T_n is a complete simple topological graph with vertices $v_1v_2, \dots v_n$ such that two edges v_iv_j and $v_{i'}v_{j'}$ cross if and only if $i < i' < j' < j$ or $i' < i < j < j'$. (See Figure 1.) A simple topological graph G is a *twisted graph* if G is weakly isomorphic to a subgraph of T_n. Twisted graphs were found in [3] as complete topological graphs with maximum number of edge-crossings but with no subgraph weakly isomorphic to the complete convex graph with 5 vertices. A version of the Erdős-Szereres Theorem for topological graphs appeared in [5]: every complete topological graph with n vertices has a topological subgraph with $m \geq c \log^{1/8} n$ edges, which is weakly isomorphic to a complete convex or twisted graph. Several problems previously studied for convex graphs were recently studied for twisted graphs [4].

We are interested in crossing numbers on twisted graphs. The *crossing number* of a topological graph D is the number of edge-crossings in D. This measure for the non-planarity of a graph has been extensively studied [7]. Some of the major motivations for investigating crossing numbers are their applications to VLSI design, to digital visual design, and to classical problems in discrete geometry. One of the fundamental results in this area is known as the *crossing lemma* [2]: for any topological graph D with n vertices and $m > 4n$ edges, $cr(D) \geq (1/64)m^3/n^2$, and this is tight except for the multiplicative constant 1/64. This constant has been progressively improved with the best current bound $cr(D) \geq (1/29)m^3/n^2$ (for $m > 7n$) [1]. It was proved in [6] that this multiplicative constant tends to a positive constant, called the *mid-range crossing constant*, when $n \to \infty$ and $n \ll m \ll n^2$.

We prove the *crossing lemma for twisted graphs* and conclude that the *mid-range crossing constant for twisted graphs* is 1/6. In fact, for every m and n, we determine the exact minimum crossing number within the class $T_{n,m}$ of twisted graphs with n vertices and m edges and provide a family of crossing optimal graphs.

2 Results

Let $cr_T(n, m)$ be the minimum number of crossings among all twisted graphs in $T_{n,m}$. Let $t_{n,m}$ be the unique integer such that $\binom{n-t_{n,m}-1}{2} \leq \binom{n}{2} - m <$

*California State Univ., Northridge, [bernardo.abrego, silvia.fernandez]@csun.edu.
†Dept. de Matemáticas, ITAM, apaulinafg@gmail.com
‡Inst. de Matemáticas, UNAM, juancho@im.unam.mx
§Dept. de Matemáticas, UAM-I, erc@xanum.uam.mx

$\binom{n-t_{n,m}}{2}$. Then
$t_{n,m} = n - \left\lfloor \frac{3}{2} + \sqrt{\left(n-\frac{1}{2}\right)^2 - 2m} \right\rfloor$.

Theorem 1 (Crossing number of twisted graphs)**.** *Let n and m be integers with $n \geq 1$ and $0 \leq m \leq \binom{n}{2}$. Then $cr_T(n,m) =$*

$$\binom{t_{n,m}}{2}m \;-\; 2\binom{t_{n,m}+1}{3}n \;+\; 3\binom{t_{n,m}+2}{4}.$$

This theorem is a direct consequence of the following two results.

Theorem 2 (Crossing inequalities)**.** *Let $G \in T_{n,m}$. For all $t \leq n$, $cr(G) \geq \binom{t}{2}m - 2\binom{t+1}{3}n + 3\binom{t+2}{4}$.*

This bound is actually tight for any n and m when $t = t_{n,m}$.

Theorem 3 (Tightness of crossing inequalities)**.** *For any $n \geq 1$ and $0 \leq m \leq \binom{n}{2}$, there exists a twisted graph G in $T_{n,m}$ such that*

$$cr(G) = \binom{t_{n,m}}{2}m - 2\binom{t_{n,m}+1}{3}n + 3\binom{t_{n,m}+2}{4}.$$

Namely, the set of edges of G is

$$\{(i,j) : 1 \leq i \leq n-1, i+1 \leq j \leq \min\{i+t, n\}\} \cup \{(i, t+1+i) : 1 \leq i \leq s\},$$

where $t = t_{n,m}$ and $s = \binom{n-t}{2} - \binom{n}{2} + m$.

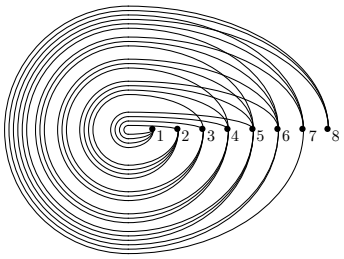

Figure 2: A twisted graph with 8 vertices, 20 edges, and $cr_T(8,20)$ crossings.

Here is how our bound relates to the classic crossing lemma and mid-range crossing constant [2, 6]. Let $n < m$ be positive integers; the notation $n \ll m \ll n^2$ stands for m is a function of n such that $lim_{n\to\infty}(n/m) = lim_{n\to\infty}(m/n^2) = 0$.

Theorem 4 (Crossing lemma for twisted graphs)**.** *Let $G \in T_{n,m}$ for integers n and m. If $n \ll m \ll n^2$, then*

$$cr(G) \geq \frac{1}{6} \cdot \frac{m^3}{n^2} - o\left(\frac{m^3}{n^2}\right).$$

If $m = cn$ for some constant $c \geq 2$ and $n > \frac{\lfloor c \rfloor^2 + 3\lfloor c \rfloor + 2}{\lfloor c \rfloor + 1 - c}$, then

$$cr(G) \geq \binom{\lfloor c \rfloor}{2}\left(\frac{3c - 2\lfloor c \rfloor - 2}{3c^3}\right)\frac{m^3}{n^2} + 3\binom{\lfloor c \rfloor + 2}{4}.$$

If $m = cn^2$ for some constant $0 < c \leq \frac{1}{2}$, then

$$cr(G) \geq \left(\frac{3\sqrt{1-2c}+1}{3(1+\sqrt{1-2c})^3} + o(1)\right)\frac{m^3}{n^2}.$$

Moreover, these inequalities are tight.

An immediate corollary of Theorem 4 is the exact value of this mid-range crossing constant.

Theorem 5 (Mid-range crossing constant for twisted graphs)**.** *Let n and m be integers such that $n \ll m \ll n^2$. Then*

$$\lim_{n\to\infty} cr_T(n,m)\frac{n^2}{m^3} = \frac{1}{6}.$$

There is a nice transition in the behavior of the constant before and after the mid-range. Namely, if $m = cn$ for some constant $c > 2$, then

$$\lim_{n\to\infty} cr_T(n,m)\frac{n^2}{m^3} = \binom{\lfloor c \rfloor}{2}\left(\frac{3c - 2\lfloor c \rfloor - 2}{3c^3}\right)$$

and

$$\lim_{c\to\infty}\binom{\lfloor c \rfloor}{2}\left(\frac{3c - 2\lfloor c \rfloor - 2}{3c^3}\right) = \frac{1}{6}.$$

Similarly, If $m = cn^2$ for some constant $0 < c \leq \frac{1}{2}$, then

$$\lim_{n\to\infty} cr_T(n,m)\frac{n^2}{m^3} = \frac{\sqrt{1-2c}+1/3}{(1+\sqrt{1-2c})^3}$$

and

$$\lim_{c\to 0^+}\frac{\sqrt{1-2c}+1/3}{(1+\sqrt{1-2c})^3} = \frac{1}{6}.$$

References

[1] E. Ackerman. On topological graphs with at most four crossings per edge. arXiv:1509.01932v1.

[2] M. Ajtai, V. Chvátal, M. Newborn, and A. Szemerédi. Crossing-free subgraphs, *Ann. Discrete Mathematics*, **12** (1982), 9-12.

[3] H. Harborth, I. Mengersen, Drawings of the complete graph with maximum number of crossings. In: Proc. 23rd Southeastern Conf. on Comb., Graph Th., and Computing, **88** (1992) 225–228.

[4] E. Omaña-Pulido, E. Rivera-Campo, Notes on the twisted graph. In: Márquez A., Ramos P., Urrutia J. (eds) EGC 2011. Lecture Notes in Computer Science **7579** (2012) 119–125.

[5] J. Pach, J. Solymosi, G. Tóth: Unavoidable configurations in complete topological graphs. *Discrete Comput. Geom.* **30** (2003) 311–320.

[6] J. Pach, J. Spencer and G. Tóth, New bounds on crossing numbers, *Discrete Comput. Geom.* **24** (2000), 623–644.

[7] M. Schaefer, The graph crossing number and its variants: A survey, *E. J. Combinatorics*, **DS21**, (2014).

Vertex Nim on Cayley Graph

Tomoaki Abuku*†

2019

1 Introduction

1.1 Impartial Game

This paper discusses "impartial" combinatorial games in normal form, that is games with the following characters:

- Two players alternately make a move.
- No chance elements (the possible moves in any given position is determined in advance).
- Both players have complete knowledge of the game states.
- The game terminates in finitely many moves.
- Both players have the same set of the possible moves in any position.
- A player who makes the last move wins.

Definition 1.1 (Outcome Classes)**.** A game position is called an $\mathcal{N}$-position (resp. a $\mathcal{P}$-position) if the first player (resp. the second player) has a winning strategy.

Clearly, all impartial game positions are classified into $\mathcal{N}$-positions or $\mathcal{P}$-positions.

Theorem 1.2. ([3]) If G is an $\mathcal{N}$-position, there exists a move from G to a $\mathcal{P}$-position. If G is a $\mathcal{P}$-position, there exists no move from G to a $\mathcal{P}$-position.

*affiliation:University of Tsukuba
†mail:buku3416@gmail.com

1.2 Rules of the Game

A game called a Vertex Nim is an impartial game played on a directed graph whose vertices are weighted by any non-negative integers [1]. The rules are as follows:

- In the starting position, a piece is placed at a vertex of the graph.
- Each player alternately moves the piece from the vertex to one of its adjacent vertices and decreases the weight of the vertex to any strictly smaller non-negative integer.

Vertex Nim is an extension of Vertex geography introduced by [2].

Definition 1.3 (Cayley Graph)**.** Let H be a finite group and S be a generating subset of H. The Cayley graph (V, E) is a graph with vertex set $V = H$ and (directed) edge set $E = \{(x, y) \mid x, y \in H, \exists s \in S, y = sx\}$.

In this paper, we discuss Vertex Nim on a Cayley graph (V, E) of finite group H generated by S.

Example 1.4. Vertex Nim on the quaternion group generated by $S = \{i, j\}$.

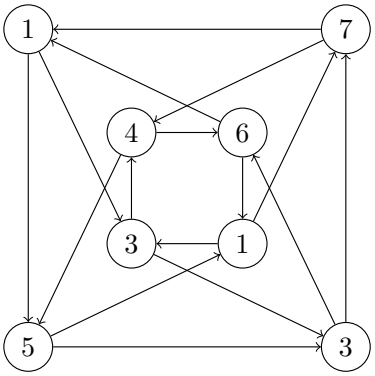

2 Winning Strategy

2.1 Quaternion Groups

Winning strategies of the game on the Cyclic group and the Dihedral group have been already given in [4]. Also a winning strategy of the game on the quaternion group has been given, but we give a simpler strategy of the game.

Lemma 2.1. If you start from one of the vertices with the least weight in the Cayley graph of the quatenion group, you are in a $\mathcal{P}$-position, namely, you have no chance to win unless the opponent makes a mistake.

Example 2.2. In the case of Example 1.4, we have the following by using Theorem 1.2 and Lemma 2.1.

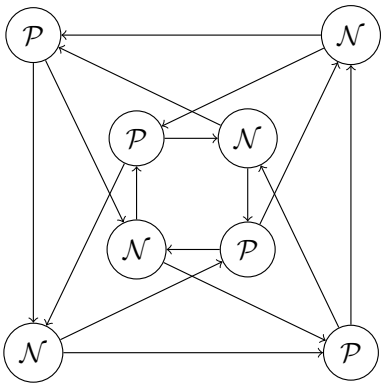

2.2 Direct product of Cyclic Groups

We give a winning strategy for Vertex Nim on $C_n \times C_m$ which is not studied in [4].

Example 2.3. Vertex Nim on $C_3 \times C_4$.

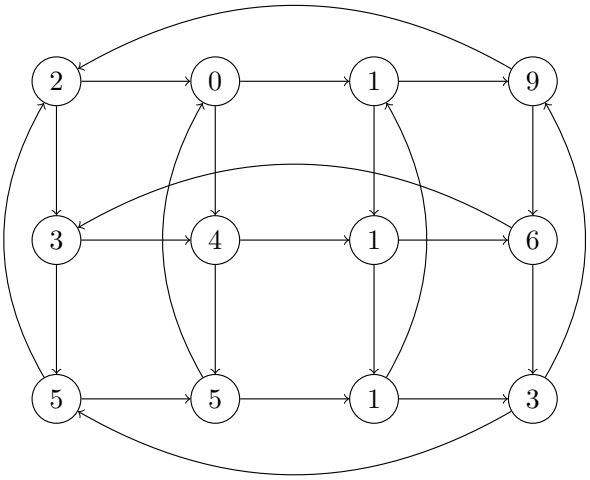

3 Acknowledgements

The author would like to thank Dr. Kô Sakai and Dr. Koki Suetsugu for useful comments and discussions.

References

[1] Burke, K. and George O., *A PSPACE-complete graph Nim*, Games of No Chance 5, 259-269, 2017.

[2] Fraenkel, A. S. Scheinerman, E, R. Ullman, D., *Undirected edge geography*, Theoretical Computer Science, Vol. 112(2), 371-381, 1993.

[3] Siegel, A. N., *Combinatorial Game Theory*, American Mathematical Society, 2013.

[4] Meyer, M., *Nim on Groups*, College of Saint Benedict and Saint John's University, Honors Theses, 2013.

Critical sets of a magic cube

Tomoko Adachi
Department of Information Sciences, Toho University
2-2-1 Miyama, Funabashi, Chiba, 274-8510, Japan
E-mail: adachi@is.sci.toho-u.ac.jp

Keywords: Critical set, Latin square, Magic cube, Magic square, Secret sharing scheme.

A magic square is known in ancient times in China and India. Many people have been interested in a magic square for hundreds years. A magic square has deeply relationship to a latin square.

A *Latin square* of order n is an $n \times n$ array in which n distinct symbols are arranged so that each symbol occurs in each row and column. A *partial Latin square* of order n is an $n \times n$ array with entries chosen from the set $\{1, 2, \cdots, n\}$ in such a way that no element occurs twice or more in any row or column. A *critical set* in a Latin square L of order n is a set $C = \{(i, j; k) \mid i, j, k \in \{1, 2, \cdots, n\}\}$ such that L is the only Latin square of order n which has symbol k in cell (i, j) for each $(i, j; k) \in C$, and no proper subset of C has above property. A critical set is called *minimal* if it is a critical set of smallest possible cardinality for L. A Latin square was studied in [4] and [3].

A *magic square* of order n is an arrangement of n^2 integers $1, 2, \cdots, n^2$ into an $n \times n$ square with the property that the sums of each row, each column, and each of the main diagonals are the same. It is known that a magic square of order n can be constructed if n is an integer for which there is a pair of orthogonal diagonal Latin squares of order n.

More generally, a *magic hypercube* of order n and dimension t is an arrangement of n^t integers $1, 2, \cdots, n^t$ into an $n \times n \times \cdots \times n$ (t times) array with the property that the sums of each 1-dimensional subarray i-th row ($i = 1, 2, \cdots, t$) and each of the main diagonals are the same. We call a magic hypercube with dimension three a *magic cube*. A magic cube was studied by Trenkler [8] and [9].

As their applications to cryptography, there is a secret shareing scheme. A *secret sharing scheme* in cryptography is developed for a set of participants to share the secret value K. The first and the most famous scheme in various secret sharing schemes, is a (t, w)-threshold scheme which was proposed by Shamir [6] in 1979. It is a method of sharing a secret value K among a finite set $\mathcal{P} = \{P_1, P_2, \cdots, P_w\}$ of w participants in such a way that any t participants can reconstruct K but no group of $t-1$ or fewer participants can reconstruct K. Each piece of information of K distributed to each participant is called a *shadow*. Secret sharing schemes using Latin squares have been investigated, for instance, Cooper's scheme [2] and Stones' scheme [7]. Both schemes make use of partial Latin squares. Cooper's scheme use critical sets of Latin squares. Stones' scheme use Latin square autotopisms. Lu and Adachi [5] introduced a construction and protocol of secret sharing schemes using magic hypercubes. In order to clarify the main ideas of using magic hypercubes for secret sharing schemes in [5], we introduce the secret sharing schemes using magic cubes in [1].

In this paper, we investigate some property of crutucal sets of a magic cube. Moreovere, we give another secret sharing scheme using magic cube. .

References

[1] T. Adachi and X. N. Lu; Magic cubes and secret sharing schemes, *Algebras, Logics, Languages and related areas, Publications of the Research Institute for Mathematical Sciences, Kyoto University,* 2096 (2018) , pp. 115-118.
http://www.kurims.kyoto-u.ac.jp/ kyodo/kokyuroku/contents/pdf/2096-17.pdf

[2] J. Cooper, D. Donovan, and J. Seberry; Secret sharing schemes arising from latin squares, *Bull. Inst. Combin. Appl.*, Vol. 12 (1994), pp. 33–43.

[3] A. D. Keedwell and J. Dénes; *Latin Squares and their applications*, 2nd editon, Elsevier, 2015.

[4] C. F. Laywine and G. L. Mullen; *Discrete Mathematics Using Latin Squares*, John Weiley & Sons, INC, 1998.

[5] X. N. Lu and T. Adachi; Secret sharing scheme using magic hypercubes, submitted.

[6] A. Shamir; How to share a secret, Communications of the ACM, 22 (1979),612-613.

[7] R. J. Stones, M. Su, X. Liu, G. Wang, and S. Lin; A Latin square aototopism secret sharing scheme, Design, Codes Cryptography, vol. 80, no. 3, pp. 635–650, 2016.

[8] M. Trenkler; Magic p-dimensional cubes, *Acta Arithmetica*, vol. 96, pp. 361–364, 1998.

[9] M. Trenkler; A construction of magic cubes, *The mathematical Gazette*, vol. 84, pp. 36–41, March 2000.

How to fold a long Conway tile into either an isotetrahedron or a rectangular dihedron

Jin Akiyama[1*] and Kiyoko Matsunaga[2*]

2019 JCDCG3, Sept. 6-8

Universidad Científica de Tokio
1-3, Kagurazaka, Shinjuku-ku, Tokyo, 162-8601, Japan
*1 : ja@jin-akiyama.com
*2 : matsunaga@mathlab-jp.com

Abstract
During the JCDCG3 2017, Eppstein and Langerman suggested us that Alexandrov theorem guaranties the foldability of every Conway tile into either an isotetrahedron (denoted by I) or a rectangular dihedron (denoted by R). Although a few results relating the topic were obtained in [1,2,3], it has not been known completely how to fold it. In this talk, we show explicitly the way to fold every Conway tile, even if it is very long, into I or R on a basis of its 4-base (Fig. 1).

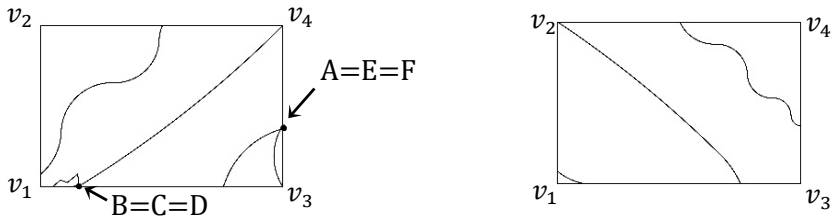

(a) Top (b) Bottom

(a) N_1 is foldable into a rectangular dihedron R

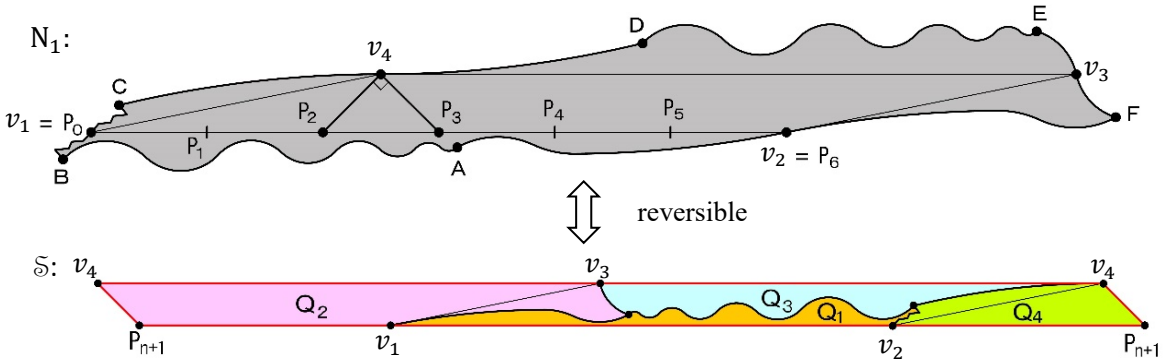

(c) N_1 is reversible into $\mathfrak{S}$

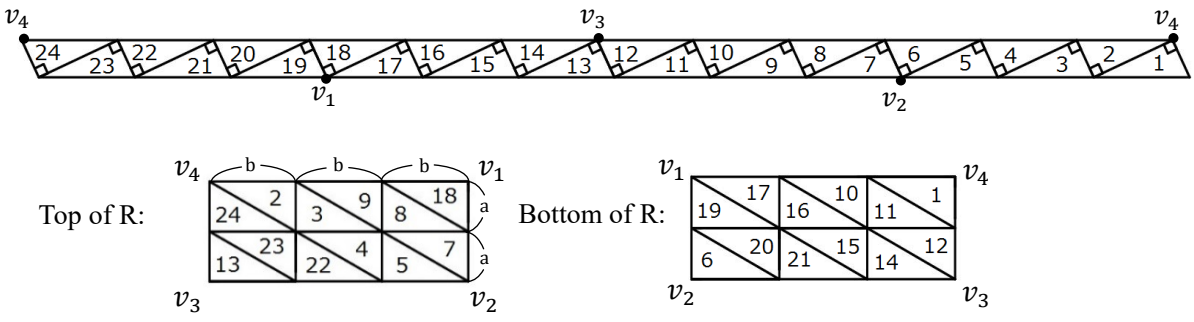

(d) $\mathfrak{S}$ is foldable into R

Fig. 1

We need the following definitions and results:
A tetrahedron is called an **isotetrahedron** if all its faces are congruent. A figure is called a **Conway tile** if it satisfies the following criterion: Its perimeter can be divided into six parts by six consecutive points A.B.C.D.E and F (all located on its perimeter) such that:

(1) The perimeter part AB is congruent by translation τ to the perimeter part ED; i.e.,$\tau(A) = E, \tau(B) = D$ and AB//ED.

(2) Each of those perimeter parts BC, CD, EF, and FA is centrosymmetric; that is, each of them coincides with itself when the figure is rotated by 180° around its midpoint.

(3) Some of the six points may coincide but at least three of them must be distinct (Fig. 2).

For a Conway tile N, we define the set of 4 midpoints v_1, v_2, v_3 and v_4 of centrosymmetric parts of N as a **4-base** of N under the agreement that midpoint of a centrosymmetric part XY is X (=Y) if X coincides with Y. Thus, there exists a 4-base for any Conway tile N (Fig. 3).

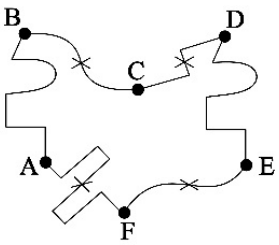

Fig. 2 Conway tile

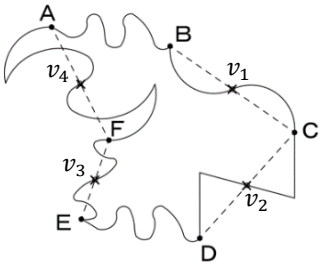

Fig. 3 4-base of N

Alexandrov's Theorem [5]
Any Alexandrov gluing corresponds to a unique convex polyhedron (where a doubly covered polygon is considered a polyhedron).

Theorem [4] *Two figures P and Q have a reversible hinged dissections if and only if P and Q are two noncrossing nets of a common polyhedron G.*

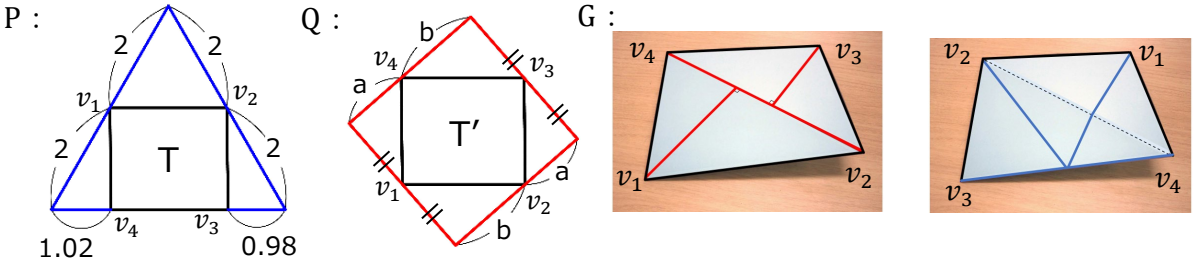

Fig. 4 P, Q are reversible, G is a common isotetrahedron

References

[1] Zachary Abel, Erik D. Demaine, Martin Demaine, Hiroaki Matsui, Günter Rote, Ryuhei Uehara, Common developments of several different orthogonal boxes, in: 23rd CCCG2011, Toronto, 2011, 77-82.

[2] J. Akiyama and K. Matsunaga, Reversibility and foldability of Conway tiles, Computatinal Geometry **64** (2017), 30-45

[3] J. Akiyama and K. Matsunaga, Unfoldings of an envelope, European Journal of Combinatorics **80** (2019), 3-16

[4] J. Akiyama, E.D. Demaine and S. Langerman, Polyhedral Characterization of Reversible Hinged Dissections, to appear in Graphs and Combinatorics.

[5] J. O'Rourke, How to Fold It: The Mathematics of Lincanges, Origami, and Polyhedra, Cambridge University Press (2011)

<邦訳：『折り紙のすうり～リンケージ・折り紙・多面体の数学』上原隆平訳、近代科学社（2012）>

Minimal Ununfoldable Polyhedron

Hugo A. Akitaya[1], Erik D. Demaine[2], David Eppstein[3], Tomohiro Tachi[4], and Ryuhei Uehara[5]

[1] Department of Computer Science, Tufts University, USA.
[2] CSAIL, MIT, USA.
[3] Department of Computer Science, University of California, Irvine, USA.
[4] Department of General Systems Studies, The University of Tokyo, Japan.
[5] School of Information Science, JAIST, Japan.

1 Introduction

In computational origami, one of the most remarkable problems asks if every convex polyhedron has an edge-unfolding to a simple and nonoverlapping polygon [3, Open Problem 21.1]. Here, an *edge-unfolding* is a set of edges of the polyhedron such that cutting along these edges unfolds the polyhedron.

There are several evidences for/against the conjecture (see [3, Sections 22.2 and 22.3]); however, it is far from to be settled. As an evidence for this conjecture, it is known that any convex polyhedron P is edge-unfoldable if P is a prismoid or a dome; however, they form a quite limited set of convex polyhedra. On the other hand, as an evidence against this conjecture, there are several edge-ununfoldable nonconvex polyhedra. In this context, a key property of a polyhedron is *topological convexity*; a polyhedron P is *topologically convex* iff there is a convex polyhedron P' such that the graph induced by its vertices and edges is isomorphic to the one induced by P. In fact, if we do not restrict to topologically convex polyhedra, it is easy to make an edge-ununfoldable polyhedron with 7 faces: take a tetrahedron and add a tetrahedral bump in the middle of one of its faces.

Research on small edge-ununfoldable nonconvex polyhedra gives us insight of the open problem. In [5], Grünbaum gives a polyhedron with 13 vertices and 13 faces that is not edge-unfoldable. We sharpen such edge-unfoldability of nonconvex polyhedra:

Theorem 1.1 *(1) There exists a topologically convex polyhedron with 7 vertices and 6 faces that is not edge-unfoldable. (2) There exists a topologically convex polyhedron with 6 vertices and 7 faces that is not edge-unfoldable. (3) Any polyhedron with less than 6 vertices or 6 faces is edge-unfoldable.*

That is, we give much smaller edge-ununfoldable polyhedra, and we also prove that they are optimal with respect to the number of faces and vertices, respectively. Note that they are not only topologically convex, but also all their faces are simple polygons (or simply connected and no holes).

2 Edge-ununfoldable polyhedra

In order to prove Theorem 1.1(1), we show a polyhedron P with 7 vertices and 6 faces s.t. any edge-unfolding of P causes an overlapping. It is as shown in Figure 1: P has an *apex* G, and the *base* of P consists of one triangle ABF and one concave pentagon $BCDEF$. The *side* of P consists of 2 triangles CDG and EDG and 2 concave quadrilaterals $ABCG$ and $AFEG$. We make P symmetric to its mirror image across the plane AGD. The key properties of the polyhedron P are the following; (a) total angle around $D > 360°$, (b) total angle around $G > 360°$, (c) $\angle CBF + \angle CBA > 360°$, and (d) $\angle ABF + \angle CBA > 300°$ and $BF < BC$.

Let $\mathcal{G} = (\mathcal{V}, \mathcal{E})$ be the graph induced by P. Then any edge-unfolding of P induces a spanning tree $\mathcal{T}$ of $\mathcal{G}$. Let $\mathcal{T}$ be any spanning tree of $\mathcal{G}$. We show that any edge-unfolding given by $\mathcal{T}$ produces overlapping. Since $\mathcal{T}$ is a tree, it has at least 2 leaves. However, from the properties (a)-(c), none of B, F, D, G can be a leaf since overlapping occurs at leaves. On the other hand, vertices A, C, E cannot be three leaves since we cannot have any spanning tree $\mathcal{T}$ that contains the edge BF with 3 leaves A, C, E. Thus $\mathcal{T}$ has only 2 leaves, i.e., $\mathcal{T}$ is a Hamilton path of $\mathcal{G}$. In most cases, $ABCG$ overlaps with $CBFED$ at vertex B by (c). The other case is shown in Figure 2. Thus the polyhedron P in Figure 1 has no edge-unfolding without overlapping. In order to prove Theorem 1.1(2), we show a polyhedron P with 6 ver-

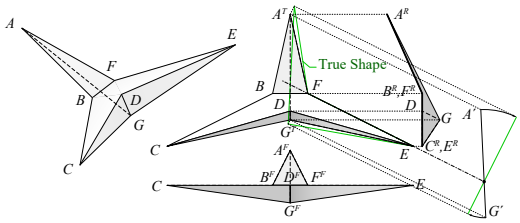

Figure 1: An edge-ununfoldable polyhedron with 7 vertices and 6 faces.

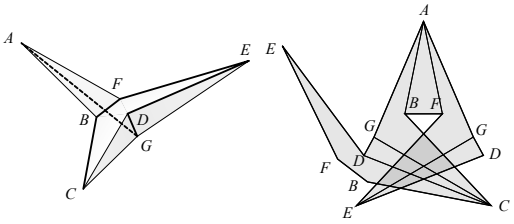

Figure 2: An edge-unfolding that causes overlapping.

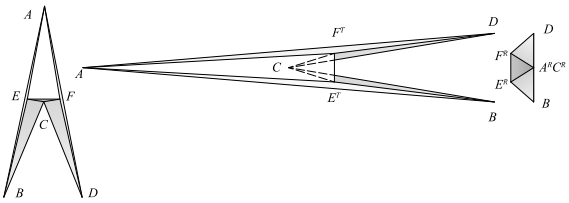

Figure 3: An edge-ununfoldable polyhedron with 6 vertices and 7 faces.

tices and 7 faces s.t. any edge-unfolding of P causes an overlapping. This polyhedron is composed of a quadrilateral $ABCD$ concave at C, connected to 2 apices E and F as in Figure 3. This polyhedron is designed to have the following properties: (a) $\angle BCE > \angle BCD$, and (b) $\angle AEB + \angle BEC + \angle CEF > 2\pi$. Property (a) forces that edges BC and CD must be cut, otherwise triangle BCE would overlap quadrilateral $ABCD$. Because A,B,D are the only vertices with positive curvature, two leaves of the spanning tree exist either on A, B, or D. If B and D are both leaves, then, the only route to A is through path $CFEA$. However, corner FEA would create an overlapping vertex by condition (b). If A and D are the only two leaves, the tree is a path $AEFDCB$. Now this again contains corner AEF, thus the unfolding overlaps by (b).

3 Edge-unfoldable polyhedra with less than 6 vertices or 6 faces

In order to prove Theorem 1.1(3),we first recall that DiBiase established that all convex polyhedra with 4, 5, or 6 vertices can be edge-unfolded [4]. Based on this result, there are only two cases to be considered; P is (a) a nonconvex square pyramid (with 5 faces and 5 vertices), or (b) a nonconvex polyhedron that consists of 6 triangles and 5 vertices with degree sequence 3,3,4,4,4. The proof that these two polyhedra are edge-unfoldable is omitted here.

4 Concluding remarks

We investigated minimal edge-ununfoldable polyhedra. We show two edge-ununfoldable polyhedra; one has 6 faces and 7 vertices, and the other has 7 faces and 6 vertices. They are optimal with respect to the number of faces and vertices for topologically convex polyhedra. Grünbaum shows an edge-ununfoldable convex faced polyhedron with 13 faces and 13 vertices [5], and Bern et al. give an edge-ununfoldable triangular faced polyhedron with 36 faces and 20 vertices [1]. Improving these upper bounds and/or showing lower bounds are future work.

Acknowledgements

David Eppstein was supported in part by NSF grants CCF-1618301 and CCF-1616248. Tomohiro Tachi was supported in part by KAKENHI 16H06106. Ryuhei Uehara was supported in part by MEXT/JSPS KAKENHI Grant Number 17H06287 and 18H04091. This work was discussed at the 34th Bellairs Winter Workshop on Computational Geometry, co-organized by Erik D. Demaine and Godfried Toussaint, held on March 22–29, 2019 in Holetown, Barbados. We thank the other participants of that workshop for providing a stimulating research environment.

References

[1] M. Bern, E. D. Demaine, D. Eppstein, E. Kuo, A. Mantler, and J. Snoeyink. Ununfoldable polyhedra with convex faces. *Computational Geometry: Theory and Applications*, 24(2):51–62, 2003.

[2] T. Biedl, E. D. Demaine, M. L. Demaine, A. Lubiw, M. Overmars, J. O'Rourke, S. Robbins, and S. Whitesides. Unfolding Some Classes of Orthogonal Polyhedra. *CCCG 98*, 1998.

[3] E. D. Demaine and J. O'Rourke. *Geometric Folding Algorithms: Linkages, Origami, Polyhedra*. Cambridge University Press, 2007.

[4] J. DiBiase. *Polytope Unfolding*. Undergraduate thesis, Smith College, 1990.

[5] B. Grünbaum. No-Net Polyhedra. *Geombinatorics*, 11:111–114, 2002.

PSPACE-completeness of Pulling Blocks to Reach a Goal

Joshua Ani* Sualeh Asif* Erik D. Demaine* Yevhenii Diomidov*
Dylan Hendrickson* Jayson Lynch* Sarah Scheffler† Adam Suhl‡

Abstract. We prove PSPACE-completeness of all variations of pulling-block path-planning puzzles (reaching a goal with or without forced pulls, of arbitrary strength, with or without gravity) that include fixed blocks or walls, with the exception of Pull?-1FG (strength 1, fixed blocks, with gravity) for which we only show NP-hardness.

In the Pull series of path-planning problems [3,4], the goal is to navigate an agent from a given starting square to a given target square within a rectangular board featuring impassable but pullable 1×1 blocks. We study several different variants of Pull, which can be combined in arbitrary combination:

1. **Strength:** In Pull-k, the agent can pull an unbroken horizontal or vertical line of up to k pullable blocks at once. In Pull-$*$, the agent can pull arbitrarily many blocks at once.
2. **Fixed blocks/walls:** In Pull-F, the board may have fixed 1×1 blocks that cannot be traversed or pulled. In the more general Pull-W, the board may have fixed thin (1×0) walls.
3. **Optional/forced pulls:** In Pull!, every agent motion that can also pull blocks must pull as many as possible (as in many video games where the player input is just a direction). In Pull?, the agent can choose whether and how many blocks to pull. (The latter is traditionally called Pull in the literature, but we use the explicit "?" to indicate optionality.)
4. **Gravity:** In Pull-G, all blocks fall maximally downward after each agent move (like gravity).

Table 1 summarizes our and known results for all variants that include fixed blocks or walls: we prove PSPACE-completeness for any strength, with optional or forced pulls, and with or without gravity, with the exception of Pull?-1FG for which we only show NP-hardness. The only previous result for this problem family is NP-hardness for Pull?-k even without fixed blocks [4]. In some cases, our results are stronger than the best known results for the corresponding Push (pushing-block) problem; see [3]. More complex variants PullPull (where pulled blocks slide maximally), PushPull (where blocks can be pushed and pulled), and Storage Pull (where the goal is to place multiple blocks into desired locations) are also known to be PSPACE-complete [3].

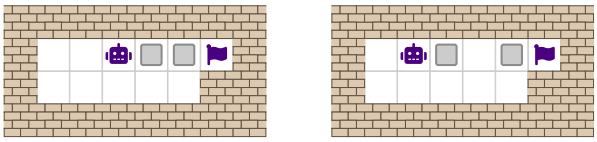

(a) Initial state **(b)** A strength-1 move

Figure 1: A pulling-block puzzle. The robot is the agent, the flag is the goal square, the light gray blocks can be moved, and the bricks are fixed in place. Robot and flag icons from Font Awesome under CC BY 4.0 License.

Our reductions are from two problems: Asynchronous Nondeterministic Constraint Logic (NCL) [2,5] and planar 1-player motion planning [1]. Without gravity, Figure 2 shows our NCL gadgets. With gravity, we reduce from the motion-planning framework [1]. For optional-pulling PSPACE-hardness (with $k \geq 2$), we use the locking 2-toggle gadget in Figure 3. For forced pulling, we introduce a new gadget, a *self-closing door*, and show it can simulate a locking 2-toggle; see Figure 4. For the one remaining case of Pull?-1FG, we show NP-hardness by constructing a crossing xor gadget (not shown here).

References

[1] Erik D. Demaine, Dylan H. Hendrickson, and Jayson Lynch. A general theory of motion planning complexity: Characterizing which gadgets make games hard. arXiv:1812.03592, 2018.

*Massachusetts Institute of Technology, Cambridge, MA, USA
†Boston University, Boston, MA, USA
‡Algorand, Boston, MA, USA

Problem	Gravity	Forced	Strength	Features	Hardness	Previous Best
PULL?-kF	no	no	$k \geq 1$	fixed blocks	PSPACE-complete	NP-hard [4]
PULL?-$*$F	no	no	∞	fixed blocks	PSPACE-complete	NP-hard [4]
PULL!-kF	no	yes	$k \geq 1$	fixed blocks	PSPACE-complete	—
PULL!-$*$F	no	yes	∞	fixed blocks	PSPACE-complete	—
PULL?-1FG	yes	no	$k = 1$	fixed blocks	NP-hard	—
PULL?-1WG	yes	no	$k = 1$	thin walls	PSPACE-complete	—
PULL?-kFG	yes	no	$k \geq 2$	fixed blocks	PSPACE-complete	—
PULL?-$*$FG	yes	no	∞	fixed blocks	PSPACE-complete	—
PULL!-kFG	yes	yes	$k \geq 1$	fixed blocks	PSPACE-complete	—
PULL!-$*$FG	yes	yes	∞	fixed blocks	PSPACE-complete	—

Table 1: New and known results for PULL variants. We omit PULL-W hardness implied by PULL-F hardness.

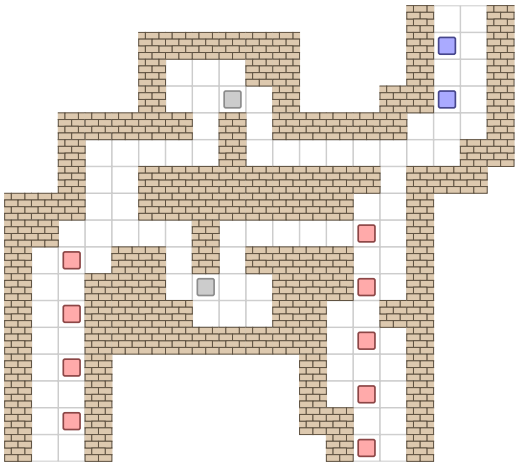

(a) NCL AND gadget for PULL-kF for $k \geq 1$. Also works for W variant and PULL-$*$.

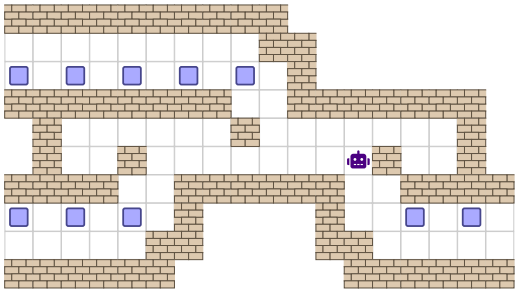

(b) NCL OR gadget for PULL-kF for $k \geq 1$ Also works for W variant and PULL-$*$.

Figure 2: Gadgets for the reduction from asynchronous NCL to PULL-kF.

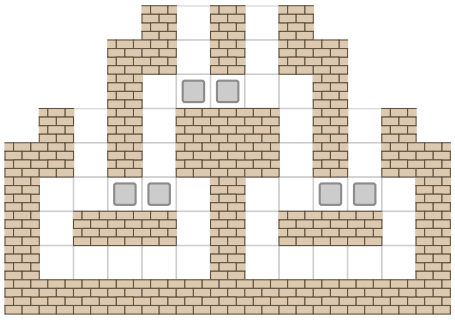

Figure 3: Construction of a locking 2-toggle (in the state where only the right tunnel is traversable, and traversing lets you optionally flip), which by [1] shows PSPACE-completeness of PULL?-kFG for $k \geq 2$. Also works for PULL?-kWG for $k \geq 1$ and for PULL?-$*$WG.

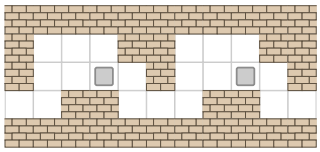

(a) Re-usable one-way "diode" gadget, denoted ▶| in Figure 4b.

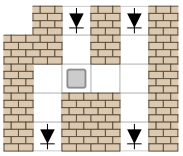

(b) This self-closing door can be "opened" from the right tunnel, and forced to "close" when traversing the left tunnel.

Figure 4: Gadgets for PULL!-1FG.

[2] Robert A. Hearn and Erik D. Demaine. *Games, Puzzles, and Computation.* A K Peters/CRC Press, 2009.

[3] André G. Pereira, Marcus Ritt, and Luciana S. Buriol. Pull and PushPull are PSPACE-complete. *Theoretical Computer Science*, 628:50–61, 2016.

[4] Marcus Ritt. Motion planning with pull moves. arXiv:1008.2952, 2010.

[5] Giovanni Viglietta. Partial searchlight scheduling is strongly PSPACE-complete. In *Proceedings of the 25th Canadian Conference on Computational Geometry*, Waterloo, Canada, August 2013.

A complete list of all convex polyhedra made by gluing regular pentagons[1]

Elena Arseneva[2], **Stefan Langerman**[3], and Boris Zolotov[4]

1. Abstract. We give a complete description of all convex polyhedra whose surface can be constructed by folding and gluing (edge-to-edge) regular pentagons.

2. Introduction. Given a collection of 2D polygons, a *gluing* describes a closed surface by specifying how to glue each polygon edge onto another edge from the collection. Alexandrov's uniqueness theorem [1] states that any gluing that is homeomorphic to a sphere and that does not yield a total facial angle more than 2π at any point, is the surface of a unique convex 3D polyhedron[5].

Unfortunately, the proof of this theorem is highly non-constructive and the only known approximation algorithm has (pseudopolynomial) running time larger than $O(n^{1116})$ (where n is the total number of edges) [7], and depends on the aspect ratio of the polyhedral metric, the Gaussian curvature at its vertices, and the desired precision of the solution. There is no known exact algorithm for reconstructing the 3D polyhedron, and in fact the polyhedron's coordinates might not even have a closed formula [5].

Enumerating all possible valid gluings is also not an easy task, as the number of gluings can be exponential even for a single polygon [2]. However one valid gluing can be found in polynomial time using dynamic programming [4, 9]. Complete enumerations of gluings and the resulting polyhedra are only known for very specific cases such as the latin cross [3] and a single regular polygon [4].

This paper continues the study, initiated by the first two authors, for the special case when the polygons to be glued together are all identical regular k-gons. For $k > 6$, the only two possibilities are two k-gons glued into a doubly covered k-gon, or one k-gon folded in half (if k is even). When $k = 6$, the number of hexagons that can be glued into a convex surface is unbounded, however there are at most 10 possible graph structures for such (non-flat) polyhedra, 6 of which have been identified, and all gluings forming doubly-covered 2D polygons have been characterized [8].

Here we study the case $k = 5$, i.e., gluing regular pentagons edge to edge. This case differs substantially from the case of hexagons, since it is not possible to produce a vertex of Gaussian curvature 0 by gluing pentagons. Therefore both the number of possible graph structures and the number of possible gluings is constant. To determine the graph structure of each gluing, we use an implementation [10] of the Bobenko-Izmestiev algorithm to obtain an approximate polyhedron P for the gluing, and then we use a computer program to generate a certificate that the approximation P has the correct graph structure if it is simplicial. For non-simplicial polyhedra, we resort to ad-hoc proofs (which appear in the full version).

3. Gluing regular pentagons together. Let P be a convex 3D polyhedron. The *Gaussian curvature* at a vertex v of P equals $2\pi - \sum_{j=1}^{t} \alpha_j^v$, where t is the number of faces of P incident to v, and α_j^v is the angle of the j-th face incident to v. Since P is convex, the Gaussian curvature at each vertex of P is non-negative. The Gauss-Bonnet theorem (1848) states that the total sum of the Gaussian curvature of all vertices of a 3D polyhedron P equals 4π.

4. How many pentagons can we glue and which vertices can we obtain? Let P be a convex polyhedron obtained by gluing several regular pentagons edge-to-edge. Vertices of P are clearly vertices of the pentagons. The sum of facial angles around a vertex v of P equals $3\pi/5$ (the interior angle of a regular pentagon) times the number of pentagons glued together at v. Since the Gaussian curvature at v is in $(0, 2\pi)$, the number of pentagons glued at v can be either one, two, or three. This yields the Gaussian curvature at v to be respectively $7\pi/5$, $4\pi/5$, or $\pi/5$.

Note that, as opposed to the case of regular hexagons, it is not possible to produce a vertex of curvature 0 (which would be a flat point on the surface of P) by gluing several pentagons. Therefore all the vertices of the pentagons must be vertices of P.

Proposition 1. *Suppose P is a convex polyhedron obtained by gluing edge-to-edge N regular pentagons. Then: (a) P has $2 + 1.5N$ vertices in total. In particular, N must be even. (b) N is at most* 12.

Enumerating all possible gluings. In order to reach our main goal and list all the convex polyhedra that can be obtained by gluing regular pentagons edge-to-edge, we used a computer program to list all the non-isomorphic gluings of this type. Our program is a simple modification of the one that enumerates the gluings of hexagons [8].

5. Determining the shape from the gluing. Consider a gluing M that satisfies Alexandrov's conditions and thus corresponds to unique polyhedron $\mathcal{P}$. Suppose we have a simplicial polyhedron P whose edge lengths and facial angles are close to those of $\mathcal{P}$. We use a program that checks whether the graph structures of P and $\mathcal{P}$ coincide.

Let V, E, F be the numbers of vertices, edges and faces of $\mathcal{P}$ respectively; $\mathcal{D}$ the maximum degree of a vertex of P; L the length of the longest edge of P; $B_r(u)$ the ball in $\mathbb{R}^3$ of radius r centered at the point u.

Vertices of P correspond to cone points of metric M, and the edges are the shortest paths between their endpoints. Thus for every edge of P we can calculate the discrepancy between its length and the corresponding length in M (which is the *intended length* of that edge). Let μ be the maximum of the discrepancy for all edges.

Similarly, a pair of adjacent edges forms an angle in both P and M. We denote the maximum discrepancy between these angle values by γ.

The basis of our procedure is an observation that each vertex of $\mathcal{P}$ lies within r–ball centered at the corresponding vertex of P, where $r = E^2 \cdot L \cdot 2\sin(\mathcal{D}\gamma/2) + E\mu$ (see Theorem 3).

Our procedure verifies that there does not exist a plane intersecting all four r–balls centered at any four vertices of P.

[1]E. A. was supported in part by F.R.S.-FNRS, and by the SNF grant P2TIP2-168563 of the Early PostDoc Mobility program. S. L. is directeur de recherches du F.R.S.-FNRS.

[2]Saint Petersburg State University, Russia
[3]Expected presenter, Université libre de Bruxelles, Belgium
[4]Saint Petersburg State University, Russia

[5]Note that the original polygonal pieces might need to be folded to obtain this 3D surface.

Theorem 2. *Given a metric M and a simplicial polyhedron P we can check in time $\mathcal{O}(E)$ that the convex polyhedron corresponding to metric M has the same graph structure as P without false-positive errors.*

False negative errors can occur if the precision is not sufficient, and a plane exists that intersects all four r–balls centered at the vertices of P even though there is an edge connecting two of the vertices. In such a case precision has to be increased by replacing P with a polyhedron that has smaller discrepancy in edge lengths and values of angles and repeating the procedure.

To obtain approximate polyhedron P one can use the existing algorithm [6, 7].

6. Precision of vertex location based on the approximation. We aim to find a small real number r such that each vertex of $\mathcal{P}$ lies within an r–ball centered at the corresponding vertex of P.

Without loss of generality, one of the vertices of both P and $\mathcal{P}$ is located at $(0, 0, 0)$, one of the edges incident to this vertex (in $\mathcal{P}$ and in P, respectively) is aligned with the x axis, and one of the faces incident to that vertex and that edge — both in $\mathcal{P}$ and P — lies on the horizontal plane $z = 0$.

We derive the following theorem, which is a key statement to prove the correctness of our main result.

Theorem 3. *Suppose μ is the maximum edge discrepancy between P and $\mathcal{P}$, γ is the maximum angle discrepancy between P and $\mathcal{P}$, $\mathcal{D}$ is the maximum degree of a vertex of P. If $\mathcal{D}\gamma < \pi/2$, then each vertex of $\mathcal{P}$ lies within an r-ball centered at the corresponding vertex of P, where $r = E^2 \cdot L \cdot 2\sin(\mathcal{D}\gamma/2) + E\mu$.*

Using this theorem we can obtain the complete list of all the polyhedra that can be obtained by gluing regular pentagons. We present this list below.

7. A complete list of all shapes obtained by gluing pentagons. Figure 1 shows all polyhedra that can be obtained by gluing regular pentagons. For those polyhedra that are simplicial, their graph structure is confirmed by applying the method of Section 6, for the others the proof is geometric, and it will apear in the full version of this note.

8. Concluding remarks and future work. The main outcome of this paper is the list of all convex polyhedra that can be made by gluing several regular pentagons edge to edge. However the way we obtained this list is interesting in its own right, and may lead to other results. While this will not always work efficiently for Alexandrov's problem on arbitrary polyhedral metric (our estimation of r depends quadratically on the number of vertices of the polyhedron), it should work well for certain classes of metrics such as metrics with small number of cone points, in particular, for metrics obtained by gluing edge-to-edge regular squares, triangles, or other polygons with fixed angles. One question that remains open is whether it is possible to deal with non-simplicial graph structures in a generic way, i.e., lift the restriction from Theorem 2 that $\mathcal{P}$ is simplicial.

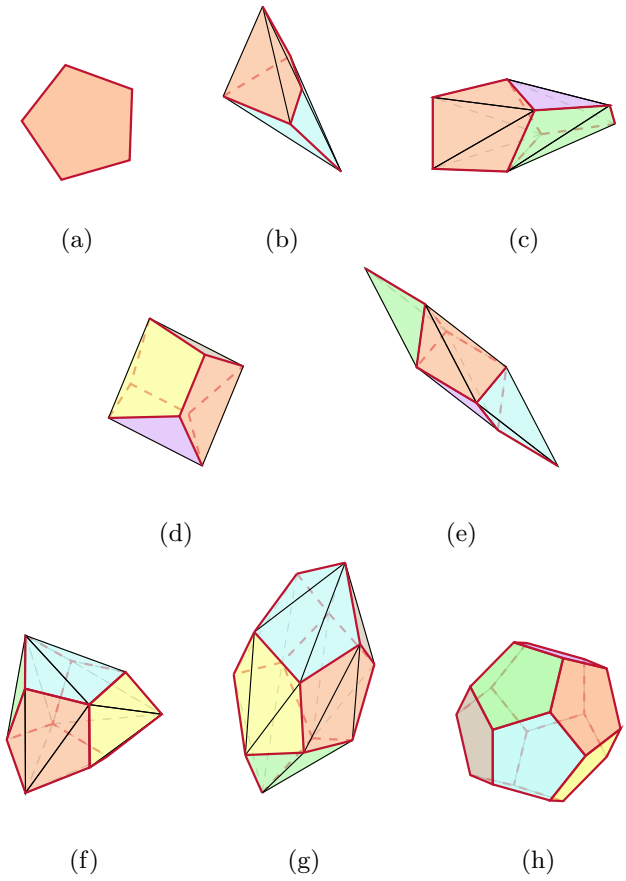

Figure 1: Polyhedra glued from regular pentagons

References

[1] A. Alexandrov. *Convex Polyhedra*. Springer-Verlag, Berlin, 2005. translation from Russian.

[2] E. Demaine, M. Demaine, A. Lubiw, and J. O'Rourke. Enumerating foldings and unfoldings between polygons and polytopes. *Graphs and Combinatorics*, 18(1):93–104, 2002.

[3] E. Demaine, M. Demaine, A. Lubiw, J. O'Rourke, and I. Pashchenko. Metamorphosis of the cube. In *Proc. SOCG*, pages 409–410. ACM, 1999. video and abstract.

[4] E. Demaine and J. O'Rourke. *Geometric folding algorithms*. Cambridge university press, 2007.

[5] D. Eppstein. Polyhedra whose vertex coordinates have no closed form formula. `https://11011110.github.io/blog/2015/12/06/polyhedra-whose-vertex.html`.

[6] A. I. Bobenko. I. Izmestiev. Alexandrov's theorem, weighted delaunay triangulations, and mixed volumes. *Annales de l'Institut Fourier*, 58(2):447–505, 2008.

[7] Daniel M Kane, Gregory N Price, and Erik D Demaine. A pseudopolynomial algorithm for alexandrov's theorem. In *WADS*, pages 435–446. Springer, 2009.

[8] E. Khramtcova and S. Langerman. Which convex polyhedra can be made by gluing regular hexagons? In *JCDCG*^{3}, 2017.

[9] A. Lubiw and J. O'Rourke. When can a polygon fold to a polytope?, 1996. Technical Report 048, Department of Computer Science, Smith College, Northampton, MA. Presented at AMS Conf., 1996.

[10] S. Sechelmann. Discrete minimal surfaces, koebe polyhedra, and alexandrov's theorem. variational principles, algorithms, and implementation. *Dipl. Thesis, TU Berlin*, 2007.

Sublinear Explicit Incremental Planar Voronoi Diagrams

Elena Arseneva[‡] John Iacono[§] Greg Koumoutsos[†]
Stefan Langerman[†¶] Boris Zolotov[*]

Abstract

A data structure is presented that explicitly maintains the graph of a Voronoi diagram of N point sites in the plane or the dual graph of a convex hull of points in three dimensions while allowing insertions of new sites/points. Our structure supports insertions in $\tilde{O}(N^{\frac{3}{4}})$ expected amortized time, where $\tilde{O}$ suppresses polylogarithmic terms. This is the first result to achieve sublinear time insertions; previously it was shown by Allen et al. that $\Theta(N^{\frac{1}{2}})$ amortized combinatorial changes per insertion could occur in the Voronoi diagram but a sublinear-time algorithm was only presented for the special case of points in convex position.

1 Introduction

Voronoi Diagrams and convex hulls are two keystone geometric structures of central importance to computational geometry. We focus the description here on planar Voronoi diagrams; the results can be extended to the dual graph of 3D-convex hulls as the structures are known to be related. We create a data structure that explicitly maintains Voronoi diagrams under insertion of new sites. The diagram is stored as a graph in adjacency list format on which primitive operations, including links and cuts, are performed. Previous work [3], which we use as a subroutine, is able to dynamically maintain a set of N points and answer nearest neighbor queries in polylogarithmic time, but this is different from maintaining the Voronoi diagram explicitly; it relies crucially on nearest neighbor being a decomposable search problem, whereas maintaining the Voronoi diagram is clearly not. In [2] it was observed that while there could be a linear number of changes to the embedded Voronoi diagram with each site insertion, this is not equivalent to the number of combinatorial changes to the graph structure of the Voronoi diagram. It was then proved by showing that the amortized number of combinatorial changes is only $\Theta(N^{\frac{1}{2}})$ per site insertion. This observation opened the possibility to maintain the Voronoi diagram graph in faster than linear time per insertion, which [2] then did for the restricted case where the sites are in convex position. Our result is a data structure that explicitly maintains the graph of a Voronoi diagram of arbitrary point sites in the plane while allowing insertions of new sites in $\tilde{O}(N^{\frac{3}{4}})$ expected amortized time, where $\tilde{O}$ suppresses polylogarithmic terms. Previously, no sublinear method was known for this problem.

2 Sketch of Data Structure

The data structure has several parts:

- An adjacency list representation of the Voronoi diagram.
- The dynamic nearest neighbor structure (DNN) [3] for the sites which supports insertion and deletion of sites and nearest neighbor queries in $\tilde{O}(1)$ expected amortized time.
- A linked list of all Voronoi cells of size at least $N^{\frac{1}{4}}$, which we call *big*.
- Call the *neighbors* of a Voronoi cell the Voronoi vertices connected to the cell by an edge. A neighbor is *relevant* if it is not incident to a big cell. For each big cell

[*]Saint Petersburg State University
[†]Partially supported by Chebyshev Laboratory and foundation Родные Города
[‡]Université libre de Bruxelles
[§]Supported by a F.R.S-FNRS MISU grant.
[¶]Directeur de recherches du F.R.S-FNRS

b_i store a circular linked list of $\Theta\left(\frac{|b_i|}{N^{\frac{1}{4}}}\right)$ data structures each associated with the consecutive range of $O(N^{\frac{1}{4}})$ neighbors of B_i. In each structure, store the Voronoi circles for those neighbors that are relevant.

- These *dynamic circle-reporting structures (DCRs)* are known variants of the DNN structure that support insertion and deletion of circles in time $\tilde{O}(1)$, and given a query point, report all k circles containing the point in time $\tilde{O}(k)$.
- For each big cell also store the vertices of the cell in circular order in a binary search tree supporting $O(\log N)$-time operations, including split and merge (such as a red-black tree).

In [1] it was shown that the number of cells of the Voronoi diagram undergoing combinatorial changes per insertion is $O(N^{\frac{1}{2}})$ amortized, there are a constant number of combinatorial changes per cell, and these cells with changes are connected. Thus, the main goal of this work is to find the cells that change. Implementing those changes is done using the techniques of [1].

Our method is to use the DNN structure to locate one Voronoi cell that must change and create a queue with this cell and all large cells. We then remove each cell from the queue, process its changes, and add into the queue any neighboring small cells with unprocessed changes; we do not have to add neighboring large cells as all of them are in the initial queue and will be processed. What we do to process small and large cells is different, but is based on the fact that given a cell with changes, the neighboring cells that change can be identified by seeing which neighbors of the cell are defined by Voronoi circles that contain the newly inserted site. For small cells we can afford to look at all $\leq N^{\frac{1}{4}}$ neighbors' circles in a brute force way, while for the large cells we use the DCRs to identify the circles containing the new site. There are a number of details, these include the possible need to propagate changes in a small cell to the DCRs of a neighboring large cell. Also, a split in a large cell could require splitting and merging a constant number of its DCR structures which is done through rebuilding.

If s small cells change, and $b_1, b_2, \ldots b_{|B|}$ are the big cells, and ℓ_i is the number of circles retuned by the DCR structures of b_i, the amortized expected runtime is

$$\tilde{O}\left(sN^{\frac{1}{4}} + \sum_{i=1}^{|B|}\left(\left\lceil\frac{|b_i|}{N^{\frac{1}{4}}}\right\rceil + \ell_i\right)\right).$$

Since s is $O(N^{\frac{1}{2}})$ amortized [1], $\sum_{i=1}^{|B|}|b_i| \leq N$, $|B| \leq N^{\frac{3}{4}}$, and $\sum_{i=1}^{|B|}\ell_i \leq sN^{\frac{1}{4}}$, this is simply $O\left(N^{\frac{3}{4}}\right)$ amortized.

3 Discussion

There remains a gap between the $\tilde{O}\left(N^{\frac{3}{4}}\right)$ expected amortized runtime of our structure and the $\Theta\left(N^{\frac{1}{2}}\right)$ amortized number of combinatorial changes to the Voronoi diagram. The randomization comes solely from the shallow cuttings used in the DNN structure [3]; it is open whether this could be removed. Maintaining the Voronoi diagram with insertions and deletions is hopeless as the $\Theta\left(N^{\frac{1}{2}}\right)$ amortized bound for insertions only becomes $\Theta(N)$ for insertions and deletions.

4 Acknowledgments

This work was completed during the Second Trans-Siberian Workshop on Geometric Data Structures. We thank the organizers and staff of Russian Railways (РЖД) for creating an ideal research environment.

References

[1] S. R. Allen, L. Barba, J. Iacono, and S. Langerman. Incremental voronoi diagrams. *Discrete & Computational Geometry*, 58(4):822–848, 2017.

[2] B. Aronov, P. Bose, E. D. Demaine, J. Gudmundsson, J. Iacono, S. Langerman, and M. H. M. Smid. Data structures for halfplane proximity queries and incremental voronoi diagrams. *Algorithmica*, 80(11):3316–3334, 2018.

[3] T. M. Chan. A dynamic data structure for 3-d convex hulls and 2-d nearest neighbor queries. *J. ACM*, 57(3):16:1–16:15, 2010.

Tetris is NP-hard even with $O(1)$ columns

Sualeh Asif* Erik D. Demaine* Jayson Lynch* Mihir Singhal*

Abstract

We prove that the classic falling-block video game *Tetris* remains NP-complete even when restricted to 8 columns, settling an open problem posed over 15 years ago [BDH+04]. Our reduction is from 3-Partition, similar to the previous reduction for unrestricted board sizes [BDH+04], but with a better packing of buckets.

In the (perfect-information) Tetris problem [BDH+04], we are given an initial board state of filled squares and a sequence of pieces that will arrive, and the goal is to place the pieces in sequence to either survive (not go above the top row) or clear the entire board. This problem was proved NP-hard for arbitrary board sizes in 2002 [BDH+04], and more recently for other polyomino pieces [DDE+17]. The variant we consider here is the *c-column Tetris problem* (abbreviated cC-Tetris), which is the Tetris problem restricted to boards with exactly c columns. The original Tetris paper [BDH+04] asked specifically about the complexity of cC-Tetris for $c = O(1)$, motivated by real-world Tetris where $c = 10$. Our main result is the following:

Theorem 1. *It is NP-complete to survive or clear the board in* cC-Tetris *for any* $c \geq 8$.

Membership in NP follows from the same result for general Tetris [BDH+04, Lemma 2.1]. Like [BDH+04], we reduce from the strongly NP-hard 3-Partition problem: given a multiset of nonnegative integers $\{a_1, \ldots, a_{3s}\}$ and a nonnegative integer T satisfying the constraints $\sum_{i=1}^{3s} a_i = sT$ and $\frac{T}{2} < a_i < \frac{T}{4}$ for all $1 \leq i \leq 3s$, determine whether $\{a_1, \ldots, a_{3s}\}$ can be partitioned into s (disjoint) triples, each of which sum to exactly T. For the reduction, we exhibit a mapping from 3-Partition instances to 8C-Tetris instances so that the following is satisfied:

Lemma 2 (Tetris $\iff$ 3-Partition)**.** *For a "yes" instance of* 3-Partition*, there is a way to drop the pieces that clears the entire board without triggering a loss. Conversely, if the board can be cleared, then the* 3-Partition *instance has a solution.*

Proof sketch. The initial board, illustrated in Figure 1(a) (where filled cells are grey and the rest of the cells are unfilled), will have 8 columns and $12sT + 48s + 26$ rows. The reduction is polynomial size.

The piece sequence is as follows. First, for each a_i, we send the following a_i *sequence* (see Figures 1(i–m)): $\langle$  $, \langle$  $\rangle^{a_i},$  $, \langle$  $\rangle$. After all these pieces, we send the following *clearing sequence* (see Figures 1(n) and (b–h)): $\langle\langle$  $\rangle^{s},$  $, \langle$  $\rangle^{6sT+24s+6},$  $, \langle$  $\rangle^{3sT+12s+4}\rangle$.

Figures 1(b–n) illustrate that a solution to 3-Partition will clear the board. To show the other direction, we progressively constrain any 8C-Tetris solution to a form that directly encodes a 3-Partition solution. Because the area of the pieces sent is exactly equal to $8(12sT + 48s + 26)$, no square can be left empty. We enumerate all possible cases to show that this goal is impossible to meet (some square must be left empty) if there is no 3-Partition solution. Figures 1(o–w) show some of the cases. □

References

[BDH+04] Ron Breukelaar, Erik D. Demaine, Susan Hohenberger, Hendrik Jan Hoogeboom, Walter A. Kosters, and David Liben-Nowell. Tetris is hard, even to approximate. *International Journal of Computational Geometry and Applications*, 14(1–2):41–68, 2004.

[DDE+17] Erik D. Demaine, Martin L. Demaine, Sarah Eisenstat, Adam Hesterberg, Andrea Lincoln, Jayson Lynch, and Y. William Yu. Total Tetris: Tetris with monominoes, dominoes, trominoes, pentominoes, ... *Journal of Information Processing*, 25:515–527, 2017.

*Massachusetts Institute of Technology, Cambridge, MA, USA

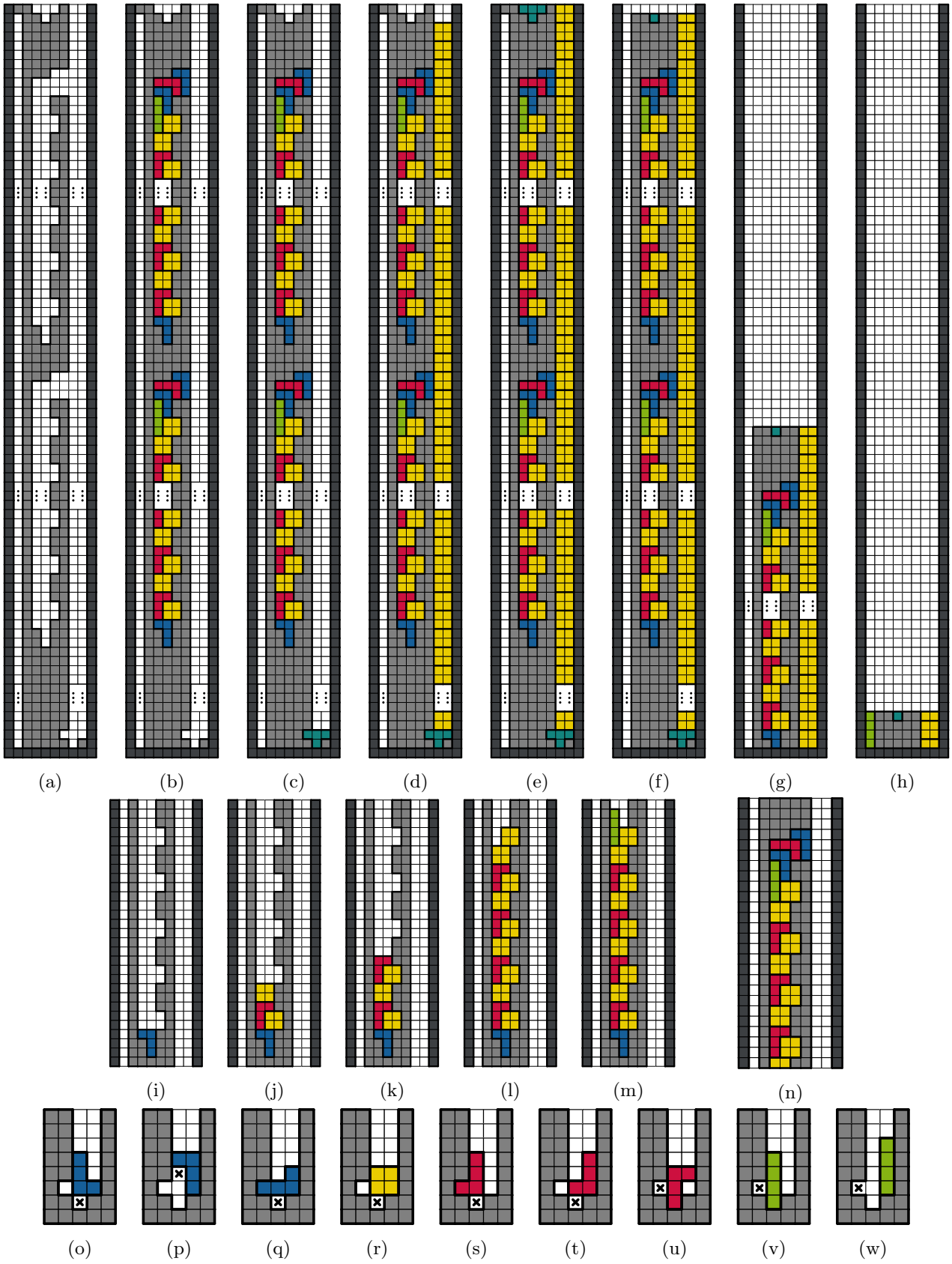

Figure 1: (a) shows the initial board. (b–d) demonstrate filling and clearing the board in the final clearing sequence. (i–m) show a valid sequence of moves for $a_i = 5$. (n) shows our bucket terminator. (o–w) show invalid possibilities for various pieces in the bucket.

RELOCATION WITH UNIFORM EXTERNAL CONTROL IN LIMITED DIRECTIONS

Jose Balanza-Martinez, David Caballero, Angel A. Cantu, Timothy Gomez, Austin Luchsinger, Robert Schweller, Tim Wylie
Department of Computer Science, University of Texas - Rio Grande Valley, Edinburg, TX 78539, USA

Abstract

We study a model where particles exist within a board and move single units based on uniform external forces. We investigate the complexity of deciding whether a single particle can be relocated to another position in the board, and whether a board configuration can be transformed into another configuration. We prove that the problems are NP-complete with 1×1 particles even when only allowed to move in 2 or 3 directions.

1 Introduction

The tilt model, proposed by Becker et al. [3], has foundations in classical motion planning. A couple of natural problems that arise in these computational systems are those of relocation and reconfiguration. *Relocation* is the problem of whether a sequence of tilts exists to relocate a tile from location a to location b. *Reconfiguration* asks if a sequence of tilts exists to transform board A to board B (specifying the location of all tiles). These were shown to be PSPACE-complete in 4-directions if a single polyomino larger than a 1×1 is in the system [1]. Here, we discuss a variant of this model (introduced in [2]) where particles exist within a board and move, in uniform, single unit distances (rather than maximally) in any of the four cardinal directions via an external force. These particles move in said direction unless the path is blocked by some "concrete" space. Figure 1 shows a simple example. We study these questions with only 1×1 tiles with limited usable directions (e.g. only tilting down and right). We further look at the complexity of the board geometry. A specific class of boards used for our relocation problem is "x/y-monotone", which can also be called vertically/horizontally monotone.

Definitions. A *board* B is a rectangular region in $\mathbb{Z}^2$ where positions are either *open* or *blocked*, meaning no tile can be on this location. A *tile/robot/particle* is a 1×1 polyomino with a label and a position at some location in B. A *configuration* $C = (B, P)$ is the board and the set of tiles with their locations. A *step* is a cardinal direction command $d = \{N, S, E, W\}$ that transforms one configuration into another by translating all tiles a unit distance in that direction unless the adjacent location is blocked or occupied by another tile. A *step sequence* is a series of steps which can be inferred from a series of directions $D = \langle d_1, \ldots, d_k \rangle$ where each $d_i \in D$ implies a step in that direction.

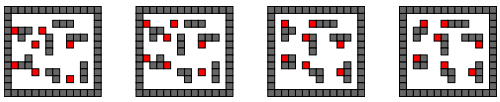

(a) Init **(b)** $\langle N \rangle$ **(c)** $\langle E \rangle$ **(d)** $\langle E \rangle$

Figure 1: An example step sequence $\langle N, E, E \rangle$. (a) The initial board configuration. (b) The resultant configuration after an N step. (c) The resultant configuration after an E step. (d) The final configuration after one more E step.

We also note that both problems are in NP, since with limited directions, there is a limited number of possible steps before the configuration cannot change, or can only move between a small number of configurations.

2 Relocation

Here we show the relocation problem is hard with limited directions (two or three) even in a monotone board via a reduction from 3-SAT.

Theorem 1. *Given a monotone board, the relocation problem in the single step model is NP-complete when limited to two or three directions.*

The 3-SAT reduction utilizes gadgets that have *binding locations* on their top and bottom locations which is how the gadgets connect to form *chains*. There are 3 chain gadgets: the *literal chain*, *clause chain*, and *validation chain*. They connect at their binding locations to form one chain representing the 3-SAT formula. Every literal is represented as one tile, and trapping it in a certain location on the board sets that literal to 'true'. We place 3 literal tiles for every clause inside a clause chain, depicted in Figure 3c, and connect them to form the clause chain.

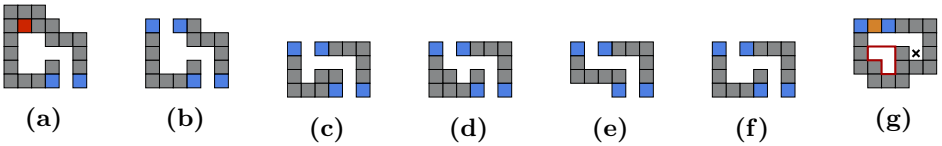

(a) **(b)** **(c)** **(d)** **(e)** **(f)** **(g)**

Figure 2: Different individual gadgets.

The tile in Figure 2a will be relocated to the gadget in Figure 2g, which is the last gadget in the validation chain. The validation chain contains tiles that force 'appropriate' assignments of the literal tiles− the validation tiles could block the relocation tile. Moreover, if any clause is not satisfied, the 'excess' tiles from the clause chain will enter the validation chain and block the relocation tile. The three chains force the proper assignment of literals and checks the satisfiability of all clauses, allowing the relocation tile to be placed only if all the clauses were satisfied.

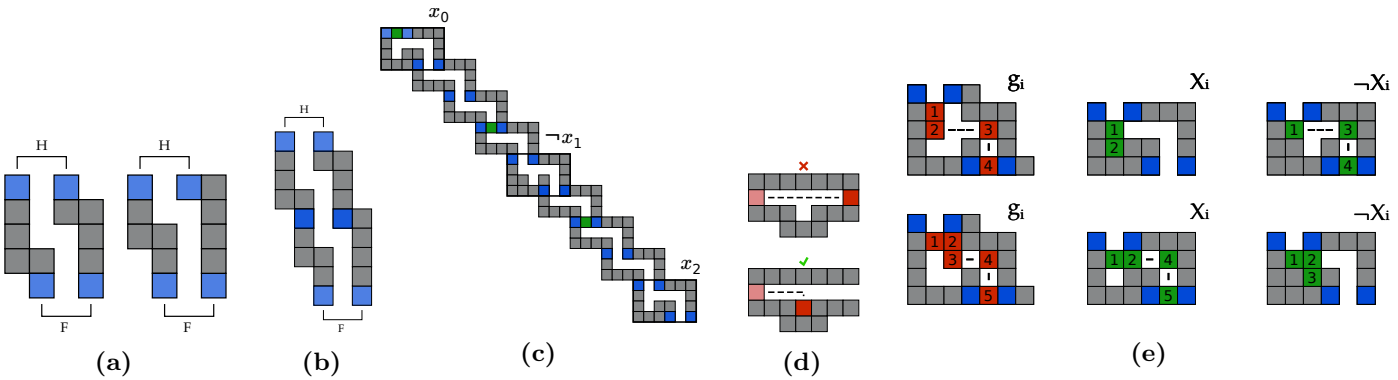

Figure 3: (a) Demonstration of two gadgets (b) binding at their bottom locations. (c) An example clause gadget. (d) Truth assignment of some literal tile. (e) A truth assignment for a variable x. The numbering on the tiles depict the step move order. Setting literal x_i to true is depicted in the upper three images, and setting it to false is depicted in the lower three.

3 Reconfiguration

Reconfiguration is a variant of relocation that ensures we know where every tile on the board is located. The input to the problem is two configurations: an initial and final. We show that in two directions the problem is NP-complete via a 3-SAT reduction. We will use South and East as the directions. Given a 3-SAT formula consisting of variables $\{x_1, x_2, x_3, ..., x_n\}$, separated into m clauses of the form $(A \vee B \vee C)$ where each A, B, C is of the form x_i or $\neg x_i$, we create an instance of the reconfiguration problem that is solvable if and only if the 3-SAT formula is satisfiable.

Theorem 2. *The reconfiguration problem in the single step model is NP-complete when limited to two directions.*

Figure 4a shows the basic structure of the clause gadgets and Figure 4b shows how variable tiles are placed. For the clause, the variables must be placed in reverse order in the three slots at the bottom right. This can only occur if one of the variables has a true value. Otherwise, one of the tiles will go into the wrong slot. In order to force the constraints, the other gadgets, shown in Figure 5, specify the location of other tiles which can only be placed correctly if the correct amount of S and E commands have been used. This prevents cheating in the clause gadgets.

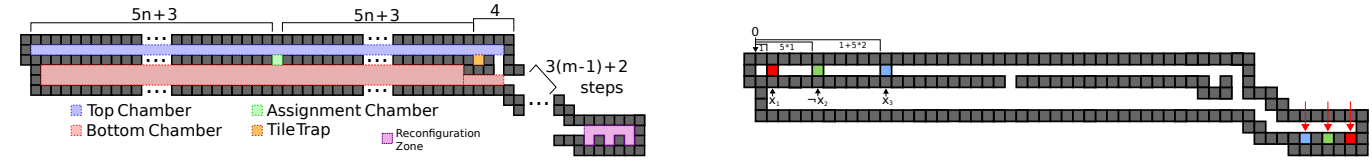

Figure 4: (a) 3-SAT clause gadget, where n is the total number of unique variables, and m indicates that this clause is the m^{th} clause in the formula. (b) Example of variable placement for clause $(x_1 \vee \neg x_2 \vee x_3)$ in a 5-variable formula. Goal locations indicated by red arrows

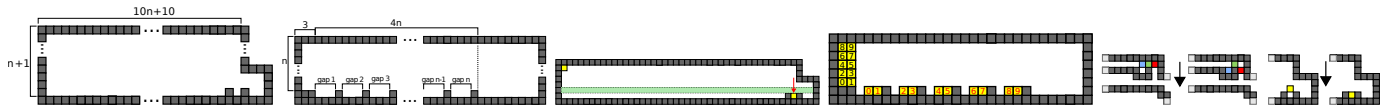

Figure 5: (a) South Limiter: Limits the amount of south steps made before all variables have been assigned. (b) South Forcer: Forces the user to make south steps at specific times. (c) Example of south limiter tile placement in a 5 variable formula. Goal location indicated by red arrow. Post assignment zone highlighted in green. (d) Example of south forcer tile placement in a 5 variable formula. Goal location indicated by red labels. (e) State of a clause gadget in which no variable tiles evaluated to a literal true before and after the forced south tilt, and the respective states of the *south limiter gadget*.

Acknowledgments. This research was supported in part by National Science Foundation Grant CCF-1817602.

References

[1] Jose Balanza-Martinez, David Caballero, Angel Cantu, Luis Garcia, Austin Luchsinger, Rene Reyes, Robert Schweller, and Tim Wylie. Full tilt: Universal constructors for general shapes with uniform external forces. In *Proceedings of the* 30^{th} *Annual ACM-SIAM Symposium on Discrete Algorithms*, SODA'19, 2019.

[2] Aaron Becker, Erik D. Demaine, Sándor P. Fekete, Golnaz Habibi, and James McLurkin. Reconfiguring massive particle swarms with limited, global control. In *Algorithms for Sensor Systems*, pages 51–66, 2014.

[3] Aaron T. Becker, Erik D. Demaine, Sándor P. Fekete, and James McLurkin. Particle computation: Designing worlds to control robot swarms with only global signals. In *Proceedings of the IEEE International Conference on Robotics and Automation*, ICRA'14, pages 6751–6756, May 2014.

Randomized Reductions and the Topology of Conjectured Classes of Uniquely Hamiltonian Graphs

Robert D. Barish[1] and Akira Suyama[1]

[1] Graduate School of Arts and Sciences,
University of Tokyo, Meguro-ku Komaba 3-8-1 Tokyo 153-8902, Japan
rbarish@genta.c.u-tokyo.ac.jp

Abstract. We utilize the hardness of the Unambiguous-SAT problem under randomized polynomial time reductions (Valiant & Vazirani; *Theoret. Comput. Sci.* **47**(1); 1986) to probe the required properties of counterexamples to (open) non-existence conjectures for uniquely Hamiltonian graphs under various topological constraints. Concerning ourselves with a generalization of Sheehan's 1975 conjecture that no uniquely Hamiltonian graphs exist in the class of $(r \in 2\mathbb{N}_{>1})$-regular graphs, Bondy & Jackson's 1998 conjecture that no uniquely Hamiltonian graphs exist in the class of planar $\cap$ minimum degree 3 graphs, and Fleischner's 2014 conjecture that no uniquely Hamiltonian graphs exist in the class of 4-vertex-connected graphs, we prove that each conjecture is false if and only if there exists a parsimonious reduction from $\#SAT$ to the problem of counting Hamiltonian cycles on each graph class in question. As the existence of a parsimonious reduction from $\#SAT$ allows for the encoding of arbitrary Unambiguous-SAT problem instances, by the Valiant-Vazirani theorem we have that hypothetical sets of counterexamples for each non-existence conjecture cannot belong to any graph class with a polynomial time testable property implying tractability for the Hamiltonian cycle decision problem (unless $NP = RP$).

Discussion. The question as to whether the members of a given graph class can be uniquely Hamiltonian (i.e. possess exactly one Hamiltonian cycle) has been the subject of considerable research in graph theory and related fields over the prior few decades. Interest in this question appears to have originated from a proof of C. A. B. Smith, reported by Tutte in 1946 [8], that the set of Hamiltonian cycles flowing through any given edge of a cubic (i.e. 3-regular) graph must have even cardinality, and therefore, that any Hamiltonian cubic graph must have at least three Hamiltonian cycles. After a bit of an incubation period, in the 1970's Thomason [6] extended the result of Smith to all graphs whose vertices uniformly have odd degree, and Entringer and Swart [2] proved that $\forall(n = 2k;\ k \geq 11)$ there exists a "nearly cubic" uniquely Hamiltonian graph on n vertices with two vertices of degree 4 and with all remaining vertices of degree 3 (see "Theorem 5" of ref. [2]).

In the 1970's, Sheehan also posed his famous conjecture [5] that no uniquely Hamiltonian 4-regular graphs can exist, which, in observation of the fact that every ($r \in 2\mathbb{N}$)-regular graph is the union of edge-disjoint spanning 2-factors, would imply that no r-regular uniquely Hamiltonian graphs exist $\forall(r \in 2\mathbb{N}_{>1})$. While there has been significant progress since this time on a proof of Sheehan's conjecture [4, 7], it remains open. This is likewise true for a related 1998 conjecture of Bondy & Jackson [1] that no uniquely Hamiltonian planar graphs exist having minimum vertex degree 3, and a more recent 2014 conjecture of Fleischner [3] that no 4-vertex-connected uniquely Hamiltonian graphs exist.

In this work, we examine the topological structure of sets of counterexamples, should they exist, to the non-existence conjectures of Sheehan [5], Bondy & Jackson [1], and Fleischner [3]. In Theorem 1 through Theorem 4 we show that each of the aforementioned conjectures is false if and only if there exists a parsimonious reduction from $\#SAT$ to the problem of counting Hamiltonian cycles on each of the relevant graph classes — i.e. ($r \in 2\mathbb{N}_{>1}$)-regular graphs in the case of Sheehan's conjecture [5], planar $\cap$ minimum degree 3 graphs in the case of Bondy & Jackson's conjecture [1], and 4-vertex-connected graphs in the case of Fleischner's conjecture [3]. We next observe that the existence of a parsimonious reduction from $\#SAT$ in each case allows us to efficiently encode arbitrary instances of a variant of satisfiability known as Unambiguous-SAT [9], where we are promised the existence of at most one satisfying assignment to a given Boolean formula. Accordingly, in Theorem 5 we use the Valiant-Vazirani theorem to show that, unless $NP = RP$, no set of counterexamples for any of the listed non-existence conjectures for uniquely Hamiltonian graphs can be contained in a graph class with a polynomial time recognizable or testable property implying an efficient solution for the Hamiltonian cycle decision problem.

References

1. J. A. Bondy and B. Jackson. Vertices of small degree in uniquely Hamiltonian graphs. *J. Combin. Theory Ser. B*, 74(2):265–275, 1998.
2. R. C. Entringer and H. Swart. Spanning cycles of nearly cubic graphs. *J. Combin. Theory Ser. B*, 29(3):303–309, 1980.
3. H. Fleischner. Uniquely Hamiltonian graphs of minimum degree 4. *J. Graph Theory*, 75(2):167–177, 2014.
4. P. Haxell, B. Seamone, and J. Verstraete. Independent dominating sets and hamiltonian cycles. *J. Graph Theory*, 54(3):233–244, 2006.
5. J. Sheehan. The multiplicity of Hamiltonian circuits in a graph. *Recent Advances in Graph Theory (M. Fiedler, Ed.)*, pages 477–480, 1975.
6. A. G. Thomason. Hamiltonian cycles and uniquely edge colourable graphs. *Ann. Discrete Math.*, 3:259–268, 1978.
7. C. Thomassen. Independent dominating sets and a second Hamiltonian cycle in regular graphs. *J. Combin. Theory Ser. B*, 72(1):104–109, 1998.
8. W. T. Tutte. On Hamiltonian circuits. *J. London Math. Soc.*, s1-21(2):98–101, 1946.
9. L. G. Valiant and V. V. Vazirani. NP is as easy as detecting unique solutions. *Theoret. Comput. Sci.*, 47:85–93, 1986.

Gossiping with interference in radio chain networks (upper bound algorithms)

Jean-Claude Bermond
Université Côte d'Azur, CNRS, Inria, I3S, France,
jean-claude.bermond@inria.fr
Takako Kodate
Department of Information and Sciences,
Tokyo Woman's Christian University, Japan,
kodate@lab.twcu.ac.jp
Joseph Yu
Department of Mathematics,
University of the Fraser Valley, B.C., Canada,
joseph.yu@ufv.ca

In this paper, we study the problem of gossiping with interference constraint in radio chain networks. Gossiping (or total exchange information) is a protocol where each node in the network has a message and wants to distribute its own message to every other node in the network. The gossiping problem consists in finding the minimum running time (makespan) of a gossiping protocol and efficient algorithms that attain this makespan.

Transmission model The radio chain network is modeled as a symmetric dipath P_n, where the vertices represent the nodes and the arcs represent the possible communications. A call (s, r) is defined as the transmission from the node s to the node r, in which s is the *sender* and r is the *receiver* and (s, r) is an arc of the dipath. The network is assumed to be synchronous and the time is slotted into *steps*. We suppose that each device is equipped with a half duplex interface, and therefore, a node cannot both receive and transmit during a step.

Interference model Furthermore, communication is subject to interference constraints. We use a binary asymmetric model of interference based on the distance in the communication digraph like the ones used in [1, 2, 5]. Let $d(s, r)$ denote the distance, that is the length of a shortest directed path, from s to r in P_n and d_I be a non-negative integer. We assume that when a node s transmits, all nodes v such that $d(s, v) \leq d_I$ are subject to the interference from the transmission at s. So two calls (s, r) and (s', r') do not interfere if $d(s, r') > d_I$ and $d(s', r) > d_I$. During a given step only non-interfering (or compatible) calls can be done and we will define a round as a set of such compatible calls. We focus here on the case where $d_I = 1$.

Main result Within this model, the problem has been studied in general in [4] where approximation results are given in particular for ring and chain networks (see also the survey [3]). We solved completely the gossiping problem in radio ring networks (work presented at JCDCG[3] 2017), and presented partial results for radio chain networks (work presented at JCDCG[3] 2018).

In this talk, we present new gossiping algorithms for chain networks which meet the lower bounds enabling us to prove the following theorem:

Theorem 1 *The minimum number R of rounds needed to achieve a gossiping in a chain network P_n $(n \geq 3)$, with the interference distance $d_I = 1$ is*

$$R = \begin{cases} 3n-5 & \text{if } n \geq 4 \\ 5 & \text{if } n = 3 \end{cases}$$

References

[1] J.C. Bermond, R. Correa and M.L. Yu.: Optimal gathering protocols on paths under interference constraints, *Discrete Mathematics* 309: 5574–5587, 2009.

[2] J.-C. Bermond, J. Galtier, R. Klasing, N. Morales, and S. Pérennes. Hardness and approximation of gathering in static radio networks. *Parallel Processing Letters*, 16(2): 165–183, 2006.

[3] L. Gąsieniec. On efficient gossiping in radio networks. Proc. Int. Conference on Theoretical Computer ScienceColloquium on structural information and communication complexity, SIROCCO 2009, Lectures Notes in Computer science, springer Verlag, vol 5869: 2–14, 2010.

[4] L. Gąsieniec and I. Potapov. Gossiping with unit messages in known radio networks. Proc. 2nd IFIP Int. Conference on Theoretical Computer Science: 193–205, 2002.

[5] R. Klasing, N. Morales, and S. Pérennes. On the complexity of bandwidth allocation in radio networks. *Theoretical Computer Science*, 406(3): 225–239, 2008.

Analyzing Novem, a Two-Player Multi-Stage Simultaneous Game

François Bonnet
School of Computing
Tokyo Institute of Technology
bonnet@c.titech.ac.jp

Introduction and motivation Novem is an abstract strategic game designed by Gil Druckman and published by Tactic in 2008. It won the "Årets Spel Best Adult Game" award in 2008 [1]. To the best of our knowledge, this game was not yet studied or solved.

While (board) games are usually played sequentially (e.g. Chess, Go, Hex, Poker, ...), Novem consists of simultaneous moves. The most famous simultaneous game is certainly Rock-Paper-Scissor (RPS), in which two (or more) players have to choose one of three hand gestures. RPS is trivially solved and the optimal strategy is the uniform strategy. There exist other simultaneous games that are (1) *interesting*, in the sense that they are played by real (human) players, and (2) *non-trivial*, which makes them worth studying. We know at least three such games that have already been studied; Colonel Blotto, Goofspiel, 10 000yens. The main difference between them and Novem lies in the duration of a game. These three games run for a finite number of rounds; 1, 10, and 13 round(s) respectively.[1] On the contrary, Novem is not a bounded game; ending a game may require an unbounded number of rounds. Note that, in Novem, there is no terminating rule similar to the 50-move rule which exists in Chess.

Rules of Novem The game is played using a 3×3 grid where tiles numbered from 1 to 9 are disposed on two layers (left of Figure 1 for initial board). At each round, the first player (P1) selects a row; A, B, or C, and the second player (P2) selects a column; 1, 2, or 3. Both choices are revealed simultaneously by the players. In the odd (resp. even) rounds, P1 (resp. P2) collects the visible tile located on the cell designed by the combined choices of row-column. If the designed cell is empty, no tile is collected in the round. The game ends as soon as one row or column is completely empty. The winner is the player whose sum of collected tiles is higher. Note that the game may end in a draw if both players collected the same total. Complete rules can be found on the publisher website [2].

We also consider a simplified version played with a single layer of tiles (right side of Figure 1).

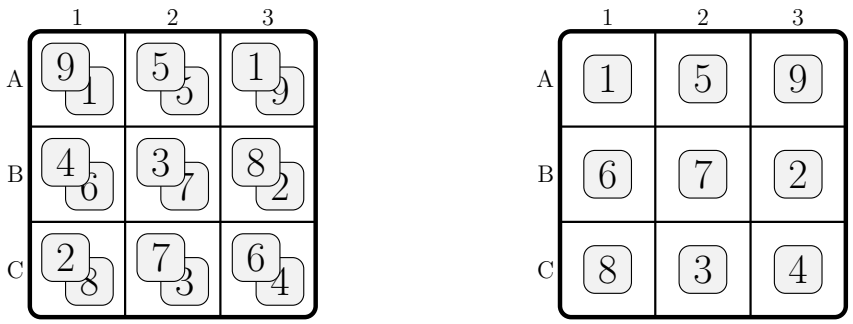

Figure 1: Initial boards of Novem (superimposed tiles are shifted to allow reading of both values)

Contributions Our goal is to *solve* the game. For Novem, it means finding *optimal strategies* and the corresponding *expected outcome*, i.e. computing Nash Equilibrium. We define the outcome as 1 if P1 wins, 0.5 if the game is drawn, and 0 if P2 wins. Our results are summarized below.

[1] Goofspiel and 10 000yens can be generalized, but the number of rounds will always be fixed.

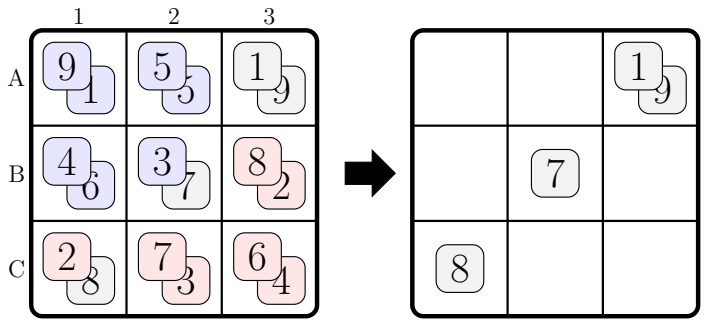

Figure 2: Deadlock configuration. Current score for P1(blue) is 33 and for P2(red) is 32.

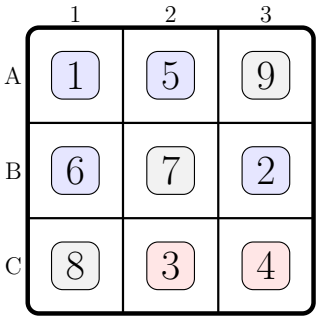

Figure 3: Configuration with irrational optimal strategies. Current score for P1(blue) is 14 and for P2(red) is 7.

1. Design issues We observed that Novem has some design issues which may lead to deadlock configurations.[2] Figure 2 depicts an execution of the game leading to a deadlock. P1(blue) collected 33 points, P2(red) collected 32 points, and there remain only four tiles on the board. To avoid an immediate loss, both players should obviously prevent their opponent to collect the tiles 7 or 8. We can also show that each player should avoid collecting the tile 1 because it would favor their opponent. The intuition is that collecting the tile 1 makes the tile 9 become visible and thus increase the winning chance of next collecting player. Therefore, no player will ever collect a tile in this configuration!

There is no such deadlock in the simplified single-layer variant, hence our decision to study it.

2. Not rationally solvable Optimal strategies cannot be expressed as rational mixing of pure strategies, not even for the single-layer version of the game. Figure 3 represents a configuration with only three tiles remaining on the board. The game ends as soon as any player collects one more tile; P1 wins if she collects any tile, while P2 wins with tiles 8 or 9, but achieves only a draw with tile 7.

Assuming P1 is next to collect, the (irrational) optimal outcome is $\frac{5+\sqrt{5}}{10} \approx 0.72$. The following (irrational) mixed strategies are optimal and unique:

- When P1 is collecting: $\{A{:}\frac{1}{3}, B{:}\frac{1}{3}, C{:}\frac{1}{3}\}$ and $\{1{:}\frac{1}{3}, 2{:}\frac{1}{3}, 3{:}\frac{1}{3}\}$.
- When P2 is collecting: $\{A{:}\frac{3-\sqrt{5}}{4}, B{:}\frac{-1+\sqrt{5}}{2}, C{:}\frac{3-\sqrt{5}}{4}\}$ and $\{1{:}\frac{3-\sqrt{5}}{4}, 2{:}\frac{-1+\sqrt{5}}{2}, 3{:}\frac{3-\sqrt{5}}{4}\}$.

Here, there is no optimal rational mixing. It is not a big problem from a theoretical point of view, but it makes exact computation much harder, that is why we computed only numerical approximations.

3. Numerical computations We computed numerical approximations of optimal strategies and expected outcome. Detailed results will appear in the longer version of the paper. For the single-layer version, when both players play optimally, the expected outcome is ≈ 0.686 which means that P1 is favored (not a surprise). With a komi of 3 ("free points" initially given to the second player), the single-layer game is almost fair; the expected outcome is approximately 0.499. With a komi of -7.5 (i.e. 7.5 points given to P1), P1 has a simple winning strategy. Conversely, to guarantee a win for P2, the game should be played with a komi of 10.5 (or $10 + \epsilon$ for any $\epsilon > 0$).

References

[1] Novem on BoardGameGeek website. `https://boardgamegeek.com/boardgame/38678/novem`. Accessed: 2019-05-24.

[2] Rule of novem. `https://web.archive.org/web/20190524073019/http://www.tactic.net/site/rules/UK/02582.pdf`. Accessed and archived: 2019-05-24.

[2] It does not really disturb real players. The game is still fun to play! But it is a problem when trying to solve the game.

Edge Matching with Inequalities, Triangles, Unknown Shape, and Two Players

Jeffrey Bosboom* Charlotte Chen* Lily Chung* Spencer Compton*
Michael Coulombe* Erik D. Demaine* Martin L. Demaine*
Ivan Tadeu Ferreira Antunes Filho* Dylan Hendrickson* Adam Hesterberg*
Calvin Hsu* William Hu* Oliver Korten† Zhezheng Luo* Lillian Zhang*

In an ***edge-matching puzzle***, we are given several tiles (usually identical in shape), where each tile has a label on each edge, and the goal is to place all the tiles into a given shape such that shared edges between adjacent tiles have compatible labels. In ***unsigned*** edge matching, labels are compatible if they are identical; in ***signed*** edge matching, labels have signs, and two labels are compatible if they are negations of each other. Physical edge-matching puzzles date back to the 1890s; perhaps the most famous example is *Eternity II* which offered a US$2,000,000 prize for a solution before 2011.

Previous work. The complexity of edge-matching puzzles has been studied since 1966. The most relevant work to this paper is from two past JCDCG conferences. In 2007, Demaine and Demaine [DD07] proved that signed and unsigned edge-matching square-tile puzzles are NP-complete and equivalent to both jigsaw puzzles and polyomino packing puzzles. In 2016, Bosboom et al. [BDD+17] proved that signed and unsigned edge-matching square-tile puzzles are NP-complete even when the target shape is a $1 \times n$ rectangle, and furthermore hard to approximate within some constant factor.

Our results. In this paper, we analyze the complexity of several variants of the edge-matching problem by varying the tile shape, target board shape, label compatibility condition, and number of players. Table 1 summarizes our results, which we now describe.

Compatibility	Board	Tiles	Players	Complexity
$<$	$1 \times n$	square	1-player	NP-complete
$\leq$	$m \times n$	square	1-player	P
Signed/unsigned	$1 \times n$	square	1-player	(2-)ASP-hard,* #P-complete
Signed/unsigned	$1 \times n$	equilateral triangle	1-player	NP-complete, #P-complete
Signed/unsigned	$1 \times n$	right triangle (hypotenuse contact)	1-player	NP-complete, #P-complete
Signed/unsigned	$\frac{\sqrt{2}}{2} \times n$	right triangle (leg contact)	1-player	P, #P-complete
Signed/unsigned	$O(1) \times n$	square/triangular with $O(1)$ colors	1-player	P
Signed/unsigned	shapeless	square	1-player	ASP-hard, #P-complete
Signed/unsigned	$1 \times n$	square	impartial 2-player	PSPACE-complete
Signed	$1 \times n$	square	partisan 2-player	PSPACE-complete

Table 1: Our results on edge-matching puzzles. *Our proof gives ASP-hardness for $1 \times n$ edge matching only when at least one boundary edge is colored; otherwise, each solution can be rotated 180 degrees to form another valid solution, so we get 2-ASP-hardness (NP-hard to find a third solution given two).

Inequality edge matching. Our most involved result is an NP-hardness proof for a new "$<$" compatibility condition, where edge labels are numbers, horizontally adjacent edges match if the left edge's number is less than the right edge's number, and vertically adjacent edges match if the top edge's number is less than the bottom edge's number. We prove NP-hardness of $<$-compatible $1 \times n$ edge matching by reduction from another new NP-hard problem, interval-pair cover. The $\leq$-compatibility condition (where equal numbers also match, or we assume all labels are distinct) turns out to be substantially easier: even rectangular puzzles turn out to be always solvable, and we give a polynomial-time algorithm.

*Massachusetts Institute of Technology, Cambridge, MA, USA
†Tufts University, Medford, MA, USA

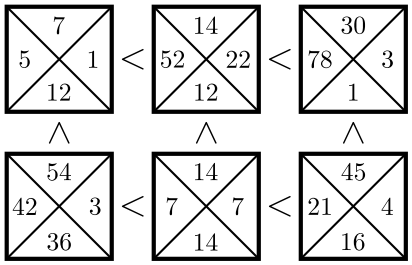

(a) A solution to a 2×3 $<$-compatible edge-matching puzzle.

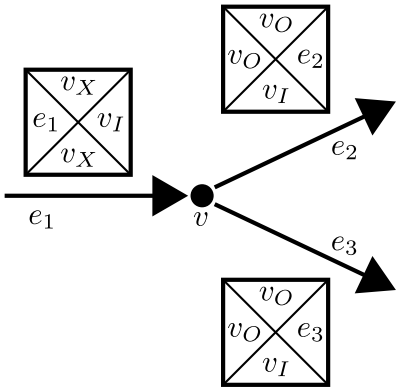

(b) A gadget from the ASP-hardness proof for $1 \times n$ edge matching.

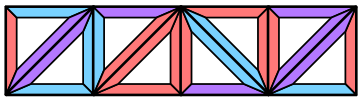

(c) Isosceles triangular edge matching with hypotenuse contact.

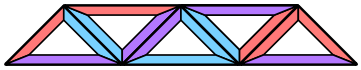

(d) Isosceles triangular edge matching with leg contact.

ASP/#P-completeness for $1 \times n$ edge matching. Of independent interest, we prove ASP-completeness of Hamiltonian path with specified start and end vertices in max-degree-3 *directed* graphs, by modifying the clause gadget from Plesník's NP-hardness proof [Ple79] and parsimoniously reducing from 1-in-3SAT instead of 3SAT. We then use this result to prove ASP-completeness for signed and unsigned $1 \times n$ edge-matching puzzles when the left boundary edge is colored (to prevent trivial rotation of solutions), and 2-ASP-hardness and #P-completeness even if the boundary is colorless.

Triangular edge matching. The conclusion of [BDD+17] claimed that the paper's results extended to equilateral-triangle edge matching, but the proposed simulation of squares by triangles is incorrect because it constrains the orientation of the simulated squares. We extend our $1 \times n$ parsimonious proof to obtain NP-hardness (but not ASP-hardness) for signed and unsigned edge matching with equilateral triangles, with or without reflection.

For right isosceles triangles, there are two natural "$1 \times n$" arrangements. For clarity, we assume the legs of the triangles have length 1. If we still want a height-1 tiling, then length-$\sqrt{2}$ hypotenuses are forced to match, so matching is NP-complete by simulation of squares. But if we ask for a height-$\frac{\sqrt{2}}{2}$ tiling, so only legs match, we show surprisingly that both signed and unsigned edge matching can be solved in polynomial time using an algorithm based on Eulerian paths.

Of independent interest, we characterize when a directed graph admits an Eulerian "path" that alternates between going forward and going backward along edges.

Shapeless edge matching. We prove that square-tile edge-matching puzzles remain NP-, ASP-, and #P-complete when the goal is to connect all tiles in any (unspecified) single connected shape, with either signed or unsigned compatibility. The proof builds a unique spiral frame that effectively forces a $1 \times n$ edge-matching puzzle with a fixed left boundary color.

2-player edge matching. We consider natural 2-player variants of $1 \times n$ edge-matching puzzles, where the players alternate placing a tile in the leftmost empty cell and the first player unable to move loses (normal play). We prove PSPACE-completeness for both signed and unsigned square-tile edge matching when players can play any remaining tile, and for signed edge matching when players play from separate pools of tiles.

References

[BDD+17] Jeffrey Bosboom, Erik D. Demaine, Martin L. Demaine, Adam Hesterberg, Pasin Manurangsi, and Anak Yodpinyanee. Even $1 \times n$ edge-matching and jigsaw puzzles are really hard. *Journal of Information Processing*, 25:682–694, 2017.

[DD07] Erik D. Demaine and Martin L. Demaine. Jigsaw puzzles, edge matching, and polyomino packing: Connections and complexity. *Graphs and Combinatorics*, 23(1):195–208, 2007.

[Ple79] Ján Plesník. The NP-completeness of the Hamiltonian cycle problem in planar diagraphs with degree bound two. *Information Processing Letters*, 8(4):199–201, April 1979.

Is Every Prime Sum Graph Hamiltonian?

Hong-Bin Chen* Hung-Lin Fu† Jun-Yi Guo‡

1 Extended Abstract

This paper is motivated from a result, by Greenfield and Greenfield in 1998 [4], concerning prime numbers.

Theorem 1.1. *[4]*
The set of integers $\{1, 2, 3, \cdots, 2n\}$, $n \geq 1$, *can be partitioned into pairs* $\{a_i, b_i\}$ *such that* $a_i + b_i$ *is prime for all* $i = 1, 2, \cdots, n$.

Theorem 1.1 was proved by L. Greenfield and S. Greenfield in 1998 [4] and reproduced by D. Galvin in 2006 [3]. This lovely result follows with an elegant proof from the well-known Bertrand's Postulate, or sometimes called Bertrand-Chebyshev Theorem [1, 6].

Theorem 1.2. *[1, 6] For any positive integer* $n > 1$, *there is at least a prime* p *such that* $n < p < 2n$.

From another point of view, it is natural to think of a graph that treats numbers as vertices where two vertices are adjacent if the sum of the corresponding numbers is a prime. We first give a formal definition of the mentioned graph. For any positive integer n, define a graph $G_n = (V, E)$ with the vertex set $V = \{1, 2, \cdots, n\}$ and $E = \{ij : i + j \text{ is prime}\}$. We call G_n the *prime sum graph* of order n. Theorem 1.1 can then be rephrased in the terminology of Graph Theory, i.e., G_{2n} has a perfect matching. Inspired by Theorem 1.1, we are interested in the structure of such a graph.

Antonio Filz [2] was the first to notice the prime circle phenomenon and calculate how many prime circles are there for $2n \leq 10$. He posed an interesting question that "are there prime circles for all $2n$?" This conjecture is also collected in the well-known

*presenter. Department of Applied Mathematics, National Chung Hsing University, Taichung 40249, Taiwan (Email: andanchen@gmail.com) The author is supported by MOST 105-2115-M-035-006-MY2 and MOST 107-2115-M-035-003-MY2, and the research is partly done while the author was a member of Department of Applied Mathematics, Feng Chia University, Taichung 40724, Taiwan.

†Department of Applied Mathematics, National Chiao Tung University, Hsinchu 30050, Taiwan (Email: hlfu@math.nctu.edu.tw) Research supported by MOST 106-2115-M-009-008

‡Department of Mathematics, National Taiwan Normal University, Taipei 11677, Taiwan (Email: davidguo@ntnu.edu.tw) Research supported by MOST 106-2115-M-003-007

book 'Unsolved Problems in Number Theory' by Richard K. Guy [5]. However, to the best of our knowledge, it has been attracted little attention and still open for decades. We reformulate it as follows.

Conjecture 1. *[2] The set of integers* $\{1, 2, 3, \cdots, 2n\}$*,* $n \geq 2$*, can be rearranged in a circle such that the sum of any two adjacent numbers is a prime. In other words,* G_{2n} *contains a Hamilton cycle.*

In this paper, we prove the following result.

Theorem 1.3. *There are infinitely many* G_{2n}*'s that have a Hamilton cycle.*

Acknowledgments

The first author would like to thank Professor Miklós Simonovits for valuable suggestions.

References

[1] J. Bertrand, *Mémoire sur le nombre de valeurs que peut prendre une fonction quand on y permute les lettres qu'elle renferme*, Journal de l'École Royale Polytechnique, Cahier 30, Vol. 18 (1845), 123-140.

[2] A. Filz, *Problem 1046*, J. Recreational Math., 14 (1982) 64.

[3] D. Galvin, *Erdős's proof of Bertrand's postulate*, April 2006.

[4] L. Greenfield and S. Greenfield, *Some problems of combinatorial number theory related to Bertrand's postulate*, J. Integer Seq. 1 (1998), Article 98.1.2.

[5] R. K. Guy, *Unsolved Problems in Number Theory*, 3rd ed. New York: Springer-Verlag, pp. 105-106, 2004.

[6] P. Tchebychev. *Mémoire sur les nombres premiers*, Journal de mathématiques pures et appliquées, Sér. 1(1852), 366-390.

The Transformation between Polycubes and the Configurations of SL Blocks

Long-Wei Chou[1], Shen-Guan Shih[2], Chih-Hung Yen[1,*]

[1]Department of Applied Mathematics

National Chiayi University, Taiwan

[2]Department of Architecture

National Taiwan University of Science and Technology, Taiwan

Abstract

Consider a 3-dimensional Euclidean space with a chosen Cartesian coordinate system of three fixed mutually perpendicular directed lines, commonly referred to as the x-axis, the y-axis and the z-axis. Let such a space be divided into unit cubes, that is, the eight corners of a cube have coordinates (x, y, z), $(x+1, y, z)$, $(x, y+1, z)$, $(x+1, y+1, z)$, $(x, y, z+1)$, $(x+1, y, z+1)$, $(x, y+1, z+1)$ and $(x+1, y+1, z+1)$ for some integers x, y and z. A polycube is defined as a finite, nonempty and connected set of unit cubes where connection is established by sharing a square face. Polycubes which just have one layer also can be viewed as polyominoes. Up to now, polycubes have been a source of topological or combinatorial problems.

SL block, proposed first by Shih [4], is an octocube consisting of an S-shaped tetracube and an L-shaped tetracube attaching to each other along sides. An SL block may interlock with other SL blocks to form variations of stable structures, and requires no nail, glue or any other adhesive material. The property of self-interlocking makes SL block expressive to explore the beauty of symmetry, which has been generally acknowledged as an essence of art and mathematics. Various shapes of octocubes have been examined based on the feasibility and flexibility of creating interlocking configurations. SL block is so far the one most interesting and promising.

In this talk, we will have a brief introduction about polycubes and SL blocks first. Then we analyse the connecting and combining ways between multiple SL blocks systematically in order to uncover all compositions of extensible and interlocking structures. Finally, we propose some results by observing an unexpected transformation between polycubes and the configurations of SL blocks.

Keywords: Polycube; SL block; Self-interlocking; Infinite extension.

*Corresponding author. E-mail address: chyen@mail.ncyu.edu.tw

References

[1] Ming-You Chen, F.K. Hwang, Chih-Hung Yen, Tessellating polyominos in the plane, Discrete Mathematics 306(12), 1139-1144, 2006.

[2] Long-Wei Chou, The study on SL-blocks, Master D. Thesis, National Chiayi University, Taiwan, January 2019.

[3] Hsuan-Huai Liu, Tessellating polycubes in the 3-dimensional space, Master D. Thesis, National Chiayi University, Taiwan, January 2015.

[4] Shen-Guan Shih, On the hierarchical construction of SL blocks - A generative system that builds self-interlocking structures, S. Adriaenssens, F. Gramazio, M. Kohler, A. Menges, M. Pauly (eds.): Advances in Architectural Geometry 2016, 124-137, 2016.

[5] Shen-Guan Shih, The art and mathematics of self-interlocking SL blocks, Bridges 2018 Conference Proceedings, 107-114, 2018.

Consistent Digital Curved Rays

Jinhee Chun[1], Kenya Kikuchi [1], and Takeshi Tokuyama[2]
[1]GSIS, Tohoku University
[2]Kwansei-Gakuin University
[1]{jinhee,kikuchi}@dais.is.tohoku.ac.jp
[2]{tokuyama}@kwansei.ac.jp

Representing a family of geometric objects in the digital world where each object is represented by a set of pixels is a basic problem in graphics and computational geometry. One important criterion is the consistency, where the intersection pattern of the objects should be consistent with axioms of the Euclidean geometry, e.g., the intersection of two lines should be a single connected component.

In geometric computation, we often experience that finite-precision computation causes geometric inconsistency. This is because the representation of geometric objects in the pixel world does not always satisfy geometric properties such as Euclidean axioms. Figure 1 shows that a naive definition of digital lines may cause inconsistency that the intersection of a pair of them may have more than one connected components.

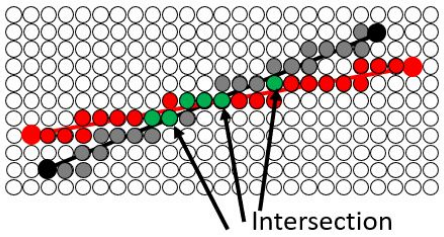

Figure 1: Inconsistency of intersection (green pixels) of two digital line segments

Thus, it is important to seek for a digital represention of a family of geometric objects such that they satisfy a digital version of geometric properties. We propose the *consistent digital curved rays* in this paper, generalising consistent digital rays for straight lines[1, 4].

We consider the triangular region $\triangle$ defined by $\{(x, y) : x \geq 0, y \geq 0, x + y \leq n\}$ in the plane, and the integer grid $G = \{(i, j) : i, j \in \{0, 1, \ldots n\}, i + j \leq n\}$ in the region. We can also handle a square region, but use $\triangle$ for ease of description of our method.

Each element of G is called a pixel (usually, a pixel is a square, but we represent it by its lower-left-corner grid point in this paper). We say a pixel is a boundary pixel if it lies on $x + y = n$. We consider an undirected graph structure under the four-neighbor topology such that $(i, j) \in G$ is connected to $(k, \ell) \in G$ if $(k, \ell) \in \{(i - 1, j), (i, j - 1), (i + 1, j), (i, j + 1)\}$.

A digital ray $S(p)$ is a path in G from the origin o to p, where $S(o) = \{o\}$ is a zero-length path. A family $\{S(p) : p \in G\}$ is called *consistent* if the following three conditions hold:

1. If $q \in S(p)$, then $S(q) \subseteq S(p)$.
2. For each $S(p)$, there is a (not necessarily unique) boundary pixel r such that $S(p) \subseteq S(r)$.
3. Each $S(p)$ is a shortest path from o to p in G.

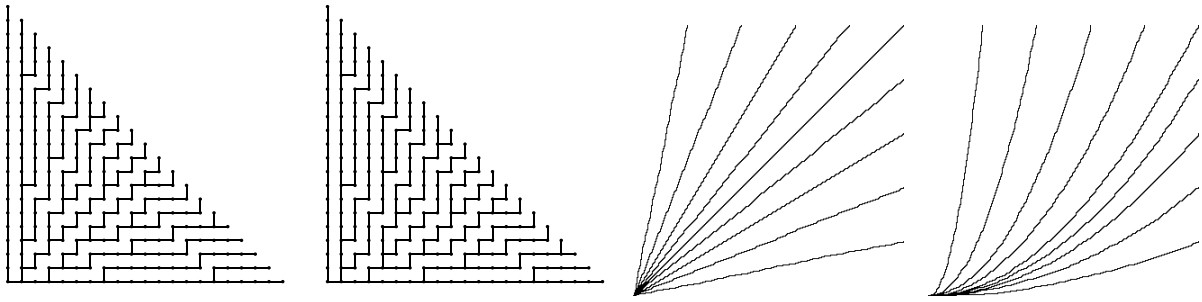

Figure 2: CDR for linear rays and parabolic rays in the triangular region of a 20×20 grid, and sampled linear and parabola digital rays in a 300×300 square grid.

The consistency implies that the union of paths $S(p)$ form a spanning tree T in G such that all leaves are boundary pixels as shown in Figure 2, and accordingly intersection of two digital rays consists of single connected component. The tree T and also the family of digital rays are called CDR (*Consistent Digital Rays*).

Previously, the theory has been considered only for digital straightness[3]. Lubby [4] first gave a construction of CDR so that each $S(p)$ simulates a linear ray within Hausdorff distance $O(\log n)$, and showed that it is asymptotically tight. The construction was re-discovered by Chun *et al.*[1] to give further investigation, and Christ *et al.*[2] gave a construction of consistent digital line segments where the lines need not go through the origin.

We will extend the theory to families of curves with the same topology as linear rays. In Figure 2, the combinatorial difference between tow CDRs can be observed. The difference leads to the visual difference of digital rays in illustrated in the second and fourth picturesin Figure 2, where it can be seen that the digital rays approximate parabolas in the right picture much better than the left one.

A family $\mathcal{F}$ of nondecreasing curves in $\triangle$ is called *ray family* if each curve goes through the origin o, and for each point $(x, y) \in \triangle \setminus \{o\}$ there exists a unique curve of $\mathcal{F}$ going through it. We call a *ray* for an element of $\mathcal{F}$. Accordingly, each pair of rays intersect each other only at the origin. A typical example is the family of parabolas $y = ax^2$ for $a \geq 0$.

We give a construction method of CDR $T_{\mathcal{F}}$ in G such that the (unique) ray of $\mathcal{F}$ connecting o and a pixel p is simulated by the path $S(p)$ well, and show an $O(\sqrt{n \log n})$ bound of the Hausdorff distance for several ray families.

Although the theoretical bound is much worse than the $O(\log n)$ for the linear ray, it is the first nontrivial result for curved rays as far as the authors know, and experimentally the construction works better.

References

[1] J. Chun, M. Korman, M. Nöllenburg, T. Tokuyama, Consistent Digital Rays, *Discrete & Computational Geometry* 42-3 (2009) pp.359-378.

[2] T. Christ, D. Pálvölgyi, M. Stojaković, Consistent Digital Line Segment, *Discrete & Computational Geometry* 47-4 (2012), pp.691-710.

[3] R. Klette, A. Rosenfeld, Digital straightness – a review *Discrete Applied Math.* 139 (2004), pp.197-230.

[4] M.G.Lubby, Grid geometries which preserve properties of euclidean geometry: A study of graphics line drawing algorithms. In NATO Conference on Graphics/CAD (1987), pp.397-432.

Forbidden triples on a finite set of 4-connected graphs

Edilberto C. Cuaresma Jr.[1,2,4,*], Reginaldo M. Marcelo[1], Agnes D. Garciano[1],

Yoshimi Egawa[3], Keiko Kotani[3], Shunsuke Nakamura[3]

[1]*Ateneo de Manila University, Quezon City, Philippines*

[2]*Caraga State University, Butuan City, Philippines*

[3]*Tokyo University of Science, Shinjuku-ku, Japan*

[4]*cuaresma810@gmail.com*

Keywords: forbidden subgraph; forbidden triple; 4-connected graph

1 Introduction

In this paper, we consider only finite undirected simple graphs.

Let G be a graph and $\mathcal{F}$ be a set of connected graphs, G is said to be *$\mathcal{F}$-free* if G does not contain any member of $\mathcal{F}$ as an induced subgraph. We let $\mathcal{G}$ denote the set of all connected graphs with order greater than or equal to 3 and for $k \geq 2$, let $\mathcal{G}_k(\mathcal{F})$ denote the set of all k-connected $\mathcal{F}$-free graphs. The members of $\mathcal{F}$ are referred to as the forbidden subgraphs. We let $\Delta(G)$ denote the maximum degree of G.

Fugisawa et.al. [2] completely determined the sets $\mathcal{F}$ with $|\mathcal{F}| = 3$ for which $\mathcal{G}_2(\mathcal{F})$ is finite. In [3], some sets $\mathcal{F}$ of forbidden triples have been identified for which $\mathcal{G}_3(\mathcal{F})$ is finite. In this study, we determine forbidden triples $\mathcal{F}$ that do not contain a star where $\mathcal{G}_4(\mathcal{F})$ is finite.

The following corollary is found in [3] .

Corollary 1.1. *Let $\mathcal{F} \subseteq \mathcal{G}$ with $|\mathcal{F}| = 3$, and suppose that $\mathcal{F}$ does not contain a star and $\mathcal{G}_4(\mathcal{F})$ is finite. Then there exists integers n, m_1, m_2 with $(n, m_1) \in \{(3,4),(3,3),(5,2),(4,2),(3,2)\}$ and $m_1 \leq m_2$ such that $\mathcal{F} = \{K_n, K_{m_1,m_2}, T\}$, where T is a tree with $\Delta(T) \leq 4$.*

In this study, we aim to give a refinement of the above Corollary by describing T more particularly.
Our notation is standard, and is mostly taken from Diestel [2]. Possible exceptions are as follows.
We let P_l denote the path of order l. A *caterpillar* is a tree for which the removal of all endvertices leaves a path. The complete bipartite graph with partite sets of cardinalities m and n is denoted by $K_{m,n}$. In particular, the $K_{1,t}$ with $t \geq 1$ is called a *star*.

Let n be an integer with $n \geq 2$. Let $P = x_1x_2\cdots x_n$ be a path of order n, and let y_1, y_2, y_3, z_1, z_2 and z_3 be six distinct vertices different from $x_1x_2\cdots x_n$. Let Y_m and Y_m^* denote the graphs defined by $V(Y_m) = V(P) \cup \{y_1, y_2\}$, $V(Y_m^*) = V(P) \cup \{y_1, y_2, z_1, z_2\}$, $E(Y_m) = E(P) \cup \{x_1y_1,\ x_1y_2\}$ and $E(Y_m^*) = E(P) \cup \{x_1y_1,\ x_1y_2,\ x_nz_1,\ x_nz_2\}$. Let X_n and X_n^* denote the graphs defined by $V(X_n) = V(P) \cup \{y_1, y_2, y_3\}$, $V(X_n^*) = V(P) \cup \{y_1, y_2, y_3, z_1, z_2, z_3\}$, $E(X_n) = E(P) \cup \{x_1y_1, x_1y_2, x_1y_3\}$ and $E(X_n^*) = E(P) \cup \{x_1y_1, x_1y_2, x_1y_3, x_nz_1, x_nz_2, x_nz_3\}$. Let Z_n^* denote the graph defined by $V(Z_n^*) = V(P) \cup \{y_1, y_2, y_3, z_1, z_2\}$ and $E(Z_n^*) = E(P) \cup \{x_1y_1, x_1y_2, x_1y_3, x_nz_1, x_nz_2\}$ (see Figure 1).

Let $\mathcal{T}_0$ be the set of trees in $\mathcal{G} \setminus \{K_{1,2}, K_{1,3}, K_{1,4}\}$ having maximum degree at most 4. Let $\mathcal{T}_1$ be the set of those caterpillars belonging to $\mathcal{T}_0$ in which no two vertices of degree 4 are adjacent. Let

$$\mathcal{T}_2 = \left\{P_s, X_{m_1}, X_{m_2}^*, Y_{n_1}, Y_{n_2}^*, Z_t^* \middle|\ s \geq 4,\ m_1, m_2, n_1, t \geq 3,\ n_2 \geq 2\right\}.$$

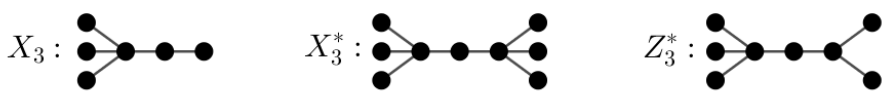

Figure 1: The following graphs are examples of X_{m_1}, $X_{m_2}^*$ and Z_t^*

2 Results

The following Theorem is our main result.

Theorem 2.1. *Let $\mathcal{F} \subseteq \mathcal{G}$ with $|\mathcal{F}| = 3$, and suppose that $\mathcal{F}$ does not contain a star and $\mathcal{G}_4(\mathcal{F})$ is finite. Then one of the following holds:*

(i) $\mathcal{F} = \{K_3, K_{m_1,m_2}, T\}$ *with* $3 \leq m_1 \leq 4$, *where* $T \in \mathcal{T}_2$;

(ii) $\mathcal{F} = \{K_{m_1}, K_{2,m_2}, T\}$ *with* $4 \leq m_1 \leq 5$ *and* $m_2 \geq 2$, *where* T *is a path or;*

(iii) $\mathcal{F} = \{K_3, K_{2,m}, T\}$ *with* $m \geq 2$, *where* $T \in \mathcal{T}_0$ *in the case where* $m = 2$, $T \in \mathcal{T}_1$ *in the case where* $3 \leq m \leq 4$ *and* $T \in \mathcal{T}_2$ *in the case where* $m \geq 5$.

In order to prove Theorem 2.1, we prove the following two lemmas.

Lemma 2.2. *Let m_1 and m_2 be integers such that $m_2 \geq m_1 \geq 2$, $m_1 \leq 4$ and $(m_1, m_2) \neq (2, 2)$. Let T be a tree with $\Delta(T) \leq 4$, and suppose that $\{K_3, K_{m_1,m_2}, T\}$ does not contain a star and $\mathcal{G}_4(\{K_3, K_{m_1,m_2}, T\})$ is finite. Then the following hold.*

(i) $T \in \mathcal{T}_1$.

(ii) *If in addition, $(m_1, m_2) \notin \{(2, 3), (2, 4)\}$, then $T \in \mathcal{T}_2$.*

Lemma 2.3. *Let m_1 and m_2 be integers such that $4 \leq m_1 \leq 5$ and $m_2 \geq 2$. Let T be a tree with $\Delta(T) \leq 4$, and suppose that $\{K_{m_1}, K_{2,m_2}, T\}$ does not contain a star and $\mathcal{G}_4(\{K_{m_1}, K_{2,m_2}, T\})$ is finite. Then T is a path.*

References

[1] Y. Egawa, J. Fujisawa, M. Furuya, M. D. Plummer and A. Saito, Forbidden triples generating a finite set of 3-connected graphs, Electron. J. Combin. 22(3) (2015), Article no. 013.

[2] R. Diestel, "Graph Theory" (5th edition), Graduate Texts in Mathematics 173, Springer(2017).

[3] J. Fujisawa, M.D. Plummer and A. Saito. Forbidden subgraphs generating a finite set, Discrete Math. 313 (2013) 1835–1842.

[4] Z. Zhao, Forbidden triples generating a finite set of graphs with high connectivity, Far East J. Appl. Math. Vol. 99 (2018) 225–233.

Perfect rainbow polygons for colored point sets in the plane

David Flores-Peñaloza[*1], Mikio Kano[†2], Leonardo Martínez-Sandoval[‡3], David Orden[§4], Javier Tejel[¶5], Csaba D. Tóth[‖6], Jorge Urrutia[**7], and Birgit Vogtenhuber[††8]

[1]Departamento de Matemáticas, Facultad de Ciencias, Universidad Nacional Autónoma de México, Mexico.
[2] Ibaraki University, Hitachi, Ibaraki, Japan.
[3] Sorbonne Université, Institut de Mathématiques de Jussieu - Paris Rive Gauche (UMR 7586), Paris, France.
[4]Departamento de Física y Matemáticas, Universidad de Alcalá, Alcalá de Henares, Spain.
[5]Departamento de Métodos Estadísticos, IUMA, Universidad de Zaragoza, Zaragoza, Spain.
[6]Department of Mathematics, California State University Northridge, Los Angeles, CA, USA.
[7]Instituto de Matemáticas, Universidad Nacional Autónoma de México, Mexico.
[8]Institute of Software Technology, Graz University of Technology, Graz, Austria.

The study of colored point sets has attracted a lot of attention, particularly for 2-, 3-, and 4-colored point sets, see [1], [2], and [3]. For every $1 \leq i \leq n$, let S_i be the set of elements of S colored with color c_i. We will assume that each S_i is non-empty and that $S = S_1 \dot{\cup} \cdots \dot{\cup} S_n$ is in general position in the plane.

Given an n-colored point set S, a simple polygon P is called a *perfect rainbow* polygon if it contains exactly one point of each color. We are interested in finding

[*]Email: dflorespenaloza@ciencias.unam.mx
[†]Email: mikio.kano.math@vc.ibaraki.ac.jp
[‡]Email: leomtz@im.unam.mx
[§]Email: david.orden@uah.es
[¶]Email: jtejel@unizar.es
[‖]Email: csaba.toth@csun.edu
[**]Email: urrutia@matem.unam.mx
[††]Email: bvogt@ist.tugraz.at

This work has received funding from the European Union's Horizon 2020 research and innovation programme under the Marie Skłodowska-Curie grant agreement No 734922.

the smallest number r_n, called *rainbow index*, such that any n-colored point set has a perfect rainbow polygon with at most r_n vertices.

It is well known that for every 3-colored point set S, there exists an empty triangle such that its vertices are in S and have different colors, that is, $r_3 = 3$. In this work, we determine the exact values of r_n up to the first case where $r_n > n$, see Table 1.

n	3	4	5	6	7
r_n	3	4	5	6	8

Table 1: Values of the rainbow index r_n up to the first case with $r_n > n$.

Moreover, for general n, we show the following lower and upper bounds on r_n:

$$\frac{20n - 28}{19} \leq r_n \leq \frac{10n}{7} + 11.$$

Acknowledgements

Research of David Flores-Peñaloza was supported by the grant UNAM PAPIIT IN117317. Research of Mikio Kano was supported by JSPS KAKENHI Grant Number 16K05248. Research of Leonardo Martínez-Sandoval was supported by the grant ANR-17-CE40-0018 of the French National Research Agency ANR (project CAPPS). Research of David Orden was supported by project MTM2017-83750-P of the Spanish Ministry of Science (AEI/FEDER, UE). Research of Javier Tejel was supported by MINECO project MTM2015-63791-R and Gobierno de Aragón under Grant E41-17R (FEDER). Research of Csaba D. Tóth was supported by NSF awards CCF-1422311, CCF-1423615, and DMS-1800734. Research of Jorge Urrutia was supported by UNAM project PAPIIT-IN102117. Research of Birgit Vogtenhuber was supported by the Austrian Science Fund within the collaborative DACH project *Arrangements and Drawings* as FWF project I 3340-N35.

References

[1] S. Bereg, F. Hurtado, M. Kano, M. Korman, D. Lara, C. Seara, R. Silveira, J. Urrutia, and K. Verbeek, Balanced partitions of 3-colored geometric sets in the plane *Discrete Applied Math.*, **181** (2015) 21–32

[2] S. Bereg, M. Kano, Balanced line for a 3-colored point set in the plane, *Electron. J. Combin.*, **19** (2012) 33.

[3] M. Kano and J. Kynčl, The hamburger theorem, *Computational Geometry: Theory and Applications*, **68** (2018) 167–173.

Optimal proper connection of graphs (Extended abstract)

Shinya Fujita
School of Data Science, Yokohama City University,
22-2 Seto, Kanazawa-ku, Yokohama 236-0027, Japan,
Email: shinya.fujita.ph.d@gmail.com

1 Introduction

All graphs considered in this paper are finite and simple. Our notation in this paper is standard. For a graph $G = (V(G), E(G))$, let $\alpha(G)$ be the independence number of G. Also, let $\alpha'(G)$ be the size of a maximum matching of G. Let $\kappa(G)$ be the vertex-connectivity of G. For other terminology and notation not defined here, we refer the reader to [12]

An edge-colored graph G is *properly colored* if no two adjacent edges share a color in G. Properly colored paths and cycles appear in a variety of fields such as genetics [4, 5] and social sciences [3]. An edge-colored connected graph G is *properly connected* if between every pair of distinct vertices, there exists a path that is properly colored. In [1], Borozan et al. defined a new notion called the *proper connection number* $pc(G)$ of a connected graph G, where $pc(G)$ is the minimum number of colors needed to color the edges of G to make it properly connected.

Recently, the notion of proper connection number attracts much attention from both theoretical and practical aspects, and thus a lot of work has been done extensively (see e.g., [2, 7, 8, 9, 11]). For details in this recent topic, we refer the reader to the nice survey of Li and Magnant [10].

In this paper, we are concerned with making an edge-colored graph properly connected efficiently. Let (G, c) be a connected graph with a given edge-coloring c. Now we consider how to make (G, c) properly connected by recoloring some edges with some colors. To minimize our effort to make G properly connected, it would be natural to focus on the minimum value on the sum of numbers of edges and colors among such recolorings. Note that, such a value should be zero when (G, c) is already properly connected.

Perhaps the most fundamental and laborious case to this problem would be the case where c assigns a common color on every edge of G, that is, the case where G is a monochromatic colored graph. Therefore, in this paper, we shall initiate this study by assuming that all edges of G have already been colored by a common color, say color 0. When $i \neq 0$, color i is called a *new color*.

Keeping this assumption in mind, we define the following cost function of edge-colored graphs called the *optimal proper connection number* for a monochromatic connected graph G.

$pc_{opt}(G) := \min\{p + q |$ we can make G properly connected
by recoloring p edges of G with q new colors$\}$.

For a monochromatic connected graph G, suppose that G becomes properly connected by recoloring p edges of G with q new colors such that $p + q = pc_{opt}(G)$. Then we call such an edge-coloring of G an *optimal recoloring of* G.

By definition, note that $pc_{opt}(K_n) = 0$ holds because any monochromatic complete graph is properly connected. Indeed, we see that a graph G satisfies $pc_{opt}(G) = 0$ if and only if G is

isomorphic to a complete graph. We can easily determine $pc_{opt}(G)$ for small graphs and some basic family of graphs. For example, we can check that $pc_{opt}(K_{2,3}) = pc_{opt}(K_{3,3}) = 3, pc_{opt}(K_{3,4}) = pc_{opt}(K_{4,4}) = 4$, $pc_{opt}(K_{1,m}) = 2m - 2$, $pc_{opt}(C_n) = pc_{opt}(P_n) = \lfloor (n-1)/2 \rfloor + 1$.

2 Main results

Our main results are following.

Theorem 1. *If G is a monochromatic connected graph of order $n \geq 1$ such that $\alpha(G) \leq 2$ then $pc_{opt}(G) \leq 3$.*

Theorem 2. *Let G be a monochromatic complete bipartite graph $K_{m,n}$ such that $m \geq n \geq 2$ and $m + n \geq 9$. Then $pc_{opt}(G) = 4$ for $n = 2, 3$, and $pc_{opt}(G) = 5$ for $n \geq 4$.*

Theorem 3. *If T is a monochromatic tree of order $n \geq 2$ then $pc_{opt}(T) = n - 2 - \alpha'(T) + \Delta(T)$.*

Please see the full paper [6] for the proofs of our main results.

References

[1] Borozan, V., Fujita, S., Gerek, A., Magnant, C., Manoussakis, Y., Montero, L., and Tuza, Z.. *Proper connection of graphs,* Discrete Math., **312** (2012), 2550–2560.

[2] Brause, C., Doan, T. D., Schiermeyer, I., *Minimum degree conditions for the proper connection number of graphs,* Gaphs and Combin., **33** (2017), 833–843.

[3] Chou, W. S., Manoussakis, Y., Megalakaki, O., Spyratos, M., and Tuza, Z., *Paths through fixed vertices in edge-colored graphs,* Math. Inform. Sci. Humaines, **127** (1994), 49–58.

[4] Dorninger, D., *Hamiltonian circuits determining the order of chromosomes,* Discrete Appl. Math., **50** (1994) 159–168.

[5] Dorninger, D., and Timischl, W., *Geometrical constraints on Bennet's predictions of chromosome order,* Heredity, **58** (1987), 321–325.

[6] Fujita, S., *Optimal proper connection of graphs,* ArXiv:1903.03311 (2019).

[7] Fujita, S., Gerek, A., and Magnant, C., *Proper connection with many colors,* J. Comb., **3** (2012), 683–693.

[8] Gu, R., Li, X., and Qin, Z., *Proper connection number of random graphs* Theoretical Computer Science, **609** (2016), 336–343.

[9] Huang, F., Li, X., and Wang, S., *Upper bounds of proper connection number of graphs,* J. Comb. Optim., **34** (2017), 165–173.

[10] Li, X., and Magnant, C., *Properly colored notions of connectivity - a dynamic survey* Theory and Applications of Graphs, **0**, Article 2.

[11] Li, X., Wei, M., and Yue, J., *Proper connection number and connected dominating sets,* Theoretical Computer Science, **607** (2015) 480–487.

[12] West, D. B., *Introduction to Graph Theory*, 2nd edition, Prentice Hall, (2001).

Connection of Two Bread Graphs

[1] Jumpei Gohara , [1] Akifumi Sako

[1] Graduate School of Science,
Tokyo University of Science, 1-3 Kagurazaka, Shinjuku-ku, Tokyo 162-8601, Japan

We show that any two bread graphs are connected by inserting a path graph of order three.

For an operator called Dirac operator in [1], Sykora studies the correspondence between Graph theory and Effective membrane theory by using deformation adjacency matrices. The lowest energy states of the Dirac operator with respect to a graph embedded in $\mathbb{R}^3$ give algebraic equations. He numerically suggests that the algebraic surface created by the equation has a form that plumped out the embedded graph.

To pursue his idea to clarify the relationship between the embedded graphs and algebraic surfaces, we introduced the following definition at the previous JCDCG^3 conference[3]. Below, all graphs $G = (V, E, W)$ represent weighted simple undirected graphs.

Definition 1 (z-axial embedding[3])**.** Let $G = (V, E, W)$ be a graph, where $V = \{v'_1, \ldots, v'_n\}$. For a vertex set V, fix $v_1 := v'_k$ and rewrite vertex indexes in order of distance of the graph $d_G(v_1, \cdot)$ from v_1 as follows. Let s_k be an element of the symmetric group S_n

$$s_k : \{v'_1, \ldots, v'_n\} \to \{v_1, \ldots, v_n\}, \quad v'_i \mapsto s_k(v'_i)$$

and the index of v_i is determined to satisfy

$$\begin{cases} i < j & if\ d_G(v_1, v_i) < d_G(v_1, v_j) \\ i < j & if\ d_G(v_1, v_i) = d_G(v_1, v_j),\ s_k(v'_l, v'_m) = (v_i, v_j),\ l < m. \end{cases}$$

The z-axial embedding $\iota : V \to \mathbb{R}^3,\ v_i \mapsto (x_i, y_i, z_i)$, for $v_i, v_j \in V$ is defined to satisfy the following two conditions: (i) if $i < j$ and $d_G(v_1, v_j) \neq d_G(v_1, v_j)$, then $z_i < z_j$. (ii) if $i < j$ and $d_G(v_1, v_j) = d_G(v_1, v_j)$, then $z_i \leq z_j$. Here, if $z_i = z_j$, then let v_i and v_j be not adjacent. Each $e_{ij} \in E$ connecting v_i and v_j is embedded as a segment $\iota(v_i)\iota(v_j)$.

Definition 2 (Deformation adjacency matrices[1])**.** For a z-axial embedding of $G = (V, E, W)$, deformation adjacency matrices $X = (X_{ij}),\ Y = (Y_{ij}),\ Z = (Z_{ij})$ of size $|G| \times |G|$ are defined as follows.

1. The diagonal entries of the matrices are

$$X_{kk} = x_k,\ Y_{kk} = y_k,\ Z_{kk} = z_k, \quad (1 \leq k \leq |G|).$$

   Here $\iota(v_k) = (x_k, y_k, z_k)$, for $v_k \in V$.

2. The off-diagonal entries of the matrices are

$$X_{jk} = X_{kj} = w_{jk} \in \mathbb{R},$$
$$Y_{jk} = -iw_{jk} = \overline{Y_{kj}}, \quad (1 \leq j, k \leq |G|,\ j \neq k)$$

where w_{jk} is the weight of edge e_{jk} connecting v_j and v_k, $\overline{Y}$ is the complex conjugate of Y and the coefficient i is an imaginary unit.

3. The other entries of the matrices are 0.

From this definition, the matrices X, Y and Z are Hermitian matrices.

Definition 3 (Dirac operator [2])**.** Let X, Y, Z be the deformation adjacency matrices of G and $(x, y, z) \in \mathbb{R}^3$ be the coordinates of the space to embed vertices. Dirac operator is defined as

$$D := \gamma^1 \otimes (X - xE) + \gamma^2 \otimes (Y - yE) + \gamma^3 \otimes (Z - zE),$$

where γ^i is Pauli matrix and E is the unit matrix.

Definition 4. (Bread graph)
For $G = (V, E, W)$, z-axial embedding ι and Dirac operator D, we define a bread graph $B(G, \iota, D)$ as

$$B(G, \iota, D) := \{(x, y, z) \in \mathbb{R}^3 \mid \det D = 0\}.$$

We discussed conditions that a bread graph and an embedded path graph are homotopic. Especially, the case that the path graph has two vertices was discussed in detail[3].

This time, we develop these discussions as follows.

Definition 5. Let G_1 and G_2 be any graphs that are not connected to each other and P_n be a path graph of order n. We defined $G(G_1, G_2)$ as a connected graph made by sharing the endpoints of P_3 by G_1 and G_2 respectively.

For the path graph P_3, we denote vertices shared in G_1 and G_2 by v_{G_1} and v_{G_2} respectively, and a vertex of degree 2 by v_2.

Theorem 0.1. *For arbitrary $G(G_1, G_2)$, if $\iota(v_{G_1}) = (0, 0, -a)$, $\iota(0, 0, a)$ for $a > 0$ and $a \leq 4r$ then $B(G(G_1, G_2), \iota, D)$ is connected, where $r = w_{2G_1} = w_{2G_2}$ is weight of edges e_{2G_1} and e_{2G_2}.*

This theorem means that a bread graph can be expanded by other graphs like a handlebody. A new bread graph with higher genus can be made by connecting several bread graphs with lower genus.

References

[1] A. Sykora. (2017). The fuzzy space construction kit. [arXiv:1610.01504 [hep-th]].

[2] Berenstein, D., Dzienkowski, E.: Matrix embeddings on flat R^3 and the geometry of membranes, Phys. Rev. D **86**, 086001 (2012).

[3] J. Gohara., K. Hasebe. and A. Sako. (2018). The Bread Graph. JCDCG^3 2018.

A New Lower Bound for Minimal-Area Convex Cover for Closed Unit Arcs

B. Grechuk[1], S. Som-am[2]

[1] *University of Leicester, UK, bg83@le.ac.uk*
[2] *University of Leicester, UK, ssa41@le.ac.uk*

1 Introduction

In 1966, Leo Moser [2] posted a famous unsolved problem in geometry which asks for the smallest area of the region in the plane, which, is possibly rotated and translated, can cover all curves of unit length. A version of this problem asks for the smallest area β of *convex* region which can cover all *closed* curves of unit length. The best known upper and lower bounds for this problem were $\beta \leq 0.11023$ [3] and $\beta \geq 0.0975$ [1].

In this work, we use geometric methods combined with the Box search algorithm to prove that the area of convex cover for the line segment of length 0.5, circle of perimeter 1, and rectangle of size 0.1727×0.3273 is at least 0.1, which implies a new lower bound $\beta \geq 0.1$.

2 Geometric Analysis

Let C be a circle of perimeter 1, R be a rectangle of size 0.1727×0.3273, and L be a line segment of length 0.5. We fix the center of circle to be $C_0(0,0)$. Let F be a regular 500-gon inscribed in C, such that the sides of R are parallel to one of the longest diagonals of F. Let X be a union $F \cup R \cup L$. X is called a *configuration*. Let $\mathscr{H}(X)$ be the convex hull of X, and $\mathscr{A}(X)$ the area of $\mathscr{H}(X)$. Let $f : \mathbb{R}^5 \to \mathbb{R}$ be a function by mapping vector $(x_1, y_1, x_2, y_2, \theta)$ to $\mathscr{A}(X)$, where $R_0(x_1, y_1), L_0(x_2, y_2)$ are the centers of R and L respectively, and θ is the angle between X axis and L_0L_2, where L_2 is a vertex of L.

Lemma 1. *Let Z be the region of points $z = (x_1, y_1, x_2, y_2, \theta)$ in $\mathbb{R}^5$ satisfying the inequalities*

$$0 \leq x_1 \leq 0.0741,\ 0 \leq y_1 \leq 0.0976,\ -0.148 \leq x_2 \leq 0.148,\ -0.148 \leq y_2 \leq 0.148,\ 0 \leq \theta \leq \pi.$$

If $f(z) > 0.1$ for all $z \in Z$, then in fact $f(z) > 0.1$ for all $z \in \mathbb{R}^5$.

Lemma 2. *For every $(x_1, y_1, x_2, y_2, \theta) \in Z$, and any $\varepsilon_i \geq 0$, $i = 1, \ldots, 5$,*

$$|f(x_1 + \varepsilon_1, y_1 + \varepsilon_2, x_2 + \varepsilon_3, y_2 + \varepsilon_4, \theta + \varepsilon_5) - f(x_1, y_1, x_2, y_2, \theta)| \leq \sum_{i=1}^{5} \varepsilon_i C_i,$$

with constants $C_1 = 0.306$, $C_2 = 0.443$, $C_3 = 0.392$, $C_4 = 0.449$, and $C_5 = 0.115$.

3 Computational results

We run the Box-search algorithm [1] by using Matlab® R2016a. The programme halts after $n = 527,754,566$ iterations. This rigorously proves that the minimal area is greater than 0.1. Numerically, the program returned value 0.10044 for this minimal area, with optimal configuration $x_1 = 0.00434$, $y_1 = 0.00648$, $x_2 = 0.00434$, $y_2 = -0.00434$, $\theta = 0.85711$

Theorem 1. *The area of convex cover S for circle of perimeter* 1*, line of length* $1/2$*, and rectangle of size* 0.1727×0.3273 *is at least* 0.1.

Corollary 3. *Any convex cover for closed unit curves has area of at least* 0.1.

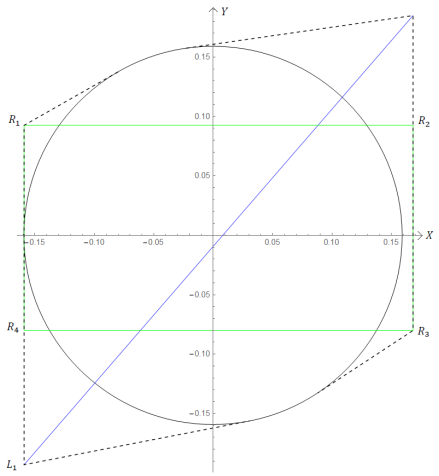

Figure 1: The convex hull of the configuration of the minimum area with 0.10044

References

[1] B. Grechuk and S. Som-am. “A convex cover for closed unit curves has area at least 0.0975”. In: *arXiv preprint math/1905.00333* (2019).

[2] L. Moser. “Poorly formulated unsolved problems of combinatorial geometry”. In: *Mimeographed list* (1966).

[3] W. Wichiramala. “A smaller cover for closed unit curves”. In: *Miskolc Mathematical Notes* 19.1 (2018), pp. 691–698.

One-question-card Version of the Hamming Code Mathemagic

Junyi Guo, Chao Yang, Hsiang-Chun Hsu

In the classic version of this magic trick, the magician asks one spectator thinking of an integer between 0 and 15 and keeping it in his mind. Then the spectator is allowed to ask four yes-or-no questions that whether the chosen number appears on the following four cards.

1	3	5	7
9	11	13	15

2	3	6	7
10	11	14	15

4	5	6	7
12	13	14	15

8	9	10	11
12	13	14	15

After that, the magician will immediately know what is the number in spectator's mind. The secret mainly depends on the encoding of these four cards. Actually, it's well-known, whether the numbers are on the i-th card is according to the i-th digit of the binary number is 1 or not. Theoretically, this trick can be extended to any n numbers with $O(\log n)$ question cards.

Richard Ehrenborg [1] and Todd Mateer [2] modified this trick to the version that the spectator is allowed to lie at most once by asking 3 more questions. After 7 yes-or-no questions, the magician reported both the number the spectator chosen and the card the spectator lied. These question cards are encoded by Hamming code. The former 4 question cards are correspondent to the 4 information bits of [7,4,3]-code, and the new 3 cards are the 3 parity-check bits.

1	2	5	6
8	11	12	15

1	3	4	6
8	10	13	15

2	3	4	5
8	9	14	15

In general, for any positive integer n, the magician also needs $O(\log n)$ question cards. In this talk, we reduce the number of question cards to $O(1)$. Actually, we need only 1 base card and 1 question card.

The main idea is de Bruijn sequence. There are $2^{2^{k-1}-k}$ different de Bruijn sequences of order k. For $k = 4$, we choose any one of the de Bruijn sequences as follows:

0000111101100101.

Its decimal sequence is: 0, 1, 3, 7, 15, 14, 13, 11, 6, 12, 9, 2, 5, 10, 4, 8. Then we put them in a circle as our base card. Besides, we just need the other circle question card with 8 holes corresponding to the odd numbers. By the property of de Bruijn sequences, we show these two cards are enough to perform the same classic magic trick by rotating the question card and putting the red hole on the top of the numbers 1, 2, 4, 9.

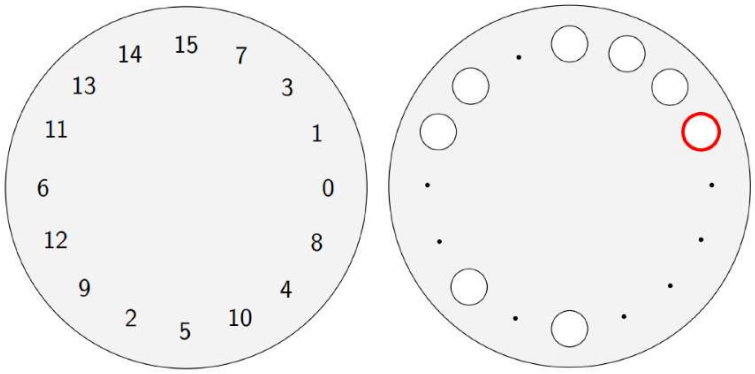

In 1-error-correcting version, this idea also works but a little differently. We remove the number 0, and to select another de Bruijn sequence carefully. This time we choose

0100110101111000.

And the base card and the question card are as follows. Then we can perform the 1-error-correcting magic trick by putting the red hole on the top of the numbers 1, 2, 4, 9, 6, 15, 5 which correspond to the 7 question cards as the former.

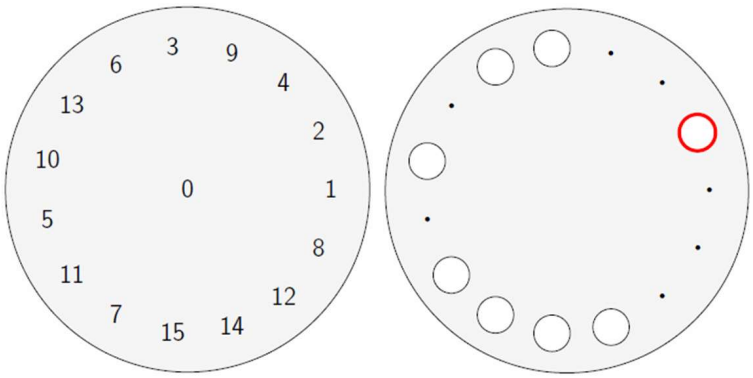

For any 2^k numbers 1-error-correcting magic trick, we prove that there exists a de Bruijn sequence of order k which can be used for the 1-question-card design.

References

1. Richard Ehrenborg, Decoding the Hamming Code, Math Horizons, 13(4) 2006 17-18. doi:10.1080/10724117.2006.11974646.
2. Todd Mateer, A Magic Trick Based on the Hamming Code, Math Horizons, 21(2) 2013 9-11. doi: 10.4169/mathhorizons.21.2.9.

Hyperfiniteness of hierarchical models for complex networks (Extended Abstract)

ITO Hiro*† HIGASHIZONO Kazuki*†
*School of Informatics and Engineering,
The University of Electro-Communications (UEC); Tokyo, Japan.
†CREST, JST; Tokyo, Japan.
*{itohiro@, h1831126@edu.cc.}uec.ac.jp

1 Introduction

Large networks such as the WWW and the protein-protein interaction network (PIN) are called complex networks. Some common properties have been found among complex networks. Many models that produce networks having such properties have been proposed, e.g., Watts-Strogatz model achieves the small-world property[8], and Barabasi-Albert model achieves the scale-free property[1]. However, the properties of complex networks are not revealed completely yet, and hence many new models that sutisfy such properties are still being proposed for interpreting complex networks. One of the attentional properties that complex networks may have is hierarchy. In 2005, Newman and Sohler presented a universal tester, which can test every property, for bounded-degree hyperfinite graphs[6]. In 2016, Ito presented a class, called $\mathcal{HSF}$, of multigraphs satisfying scale-freeness and hierarchy, and showed that Newman and Sohler's algorithm can be applied even though the class is not bounded-degree[5]. From the observation of it, if a graph class satisfies both scale-freeness and hyperfiniteness, the algorithms of [6] can be also applied. In this talk, we show that three well-known models of complex networks that obey hierarchy are all hyperfinite. Consequently, we proved that every property is testeble on these classes.

2 Definitions

Two graphs $G_1 = (V_1, E_1)$ and $G_2 = (V_2, E_2)$ are *isomorphic* if there is a one-to-one correspondense $\pi : V_1 \to V_2$ such that $(u, v) \in E_1$ if and only if $(\pi(u), \pi(v)) \in E_2$ for every pair $u, v \in V_1$. A *graph property* (or *property* , in short) is a family of graphs, that is closed under isormophism. For two graphs $G_1 = (V_1, E_1)$ and $G_2 = (V_2, E_2)$ with $|V_1| = |V_2| = n$, $m(G_1, G_2)$ is the number of edges that we need to delete or insert in order to make G isomorphic to G'. *Distance* $\mathrm{dist}(G_1, G_2)$ between G_1 and G_2 is defined as $m(G_1, G_2)/n$. For a graph G and a family of graphs $\mathcal{H}$, $\mathrm{dist}(G, \mathcal{H}) = \min_{G' \in \mathcal{H}} \mathrm{dist}(G, G')$. For a real number $\epsilon > 0$ and two n vertex graphs G_1 and G_2, if $\mathrm{dist}(G_1, G_2) \leq \epsilon$, then G_1 and G_2 are *ϵ-close*, otherwise *ϵ-far*. For a property $\mathcal{P}$, if $\mathrm{dist}(G, \mathcal{P}) \leq \epsilon$, then G is ϵ-close from $\mathcal{P}$, otherwise ϵ-far.

Definition 1 (Tester) *For a property $\mathcal{P}$, a tester is an algorithm that, given query access to a graph G, accepts every graph in $\mathcal{P}$ with a probability at least $2/3$, and rejects every graph that are ϵ-far from the property with a probability at least $2/3$. If a tester runs in constant time, $\mathcal{P}$ is testable.*

Definition 2 (Hyperfinite) *For real numbers $s, \epsilon > 0$, an n vertex graph G is called (s, ϵ)-hyperfinite if it can remove at most ϵn edges to obtain a graph whose connected compornents have size at most s. For a function $\rho : \mathbb{R}^+ \to \mathbb{R}^+$, G is ρ-hyperfinite if it is $(\rho(\epsilon), \epsilon)$-hyperfinite for every $\epsilon > 0$. A family $\mathcal{G}$ of graphs is ρ-hyperfinite if every $G \in \mathcal{G}$ is ρ-hyperfinite. If there exists such a function ρ, $\mathcal{G}$ is called hyperfinite.*

3 Hirearchical models

Dorogovtsev[3], Barabási[2], and Ravasz[7] models are well-known hierarchical models of complex networks. The generating algorithms are shown as follows. From the restriction of the space, we omit an explanation of Barabasi's model, which is close to Ravasz's model.

Algorithm 1 Dorogovtsev model (Fig.1)

Step 1 : Put two vertices, and connect them.
Step 2 : Add one vertex for every edge and connect it to the end vertices of the edge.
Step 3 : Repeat Step 2.

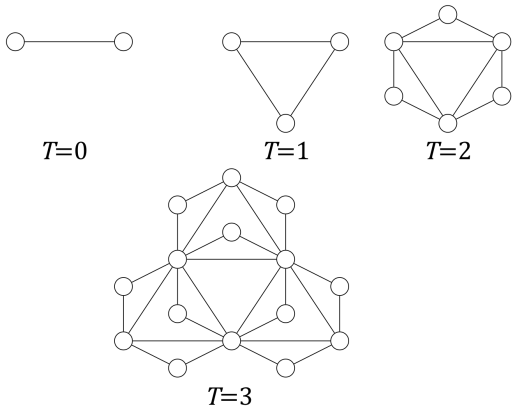

Figure 1: Dorogovtsev model

Algorithm 2 Ravasz model (Fig. 2)

Step 1 : Put a vertex, and let it be a root vertex.
Step 2 : Put α copies of the root, and let them be verge. Let B be a set of verges. Connect verges to the root.
Step 3 : Put α copies of the present graph, add the copied of verges to B, and remove the verges of the original graph from B. Connect every vertices in B to the root.
Step 4 : Repeat step 3.

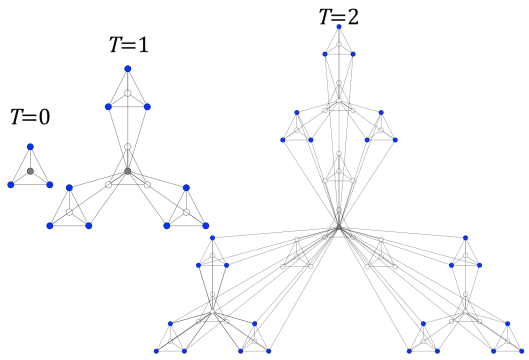

Figure 2: Ravasz model($\alpha = 3$)

4 Results

We prove the following theorem.

Theorem 1 *For a real number $\epsilon > 0$, there exists a constant number $s = s(\epsilon)$ such that every graph generated by Dorogovrsev, Barabási, or Ravasz models is (s, ϵ)-hyperfinite.* □

By considering the results on scale-freeness on [5] with this theorem, we get the following corollary.

Corollary 1 *Every property is constant-time testable on Dorogovtsev, barabási, and Ravasz models.* □

5 Conclusion and future work

We proved that three hierarchical models are hyperfinite, similarly to $\mathcal{HSF}$. However, we expect that they are not in $\mathcal{HSF}$. Therefore, in the future work, we should define new graph class which contains these hierarchical models.

Acknowledgements

This work is partially supported by CREST, JST (Grant Number JPMJCR1402).

References

[1] A. -L. Barabási and R. Albert, "Emergence of Scaling in Random Networks," Science, vol. 286, pp. 509–512, 1999.

[2] A. -L. Barabási and E. Ravasz, "Deterministic scale-free networks," Physica A, vol. 299, pp. 559–564, 2001.

[3] S. N. Dorogovtsev, A. V. Goltsev, and J. F. F. Mendes, "Pseudofractal scale-free web," Physical Review E, vol. 65, No. 066122, 2011.

[4] O. Goldreich (Ed.), Property Testing — Current Research and Surveys, LNSC 6390, Springer, pp. 105–141, 2010.

[5] H. Ito, "Every property is testable on a natural class of scale-free multigraphs," Proc. ESA, pp. 51:1–51:12, 2016.

[6] I. Newman and C. Sohler, "Every property of hyperfinite graphs is testable," Proc. STOC, pp. 675–684, 2011.

[7] E. Ravasz and A. -L. Barabási, "Hierarchical organization in complex networks," Physical Review E, vol. 67, No. 026112, 2003.

[8] D. J. Watts and H. S. Strogatz, "Collective dynamics of ' small-world ' networks", Nature, vol. 393, pp. 440–442, 1998.

An Improved Searching Algorithm on a Line by Four Truthful Robots and Two Byzantine Robots*

Michael Hoffmann† Malte Milatz† Yoshio Okamoto‡ Manuel Wettstein†

We study the following one-dimensional online search problem. A collection of n robots starts at the origin of the real line, seeking to find a treasure that is hidden at an unknown location $g \in \mathbb{R}$. The robots can move independently at unit speed and are capable to detect (and report) the treasure whenever they are at the same position g. The goal is to design an algorithm that allows to locate the treasure quickly, regardless of where it is located.

The problem here comes with an additional twist, as introduced by Czyzowicz et al. [1]. Among the n robots there are f that are *Byzantine*, which may provide false reports. That is, they may report a treasure at a position where it is not, and they may be silent at a position where the treasure is. A robot that is not Byzantine is referred to as *truthful*.

As usual in an online setting, we measure the performance of a strategy by its worst case *competitive ratio*, that is, in relation to an optimal offline algorithm that knows the target position g in advance. In this problem, the optimal offline algorithm is obvious: Directly move all robots from the origin to the goal location g. This takes $|g|$ time units. Hence, an algorithm that uses t time units to find the treasure at position g is said to have competitive ratio $t/|g|$.

Among others, the case $(n, f) = (6, 2)$ was studied by Czyzowicz et al. [1]. They claimed an algorithm with competitive ratio 4 and gave a lower bound of 3. We improve the upper bound.

Theorem 1. *There is an algorithm to find a treasure on a line with six robots, two of which are Byzantine with competitive ratio at most* $\sqrt{13} < 3.61$.

In this abstract, we only give an outline of the algorithm, and the analysis will be omitted.

*The work was done at 15th Gremo's Workshop on Open Problems, Pochtenalp, Switzerland. The authors thank the participants for an inspiring atmosphere. The work by M.H. was supported by the Swiss National Science Foundation within the collaborative DACH project *Arrangements and Drawings* as SNSF Project 200021E-171681. The work by Y.O. was partially supported by JSPS KAKENHI 15K00009 and JSPS CREST JPMJCR1402.

†ETH Zurich, Switzerland.

‡The University of Electro-Communications, Japan and RIKEN Center for Advanced Intelligence Project, Japan.

The algorithm consists of up to five phases. In the first phase, the robots are split into two groups of size three arbitrarily. One group moves left and the other group moves right. The first phase ends as soon as a robot reports the treasure. Let k denote the time at which this report occurs, which is the same as the distance of both groups from the origin at the end of Phase 1. Suppose without loss of generality that a report at time k comes from the group of robots in the positive halfline. We distinguish two cases.

Case 1: two or more robots report the treasure at position k. Then, we let the two groups of robots move to exchange their position. At time $3k$, all robots have visited the location k and so we know by majority vote if this is the treasure location. If so, we are done. If not, then we know the two Byzantine robots and discard them from consideration. We continue by moving the group at position k to the right and the group at position $-k$ to the left. As soon as one robot reports the treasure, we are done.

Case 2: exactly one robot reports the treasure at position k. Then, Phase 2 of the algorithm begins. We discard the robot that issued the report from consideration so that only two robots remain in the group at position k. At the beginning of Phase 2, one of the remaining robots from each group switches back and reverses direction. We let the robots move in this way for some time $\alpha \in [0, k]$, where $\alpha = (\sqrt{13} - 3)k/2 < 0.303k$ is a good choice for this parameter. In other words, during Phase 2 there are four groups of robots moving together: one robot in $[k, 2k]$ moving right, one robot in $[0, k]$ moving left (called the *green robot*), one robot in $[-k, 0]$ moving right (the *blue robot*), and two robots in $[-2k, k]$ moving left.

At time $k + \alpha$, the second phase ends. At the beginning of the third phase, one robot (the *red robot*) from the leftmost group of two robots (at position $-k - \alpha$) switches back and reverses direction. The third phase ends when the blue robot reaches position k at time $3k$. We distinguish three cases.

Case 2.1: At some point during Phase 2 or Phase 3 another robot reports the treasure. If it is one of the three colored robots (red, blue, or green), then we can immediately conclude that it is Byzan-

tine. As we have at most two Byzantine robots, we conclude that both reports are wrong. We simply continue to sweep the line with the two black robots in extreme position and will eventually find the treasure at a position g in optimal time $|g|$.

It remains to consider the case that one of the uncolored (*black*) robots reports the treasure at a position $k' \in (k, 3k]$. We discard the reporting robot from consideration so that only four robots remain. We let all remaining robots run their course and continue in whatever direction they are heading.

At time $3k$ the blue robot reaches k. If it confirms the treasure at k, then—one way or another—two robots lied at k. Therefore, the treasure is at either k or k' and we know where as soon as the red robot reaches k at time $3k + 2\alpha$.

Otherwise, the blue robot denies a treasure at k and we conclude that the initial report at k was wrong. We send the red robot to k' and let the other robots continue in their current direction. We consider three subcases depending on the position of k'. Note that at time $3k$, the red robot is at position $k - 2\alpha > 0$.

Case 2.1.1: $-k - \alpha \leq k' < -k$. Then, the red robot has already seen k' and remained silent. Hence, when the green robot reaches k' at time $k' + 2k$ we know if the treasure is there. If so, we are done. Otherwise, we found the two Byzantine robots and either the right black robot finds the treasure in optimal time, or the green robot finds it at $g < -k$.

Case 2.1.2: $k' < -k - \alpha$. Then the red robot reaches k' at time $4k + |k'| - 2\alpha$. In addition to the reporting black robot, both the green and the red robot have visited k' at this point. Thus we know whether or not the treasure is there by a majority vote. If the treasure is at k', then we found it at time at most $\sqrt{13}k$. Otherwise, we found the two Byzantine robots and either the right black robot finds the treasure in optimal time, or the green robot finds it at a position $g < k'$.

Case 2.1.3: $k < k'$. Then, the red robot reaches k' at time $\sqrt{13}k'$. At this point, three robots (black, blue, and red) have seen k' and so we know whether or not the treasure is there by a majority vote. Therefore, if the treasure is at k', then we are done. Otherwise, we found the two Byzantine robots and either the left black robot finds the treasure in optimal time, or the red robot finds it at $g > k'$.

This completes the analysis of Case 2.1. Hence in the following we may assume that no robot reports the treasure during Phases 2 and 3. We continue our analysis at the end of Phase 3.

Case 2.2: the blue robot reports the treasure at position k, when reaching it at time $3k$ at the end of Phase 3. We discard the blue robot from consideration and wait for the red robot to arrive at k. Both extreme black robots continue in their current direction. The red robot reaches k at time $\sqrt{13}k$. If it confirms the treasure at k, then we are done. Otherwise, all remaining robots are truthful and one of the black robots finds the treasure at a position g, with $|g| > 3k$. and we know by time $2|g|$ that the report is correct.

Case 2.3: the blue robot does not report the treasure at position k at the end of Phase 3. Then, we know that the first report was wrong and only one Byzantine robot remains. We enter Phase 4, where all robots continue in their current direction except for the red robot, which switches back to the origin. Phase 4 ends when the red robot reaches the origin at time $4k - 2\alpha$.

If no robot reports the treasure during Phase 4, then Phase 5 starts where the red robot remains at the origin while the other four robots continue in their current direction. Ultimately either the blue or the green robot reports the treasure at a position g, with $|g| \geq 2(k - \alpha)$. (If one of the black robots reports it, then it is even better.) We immediately send the red robot over to check, while letting all other robots continue in their current direction.

It remains to consider the case that a robot reports the treasure at a position g during Phase 4. If the report comes from a black robot, then we can simply wait until the blue or green robots reaches g. At this point the red robot will have reached the origin and we can argue as above for Phase 5. Hence, suppose that the blue or green robot reports the treasure. There are two final cases.

Case 2.3.1: the blue robot reports the treasure during Phase 4 at a position $k' \in (k, 2(k - \alpha)]$. Then, we immediately switch around the red robot to head for k'. If the treasure is at k', then we are done. Otherwise, the remaining robots are truthful and we eventually find the treasure with a black robot in optimal time.

Case 2.3.2: the green robot reports the treasure during Phase 4 at a position $k' < -k$. If $k' \geq -k - \alpha$, we immediately know that the report at k' is wrong and continue as before with the remaining black robots, both of which are truthful.

Hence we may suppose that $k' < -k - \alpha$. The green robot reaches k' at time $|k'| + 2k$, and the red robot reaches k' at time at most $\sqrt{13}k'$.

References

[1] J. Czyzowicz, K. Georgiou, E. Kranakis, D. Krizanc, L. Narayanan, J. Opatrny, and S. M. Shende. Search on a line by Byzantine robots. In *ISAAC 2016*, pp. 27:1–27:12, 2016.

Mind *The Mind* with Synchronous Clocks

Takashi Horiyama* Kazuhiro Kurita† Yoshio Okamoto‡ Kei Uchizawa§
Ryuhei Uehara¶

1 Introduction

The Mind is a card game developed by Wolfgang Warsch, and published by Nürnberger-Spielkarten-Verlag, Germany, in 2018. The game aquired a good reputation, and it was nominated for several honors, including *Spiel des Jahres* 2018.

The game set consists of one hundred cards, numbered from 1 to 100. The same number of cards are dealt to each player, and each player can check her own cards, but not the others' cards. The players cooperatively try to play the dealt cards in ascending order, but the twist is that the players are not allowed to communicate with each other. The absence of communication makes the game exciting.

A usual strategy for the players is to try to synchronize their mental clocks, count seconds, and play card i at time i. If the clocks really synchronize, then the players can win after 100 seconds. However, spending 100 seconds sounds a waste of time, for example, if there are only four players, and only one card is dealt to each player.

Therefore, as a secondary goal (that is not specified by the game), the players want to reduce the time spent in the game. On the other hand, they should know a risk of failure by reduction; there should be a trade-off between the success probability and the length of a time interval.

The goal of this study is to uncover this trade-off by mathematically modeling the situation above. As a result, when only one card is dealt to each player, we characterize optimal strategies for the players, and derive a recursive formula to compute the maximum success probability.

Due to space constraints, proofs are suppressed.

*Saitama University, Japan
†Hokkaido University, Japan
‡The University of Electro-Communications, Japan and RIKEN Center for Advanced Intelligence Project, Japan
§Yamagata University, Japan
¶Japan Advanced Institute of Science and Technology, Japan

2 Set-up

The game is parametrized by four positive integers N, K, M and T. We assume $MK \leq N$.

In the game, we use N cards numbered from 1 to N. A card with number $c \in \{1, 2, \ldots, N\}$ will simply be called a card c. There are K players, and a player is identified with a number from $\{1, 2, \ldots, K\}$. To each player, M cards are dealt, and the players see their own cards. No player sees the others' cards, nor the cards that are not dealt. Players are not allowed to establish any communication with other players.

The players share a synchronous clock. The time is counted discretely from $1, 2, \ldots,$ up to T.

At time $t \in \{1, 2, \ldots, T\}$, each player makes a decision: whether she plays one of her cards or not. The players can see the played cards of other players. After the decision, time is incremented by one, and the game proceeds.

The players lose if one of the following three conditions is satisfied.

1. Two or more cards are played at the same time.
2. The played card has a larger number than a card of a player that was not yet played.[1]
3. After time T, there is still a player who owns a card at hand.

If none of the conditions is satisfied at any time, then the players win.

For the sake of theoretical analysis, we assume that cards are dealt uniformly at random among the players. We concentrate on the case where $M = 1$.

The goal of this work is to establish the players' strategies that maximize the winning probability for any given N, K, and T. Such strategies are called *optimal*.

3 Optimal Strategies

A strategy of a player may depend on the game situation. At time $t = 1$, each player i decides

[1] This already implies that each player should play her cards in ascending order.

whether she plays a card or not, and if she plays a card, she decides which card she plays. This means that player i has a set $\mathcal{S}(i) \subseteq \{1, 2, \ldots, N\}$ of cards such that if she has a card in $\mathcal{S}(i)$, then she plays that card at time $t = 1$; otherwise she does not play a card at time $t = 1$. Thus, the players' strategy at time $t = 1$ can be identified with an ordered family of sets $\langle \mathcal{S}(i) \mid i \in \{1, 2, \ldots, K\} \rangle$.

A strategy $\mathcal{S}(i)$ of player i is a *prefix* strategy if there exists $N(i)$ such that $\mathcal{S}(i) = \{1, 2, \ldots, N(i)\}$.

Lemma 1. *In every optimal strategy of the players, each player takes a prefix strategy.*

Thanks to Lemma 1, in an optimal strategy $\langle \mathcal{S}(i) \rangle$, we denote $\mathcal{S}(i) = \{1, 2, \ldots, N(i)\}$ for some $N(i) \in \{1, 2, \ldots, N\}$.

The players' strategy $\langle \mathcal{S}(i) \rangle$ is called *uniform* if there exists a set $\mathcal{S} \subseteq \{1, 2, \ldots, N\}$ of cards such that $\mathcal{S}(i) = \mathcal{S}$ for all players i.

Lemma 2. *Every optimal strategy is a uniform strategy.*

Following Lemmas 1 and 2, we may restrict to the following *uniform prefix strategy*.

> **Uniform prefix strategy:** Fix a number N'. Each player i plays her card if and only if she owns a card with number smaller than or equal to N'. In other words, $\mathcal{S}(i) = \{1, 2, \ldots, N'\}$ for all i.

Here, N' depends on N, K, and T, but is independent of player i.

Theorem 1. *When $M = 1$, every optimal strategy is a uniform prefix strategy.*

4 Recursion

From Theorem 1, we are able to obtain a recursive formula to compute the winning probability in *The Mind*. We denote by $p(N, K, T)$ the winning probability when the players follow optimal strategies.

For base cases (or easy cases), we have the following:

$$p(N,K,T) = \begin{cases} 0 & (\text{if } T \le 0), \\ 1 & (\text{if } K = 1 \text{ and } T \ge 1), \\ 0 & (\text{if } K = 1 \text{ and } T \le 0), \\ 0 & (\text{if } N < K), \\ 0 & (\text{if } N = K \text{ and } T < N), \\ 1 & (\text{if } N = K \text{ and } T \ge N). \end{cases}$$

For a general case where $N > K$, $K \ge 2$, and $T \ge 1$, we obtain the following recurrence:

$$p(N,K,T) = \max_{N'} \{P \cdot p(N - N', K, T - 1) + Q \cdot p(N - N', K - 1, T - 1)\},$$

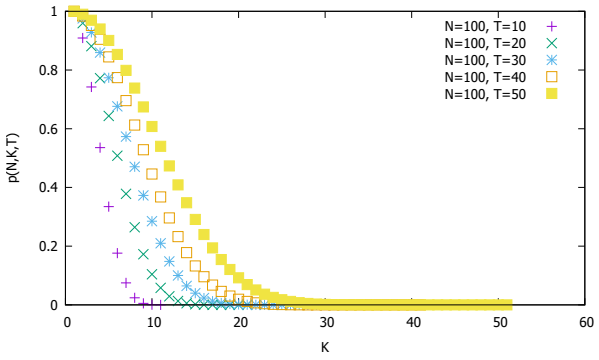

Figure 1: The maximum winning probability when $N = 100$. The horizontal axis represents K.

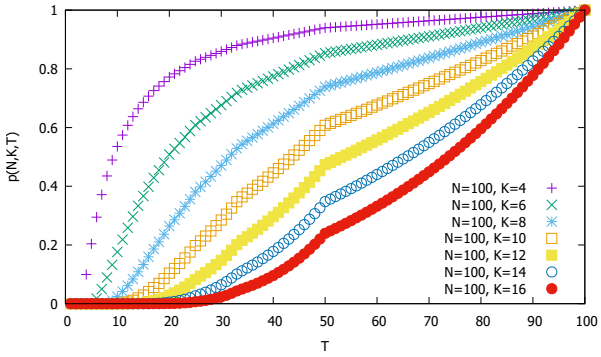

Figure 2: The maximum winning probability when $N = 100$. The horizontal axis represents T.

where the maximum is taken over all $N' \in \{1, 2, \ldots, N - K + 1\}$, P is the probability that no player owns card in $\{1, 2, \ldots, N'\}$ and Q is the probability that a single player owns her card in $\{1, 2, \ldots, N'\}$ while the other players own cards in $\{N' + 1, N' + 2, \ldots, N\}$.

The probabilities P and Q can be calculated explicitly:

$$P = \frac{(N - N')!(N - K)!}{N!(N - N' - K)!};$$
$$Q = \frac{KN'(N - N')!(N - K)!}{N!(N - N' - K + 1)!}.$$

5 Final Remarks

Figures 1 and 2 show the result of calculations based on the recursion above. We were not able to derive an explicit formula for the probability. This remains an open question.

This work focused on the case where $M = 1$. The case where $M \ge 2$ remains unsolved.

Acknowledgements This work was partially supported by JSPS KAKENHI 15H05711.

Another Representation of Rhombus Tilings

Takashi Horiyama[1] Tomohiro Tachi[2] Asao Tokolo[3]

[1] Saitama University, Saitama, Japan. horiyama@al.ics.saitama-u.ac.jp
[2] The University of Tokyo, Tokyo, Japan. tachi@idea.c.u-tokyo.ac.jp
[3] TOKOLO.com, Tokyo, Japan. info@tokolo.com

1 Introduction

A rhombus tiling is a set of rhombus tiles which covers a domain D without overlaps nor gaps. Let $\vec{u}_0, \vec{u}_1, \ldots, \vec{u}_{n-1}$ be pairwise non-collinear unit vectors of a 2 dimensional plane. Then, we have $\binom{n}{2}$ kinds of rhombus tiles defined as $R_{i,j} := \{a_i\vec{u}_i + a_j\vec{u}_j \mid 0 \leq a_i, a_j \leq 1\}$. In this paper, we focus on a zonotopal domain D which is defined as $D := \{\sum a_i\vec{u} \mid 0 \leq a_i \leq d_i\}$, where d_i's are some fixed constant integers. For ease of discussion, we assume $d_1 = d_2 = \cdots = d_n = d$ for some integer d (We can easily extend our discussion to general d_i's). In a rhombus tiling, rhombus tiles are placed in D so that (1) all points in D are covered, and (2) any two different tiles have no intersection (i.e., they are nonadjacent), or they share a vertex or an edge of their rhombuses (i.e., they are adjacent).

Figure 1 (a) illustrates a rhombus tiling for $n = 3$ and $d = 2$. For understanding rhombus tilings, de Bruijn introduced ribbons of rhombus tiles (now, called de Bruijn lines) [2]). The rhombus tiles denoted in bold lines in Figure 1 (a) is an example of a de Bruijn line, which is obtained by concatenating adjacent rhombus tiles that have edges parallel to $\vec{u}_0$. By replacing de Bruijn lines with pseudolines, rhombus tilings can be represented by the arrangements of pseudolines (see e.g., [1, 3]). Figure 1 (b) illustrates an arrangement of pseudolines corresponding to the rhombus tiling in Figure 1 (a).

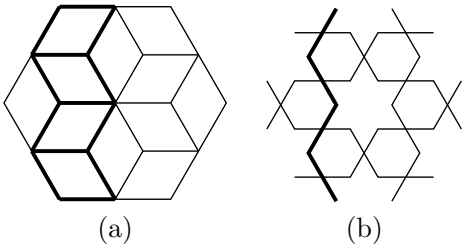

Figure 1: A rhombus tiling for $n = 3$ and $d = 2$, and its corresponding arrangement of pseudolines. A ribbon and its corresponding pseudoline are given in bold.

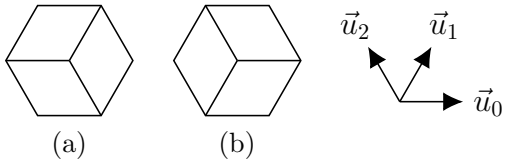

Figure 2: Two rhombus tilings for $n = 3$ and $d = 1$.

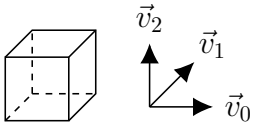

Figure 3: 3-dimensional cube with 3-dimensional unit vectors $\vec{v}_0$, $\vec{v}_1$ and $\vec{v}_2$.

The bold pseudolines corresponds to the de Bruijn line in bold in Figure 1 (a).

In this paper, we propose another way for representing rhombus tilings. Our idea is to introduce a set of (2-dimensional) faces in an n-dimensional hypercube, and to project it into a 2-dimensional plane. We will explain the relation between the faces in n-dimensional hypercube and their projection, and then give the condition on the faces so that the projection makes a valid rhombus tiling. Our method also extends to the tilings of 3-dimensional rhombohedra (or rhombotopes in higher dimensions).

2 Case $n = 3$

First, to illustrate our idea, we start from the case $n = 3$ with $d = 1$. We have two rhombus tilings for this case, as illustrated in Figure 2. The tiling in Figure 2 (a) consists of the following three faces: $([0,1],0,[0,1])$, $(1,[0,1],[0,1])$ and $([0,1],[0,1],1)$, where a domain $([a_{0,0},a_{0,1}],[a_{1,0},a_{1,1}],[a_{2,0},a_{2,1}])$ represents $\{\sum_{i=0}^{2} a_i\vec{u}_i \mid a_{i,0} \leq a_i \leq a_{i,1}\}$ and $[a_i,a_i]$ is abbreviated as a_i. Similarly, the tiling in Figure 2 (b) consists of the following three faces: $([0,1],1,[0,1])$, $(0,[0,1],[0,1])$ and $([0,1],[0,1],0)$.

Now, tiling in Figure 2 can be observed as the

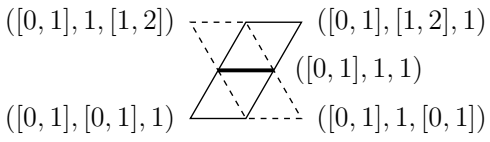

Figure 4: Four 3-dimensional faces sharing a line segment $([0,1],1,1)$.

isometric projection of a subset of faces of 3-dimensional cube illustrated in Figure 3. The edges are in the directions of the (3-dimensional) unit vectors $\vec{v}_0 = (1,0,0)$, $\vec{v}_1 = (0,1,0)$ and $\vec{v}_2 = (0,0,1)$. With these unit vectors, face $([0,1],0,[0,1])$ can be interpreted as the top face of the cube. From this view point, the faces in Figure 2(a) represent the front, right, and top faces of the cube, respectively. Similarly, the faces in Figure 2(b) represent the back, left and bottom faces of the cube, respectively.

For general d, we consider $d \times d \times d$ lattice of cubes. Namely, we have a cube domain of edge length d with 3-dimensional unit vectors $\vec{v}_0$, $\vec{v}_1$ and $\vec{v}_2$. A (2-dimensional) face in this cube lattice is represented as a domain $([a_{0,0}, a_{0,1}], [a_{1,0}, a_{1,1}], [a_{2,0}, a_{2,1}])$, where $a_{i,j}$'s are integers, exactly two $i \in \{0,1,2\}$ satisfies $a_{i,1} = a_{i,0} + 1$, and another i satisfies $a_{i,1} = a_{i,0}$. The unit vectors $\vec{v}_0$, $\vec{v}_1$ and $\vec{v}_2$ are projected to the 2-dimensional unit vectors $\vec{u}_0$, $\vec{u}_1$ and $\vec{u}_2$. By this projection, faces in 3-dimensional space is projected to rhombuses in 2-dimensional space.

Note that some faces and edges in the cube do not appear in the rhombus tilings. In other words, by selecting a set of faces in the cube lattice, their projection makes a valid rhombus tiling. Our goal is to characterize such set of faces F.

The rhombus tiles a plane if and only if (1) the internal edge is shared by two tiles and the boundary edge is owned by a tile, and (2) the tiles do not intersect. Condition (1) can be described in terms of the cube lattice as follows. Each line segment in the cyclic domains $([0,d],0,0)$, $(d,[0,d],0)$, $(d,d,[0,d])$, $([0,d],d,d)$, $(0,[0,d],d)$ and $(0,0,[0,d])$, called the *boundary line segments*, (projected to the boundary of the 2D domain), is adjacent to exactly one face in F. Every other line segment is adjacent to zero or two faces in F.

For condition (2), we need a careful observation on two adjacent faces. Figure 4 illustrates the projected rhombus of four 3-dimensional faces sharing a line segment $([0,1],1,1)$, which is parallel to $\vec{v}_0$. From the line segment, face $([0,1],[1,2],1)$ is in the direction of $\vec{v}_2$. Similarly, faces $([0,1],1,[1,2])$, $([0,1],[0,1],1)$ and $([0,1],1,[0,1])$ are in the directions of $\vec{v}_3$, $-\vec{v}_2$, $-\vec{v}_3$, respectively. If two faces in projection are on the same side from the line segment, those two have an overlap. Thus, to achieve a rhombus tiling, we need to select two faces so that one is above the line segment and the other is below the line segment.

3 General n

In general, we make a projection from n-dimensional unit vectors $\vec{v}_0 = (1,0,0,\ldots,0)$, $\vec{v}_1 = (0,1,0,\ldots,0)$, ..., and $\vec{v}_{n-1} = (0,0,0,\ldots,1)$ to 2-dimensional unit vectors $\vec{u}_i = (\cos\frac{i}{n}\pi, \sin\frac{i}{n}\pi)$ $(i = 0,1,\ldots,n-1)$. We select a set F of faces in an n-dimensional hypercube of edge length d. The n-dimensional line segments cyclically connecting $2n$ vertices $(0,0,\ldots,0)$, $(d,0,\ldots,0)$, ..., $(d,d,\ldots,d)$, $(0,d,\ldots,d)$, ..., and $(0,0,\ldots,0,d)$ are boundary line segments. Each of the line segments has an adjacent face in F. Every other line segment has zero or two adjacent faces in F, where, in case two faces are adjacent, one is above and the other is below the line segment.

We can further rewrite this "above or below" discussion in terms of consistent orientation. Consider two faces sharing an edge of direction $\vec{v}_i$ extending to $\sigma_j\vec{v}_j$ and $\sigma_k\vec{v}_k$ directions ($\sigma_j = \pm 1$, $\sigma_k = \pm 1$), respectively. They have consistent normals $\vec{v}_i \times \sigma_j\vec{v}_j$ and $(-\vec{v}_i) \times \sigma_k\vec{v}_k$, respectively. The orientation needs to be consistent also in the projection, i.e., $\sigma_j \det\begin{bmatrix}\vec{u}_i & \vec{u}_j\end{bmatrix}$ and $\sigma_k \det\begin{bmatrix}-\vec{u}_i & \vec{u}_k\end{bmatrix}$ have the same sign. This representation makes our model further ready for rhombohedral tiling and the tiling in a higher dimension.

We have enumerated the sets of faces that satisfy the constraints as above. That is to say, the constraints on the faces of n-dimensional hypercube for a rhombus tiling. The experimental results match the known results [4] on $d = 1$ when n is up to 8, and on $d = 2$ when n is up to 6.

References

[1] O. Bodini, T. Fernique, M. Rao, E. Remila, Distance on Rhombus Tilings, Theoretical Computer Science, 412, pp. 4787–4794, 2011.

[2] N. G. De Bruijn, Algebraic Theory of Penrose's Non-Periodic Tilings of the Plane, Indagationes Mathematicae, 43, pp. 39–66, 1981.

[3] H. Hamanaka, T. Horiyama, and R. Uehara, On the Enumeration of Chequered Tilings in Polygons, Bridges Conference, pp. 423–426, 2017.

[4] M. Widom, N. Destainville, R. Mosseri, and F. Bailly, Random Tilings of High Symmetry: II. Boundary Conditions and Numerical Studies, arXiv:cond-mat/0310515, 2017.

Representations of Generalized Symmetric Groups and Sums of Welter's Game

Yuki Irie*

We present a relation between irreducible representations of generalized symmetric groups and sums of Welter's game. Mikio Sato [5, 6] conjectured that Welter's game is related to representations of groups. In support of this conjecture, he pointed out that the Sprague-Grundy function of this game can be expressed in a form similar to the hook-length formula. A relation between them was established in [3]. In this talk, we generalize this result to generalized symmetric groups.

1. Welter's game

Welter's game is a two-player game played with a Young diagram. A Young diagram is a collection of cells and represents a partition. For example, the Young diagram in Figure 1 (a) represents the partition $(4, 3, 2)$. We identify a partition with its Young diagram.

To define Welter's game, we introduce some notation. For a cell c in a Young diagram, the *hook* of c consists of the cells to the right of and below c, and including c. Figure 1 (b) shows the hook of the cell $(1, 2)$. The number of cells in the hook of c is called the *hook-length* of c. Figure 1 (c) shows the hook-lengths of $(4, 3, 2)$.

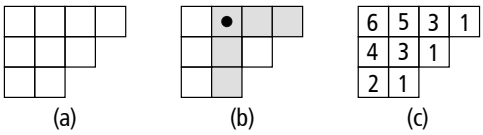

Figure 1: Young diagram (4,3,2)

We now define Welter's game. In this game, two players alternately remove a hook. Figure 2 shows the result of removing the hook of (1,2). The player who removes the hook last wins.

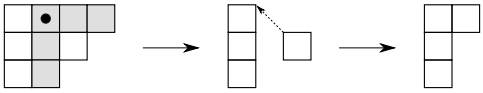

Figure 2: Removal of the hook of (1,2)

Impartial games such as Welter's game can be solved using Sprague-Grundy functions (see, for example, [1, 2]). Sato [5] obtained the following formula for the Sprague-Grundy function of Welter's game. For a Young diagram Y, let $H(Y)$ be the multiset of hook-lengths of Y. If we think of Y as a position in Welter's game, then the Sprague-Grundy value of Y can be expressed as

$$\mathrm{sg}_W(Y) = \bigoplus_{h \in H(Y)}{}_2 \; 2^{\mathrm{ord}_2(h)+1} - 1,$$

where $\oplus_2$ is addition without carry in base 2 and $\mathrm{ord}_2(h)$ is the 2-adic order of h. For example, $1 \oplus_2 3 = 2$ and $\mathrm{ord}_2(12) = 2$.

2. Representations

Let G be a finite group and V a finite dimensional vector space over $\mathbb{C}$. A group homomorphism R from G to the general linear group $GL(V)$ is called a *representation* of G. The dimension of V is called the *degree* of R. For a subgroup H of G, the *restriction* of R to H is the representation $R|_H : H \to GL(V)$. It is known that every representation of G can be decomposed to a direct sum of irreducible representations.

Irreducible representations of symmetric group $\mathrm{Sym}(n)$ are in one-to-one correspondence with Young diagrams with n cells (see, for example, [4]). For a Young diagram Y, let R^Y denote the irreducible representation corresponding to Y. Then

$$\deg R^Y = \frac{n!}{\prod_{h \in H(Y)} h} \qquad \text{and}$$

$$R^Y|_{\mathrm{Sym}(n-1)} = \bigoplus_{Y^-} R^{Y^-},$$

where the direct sum runs over all Young diagrams Y^- obtained from Y by removing a hook of length 1. For example,

$$\deg R^{\ydiagram{4,3,1}} = \frac{9!}{6 \cdot 5 \cdot 4 \cdot 3^2 \cdot 2} = 168 \qquad \text{and}$$

$$R^{\ydiagram{4,3,1}}|_{\mathrm{Sym}(8)} = R^{\ydiagram{4,3}} \oplus R^{\ydiagram{3,2,1}} \oplus R^{\ydiagram{3,3}}.$$

One of the central problems of representation theory is the McKay conjecture [1] about representations with

*Research Alliance Center for Mathematical Sciences, Tohoku University, yirie@tohoku.ac.jp

[1] McKay conjectured that the number of irreducible representations of G with degree prime to p is equal to that of $N_G(P)$, where P is a Sylow p-subgroup of G and $N_G(P)$ is the normalizer of P in G.

degree prime to p. Such representations play an important role to connect representations and games. Let p be a prime. Define

$$\psi^p(Y) = \bigoplus_{h\in H(Y)} p \quad p^{\mathrm{ord}_p(h)+1} - 1,$$

where $\oplus_p$ is addition without carry in base p and $\mathrm{ord}_p(h)$ is the p-adic order of h. Note that $\psi^2(Y) = \mathrm{sg}_{\mathcal{W}}(Y)$.

Theorem 2.1 ([3]). *The restriction of R^Y to $\mathrm{Sym}(\psi^p(Y))$ has an irreducible component with degree prime to p.*

Example 2.2. Let $p = 2$ and $Y = (4, 3, 2)$. Then $\psi^2(Y) = 7$, so Theorem 2.1 asserts that $R^Y|_{\mathrm{Sym}(7)}$ has an irreducible component with odd degree. Indeed, $R^{(3,3,1)}$ is its irreducible component and $\deg R^{(3,3,1)} = 7!/(5 \cdot 4 \cdot 3 \cdot 2^2) = 21$.

3. Games and Representations

Let $\mathcal{W}^p$ be a p-saturated (see Appendix A) Welter's game. In fact, we can prove that the Sprague-Grundy function $\mathrm{sg}_{\mathcal{W}^p}$ of $\mathcal{W}^p$ is equal to ψ^p using Theorem 2.1. Therefore, this theorem can be reformulated as follows.

Theorem 3.1 ([3]). *The restriction of R^Y to $\mathrm{Sym}(\mathrm{sg}_{\mathcal{W}^p}(Y))$ has an irreducible component with degree prime to p.*

We can generalize Theorem 3.1 to generalized symmetric groups $(\mathbb{Z}/m\mathbb{Z})\wr\mathrm{Sym}(n)$. Irreducible representations of $(\mathbb{Z}/m\mathbb{Z}) \wr \mathrm{Sym}(n)$ are in one-to-one correspondence with m-tuples of Young diagrams with n cells in total. For an m-tuple of Young diagrams $(Y_1, \ldots, Y_m)$, let $R^{Y_1,\ldots,Y_m}$ the corresponding irreducible representation of $(\mathbb{Z}/m\mathbb{Z}) \wr \mathrm{Sym}(n)$. The degree and restrictions of $R^{Y_1,\ldots,Y_m}$ can be computed in a similar way to R^Y.

Theorem 3.2. *The restriction of $R^{Y_1,\ldots,Y_m}$ to $(\mathbb{Z}/m\mathbb{Z})\wr \mathrm{Sym}(\mathrm{sg}_{\mathcal{W}^p}(Y_1) \oplus_p \cdots \oplus_p \mathrm{sg}_{\mathcal{W}^p}(Y_m))$ has an irreducible component with degree prime to p.*

Example 3.3. Let $p = 2$, $m = 2$, $Y_1 = (4, 4, 2)$, and $Y_2 = (2, 1)$. Then $\deg R^{Y_1,Y_2} = 13!/(6 \cdot 5^2 \cdot 4 \cdot 3^2 \cdot 2^3) = 144144$ and $\mathrm{sg}_{\mathcal{W}^2}(Y_1) \oplus_2 \mathrm{sg}_{\mathcal{W}^2}(Y_2) = 6 \oplus_2 1 = 7$. Theorem 3.2 asserts that $R^{Y_1,Y_2}|_{\mathrm{Sym}(7)}$ has an irreducible component with odd degree. Indeed, $R^{(2,2,1),(2)}$ is its irreducible component and $\deg R^{(2,2,1),(2)} = 7!/(4\cdot3\cdot2^2) = 105$.

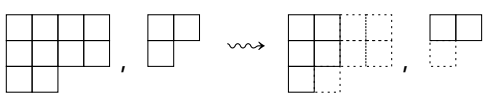

A. p-saturations

A.1. Subtraction games

Let $\mathcal{P} \subseteq \mathbb{N}^k$ and $\mathcal{C} \subseteq \mathbb{N}^k \setminus \{(0, \ldots, 0)\}$, where $\mathbb{N}$ is the set of nonnegative integers. We consider the following game. Before the game, we pick a start position $X_0 \in \mathcal{P}$. The two players alternately subtract some $C \in \mathscr{C}$ from the current position. The player who subtracts last wins. Let $\Gamma(\mathcal{P}, \mathcal{C})$ denote this game.

Example A.1. Let $\mathcal{P} = \mathbb{N}^k$ and $\mathcal{C} = \{C \in \mathbb{N}^k : \mathrm{wt}(C) = 1\}$, where $\mathrm{wt}(C)$ is the Hamming weight of C. Then $\Gamma(\mathcal{P}, \mathcal{C})$ is Nim. Welter's game can be described as a subtraction game. Let $\mathcal{P} = \{X \in \mathbb{N}^k : x_i \neq x_j\}$, where $X = (x_1, \ldots, x_k)$. Then $\Gamma(\mathcal{P}, \mathcal{C})$ is another form of Welter's game. The correspondence between the two forms of Welter's game is given by $\Phi : X \mapsto (x_{\sigma(1)}, x_{\sigma(2)}, \ldots, x_{\sigma(k)}) - (k-1, k-2, \ldots, 0)$, where $\sigma \in \mathrm{Sym}(k)$ with $x_{\sigma(1)} > x_{\sigma(2)} > \cdots > x_{\sigma(k)}$. For example, $\Phi((4, 6, 2)) = (4, 3, 2)$.

A.2. p-saturations

Using p-saturations, we can construct games whose Sprague-Grundy function can be expressed by arithmetic modulo p.

Let $\mathscr{C}^\beta$ be the set of $C \in \mathbb{N}^k \setminus \{(0, \ldots, 0)\}$ satisfying

$$\mathrm{ord}_p\left(\sum c_i\right) = \min\{\mathrm{ord}_p(c_i) : 1 \leqslant i \leqslant k\}.$$

Then $\Gamma(\mathcal{P}, \mathcal{C})$ said to be *p-saturated* if its Sprague-Grundy function is equal to that of $\Gamma(\mathcal{P}, \mathscr{C}^\beta)$.

Example A.2 ([3]). Let $\mathcal{N}^p$ be a p-saturated Nim. Then $\mathrm{sg}_{\mathcal{N}^p}(X) = x_1 \oplus_p \cdots \oplus_p x_k$.

References

[1] E. R. Berlekamp, J. H. Conway, and R. K. Guy. *Winning Ways for Your Mathematical Plays.* A.K. Peters, Natick, Mass., 2nd edition, 2001.

[2] J. H. Conway. *On Numbers and Games.* A.K. Peters, Natick, Mass., 2nd edition, 2001.

[3] Y. Irie. p-Saturations of Welter's game and the irreducible representations of symmetric groups. *J. Algebraic Combin.*, 48:247–287, 2018.

[4] B. Sagan. *The Symmetric Group: Representations, Combinatorial Algorithms, and Symmetric Functions.* Graduate Texts in Mathematics. Springer-Verlag, New York, 2001.

[5] M. Sato. On a game (notes by Kenji Ueno)(in Japanese). In *Proceedings of the 12th Symposium of the Algebra Section of the Mathematical Society of Japan*, pages 123–136, 1968.

[6] M. Sato. *Lecture Notes in Kyoto University (1984-1985)(notes by Toru Umeda)(in Japanese).* Number 5 in Surikaiseki Lecture Note. 1989.

Strip flat folding with parallel oblique or orthogonal zigzag mountain-valley-assigned creases (Extended Abstract)

Hiro Ito* Chie Nara† Izumi Shirahama‡ Mizuho Tomura*
*School of Informatics and Engineering,
The University of Electro-Communications (UEC); Tokyo, Japan.
†Institute of Advanced Study of Mathematical Sciences,
Meiji University; Tokyo, Japan.
‡ECBEING CORP. Tokyo, Japan.
*{itohiro@, t1831105@edu.cc.}uec.ac.jp,
†cnara@jeans.ocn.ne.jp, ‡izmrhythm@gmail.com

1 Introduction

The flat foldability problem, which asks whether or not a given piece of paper with creases each of which has a mountain-valley assignment is flat foldable, is a typical problem of origami mathematics. This problem is know to be in NP-complete [2]. However, in the case that the paper is limited to a rectangular strip and the creases are perpendicular to the long axis of the strip, which is called one-dimensional flat folding problem (with mountain-valley-assigned creases), a linear time algorithm is known [1][3]. We consider two problems: One is that the angle formed by creases is equal to an arbitrary angle, which is not limited to $\pi/2$, i.e., all creases are parallel; and the other is that only two types of creases that are orthogonal each other are allowed and creases are arranged in a zigzag pattern. We show that the former can be solved in linear time, and the latter is always foldable.

2 Preliminaries

The piece of paper is restricted to a long rectangular strip. A crease is a line segment on a piece of paper.

An angle formed by a crease is the angle at which the crease rotates in the positive direction from the x-axis, where the long axis of the strip is the x-axis. A crease is folded into either a mountain fold (M) forming a protruding ridge, or a valley fold (V) forming an indented trough. A mountain crease is illustrated by a one-dot-chain line, and a valley crease is illustrated by a broken line. We must fold every crease according to the given mountain/valley assignment in 180°. The paper should not be stretched, be torn, nor penetrate itself. When we fold a piece of paper, it continuously changes its form from the initial flat form to the final folded state. The paper can not self-intersect, but can overlap. A folding such that every crease is folded according to the given direction of mountain/valley assignment and the final state becomes flat is called a *flat folding*. If a piece of paper with mountain-valley-assigned creases has a flat folding, it is said *flat foldable*.

3 Definitions of the problems and our results

3.1 Parallel oblique creases

In this section we consider a problem in which all creases are parallel, but the angle may not be $\pi/2$, i.e., this problem is a generalization of the one-dimensional flat folding problem.

$n+2$ real values c_0, c_1, …, c_{n+1} (where $c_0 < c_1 < \cdots < c_{n+1}$) and a label function L: $\{1, \ldots, n\} \to \{M, V\}$ are given. The piece of paper is a parallelogram strip whose vertex coordinates on the plane are $(c_0, 0)$, $(c_{n+1}, 0)$, $(c_{n+1} + \cot\theta, 1)$, and $(c_0 + \cot\theta, 1)$, and the width (height) is 1. If $L(i) = M$, then c_i is a mountain crease and if $L(i) = V$, then c_i is a valley crease.

It has n creases c_i ($i \in \{1, \ldots, n\}$) and the angle formed by a crease and the long edge of the strip is θ, where $0 < \theta < \pi/2$ i.e., the short edges of the strip and all of the creases are parallel (see Fig. 1).

An instance is expressed by $I = (c_0, \ldots, c_{n+1}; L, \theta)$. This problem is formulated as follows.

Problem: Strip flat folding problem with parallel oblique mountain-valley-assigned creases

Input: $I = (c_0, \ldots, c_{n+1}; L, \theta)$

Request: Determine whether or not I is flat foldable.

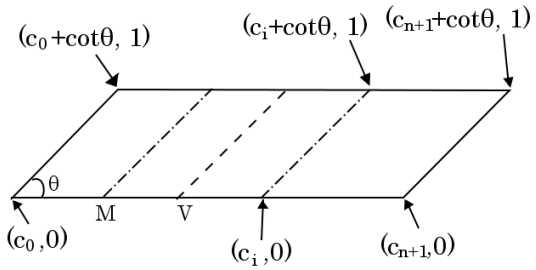

Figure 1: An instance of the strip flat folding problem with parallel oblique mountain-valley-assigned creases

For this problem, we give a linear-time algorithm.

3.2 Zigzag creases

In this section, we consider a problem in which only two angles of creases orthogonal each other are allowed and all creases form a zigzag pattern. In this problem we allow a label of a crease "unfold" (N) besides M and V. If the label of a crease is N, the crease is not folded (i.e., it is not a "crease," but a mere line segment).

An integer n which is the number of creases and a label function L: $\{1, \ldots, n\} \to \{M, V, N\}$ are given. The shape of the strip is a parallelogram if n is odd and an isosceles trapezoid if n is even. For both shapes, the hight is one and the inner angles of the four vertices are θ or $\pi - \theta$, where $0 < \theta < \pi/2$ is a given real number. The angle that a crease makes with the long edge (base) of the strip is θ or $\theta + \pi/2$ and the creases form a zigzag pattern shown as Fig. 2.

An instance is expressed by $I = (n, L, \theta)$. This problem can be formulated as follows.

Problem: Strip flat folding problem with orthogonal zig-zag mountain-valley-assigned creases

Input: $I = (n, L, \theta)$

Request: Determine whether or not I is flat foldable.

Figure 2: An instance of the strip flat folding problem with orthogonal zig-zag mountain-valley-assigned creases

For this problem we show that every instance is flat foldable.

4 Summary and future work

We present a linear time algorithm for the strip flat folding problem with parallel oblique mountain-valley-assigned creases.

Furthermore, we prove that the strip flat folding problem with orthogonal zig-zag mountain-valley-assigned creases is always flat foldable.

For future work, we will try to relax the restrictions. The general strip flat folding problem, i.e. arbitrary creases without crossing are given on a strip, has been shown to be weakly NP-hard if the pieces are rigid [4]. However, if the rigidity constraint does not exist, a polynomial-time algorithm may exist.

References

[1] E. M. Arkin, M. A. Bender, E. D. Demaine, M. L. Demaine, J. S. B. Mitchell, S. Sethia, and S. S. Skiena, "When can you fold a map?," Computational Geometry, vol. 29, Issue 1, pp. 23–46, September, 2004.

[2] M. Bern and B. Hayes, "The complexity of flat origami," Proc. 7th ACM-SIAM Sympos. Discrete Algorithms, pp. 175–183, Atlanta, USA, January, 1996.

[3] E. D. Demaine and J. O'Rourke, Geometric Folding Algorithms: Linkages, Origami, and Polyhedra, Cambridge University Press, Cambridge, 2007.

[4] E. D. Demaine, private communications, 2016.

Continuous Flattening of the 2-Dimensional Skeleton of a Regular 24-Cell

Jin-ichi Itoh[1] and Chie Nara[2]

[1] School of Education, Sugiyama Jyogakuen University, Chikusa-ku, Nagoya, Japan,j-itoh@sugiyama-u.ac.jp
[2] Meiji Institute for Advanced Study of Mathematical Sciences, Meiji University, Nakano, Tokyo 164-8525, Japan, cnara@jeans.ocn.ne.jp

Abstract. It is known that we can continuously flatten the surface of any given regular polyhedron onto any of its faces by moving creases to change the shapes of some faces successively. This result was extended by the authors to regular polytopes such as simplexes, hypercubes, and cross-polytopes. There are three more types of regular polytopes, the 24-cell, the 120-cell, and the 600-cell. In this talk we show that for a regular 24-cell P the 2-dimensional skeleton of P can be continuously flattened onto any of its faces F so that 9/16 of the edges and all six faces parallel to F are rigid during the motion.

1 Introduction

Can we flatten a polyhedron of flexible material such as a piece of paper without cutting and stretching? (See [1]). We proved in [4] that there are infinitely many ways to do so for a convex polyhedron. In this paper we work on a related topic for higher dimensional polytopes.

Definition 1. *Let P be an n-dimensional regular polytope. Let S be the set of the 2-dimensional faces in P. We call S the 2-dimensional skeleton (2-skeleton for short) of P.*

The authors showed in [2, 3] that for any dimension n the 2-skeleton S of each of an n-hypercube, n-simplex, and n-cross-polytope can be continuously flattened onto any of its 2-dimensional face F so that a large number of the edges are rigid and that in the case of hypercube all the square faces parallel to F are rigid during the motion. For the 4-dimensional case, there are three more types of regular polytopes, the 24-cell, the 120-cell, and the 600-cell. In this talk we work on the 24-cell.

A regular 24-cell is composed of 24 regular octahedra. Let Q be the cuboctahedron in the 4-dimensional Euclidean space with x-, y-, z-, and w-axes, whose 12 vertices are $(\pm1, \pm1, 0, 0)$, $(\pm1, 0, \pm1, 0)$, and $(0, \pm1, \pm1, 0)$ (see Fig. 1 (a)). Let W^+ and W^- be regular octahedra with vertices $(\pm1, 0, 0, \epsilon)$, $(0, \pm1, 0, \epsilon)$, and $(0, 0, \pm1, \epsilon)$ where $\epsilon = \pm1$, respectively (Fig. 1 (b)). The surface of the convex hull of the union $Q \cup W^+ \cup W^-$ is a regular 24-cell and denoted by P. Note that lengths of its edges are all equal to $\sqrt{2}$.

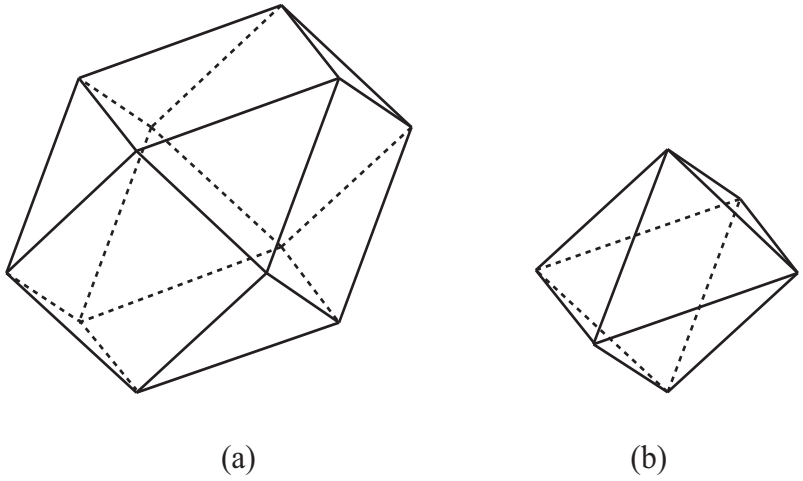

Fig. 1. A regular 24-cell: (a) A cuboctahedron in xyz-space with $w = 0$; (b) a regular octahedron congruent to the one in the hyperspace with $w = 1$ or $w = -1$.

2 Theorem

A regular 24-cell P is composed of 24 vertices, 96 edges, and 96 faces.

Theorem 1. *Let P be a regular 24-cell. There is a continuous folding process from the 2-dimensional skeleton of P onto the surface of an octahedron congruent to a facet of P so that 72 edges are rigid and each of the other 24 edges is deformed into two connected edges folded at its midpoint, and that 24 faces are rigid during the motion.*

We also show that the 2-skeleton of a regular 24-cell can be continuously folded onto any of its faces F so that 54 edges and all six faces parallel to F are rigid during the motion.

References

1. E. D. Demaine and J. O'Rourke, *Geometric Folding Algorithms: Linkages, Origami, Polyhedra*, Cambridge University Press, 2007.
2. J. Itoh, C. Nara, Continuous flattening of the 2-dimensional skeleton of the square faces in a hypercube. Submitted.
3. J. Itoh, C. Nara, Continuous flattening of the 2-dimensional skeletons of higher-dimensional simplexes and cross-Polytopes. Submitted.
4. J. Itoh, C. Nara, and C. Vîlcu, Continuous flattening of convex polyhedra. In *Revised Papers, 16th Spanish Meeting on Computational Geometry (EGC 2011)*, LNCS, vol. 7579, pp. 85–97. Springer, 2012.

Efficient Algorithm for $2 \times n$ Map Folding with Diagonal Creases

Yiyang Jia[1], Jun Mitani[1], and Ryuhei Uehara[2]

yiyangjia@cgg.cs.tsukuba.ac.jp, mitani@cs.tsukuba.ac.jp, uehara@jaist.ac.jp
[1] Tsukuba University, Japan.
[2] School of Information Science, JAIST, Japan.

1 Introduction

In computational origami, one of the most popular problems is the *flat folding*, which asks whether a given crease pattern can be folded in flat or not. When a given crease pattern has only one vertex at the center, the flat folding problem asks the *local flat foldability*. For this simple and basic problem, two conditions about angles and assignment of mountain/valley foldings are well known:

[**Kawasaki=Justin Theorem**] For a vertex to be flat-foldable, the alternate angles between adjacent creases must sum up to π.

[**Maekawa=Justin Theorem**] For a vertex to be flat-foldable, the difference of the numbers of its related creases assigned to be mountain and valley is ± 2.

However, when a given crease pattern contains n vertices, the *global flat foldability* is intractable. Since Bern and Hayes first showed that the flat folding problem is NP-hard in general [3], this problem has been widely investigated in many variants.

As a simpler version, map folding problem has been studied for almost 40 years. However, even in this restricted case, there are still many unsolved problems [2]. In the basic map folding problem, a map is defined by a rectangular sheet with a grid pattern. Specifically, the sheet is partitioned into an $m \times n$ regular square grid. Its mountain-valley assignment is defined as a mapping from the collection of non-boundary grid edges to the set $\{M, V\}$, where M and V mean mountain and valley foldings, respectively.

In [2], they mainly investigate the map folding problem on a *simple folding model*. In this simple model, they show weakly NP-completeness for the map folding problem for maps of size $m \times n$. Recently, some hardness results are extended and strengthened to more general simple folding models in [1].

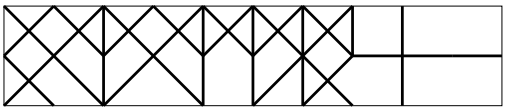

Figure 1: An instance of our problem.

When we turn to the general folding model, the map folding problem asks if a feasible folded state consistent to a given crease pattern with/without MV assignment exists or not. This problem has the different aspect comparing to the simple folding model.

The MV assignment apparently has a significant effect on the difficulty of the map folding problem. Conversely, it is trivial to fold any ordinary square grid without MV assignment. From this viewpoint, two extensions are investigated. One is the extension from square grids to square and diagonal grids, which means, diagonal crease lines of angle 45° are allowed. The other is assigning "not folded" besides M and V, that is, allowing some crease lines in the grid not folded. Both of them are natural assumptions from the viewpoint of origami.

In this context, recently, the map folding problem of size $1 \times n$ is investigated by the first two authors [4]. Namely, an instance is a paper strip of size $1 \times n$, with a crease pattern as a part of a square and diagonal grid, and with no MV assignment. In this case, they proved that every such instance can be folded in flat. In this paper, we extend this result to a map of size $2 \times n$ (Figure 1). The main theorem is as follows:

Theorem 1.1 *Let P be a sheet of paper of size $2 \times n$ with a crease pattern. Here, the crease pattern is a subgraph of a square and diagonal grid of size $2 \times n$, and MV assignment is not given. Then, any P satisfying local flat foldability can be folded in flat. Moreover, a corresponding folding motion can be found in linear time.*

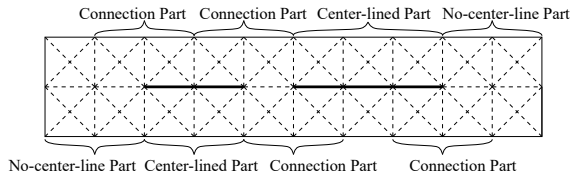

Figure 2: A separation with respect to the horizontal center line (Sections each with two, one, or none horizontal crease belongs to a center-line part, a connection section, or a no-center-line part, respectively).

Collections	Patterns	Operations
Center-lined Part	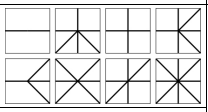	Direct Folding
Connection Part	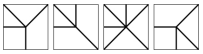	
No-center-line Part	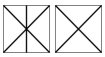	
	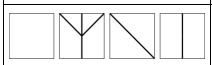	Combination Folding

Table 1. Patterns and way of folding.

2 Outline of the Proof

For a given P, the vertices inside of P can be classified into two groups. The first group consists of the vertices that can have the degree at most 4 in the crease pattern. A previous work in [4] about maps of size $1 \times n$ provides some available results, while it only analyzed the properties of the degree at most 4 in the crease pattern. Since our study is about maps of size $2 \times n$, the other group consisting of the vertices each has a degree at most 8 in the crease pattern becomes the main target through our proof.

Based on analysis on the second group, we give a general way to fold P to a zigzag pleat. The key to avoid self-intersection during the folding is: Always keeping the layers already folded below the ones to be folded along a fixed direction. In the proof, we analyze a set Ω composed by $n-1$ consecutive sections, each of which is a square of size 2×2 (whose center points are the vertices from the second group). P can be flat-folded via a folding process f if (1) each element in Ω satisfies no self-intersection happens within itself, and (2) the sections left to it in the initial state are folded to layers below it while the sections right to it are folded to layers above it.

We here give a brief idea for proving claim (2). For a vertex in the second group, there are 18 patterns with respect to symmetry if it is locally flat-foldable. These patterns and their corresponding way of folding are summarized in Table 1. The patterns are classified into three groups with respect to the number of creases k on the horizontal line as *Center-lined Part* ($k = 2$), *Connection Part* ($k = 1$), and *No-center-line Part* ($k = 0$) in Figure 2. The way of folding is mainly decided by this classification as shown in Table 1. Every section is considered to be folded with either *Direct Folding* (fold without any unfold operation) or with *Combination Folding* (a combination of both fold and unfold operations). The outline of our proof is as follows: First, show that every *Center-lined Part* and every *No-center-line Part* can be folded into a zigzag pleat with a corresponding folding operation respectively; Then, prove that every possible *Connection Part* between a *Center-lined Part* and a *No-center-line Part* can be effectively folded in order to obtain a final flat-folded state of P without self-intersection. During each step, we specify reasonable MV assignments for each pattern itself and the possible combinations involving it, which always leads to a flat-folded state in the shape of a zigzag pleat. Based on the MV assignment given step by step and a combination of these folding operations, P can be folded into a zigzag flat-folded state.

Throughout these operations, we can conclude that P can be folded flat if and only if each of the vertices inside of P is locally flat-foldable. Therefore, we can decide it in linear time by checking locally one by one.

References

[1] H. A. Akitaya, E. D. Demaine, and J. S. Ku. Simple Folding is Really Hard. *Journal of Information Processing*, 25:580–589, 2017.

[2] E. M. Arkin, M. A. Bender, E. D. Demaine, M. L. Demaine, J. S. B. Mitchell, S. Sethia, and S. S. Skiena. When Can You Fold a Map? *Computational Geometry: Theory and Applications*, 29(1):23–46, 2002.

[3] M. Bern and B. Hayes. The Complexity of Flat Origami. In *Ann. ACM-SIAM Symposium on Discrete Algorithms*, pages 175–183. ACM, 1996.

[4] Y. Jia, Y. Kanamori, and J. Mitani. Flat-foldability for $1 \times n$ maps with square/diagonal grid patterns. In *International Conference and Workshop on Algorithms and Computation (WALCOM 2019)*, pages 135–147. Lecture Notes in Computer Science Vol. 11355, Springer-Verlag, 2019.

Maximum Overlaps of Folded Triangles and Quadrilaterals

Mikio Kano* Evangelos Kranakis† Toshinori Sakai‡
Jorge Urrutia§

Extended Abstract

Let $\triangle ABC$ denote a triangle with vertices A, B and C. A *non-obtuse* triangle is a triangle without an obtuse angle. For a connected plane figure F, let $\mathcal{L} = \mathcal{L}_F$ denote the set of straight lines in the plane, intersecting F. For $\ell \in \mathcal{L}$, let $\mathrm{ov}(F;\ell)$ denote the area of the overlap of F for the folding along ℓ (Figure 1). For a measurable subset S in the plane, let $m(S)$ denote the area of S.

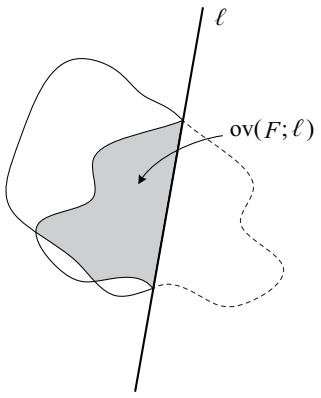

Figure 1: A folding and the overlap.

For a triangle $\triangle ABC$, write $|BC| = a$, $|CA| = b$, $|AB| = c$, $\angle CAB = \alpha$, $\angle ABC = \beta$ and $\angle BCA = \gamma$, where for two points X and Y, $|XY|$ denotes the length of the line segment XY. In this presentation, we first show the following theorem [1]:

Theorem 1 *For any triangle $\triangle ABC$ with $a \le b \le c$,*

$$\max_{\ell \in \mathcal{L}} \frac{\mathrm{ov}(\triangle ABC;\ell)}{m(\triangle ABC)} = \max\left\{ \frac{b}{b+c}, \frac{a}{a+b}, \frac{c^2}{2c^2+b^2-a^2} \right\}.$$

More specifically, the maximum is $b/(b+c)$, $a/(a+b)$ or $c^2/(2c^2+b^2-a^2)$ if the point $(a/c, b/c)$ belongs to the region I, II or III in Figure 2, respectively.

*Ibaraki University, Japan, mikio.kano.math@vc.ibaraki.ac.jp
†Carleton University, Canada, kranakis@scs.carleton.ca
‡Tokai University, Japan, sakai@tokai-u.jp
§Universidad Nacional Autónoma de México, México, urrutia@matem.unam.mx

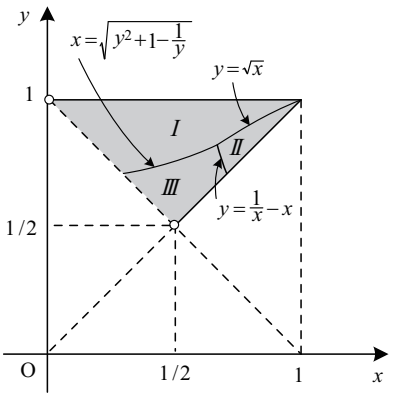

Figure 2: The regions I, II and III. (Since $a \leq b \leq c$ by assumption and since $c < a + b$ by the triangle inequality, we have $x \leq y \leq 1 < x + y$, where $x = a/c$ and $y = b/c$.)

As immediate corollaries, we obtain:

Corollary 1 *For any triangle $\triangle ABC$,*

$$\max_{\ell \in \mathcal{L}} \frac{\mathrm{ov}(\triangle ABC; \ell)}{m(\triangle ABC)} > \sqrt{2} - 1 = 0.41421... \left(= \frac{1}{\sqrt{2}+1} \right),$$

and this bound is tight.

Corollary 2 *For any non-obtuse triangle $\triangle ABC$,*

$$\max_{\ell \in \mathcal{L}} \frac{\mathrm{ov}(\triangle ABC; \ell)}{m(\triangle ABC)} \geq \frac{1}{\sqrt[3]{2}+1} = 0.44249...,$$

and this bound is tight.

For a convex quadrilateral Q, we label its vertices by A, B, C and D in this order along the perimeter, in such a way that

$$\angle DAB + \angle ABC \leq \pi \quad \text{and} \quad \angle CDA + \angle DAB \leq \pi. \tag{1}$$

Theorem 2 *For a convex quadrilateral Q with (1), $AC \geq AD$ and $AC \geq AB$,*

$$\max_{\ell \in \mathcal{L}} \frac{\mathrm{ov}(Q; \ell)}{m(Q)} \geq \frac{\sqrt{2}+1}{6} = 0.40236....$$

We also show some other results for convex quadrilaterals.

References

[1] Kano, M., Kranakis, E., Sakai, T.,Urrutia, J.: Maximum overlaps of folded triangles. submitted.

Enumerating associative magic squares of order 7

Go Kato*[1] and Shin-ichi Minato†[1]

[1]Kyoto University

A magic square of order n is an $n \times n$ square grid such that the sums of the numbers in each row, column, and diagonal are equal. An associative magic square is a magic square such that the sum of any 2 cells at symmetric positions with respect to the center is constant. Although it is known that there are many associative magic squares of order 7, the exact number was not known until this report. The total number of associative magic squares of order 7 is enormous, and thus, it is not realistic to obtain the number by simple backtracking. As a recent result, Artem Ripatti reported the number of semi-magic squares of order 6 (the magic squares of 6×6 without diagonal sum conditions) in 2018[1]. In this research, with reference to Ripatti's method of enumerating semi-magic squares, we have calculated the total number of associative magic squares of order 7. There are exactly 1,125,154,039,419,854,784 associative magic squares of order 7, excluding symmetric patterns.

In Ripatti's paper, he considered some equivalent classes, defined the representative patterns and counted only representative patterns. Then, he divided squares into two parts and enumerates each part independently. Finally, he combined the results of each part to get the total number of semi-magic squares of order 6. We extend Ripatti's method for semi-magic squares to associative magic squares and propose an algorithm to calculate the number of associative magic squares of order 7.

Associative magic squares of order 7 can be transformed into $48 \times 48 = 2304$(48 row rearrangements and 48 column rearrangements) associative magic squares by symmetrical swapping of rows and columns with respect to the center as exemplified in Figure 1. We define a canonical associative magic square of order 7 that represents the 2304 associative magic squares made by the transformations, and count only the canonical associative magic squares.

It is an important issue how to split the square to enumerate each part independently. We can enumerate 3 center rows and 4 outer rows more independently than many other partitions. Thus, we will consider counting associative magic squares of order 7 by dividing up the square as shown in Figure 2.

*kato.go.46a@st.kyoto-u.ac.jp

†minato@i.kyoto-u.ac.jp

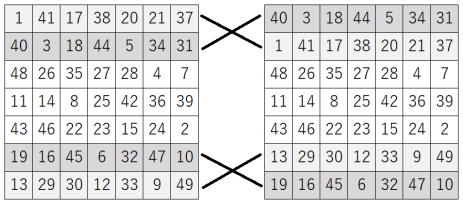

1	41	17	38	20	21	37
40	3	18	44	5	34	31
48	26	35	27	28	4	7
11	14	8	25	42	36	39
43	46	22	23	15	24	2
19	16	45	6	32	47	10
13	29	30	12	33	9	49

40	3	18	44	5	34	31
1	41	17	38	20	21	37
48	26	35	27	28	4	7
11	14	8	25	42	36	39
43	46	22	23	15	24	2
13	29	30	12	33	9	49
19	16	45	6	32	47	10

Figure 1: one of 48 row rearrangements

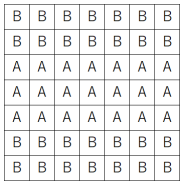

B	B	B	B	B	B	B
B	B	B	B	B	B	B
A	A	A	A	A	A	A
A	A	A	A	A	A	A
A	A	A	A	A	A	A
B	B	B	B	B	B	B
B	B	B	B	B	B	B

Figure 2: 3 center rows and 4 outer rows

Let S_A be the set of elements in the center part and S_B be the set of elements in the outer part. We count canonical associative magic squares for each (S_A, S_B). Let X_{ij} be the i-th row, j-th column element of the square. We define the profile of the center parts as $(\sum_{i=3}^{5} X_{i1},\ \sum_{i=3}^{5} X_{i2},\ \sum_{i=3}^{5} X_{i3})$ and define the profile of the outer parts as $(175 - X_{11} + X_{21} + X_{61} + X_{71}, 175 - X_{12} + X_{22} + X_{62} + X_{72}, 175 - X_{13} + X_{23} + X_{63} + X_{73})$. In these definitions, the center part and the outer part must have the same profile in order for the combination of the center and the outer part to become an associative magic square. Therefore, for each profile p, we can count the number of canonical center parts $N_A[p]$ and canonical outer parts $N_B[p]$ then calculate the number of canonical associative magic squares in one pair (S_A, S_B) as $\sum_p (N_A[p] \times N_B[p])$

We have calculated the total number of associative magic squares of order 7 up to reflections and rotations: 1,125,154,039,419,854,784. This is the first result to show the exact number of 7×7 associative magic squares. The calculation was executed on 16 threads, and took about 2 weeks. We submitted our results to the On-Line Encyclopedia of Integer Sequences (OEIS), and it was accepted on December 10, 2018[2].

Walter Trump[3] estimated the number of associative magic squares of order 7 to be within the range $(1.125151 \pm 0.000051) \times 10^{18}$ with a probability of 99 %. Our result, 1,125,154,039,419,854,784, is within the range of this estimate. Trump also confirmed the number of 7×7 associative magic squares of one (S_A, S_B) with backtracking and confirmed our total results with his own program based on our method. Our results have been confirmed by a probabilistic estimation, Trump's implementation, and some properties of associative magic squares.

References

[1] A. Ripatti. On the number of semi-magic squares of order 6. arXiv preprint arXiv:1807.02983. 2018

[2] The On-Line Encyclopedia of Integer Sequences, published electronically at https://oeis.org, 2018, Sequence A081262

[3] W. Trump. How many magic squares are there? http://www.trump.de/magic-squares/howmany.html (2018.12.14).

Constructive Characterization of Critical Bidirected Graphs

Nanao Kita
Tokyo University of Science
kita@rs.tus.ac.jp

In this talk, we define a class of bidirected graphs called *radials* that is a generalization of factor-critical graphs in matching theory, and provide a constructive characterization of radials that contains Lovász's classical theorem on factor-critical graphs. This is a piece from a series of works that establish a strong component decomposition for bidirected graphs with respect to directed trails.

Bidirected graphs are a common generalization of digraphs and signed graphs. A *bidirected graph* is a graph in which a sign + or − is assigned to each end of each edge. A *digraph* is a special bidirected graph in which the ends of an edge have distinct signs. A *signed graph* is a graph in which a single sign is assigned to each edge, and can be considered as a bidirected graph in which the ends of each edge have the same sign. The concept of bidirected graphs is first proposed by Edmonds and Johnson [1] in 1970 to provide an integer linear programming framework that integrates various problems in matchings, coverings, and network flows.

We can naturally define a bidirected counterpart of directed paths (*dipaths*) and trails (*ditrails*) in digraphs; however, we should note that general bidirected graphs have the following two features that digraphs do not possess, which make the structure of bidirected graphs rich and complicated. First, general bidirected graphs have four types of dipaths or ditrails, that is, dipaths or ditrails that start and end with − and − or + and +, in addition to those with + and − or − and +. Second, in bidirected graphs, even if two vertices are connected by a ditrail, it does not necessarily follow that these vertices are connected by a dipath. This implies that we need distinct strong connectivity theories for bidirected graphs, that is, those regarding dipaths and ditrails.

We define *radials* as follow: a bidirected graph with a vertex r is a radial with root r if every vertex can reach r with a ditrail starting and ending with − and +, respectively. Radials are a common generalization of the *factor-critical graphs* and *flowgraphs*. An undirected graph is *factor-critical*

if deleting any arbitrary single vertex makes a graph with perfect matchings. Under the correspondence between matchings in undirected graphs and a special singed graphs, factor-critical graphs corresponds to a special class of radials. Factor-critical graphs are a classical concept in matching theory and appear in the Gallai-Edmonds structure theorem and Edmonds' blossom algorithm for solving the maximum matching problem [2]. In 1972, Lovász gave a constructive characterization of the factor-critical graphs that uses the ear decomposition. This celebrated characterization has shown its power in numerous works in matching theory where the Gallai-Edmonds structure theorem or the maximum matching problems are involved. A digraph with root r is a *flowgraph* with root r if every vertex can reach r with a directed path. From the strong component decomposition for digraphs and the classical characterization of strongly connected digraphs that uses the ear decomposition, a constructive characterization of flowgraphs is obvious.

In this study, we provide a constructive characterization of the radials. This is a common generalization of the above mentioned Lovász's characterization of factor-critical graphs and the characterization of flowgraphs. We first define *semiradials*, a wider concept that includes radials. We then define two classes of semiradials: *absolute* semiradials and *linear* semiradials. Two special classes are also defined for the first one: *strong* radials and *almost strong* radials. We provide constructive characterizations for each of these four classes of radials or semiradials, and then use characterization to obtain a constructive characterization of general radials.

References

[1] J. Edmonds and E. L. Johnson, *Matching: a well-solved class of integer linear programs*, Combinatorial structures and their applications, 1970, pp. 89–92.

[2] L. Lovász and M. D. Plummer, *Matching theory*, AMS Chelsea Publishing, 2009.

A Phase Transition Concerning the Boundedness of Orbits on a Pointset

Evangelos Kranakis[1,2]

[1] School of Computer Science, Carleton University, Ottawa, Ontario, Canada.
[2] Research supported in part by NSERC Discovery grant.

Abstract. We investigate the phase transition of a dynamical system generating an infinite orbit of points. The points of the orbit are generated according to the following basic *antipodal operation*. Given a positive real number a, called the expansion factor, and two points p, q at Euclidean distance $|pq|$ we determine the unique point p' on the straight line passing through p and q which is antipodal to the point p with respect to q and at Euclidean distance $a|pq|$ from q. The operation on points previously defined is denoted by $p \Rightarrow_{a,q} p'$.

Let $\mathbf{a} := (a_0, a_1, \ldots, a_{n-1})$ be an arbitrary but fixed positive real numbers and $\mathbf{q} := (q_0, q_1, \ldots, q_{n-1})$ n (anchor) points. An orbit consisting of an infinite sequence $p_0, p_1, \ldots, p_m, \ldots$ of points in the plane is generated by using the anchor points as follows. The orbit is initiated with the point $p_0 := p$ and for all integers $m \geq 1$, satisfies $p_m \Rightarrow_{a_{m \bmod n}, q_{m \bmod n}} p_{m+1}$ so that $p_{m+1} := (p_m)'$; the resulting sequence of points is called the $(\mathbf{a}, \mathbf{q})$-orbit of p.

For any starting point p and any pair $(\mathbf{a}, \mathbf{q})$ we characterize the boundedness of $(\mathbf{a}, \mathbf{q})$-orbits. Namely, it is shown that there is a phase transition concerning the boundedness of the resulting $(\mathbf{a}, \mathbf{q})$-orbit which depends on whether or not the product of the expansion factors is less than one, i.e., $a_0 a_1 \cdots a_{n-1} < 1$. The "boundedness" phase transition phenomenon described above is shown to be valid for any dimension $d = 1, 2, 3$ in the Euclidean space.

Boundedness of Orbits from Anchor Points

We consider a new problem on the boundedness of orbits. Suppose that n points $\mathbf{q} = (q_0, q_1, \ldots, q_{n-1})$, also called *anchors*, are located in arbitrary but fixed positions in the plane. Further, assume that each point q_i is associated with a positive real number a_i called the *expansion factor* (or *ratio*) of q_i. Let $\mathbf{a} = (a_0, a_1, \ldots, a_{n-1})$ be the sequence of expansion factors. Let p be any point in the plane. The $(\mathbf{a}, \mathbf{q})$-orbit with respect to the

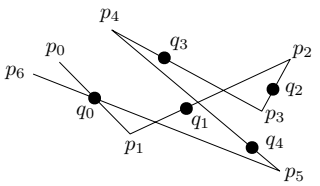

Fig. 1. The first seven points $p_0, p_1, p_2, p_3, p_4, p_5, p_6$ in a $(\mathbf{a}, \mathbf{q})$-orbit with five anchor points q_0, q_1, q_2, q_3, q_4 in the plane and respective expansion ratios a_0, a_1, a_2, a_5, a_4. The sequence of points p_i continues indefinitely.

sequence $\mathbf{q}$ of anchors consists of an infinite sequence $p_0, p_1, \ldots, p_m, \ldots$ of points which is generated by using the antipodal operation (defined in the abstract above) on points $q_0, q_1, \ldots, q_{n-1}$ so that point p_{m+1} is antipodal to p_m with respect to the point $q_{m \bmod n}$ (see Figure 1).

Given the setting considered above we prove the following result concerning the boundedness of orbits generated from an anchor point set.

Theorem 1 (2D Orbits from n anchors). *Consider n anchor points $\mathbf{q} = (q_0, q_1, \ldots, q_{n-1})$ in the plane with corresponding expansion factors $\mathbf{a} = (a_0, a_1, \ldots, a_{n-1})$, respectively, and a point p in the plane.*

1. *If $a_0 a_1 \cdots a_{n-1} > 1$ and the distance of p from the point set $\{q_0, q_1, \ldots, q_{n-1}\}$ is at least*

$$\Omega\left(\delta \max_{1 \le i < b} \left\{ \frac{1}{a_0} + \frac{1}{a_0 \cdots a_i} \right\}\right),$$

   where δ is the diameter of the point set, then p has an unbounded $(\mathbf{a}, \mathbf{q})$-orbit.
2. *If $a_0 a_1 \cdots a_{n-1} < 1$ then p has a bounded $(\mathbf{a}, \mathbf{q})$-orbit.*
3. *If $a_0 a_1 \cdots a_{n-1} = 1$ then p has a bounded $(\mathbf{a}, \mathbf{q})$-orbit for $n > 2$, and an unbounded $(\mathbf{a}, \mathbf{q})$-orbit for $n = 2$.*

The result above generalizes easily to three-dimensional space.

Related Work on Outer Billiards

We now contrast our work with outer billiards, a dynamical system defined in the Euclidean plane which involves a discrete sequence of moves taking place outside a given bounded convex set K. Assume the boundary of K is a convex polygon. In addition, let a be an arbitrary positive real number. To form an outer billiard orbit, one starts with an arbitrary point $p := p_0$ which lies outside the convex polygon K. Draw the straight line emanating from p_0 and intersecting K at a vertex, say p_{01}, so that K is to the right of this line. Let p_1 be the point on this line antipodal to p_0 with respect to p_{01} so that $|p_0 p_{01}| = a|p_{01} p_1|$. The sequence of points resulting when we iterate this operation is called forward a-orbit (see Figure 2). The

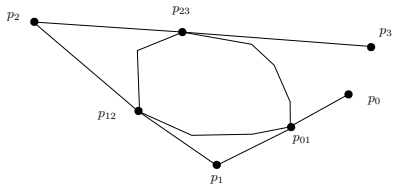

Fig. 2. The first three points p_0, p_1, p_2, p_3 in a a-forward outer billiard (orbit) for a bounded convex polygon with starting point p_0. By reversing direction p_3, p_2, p_1, p_0 this can also be considered as an a-backward orbit.

definition of outer billiard generalizes an analogous definition restricted to $a = 1$ and which can be found in Schwartz [5]. Moser [2][p. 11] attributes the following question to Neumann [3]: Assume $a = 1$. "Is there an outer billiards system with an unbounded orbit?" as an idealized version of the question about the stability of the solar system. Neumann [3] was the first to introduce outer billiards in the late 1950s. In the 1970s, J. Moser [1] popularized outer billiards as a toy model for celestial mechanics. Only outer orbits on Penrose kites are known to be unbounded [4]. For a book length treatment of the topic as well as a chronological list of most of the known work related to the question of the boundedness of the orbit when $a = 1$ the reader is referred to the following book by Schwartz [5]. For general, related work on billiards the reader is referred to the books [6, 7] by Tabachnikov.

References

1. J. Moser. Is the solar system stable? *The Mathematical Intelligencer*, 1(2):65–71, 1978.
2. J. Moser. *Stable and random motions in dynamical systems: with special emphasis on celestial mechanics (AM-77)*. Princeton university press, 2016.
3. B. H. Neumann. Sharing ham and eggs. *Iota, Manchester University*, pages 14–18, 1959.
4. R. E. Schwartz. Unbounded orbits for outer billiards I. *Journal of Modern Dynamics*, 1(3):371–424, 2007.
5. R. E. Schwartz. *Outer Billiards on Kites (AM-171)*, volume 191. Princeton University Press, 2009.
6. S. Tabachnikov. *Billiards*, volume I. Société Mathématique de France, Panoramas et Syntheses, 1995.
7. S. Tabachnikov. *Geometry and billiards*, volume 30. American Mathematical Soc., 2005.

Applications of Combinatorial Nullstellensatz in Additive Coloring of Halin Graphs

Hsin-Hao Lai

Department of Mathematics, National Kaohsiung Normal University, Kaohsiung, Taiwan

hsinhaolai@nknucc.nknu.edu.tw

Let G be a graph. An *additive coloring* of a graph G is a labeling from the vertex set of G to the set of integers such that for every two adjacent vertices the sums of integers assigned to their neighbors are different.

The definition of additive chromatic number was first introduced in [4]. The *additive chromatic number* of G is the least integer k such that G has an additive coloring from the vertex set of G to $\{1, 2, \ldots, k\}$. It is conjectured in [4] that for every graph G, the chromatic number of G is an upper bound of the additive chromatic number of G.

The definition of additive choice number was first introduced in [1]. A *list* L of a graph G is a mapping that assigns a finite set of integers to each vertex of G. A list is a *k-list* if for each vertex is assigned at least k integers. An additive coloring f of G such that $f(v)$ is an element in $L(v)$ for each vertex v is called an *additive L-coloring* of G. The *additive choice number* is the least integer k such that G has an additive L-coloring for any k-list L. The additive choice number is an upper bound of the additive chromatic number for any graph G.

The definition of sigma chromatic number was first introduced in [3]. The *sigma chromatic number* of G is the minimum number of colors required in an additive coloring of G. The additive chromatic number is an upper bound of the sigma chromatic number for any graph G.

A *Halin graph* is a plane graph H constructed as follows. Let T be a tree of order at least 4. All vertices of T are either of degree 1 or of degree at least 3. Let C be a cycle connecting the leaves of T in such a way that C forms the boundary of the unbounded face. The tree T is called the characteristic tree of H.

Combinatorial Nullstellensatz was introduced in [2] and became a powerful tool in many fields of combinatorics, including additive combinatorics, combinatorial geometry and graph theory.

In this paper, I will introduce some applications of Combinatorial Nullstellensatz in the study of additive coloring of Halin graphs and present new upper bounds on additive chromatic number and additive choice number of cubic Halin graphs. And I will prove that if H is a Halin graph and the characteristic tree of H has even leaves, then H has an additive coloring from the vertex set of H to $\{1, 2, d\}$ with d is upper bounded by 1 plus 3 times the maximum degree of H.

Keywords: additive coloring, additive chromatic number, additive choice number, sigma chromatic number, Halin graph, Combinatorial Nullstellensatz.

References

[1] S. Akbari, M. Ghanbari, R. Manaviyat and S. Zare, On the lucky choice number of graphs, Graphs Combin. 29 (2013), 157-163.

[2] N. Alon, Combinatorial Nullstellensatz, Combin. Prob. Comp. 8 (1999), 7-29.

[3] G. Chartrand, F. Okamoto and P. Zhang, The sigma chromatic number of a graph, Graphs Comb. 26 (2010), 755-773.

[4] S. Czerwiński, J. Grytczuk and W. Żelazny, Lucky labelings of graphs, Inform. Process. Lett. 109 (2009), 1078-1081.

An Infinite Series of Counterexamples to the Annihilation Number Conjecture

Eugen Mandrescu
Holon Institute of Technology, Israel

Joint work with Vadim E. Levit, Ariel University, Israel

For a graph G, let $n(G), m(G), \alpha(G), \mu(G)$ denote the order, the size, the cardinality of a maximum independent set, and the cardinality of a maximum matching, respectively. Let $\Omega(G)$ stand for the family of all maximum independent sets. If $\alpha(G)+\mu(G)=n(G)$, then G is a *König-Egerváry graph* [3, 10]. For instance, each tree is a König-Egerváry graph.

Let $d_1 \leq d_2 \leq \cdots \leq d_{n(G)}$ be the degree sequence of a graph G. Pepper [9] defined the *annihilation number* $h(G)$ as the largest integer k such that $\sum_{i=1}^{k} d_i \leq |E|$. For $A \subseteq V$, let $\deg(A) = \sum_{v \in A} \deg(v)$. Every $A \subseteq V$ satisfying $\deg(A) \leq m(G)$ is an *annihilating set*. An annihilating set A is *maximal* if $\deg(A \cup \{v\}) > m(G)$, for every $v \in V - A$, and it is *maximum* if $|A| = h(G)$ [9]. The relation between the annihilation number and various parameters of a graph were studied in [1, 2, 4, 6, 8].

Theorem 1 *[7] For a graph G with $h(G) \geq \frac{n(G)}{2}$, $\alpha(G) = h(G)$ if and only if G is König-Egerváry and every maximum independent set is **maximum** annihilating.*

Conjecture 2 *[7] Let G be a graph with $h(G) \geq \frac{n(G)}{2}$. Then $\alpha(G) = h(G)$ if and only if G is König-Egerváry and every maximum independent set is **maximal** annihilating.*

Consider the tree from Figure 1: T has the degree sequence $(1,1,1,1,1,1,2,2,3,3,4)$, $m(T) = 10$, $h(T) = 8 > \alpha(T)$, $\Omega(T) = \{S\}$, where $S = \{x_1, x_2, x_3, x_4, x_5, x_6, x_7\}$ has $\deg(S) = 8$. Thus S is a (unique) maximum independent set but not a **maximal annihilating set**.

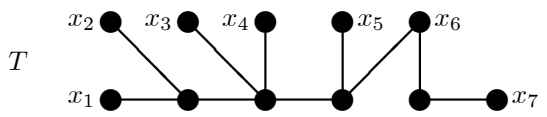

Figure 1: A tree with $\alpha(T) = 7$.

Combining several related results on strong unique maximum independence trees [5], we disprove Conjecture 2, by proving the following.

Theorem 3 *There exist a tree T of order $2k+1, k \geq 4$ and a tree of order $2k+4, k \geq 3$, such that $h(T) \geq \frac{n(T)}{2}$ and each $S \in \Omega(T)$ is a* ***maximal non-maximum*** *annihilating set. For instance, the trees from Figure 2.*

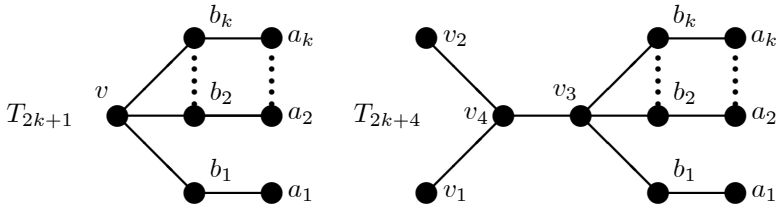

Figure 2: Odd and even tree counterexamples.

References

[1] H. Aram, R. Khoeilar, S. M. Sheikholeslami, L. Volkmann, *Relating the annihilation number and the Roman domination number*, Acta Math. Univ. Comenian. **87** (2018) 1–13.

[2] C. Bujtás, M. Jakovac, *Relating the total domination number and the annihilation number of cactus graphs and block graphs*, Ars Math. Contemp. **16** (2019) 183–202.

[3] R. W. Deming, *Independence numbers of graphs - an extension of the König-Egerváry theorem*, Discrete Math. **27** (1979) 23–33.

[4] W. J. Desormeaux, T. W. Haynes, M. A. Henning, *Relating the annihilation number and the total domination number of a tree*, Discrete Appl. Math. **161** (2013) 349–354.

[5] G. Hopkins, W. Staton, *Graphs with unique maximum independent sets*, Discrete Math. **57** (1985) 245–251.

[6] M. Jakovac, *Relating the annihilation number and the 2-domination number of block graphs*, Discrete Appl. Math. **260** (2019) 178–187.

[7] C. E. Larson, R. Pepper, *Graphs with equal independence and annihilation numbers*, Electron. J. Combin. **18** (2011) #P180.

[8] W. Ning, M. Lu, K. Wang, *Bounding the locating-total domination number of a tree in terms of its annihilation number*, Discuss. Math. Graph Theory **39** (2019) 31–40.

[9] R. Pepper, *On the annihilation number of a graph*, in: Recent Advances in Electrical Engineering: Proc. of the 15^{th} American Conf. on Appl. Math. (2009), 217–220.

[10] F. Sterboul, *A characterization of the graphs in which the transversal number equals the matching number*, J. Combin. Theory **B 27** (1979) 228–229.

SOME GENERATOR SUBGRAPHS OF THE SQUARE OF A CYCLE

Realiza M. Mame[1], Neil M. Mame [2]

[1]Batangas State University, Batangas City, Philippines, email :reamame@yahoo.com.ph

[2]Batangas State University, Batangas City, Philippines, email :mameneil10@yahoo.com

Abstract

Graphs considered in this paper are finite simple graphs. The problem on generator subgraphs of a graph was introduced by Gervacio in 2008. Let G be a graph with $E(G) = \{e_1, e_2, \ldots, e_m\}$, for some positive integer m. The *edge space* of G, denoted by $\mathscr{E}(G)$, is a vector space over the field $\mathbb{Z}_2 = \{0, 1\}$. The elements of $\mathscr{E}(G)$ are all the subsets of $E(G)$. Vector addition is defined as $X + Y = X\Delta Y$, the symmetric difference of X and Y, for $X, Y \in \mathscr{E}(G)$. Scalar multiplication is defined as $1 \cdot X = X$ and $0 \cdot X = \emptyset$, for $X \in \mathscr{E}(G)$. The set $S \subseteq \mathscr{E}(G)$ is called a generating set if every element of $E(G)$ is a linear combination of the elements of S. For a nonempty set $X \in \mathscr{E}(G)$, $G[X]$ denotes the smallest subgraph of G with edge set X. If H is an arbitrary subgraph of G, then the set $E_H(G) = \{A \in \mathscr{E}(G) : G[A] \simeq H\}$ denotes the *uniform set* of H with respect to G while $\mathscr{E}_H(G)$ denotes the subspace of $\mathscr{E}(G)$ generated by $E_H(G)$. If $E_H(G) = \mathscr{E}(G)$, that is $E_H(G)$ is a generating set, then we call H a *generator subgraph* of G. Let x and y are vertices of a graph G. The distance between x and y in G, denoted by $d(x, y)$, is the length of the shortest path joining x and y. The square of the cycle C_n, denoted by C_n^2, is the graph obtained from C_n by adding the edge $[x, y]$ to the cycle C_n if and only if $d(x, y) = 2$. We identify some classes of generator subgraphs of C_n^2. The following are the results:

Theorem 1. *Let p and k are positive integers. Then the star graph S_p is a generator subgraph of C_n^2 if and only if $p = 1$ or $p = 3$.*

Theorem 2. *Let k and n are positive integers. Then the path P_k is a generator subgraph of C_n^2 if and only if k is even and $2 \leq k \leq n$.*

Theorem 3. *Let n and r be positive integers. Then the tadpole graph $T_{3,r}$ is a generator subgraph of C_n^2 if and only if r is even and $2 \leq r \leq n - 3$.*

Moreover, we established a sufficient condition for the generator subgraphs of C_n^2. A *pendant* P_3 in a graph, as defined by Gervacio [5], is an induced subgraph isomorphic to P_3 where one vertex has degree 1, the second vertex is adjacent only to the other two vertices.

Theorem 4. *Let H be a subgraph of C_n^2. If*

i. $|E(H)|$ is odd; and

ii. H contains a pendant P_3

then H is a generator subgraph of C_n^2.

Keywords: Edge Space, Square of a Cycle, Edge-Induced Subgraph, Uniform Set, Generator Subgraph.
Mathematics Subject Classification: 05C25

References

[1] G. Chartrand and P. Zhang, *Introduction to Graph Theory*, Mc Graw Hill, Reading, Singapore, 2005.

[2] S. V. Gervacio, Generator Graphs, *contributed paper,* 4^{th} *International Conference On Combinatorial Mathematics and Combinatorial Computing*,U.A., New Zealand, Dec 15-19, 2008.

[3] Gervacio S. V., M. T. C. Valdez, & D. F. Bengo, Generator Subgraphs of Fans and Wheels, Proc., *Osaka University - De La Salle University Academic Research Workshop*, Manila, August 2008.

[4] S. V. Gervacio & N. M. Mame, Universal and Primitive Graphs, *Proc., Osaka University-De La Salle University Academic Research Workshop*, Manila, August 2007, pp. 51–53.

[5] Gervacio S. V., Determination of Uniform Generating Sets of the Edge Space of Some Graphs, *research project under URCO*, De La Salle University-Manila, April 2009.

[6] N. M. Mame, Generator Subgraphs of Some Classes of Graphs, *Ph.D. Dissertation*, De La Salle University, Taft Avenue Manila, 2011.

[7] N. M. Mame, S. V. Gervacio, Generator Subgraphs of the Wheel, contributed paper, *2016 Asian Mathematical Conference*, Bali, Indonesia, July 2016.

Note on continuous flattening of multilayer pyramidal faces inscribed inside a belt

Kazuki Matsubara[1] and Chie Nara[2]

[1] Faculty of Commerce, Chuo Gakuin University,
Chiba, 270-1196, Japan.
additivestructure@gmail.com

[2] Meiji Institute for Advanced Study of Mathematical Sciences,
Meiji University, Tokyo, 164-8525, Japan.
cnara@jeans.ocn.ne.jp.

We use the terminology *polyhedron* for a polyhedral surface in $\mathbb{R}^3$ which is permitted to touch itself but not self-intersect. A *flat folding* of a polyhedron is a folding by creases, without self-crossing, into a multilayered flat folded state so that the number of creases is finite. There are several ways to continuously flatten polyhedra in [1–5]. Recently, the second author proposed the problem of continuous flattening of polyhedra with some divisions, i.e., some of whose edges are incident to three or more faces (see [6]). In this talk, we mean a belt as the set of side faces of a right prism, and call a set of (multilayer) pyramidal faces (or polygonal faces) inscribed inside the belt a *pyramidal complex*. We discuss continuous flattening of pyramidal complexes.

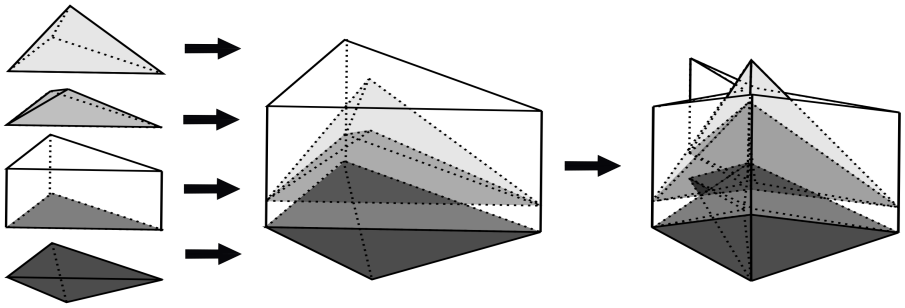

Figure 1: A flattening motion of a pyramidal complex composed of 4-layers inscribed inside a belt.

Figure 1 shows an example of continuous flattening of a pyramidal complex of 4-layers composed of three pyramidal faces and a base of the belt. By further elaboration of the folding methods discussed in [4,5], continuous flattening motions of various type of pyramidal complexes can be obtained.

For each pyramidal face composed of n triangles, each of n edges adjacent to the top vertex and each of n bottom edges are called a *radial edge* and a *horizontal edge*, respectively. Especially, we focus on the continuous flattening motion so that every radial edge is rigid. This implies that every radial edge

can be made by rigid materials.

The purpose of this talk is to find continuous flattening motions for some classes of pyramidal complexes so that every radial edge is rigid. We provide some conditions for the existence of continuous flattening motions of pyramidal complexes, and also present an example which does not satisfy those conditions and cannot be flattened continuously in our method. Furthermore, we discuss the rigidity of the horizontal edges during the flattening motions.

References

[1] Z. Abel, E. D. Demaine, M. L. Demaine, J. Itoh, A. Lubiw, C. Nara, and J. O'Rourke, Continuously flattening polyhedra using straight skeletons, *Proc. 30th Annual Symposium on Computational Geometry (SoCG)*, pp. 396–405 (2014).

[2] E. D. Demaine and J. O'Rourke, *Geometric Folding Algorithms: Linkages, Origami, Polyhedra*, Cambridge University Press (2007).

[3] J. Itoh, C. Nara and C. Vîlcu, Continuous flattening of convex polyhedra, *Proc. 16th Spanish Meeting on Computational Geometry (EGC 2011)*, LNCS, Vol. 7579, pp. 85–97, Springer (2012).

[4] K. Matsubara and C. Nara, Continuous flattening of α-trapezoidal polyhedra, *J. Inf. Process.* Vol. 25, pp. 554–558 (2017).

[5] C. Nara, Continuous flattening of some pyramids. *Elem. Math.* Vol. 69(2), pp. 45–56 (2014).

[6] C. Nara and J. Itoh, Continuous flattening of extended bipyramids with rigid radial edges. In The Proceedings from 7OSME, 2, tarquin, Oxford, 561–571 (2018).

On the diameter of bisubmodular polyhedra

Yasuko Matsui[*] Noriyoshi Sukegawa[†] Ping Zhan[‡]

1 Introduction

Finding good upper bounds on the diameter of polyhedra is a fundamental problem in polyhedral combinatorics theory. The diameter $\delta(P)$ of a polyhedron P is the graph diameter of its 1-skeleton. In other words, it is the smallest number k such that every pair of the vertices of P can be connected by using at most k edges of P.

The diameter of polyhedra has an important application in complexity analyses of the simplex method. In this context, a major open problem is the polynomial Hirsch conjecture, which asks for a polynomial upper bound $p(d, n)$ on the maximum possible diameter of d-dimensional polyhedron with n facets; see e.g. [6, 10]. Another major open problem is concerned with lattice polytopes, to which one can apply more geometrical tools [2, 3, 7].

On the other hand, it is also important to understand the behavior of the diameter using specific polyhedra. A good example would be the zonotope, which was utilized in [4] to analyze the diameter of lattice polytopes. Other important examples are the associahedra [8] and the permutahedra, to which we have the sharp estimates on the diameter.

2 Main result

In this talk, we give a sharp estimate on the diameter of the bisubmodular polyhedra. The bisubmodular polyhedron generalizes several important polyhedra and is related to the permutahedron since a permutahedron can be regarded as a facet of a submodular polyhedron.

For a finite set D with size d, let $3^D = \{(X, Y) \mid X, Y \subseteq D, X \cap Y = \emptyset\}$. We define two binary operations, *reduced union* $\sqcup$ and *intersection* $\sqcap$ on 3^D as

$$(X_1, Y_1) \sqcup (X_2, Y_2) = ((X_1 \cup X_2) - (Y_1 \cup Y_2), (Y_1 \cup Y_2) - (X_1 \cup X_2)),$$
$$(X_1, Y_1) \sqcap (X_2, Y_2) = (X_1 \cap X_2, Y_1 \cap Y_2)$$

for each $(X_1, Y_1), (X_2, Y_2) \in 3^D$. A function $f : 3^D \to \mathbb{R}$ is called *bisubmodular* if

$$f(X_1, Y_1) + f(X_2, Y_2) \geq f((X_1, Y_1) \sqcup (X_2, Y_2)) + f((X_1, Y_1) \sqcap (X_2, Y_2))$$

holds for each $(X_1, Y_1), (X_2, Y_2) \in 3^D$. A polyhedron defined by

$$\mathrm{P}(f) = \left\{ x \ ; \ x \in \mathbb{R}^D, \ \forall (X, Y) \in 3^D, \ \sum_{i \in X} x(i) - \sum_{i \in Y} x(i) \leq f(X, Y) \right\},$$

[*]Department of Mathematical Sciences School of Science, Tokai University; yasuko@tokai-u.jp
[†]Department of Information and Computer Technology, Tokyo University of Science; sukegawa@rs.tus.ac.jp
[‡]Department of Communication and Business, Edogawa University; zhan@edogawa-u.ac.jp

is called *bisubmodular polyhedron* if f is bisubmodular.

We show that the diameter of the bisubmodular polyhedra is at most d^2. Recall that d corresponds to the dimension. We also show that this bound is tight, and is also valid for *monotonic* diameter. The key ingredients of our proof are from [1, 5, 9].

References

[1] K. Ando and S. Fujishige. On structures of bisubmodular polyhedra. *Mathematical Programming* 74 (1996) 293–317.

[2] A. Del Pia and C. Michini. On the diameter of lattice polytopes. *Discrete and Computational Geometry* 55 (2016) 681–687.

[3] A. Deza and P. Lionel. Improved bounds on the diameter of lattice polytopes. *Acta Mathematica Hungarica* 154 (2018) 457–469.

[4] A. Deza. G. Manoussakis, and S. Onn. Primitive zonotopes. *Discrete and Computational Geometry* 60 (2018) 27–39.

[5] S. Fujishige. Submodular Function and Optimization, Second Edition (Elsevier, 2005).

[6] G. Kalai and D.J. Kleitman. A quasi-polynomial bound for the diameter of graphs of polyhedra. *Bulletin of the American Mathematical Society* 26 (1992) 315–316.

[7] P. Kleinschmidt and S. Onn. On the diameter of convex polytopes. *Discrete mathematics* 102 (1992) 75–77.

[8] L. Pournin. The diameter of associahedra. *Advances in Mathematics* 259 (2014) 13–42.

[9] V. Reiner. Signed posets. *Journal of Combinatorial Theory Ser. A* 62 (1993) 324–360.

[10] N. Sukegawa. An asymptotically improved upper bound on the diameter of polyhedra. *Discrete and Computational Geometry*, to appear.

Wythoff's Game with a Pass

Mariko Kashiwagi[1] Akira Murakami[1] Keito Tanemura[1] Itsuki Kitagawa[1]
Kazuya Hiramatsu[1] Masanori Fukui[2] Sintarou Kaimoto [1] Ryohei Miyadera[1]
[1]Kwansei Gakuin University / High School [2]Hiroshima University

1. Wythoff's Game

We study a variant of the classical Wythoff's game. The classical Wythoff's game is played with two piles of stones, and two players take turns to remove stones from one or both piles. When removing stones from both piles, an equal number must be removed from each. The player who removes the last stone(s) is the winner.

An interesting question in combinatorial game theory has been to determine what happens when the rules are modified to allow for a one-time pass, that is, a pass move that may be used at most once in a game, and not from a terminal position. Once the pass has been used by either player, it is no longer available. Combinatorial games with a pass have been studied by many mathematicians (see [2] and [3]); however, difficulties related to the underlying structure of the game and the theory of games with a pass have not yet been resolved. The classical Nim with three piles becomes a very complicated game when the pass move is introduced. The authors have also studied a combinatorial game with a pass; see [1].

In the present research, the authors studied Wythoff's game with a pass and discovered the following facts (a) and (b). Fact (a) may be surprising for some experts of combinatorial game theory, and (b) follows from (a) and the result of Horrocks and Nowakowski [3].
(a) When the pass move is still available, the $\mathcal{P}$-positions of the Wythoff's game with a pass are almost the same as those of Grundy value 1 in Wythoff's original game.
(b) The graph of $\mathcal{P}$-positions in Wythoff's game with a pass when the pass is still available is very similar to the graph of $\mathcal{P}$-positions in the classical Wythoff's game.
We denote by $\{x, y, p\}$ the condition of the game, where x, y define the numbers of stones on the piles, and additional parameter p denotes whether the pass is still available ($p = 1$) or has already been used ($p = 0$). When $p = 0$, the game is mathematically identical to the classical Wythoff's game.

Definition 1. We define the movements of stones in Wythoff's game with a pass as follows.
(i) For $x, y \in Z_{\geq 0}$, let $move(x, y, p) = \{(x - s, y, p) : 1 \leq s \leq x\} \cup \{(x, y - t, p) : 1 \leq t \leq y\} \cup \{(x - s, y - s, p) : 1 \leq s \leq \min(x, y)\} \cup \{(x, y, 0)\}$ if $x + y > 0$ and $p = 1$.
(ii) $move(x, y, p) = \{(x-s, y, p) : 1 \leq s \leq x\} \cup \{(x, y-t, p) : 1 \leq t \leq y\} \cup \{(x-s, y-s, p) : 1 \leq s \leq \min(x, y)\}$ if $x + y = 0$ or $p = 0$.

We review some necessary concepts in combinatorial game theory; see [6].

Definition 2. (i) The *minimum excluded value* (*mex*) of a set S of non-negative integers is the least non-negative integer that is not in S.
(ii) Each position (x, y, p) has an associated Grundy number $\mathcal{G}(x, y, p)$.
The Grundy number is calculated recursively as $\mathcal{G}(x, y, p) = mex\{\mathcal{G}(u, v, q) : (u, v, q) \in move(x, y, p)\}$.
Two positions of the game are of particular importance:
(iii) From $\mathcal{N}$-positions, the next player can force a win, as long as the player plays correctly at every stage.
(iv) From $\mathcal{P}$-positions, the previous player (who will play again after the next player) can force a win, as long as that player plays correctly at every stage.

Theorem 1. (x, y, p) is a $\mathcal{P}$-position if and only if $\mathcal{G}(x, y, p) = 0$.

This is a well-known theorem, and the positions of Grundy value 0 are important because of this theorem.

Definition 3. Let $A = \{(0, 1), (1, 0), (2, 2), (3, 6), (6, 3), (5, 7), (7, 5)\}$ and $B = \{(0, 0), (1, 3), (3, 1), (2, 5), (5, 2), (6, 7), (7, 6)\}$.

The following theorem proves fact (a).

Theorem 2. $\{(x, y) : \mathcal{G}(x, y, 1) = 0\} = \{(x, y) : \mathcal{G}(x, y, 0) = 1\} \cup B - A$.

$\mathcal{G}(x, y, 1) = 0$ if and only if $(x, y, 1)$ is the $\mathcal{P}$-position of the Wythoff's game with a pass when the pass move is still available, and $\mathcal{G}(x, y, 0) = 1$ if and only if $(x, y, 0)$ is the position of Grundy value 1 of Wythoff's original game. Therefore, by Theorem 2 and the fact that A and B are a finite set with eight elements, we prove fact (a).

Lemma 1. For each position $(x, y) \in T_1$, there exists some $(x', y') \in T_0$ such that $\mid x - x' \mid \leq 2$ and $\mid y - y' \mid \leq 4$.

Proof. This follows from Corollary 5.14 in [5]. □

By Lemma 1 and Theorem 2, the graph in Figure 1 is very similar to the graph in Figure 2, which is in line with fact (b) mentioned earlier.

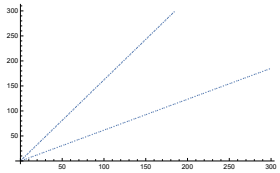

Figure 1. Graph of $\mathcal{P}$-positions in the classical Wythoff's game.

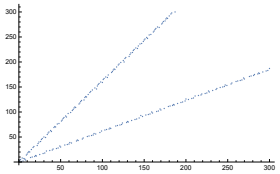

Figure 2. Graph of $\mathcal{P}$-positions in the Wythoff's game with a pass when the pass is still available.

By Theorem 2, we prove that when the pass move is still available, $\mathcal{P}$-positions of the Wythoff's game with a pass are almost the same as the positions of Grundy value 1 of Wythoff's original game.

Then, it is natural to look for other combinatorial games that have the same type of features. There are variants of Wythoff's game very similar to the original Wythoff's game. What type of features do these games have when we introduce a pass move?

Definition 4. (i) A variant of Wythoff's game wherein the players are not allowed to remove stones from the smaller pile when the two entries are not equal.
(ii) A variant of Wythoff's game with an extra move allowing players to remove h stones from the smaller pile and k stones from the larger pile, where h and k are arbitrary natural numbers such that they are smaller than the number of stones in the smaller and larger piles, respectively, and $k < h$.

Theorem 3. The following sets (i), (ii), and (iii) are the same.
(i) The set of $\mathcal{P}$-positions of the variant of (i) in Definition 4,
(ii) The set of $\mathcal{P}$-positions of the variant of (ii) in Definition 4, and
(iii) The set of $\mathcal{P}$-positions of the original Wythoff's game (without a pass).

For a proof, see [7].

The authors discovered facts that are similar to the fact presented in Theorem 2 for the variant of (ii) in Definition 4 through computer calculations. They presented these facts in Example 1, but they have not managed to prove them.

Example 1. When a pass move is introduced, the variant of Wythoff's game of (ii) of Definition 4 has a characteristic very similar to that of Wythoff's game with a pass. We have discovered the following fact through calculation using the software Mathematica.
For $x, y \leq 650$, the number of elements in $\{(x, y) : \mathcal{G}(x, y, 1) = 0\}$ is 497, and the number of elements in $\{(x, y) : \mathcal{G}(x, y, 1) = 0$ and $\mathcal{G}(x, y, 0) = 1\}$ is 475. Since $475/497 = 0.9557$, it seems that a large majority of elements of set $\{(x, y) : \mathcal{G}(x, y, 1) = 0\}$ belong to set $\{(x, y) : \mathcal{G}(x, y, 0) = 1\}$. This is very similar to fact (a) and Theorem 2.
For the variant of Wythoff's game of (i) in Definition 4, there does not exist any such fact.

References

[1] S. Nakamura and R. Miyadera, Impartial Chocolate Bar Games, Integers 15 (2015).
[2] R. Berlekamp, J.H. Conway, and R.K. Guy, Winning Ways for Your Mathematical Plays (Academic, London), Chap. IX, 1979.
[3] G. Horrocks and R.J. Nowakowski, Regularity in the G-Sequences of Octal Games with a Pass, Integers 3(G1) (2003), 10.
[4] R.E. Morrison, E.J. Friedman, and A.S. Landsberg, Combinatorial Games with a Pass: A Dynamical Systems Approach, Chaos: An Interdisciplinary Journal of Nonlinear Science 21 (2011), 043108.
[5] U. Blass and A.S. Fraenkel, The Sprague–Grundy Function for Wythoff's Game, *Theoretical Computer Science* **7** (1990), 311-333.
[6] M.H. Albert, R.J. Nowakowski, and D. Wolfe, *Lessons in Play* (A K Peters/CRC Press, Location), 2007, 139.
[7] Nhan Bao Ho, Two Variants of Wythoff's Game Preserving its P-positions, *Journal of Combinatorial Theory*, Series A 119, (2012), 1302-1314

Chocolate Games With an Upper Bound for the Number of Columns and Rows That Can Be Removed in a Turn

Yushi Nakaya [1] Mariko Kashiwagi [2] Michitada Hayashi [3]
Sintarou Kaimoto [2] Ryoji Takano [2] Kazunari Mizuta [2] Nazuki Terakawa [2]
[1]Tohoku University [2]Kwansei Gakuin University and High School [3]Kobe High School

1. Chocolate Games

Here, the authors present formulas of Grundy numbers for a chocolate game. This chocolate is a variant of the chocolate presented in $JCDCG^3$ 2016 [1], as well as of the chocolate game presented in [2].First, we describe the rule of the chocolate game.
(i) A chocolate bar is a rectangular array of squares, but with some squares removed. There is a poisoned square at the bottom left of the bar. Each player, in turn, breaks the bar in a straight line along the grooves and eats the piece he/she broke off. The player who manages to leave an opponent with the single bitter block (black block) is the winner.
(ii) There is an upper bound for the number of columns and rows that can be removed in a turn.

Because of (ii), the mathematical structure of the chocolate game in this article is very different from that of the game in $JCDCG^3$ 2016 [1] and [2]. Our main results are Theorem 2 and Theorem 3, whereas the main result of [2] is Theorem 4, and the result of [1] is a generalization of Theorem 4.

The chocolate game in Figure 1 is mathematically equivalent to the game with a pile of two stones and a pile of five stones; thus, we concentrate on the games demonstrated in Figure 2.

Figure 1. 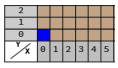

Figure 2. 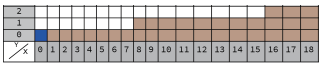

In this study, we consider the Grundy numbers of a chocolate bar.
We now determine the shape of the bar. Let $Z_{\geq 0}$ be the set of non-negative integers.

Definition 1. Let k be a natural number, and let $f(x) = \lfloor \frac{x}{4k} \rfloor$.
For $x, y \in Z_{\geq 0}$, the chocolate bar will consist of $x+1$ columns, where the 0-th column is the bitter square, and the height of the i-th column is $t(i) = \min(f(i), y) + 1$ for $i = 0, 1, ..., x$. We will denote this by $CB(f, x, y)$. Thus, the height of the i-th column is determined by f, i, and y.

Note that the chocolate in Figure 2 is $CB(f, 18, 2)$, where $f(x) = \lfloor \frac{x}{8} \rfloor$. We briefly review some necessary concepts of combinatorial game theory; see [3] for more details.

Definition 2. (a) $\mathcal{P}$-positions are winning positions for the previous player (the player who just moved), as long as that player plays correctly at every stage.
(b) $\mathcal{N}$-positions are winning positions for the next player, as long as that player plays correctly at every stage.

Definition 3. (i) Let x, y be non-negative integers. We represent them in base 2, so that $x = \sum_{i=0}^{n} x_i 2^i$ and $y = \sum_{i=0}^{n} y_i 2^i$ with $x_i, y_i \in \{0, 1\}$. We define the nim-sum $x \oplus y = \sum_{i=0}^{n} w_i 2^i$, where $w_i = x_i + y_i \ (mod\ 2)$.
(ii) The *minimum excluded value* (mex) of a set S of non-negative integers is the least non-negative integer that is not in S.
(iii) Let $\mathbf{p}$ be a position of an impartial game. The associated Grundy number is denoted by $G(\mathbf{p})$ and is recursively defined by $G(\mathbf{p}) = mex\{G(\mathbf{h}) : \mathbf{h} \in move(\mathbf{p})\}$.

Theorem 1. $G_{\mathbf{G}}(\mathbf{g}) = 0$ if and only if $\mathbf{g}$ is a $\mathcal{P}$-position.

For a fixed function f, the position of $CB(f, x, y)$ will be denoted by coordinates $\{x, y\}$.

Definition 4. For $x, y \in Z_{\geq 0}$, we define $move_f(\{x, y\})$, which is the set of positions that can be reached by making precisely one move from $\{x, y\}$.
Let $move_f(\{x, y\}) = \{\{x, v\} : v < y\} \cup \{\{w, \min(y, f(w))\} : w < x\}$, where $v, w \in Z_{\geq 0}$.

Example 1. Here, we explain $move_f$ when $f(t) = \lfloor \frac{t}{8} \rfloor$. If we start with the chocolate bar in Figure 3, whose coordinates are $\{x, y\} = \{18, 2\}$, and reduce $y = 2$ to $y = 1$ by cutting horizontally, then we have the bar in Figure 4, whose coordinates are $\{x, y\} = \{18, 1\}$.

If we start with the chocolate bar in Figure 3 and reduce $x = 18$ to $x = 16$ by cutting vertically, then we have the bar in Figure 5, whose coordinates are $\{x, y\} = \{16, 2\}$. We note that $\{16, \min(2, \lfloor \frac{16}{8} \rfloor)\} = \{16, 2\}$, and the reduction of z does not affect y.

If we start with the chocolate bar in Figure 3 and reduce $x = 18$ to $x = 13$ by cutting vertically, then we have the bar in Figure 6, whose coordinates are $\{x, y\} = \{13, 1\}$. We note that $\{13, \min(2, \lfloor \frac{13}{8} \rfloor)\} = \{13, 1\}$, and the reduction of x decreases the value of y. Therefore, we have $\{18, 1\}$, $\{16, 2\}$, $\{13, 1\} \in move_f(\{18, 2\})$.

Figure 3. $CB(f, 5, 11)$ 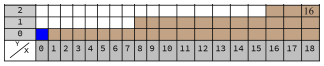

Figure 4. $CB(f, 3, 11)$ 

Figure 5. $CB(f, 5, 10)$ 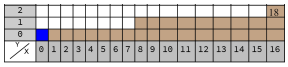

Figure 6. $CB(f, 4, 8)$ 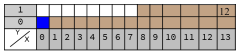

The authors discovered the following facts (a) and (b) for the chocolate game $f(t) = \lfloor \frac{t}{4k} \rfloor$.
(a) When the upper limit for the number of columns and rows to be taken is $8k$, we have eight formulas for Grundy numbers. See Theorem 2.
(b) When the upper limit is smaller than $4k$, the formula for Grundy numbers can be expressed by two simple equations. See Theorem 3.
Next, we study these facts (a) and (b) one by one.
(a) When the upper limit is $8k$, there are eight formulas for Grundy numbers.

Theorem 2. Suppose that the upper limit is $8k$ for a natural number k. Let $\mathcal{G}(x, y)$ be the Grundy number of $CB(f, x, y)$ for $f(t) = \lfloor \frac{t}{4k} \rfloor$. Then, we have the following statements.
(i) $\mathcal{G}(x, y) = x \oplus y$ for any $x \leq 8k$.
(ii) $\mathcal{G}(x, y) = 8k$ for $(x, y) = (8k + 1, 1)$ or $(8k + 2, 2)$.
(iii) $\mathcal{G}(x, y) = 8k + 1$ for $(x, y) = (8k + 1, 2)$.
(iv) $\mathcal{G}(x, y) = 8k + 3$ for $(x, y) = (12k, 3)$.
(v) $\mathcal{G}(x, y) = 8k + 4$ for $(x, y) = (16k, 4)$.
(vi) $\mathcal{G}(x, y) = 8k + 1$ for (x, y) such that $y = x/(4k)$ and $y = 2$ $(mod\ 3)$.
(vii) $\mathcal{G}(x, y) = 8k + 2$ for (x, y) such that $y = x/(4k)$ and $y = 0$ $(mod\ 3)$.
$(viii)$ $\mathcal{G}(x, y) = 8k + 3$ for (x, y) such that $y = x/(4k)$ and $y = 1$ $(mod\ 3)$.
(ix) $\mathcal{G}(x, y) = x - y\ mod\ 8k + 1$ for x, y that do not satisfy either of the above conditions (i),...$(viii)$.

(b) When the upper limit is smaller than $4k$, the mathematical structure becomes very simple. There are two formulas for Grundy numbers.

Theorem 3. Let $f(t) = \lfloor \frac{t}{2k} \rfloor$. Let u be the upper limit of the number of columns and rows of chocolates to be cut. If u is smaller than $2k$, then we have the following statements.
(i) $\mathcal{G}(x, y) = u + 1$ for $(x, y) = (2k, f(2k))$.
(ii) $\mathcal{G}(x, y) = x - y$ $(mod\ u + 1)$.

(c) If there is no upper limit for the number of columns and rows to be cut, the mathematical structure of the game is almost the same as that of the classical nim.

Theorem 4. Let $\mathcal{G}(x, y)$ be the Grundy number of $CB(f, x, y)$ for $f(t) = \lfloor \frac{t}{4k} \rfloor$. Then, $\mathcal{G}(x, y) = x \oplus y$.

For a proof of this theorem, see [2].

References

[1] R. Miyadera et al., Grundy Numbers of Impartial Three Dimensional Chocolate Bar Games, $JCDCG^3$, (2016).

[2] S. Nakamura and R. Miyadera, Impartial Chocolate Bar Games, Integers 15 (2015).

[3] M. H. Albert, R. J. Nowakowski and D. Wolfe, Lessons in Play (A K Peters, Location), 139.

Connected Interior Domination in Graphs and Some Realization Problems

Shiela Mae B. Pacardo
College of Arts and Sciences
Notre Dame of Marbel University
Alunan Avenue, 9506 Koronadal City, Philippines
shielamae.pacardo@g.msuiit.edu.ph

Helen M. Rara
Department of Mathematics and Statistics
College of Science and Mathematics
Center of Graph Theory, Algebra and Analysis
Premier Research of Institute of Science and Mathematics
Mindanao State University-Iligan Institute of technology
Tibanga Highway, 9000 Iligan City, Philippines
helenrara@yahoo.com

Extended Abstract

Let G be a simple graph. A set $S \subseteq V(G)$ is called a *connected interior dominating set* of G if S is an interior dominating set of G and the induced subgraph $\langle S \rangle$ is connected. The minimum cardinality of a connected interior dominating set in G is called *connected interior domination number* of G and is denoted by $\gamma_{cId}(G)$. A connected interior dominating set in G with cardinality $\gamma_{cId}(G)$ is referred to as γ_{cId}-set. In this paper, we provide some basic properties of the connected interior dominating sets and characterize the connected interior dominating sets under the join and corona of graphs. Then we determine the corresponding connected interior domination number of these graphs. The study of these concepts is motivated with application of locating domination in graphs. The following are some important results of this paper:

Remark 1. Let G be a connected graph of order $n \geq 3$. Then $1 \leq \gamma_{Id}(G) \leq \gamma_{cId}(G) \leq |Int(G)|$.

Theorem 2. Let G be a graph of order $n \geq 4$. Then $\gamma_{cId}(G) = 2$ if and only if $\gamma_{It}(G) = 2$.

Theorem 3. Let G and H be connected graphs. If $\gamma_{cId}(G) = 1$ and $\gamma_{cId}(H) = 1$, then the connected interior dominating set of $G + H$ does not exist.

Theorem 4. Let G and H be connected graphs such that $G + H$ admits a connected interior dominating set. Then $S \subseteq V(G + H)$ is a connected interior dominating set of $G + H$ if and only if at least one of the following is true:

(i) $S \subseteq V(G)$, S is a connected interior dominating set of G and $\gamma(H) \neq 1$.

(ii) $S \subseteq V(H)$, S is a connected interior dominating set of H and $\gamma(G) \neq 1$.

(iii) $S \cap V(G)$ and $S \cap V(H)$ are nonempty subsets of the interior sets of G and H, respectively and $\gamma(G) \neq 1$ and $\gamma(H) \neq 1$.

Lemma 5. Let G be a connected graph and H be any graph. Then the subgraph $\langle V(G) \rangle$ induced by $V(G) \subseteq V(G \circ H)$ is a connected subgraph of $G \circ H$.

Theorem 6. Let G be a nontrivial connected graph and H be any graph. Then $S \subseteq V(G \circ H)$ is a connected interior dominating set of $G \circ H$ if and only if $S = V(G)$.

Corollary 7. Let G be a nontrivial connected graph and H be any graph. Then $\gamma_{cId}(G \circ H) = |V(G)| = \gamma_{Id}(G \circ H)$.

Theorem 8. Let a and b be positive integers such that $a \leq b$ and $b = 2a - 1$ for $a < b$. Then there exists a connected graph G such that $\gamma_{Id}(G) = a$ and $\gamma_{cId}(G) = b$.

Theorem 9. Let a, b and c be positive integers such that $2 \leq a \leq b \leq c$ and $2c = 3a - 2$ if a is even and $2c = 3a - 3$ if a is odd when $a = b < c$, $2b = 3a$ and $c = 2a - 1$ if a is even and $2b = 3a + 1$ and $c = 2a - 1$ if a is odd when $a < b < c$. Then there exists a connected graph G such that $\gamma_{Id}(G) = a$, $\gamma_{It}(G) = b$ and $\gamma_{cId}(G) = c$.

Corollary 10. Given a positive integer n, there exists a connected graph G such that $\gamma_{cId}(G) - \gamma_{It}(G) = n$, that is, the difference $\gamma_{cId} - \gamma_{Id}$ can be made arbitrarily large.

Keywords: interior domination, connected interior domination, join, corona

References

[1] A.Anto Kinsley, C.Caroline Selvaraj, *A Study on Interior Domination in Graphs*, IOSR Journal of Mathematics, Vol. 12, pp 55-59, 2016

[2] L. Casinillo, E. Lagumbay, H. Abad *A note on Connected Interior Domination in Join and Corona of Two Graphs*, IOSR Journal of Mathematics, Vol (13), 2017.

[3] S.M.Pacardo and H.M. Rara, *Interior Domination in Graphs under some binary Operations*. Applied Mathematical Sciences, Vol.12, 2018, no. 14, 677-690.

[4] C.E. Go, and S.R. Canoy, Jr., *Domination in the corona and join of graphs*. International Mathematical Forum, 6 (2011), no. 16, 763-771.

[5] Canoy, S.R. Jr., Malacas, G.A., Tarepe, D., *Locating-Dominating Sets in Graphs*, Applied Mathematical Sciences 8 (88), 4381-4388

On open neighborhood locating-dominating set of Mycielski graphs

Suhadi Wido Saputro

Bandung Institute of Technology, Indonesia

A monitored system can be modelled as a graph G. It is generally assumed that a detection device located at vertex v in G, can detect an intruder only if the intruder is at v or at a vertex which is adjacent to v. The placing monitoring device in the system can be considered as an open neighborhood locating-dominating problem. An open neighborhood locating-dominating set (OLD-set) S in a graph G is a vertex set of G such that for every vertex v in G, its open neighborhood has a unique non-empty intersection with S. The minimum cardinality of an OLD-set of G is called as the open neighborhood locating-dominating number of G, denoted by $OLD(G)$. In this paper, we consider a Mycielski graph of G, denoted by $\mu(G)$. For any connected graphs G, we determine the relation between $OLD(\mu(G))$ with $OLD(G)$, order of G, or the maximum degree of G. This talk is based on joint work with Wedyata Larasartika (Bandung Institute of Technology).

Gene of Wythoffian polytopes belong to D/E finite reflection groups

Ikuro Sato[1] and Jin Akiyama[2]

2019 JCDCG3, Sept. 6-8

1. Miyagi Cancer Center
sato-ik510@miyagi-pho.jp
2. Tokyo University of Science
ja@jin-akiyama.com

Abstract

Regular and semi-regular polytopes are studied widely, but there are still many unknown parts remained [1]. Wythoffian is a generalization of regular and semi-regular polytope. It is shown in [2] that a combinatorial and topological calculation (without use of coordinates) for the global and local metric of Wythoffians whose finite reflection groups belong to A_n, B_n, C_n, F_4, G_2, H_3, H_4 and $I_2(p)$. At that time, D_n, E_6, E_7 and E_8 were 'empty' because of several difficulties; (1) two kinds of constituents (α_{n-1} and $h\gamma_{n-1}$ in D_n, α_{n-1} and β_{n-1} in E_n), (2) bifurcation of Coxeter-Dynkin diagram and (3) duality vanished and triality newly appears. In this talk, we will give a recurrence algorithm for them beyond the difficulties.

To show the effectiveness of calculation called Wythoff arithmetic, let us take a 6-Wythoffian polytope P belonging to E_6 which is expressed as Fig. 1 or D_5 as Fig. 2 by Coxeter-Dynkin diagram. Denoting by f_k the number of k-faces of P, it is calculated by the arithmetic;
(a) $f_0 = 432,\ f_1 = 3240,\ f_2 = 7920,\ f_3 = 7200,\ f_4 = 2430$ and $f_5 = 342$ (Table 1)
(b) $f_0 = 480,\ f_1 = 1200,\ f_2 = 1040,\ f_3 = 360$ and $f_4 = 42$ (Table 2), respectively.

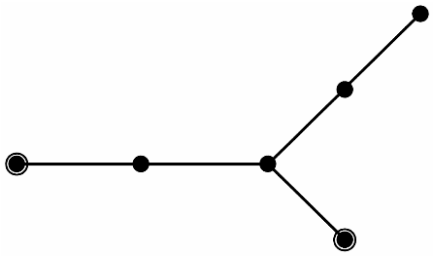

Fig. 1

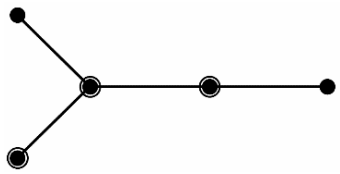

Fig. 2

$$\begin{bmatrix} 16 & 0 & 0 & 0 & 0 & 0 & 0 \\ 80 & 5 & 0 & 0 & 0 & 0 & 0 \\ 160 & 10 & 2 & 0 & 0 & 0 & 0 \\ 120 & 10 & 1 & 1 & 0 & 0 & 0 \\ 26 & 5 & 0 & 0 & 1 & 0 & 0 \\ 1 & 1 & 0 & 0 & 0 & 1 & 0 \\ 0 & 0 & 0 & 0 & 0 & 0 & 1 \end{bmatrix} \begin{bmatrix} 27 \\ 216 \\ 720 \\ 1080 \\ 648 \\ 99 \\ 1 \end{bmatrix},$$

Table1

$$\begin{bmatrix} 60 & 6 & 0 & 0 & 0 & 0 \\ 120 & 9 & 0 & 0 & 0 & 0 \\ 80 & 5 & 1 & 0 & 0 & 0 \\ 20 & 1 & 0 & 1 & 0 & 0 \\ 1 & 0 & 0 & 0 & 1 & 0 \\ 0 & 0 & 0 & 0 & 0 & 1 \end{bmatrix} \begin{bmatrix} 16 \\ -80 \\ 160 \\ 120 \\ 26 \\ 1 \end{bmatrix}$$

Table2

References

[1] Coxeter, H. S. M., Wythoff's construction for uniform polytopes, *Proc. London Math. Soc.*, **38**, 327-339 (1934).
[2] Akiyama, J. Hitotumatu, S., Ishii, M., Matsuura, A., Sato, I., and Toyoshima, S., A recursive Algorithm for the k-face Numbers of Wythoffian-n-polytopes Constructed from Regular Polytopes, *J. Information Processing*, **25**, 528-536 (2017).

A grammatical approach to the analysis and operations of semi-interlocking constructions of SL blocks

Shen-Guan Shih;
Dept. of Architecture, National Taiwan University of Science and Technology,
sgshih@mail.ntust.edu.tw

Abstract
SL block is a kind of octocube that can be used as a building element to construct semi-interlocking structures of various shapes [1]. It was uncovered that conjugate pairs of SL blocks can be sequentially concatenated into strands that are extensible in three orthogonal directions [2]. Semi-interlocking is defined as a property of composite structures that allows some parts of the assembly not entirely locked within the configuration, but with one direction held to the structure by friction and can be removed by force. A fully interlocked structure can be strong and stable but would certainly allow no feasible process to construct. A semi-interlocked structure may remain stable under forces from various directions, and yet allows at least one feasible sequence for assembling and disassembling. SL strands may form enclosed loops if both ends meet at the same location. All looping SL strands are semi-interlocking.

String re-write grammars can be used to define languages of SL strands. Generative processes are defined to create stylish configurations of SL constructions based on some grammar definitions. Syntax-directed translations can be applied to convert one SL strand to some others by replacing re-write rules of one grammar with re-write rules from some others. Experiments were carried out and interesting results are displayed and discussed.

Looping SL strands can be represented as sequences of concatenations. An algorithm to derive feasible sequences for assembling and disassembling of semi-interlocked SL strands is presented. The algorithm is based on syntax directed translations of an input grammar that defines possible concatenations of SL conjugate pairs and an output grammar that generates assembling processes for SL strands. In the translation process, an attributed input grammar is used to parse the syntactic structures of the processed SL strand. The syntactic structures are used to guide the output grammar to generate assembling sequences for construction. The reverses of

generated sequences would also imply feasible ways for disassembling.

With the grammatical approach, it might be possible to define high level operations and analysis that enable the design and assessment of very complicated constructions that are made of very simple and primitive elements such as SL blocks. Future study may be directed towards the interactions between generative processes of grammars and the context where the deviations take place.

[1] Shen-Guan Shih, On the hierarchical construction of SL blocks - A generative system that builds self-interlocking structures, S. Adriaenssens, F. Gramazio, M. Kohler, A. Menges, M. Pauly (eds.): *Advances in Architectural Geometry 2016*, 124-137, 2016.

[2] Shen-Guan Shih, The art and mathematics of self-interlocking SL blocks, *Bridges 2018 Conference Proceedings*, 107-114, 2018.
http://archive.bridgesmathart.org/2018/bridges2018-107.pdf

The Huffman Tree Problem with Linear Functions with Upper Bounds

Yuichi Shirai* Hiroshi Fujiwara* Hiroaki Yamamoto*

The Huffman tree problem [Huf52] is a problem in which for a sequence of n weights, the task is construct a full binary tree that minimizes the weighted sum of depths of the leaves each corresponding to a weight. The General Cost Huffman Tree Problem [FJ14] is an extension of the Huffman tree problem. The input is a sequence of n functions. The task is to obtain a full binary tree that minimizes the sum of the function values with respect to the depths of the leaves each corresponding to a function. Formally, this problem is formulated as below.

General Cost Huffman Tree Problem

Input: A sequence of functions $f_1, f_2, \ldots, f_n : \mathbb{N} \to \mathbb{Q}$.

Output: A binary tree T having leaves $l_1, l_2, \ldots, l_n$.

Objective: Minimize $\sum_{i=1}^{n} f_i(\mathrm{depth}(l_i, T))$.

Here, $\mathrm{depth}(l_i, T)$ represents the length of the path from the root of T to the leaf l_i.

The difficulty of the problem depends on what class the functions in the input sequence belong to. Table 1 summarizes previous works and our results. Fujiwara and Jacobs [FJ14] proved the General Cost Huffman Tree Problem to be NP-hard even for 0-1 functions. In contrast, the original Huffman tree problem [Huf52], which is a special case of the General Cost Huffman Tree Problem, admits an $O(n \log n)$-time algorithm. Fujiwara, Nakamura, and Fujito [FNF15] gave an $O(n \log n)$-time algorithm for the case of unit step functions. Fujiwara and Jacobs [FJ14] provided an $O(n^2 \log n)$-time algorithm for non-decreasing convex functions. It is open whether the General Cost Huffman Tree Problem with non-decreasing non-convex functions can be solved in polynomial time or not.

We study two subclasses of non-decreasing non-convex functions and give polynomial-time algorithms for each. Our target is linear functions with upper bounds, represented as:

$$f_i(x) = w_i \cdot \min\{x, t_i\}$$

Table 1: Complexity results for the General Cost Huffman Tree Problem.

class of functions	time complexity
linear	$O(n \log n)$ [Huf52]
unit step	$O(n \log n)$ [FNF15]
class 1	$O(n^2)$ [this paper]
class 2	$O(n^2 \log n)$ [this paper]
non-decreasing convex	$O(n^2 \log n)$ [FJ14]
general	NP-hard [FJ14]

[0]This work was supported by KAKENHI (16K00033, 17K00013, and 17K00183).

*Shinshu University

with $w_i \geq 0$ and $t_i \geq 0$ for all $i \in \{1, 2, \ldots, n\}$. We investigate the following two classes:

- Class 1: sequences of functions $\{f_i\}$ such that $w_1 = w_2 = \cdots = w_n$.
- Class 2: sequences of functions $\{f_i\}$ such that $t_1 = t_2 = \cdots = t_n$.

Theorem 1. *There exists an $O(n^2)$-time algorithm for the General Cost Huffman Tree Problem for class 1 functions.*

Theorem 2. *There exists an $O(n^2 \log n)$-time algorithm for the General Cost Huffman Tree Problem for class 2 functions.*

Our two algorithms have the same structure: Sort the input sequence, solve subproblems, and then choose the best solution. The key idea behind is the fact that: if the input sequence is sorted (specifically, in a descending order of t_i for class 1, and in a descending order of w_i for class 2), the set of functions such that $\mathrm{depth}(l_i, T) < t_i$ in an optimal solution is some *prefix* of $\{1, 2, \ldots, n\}$. Hence, it is sufficient to check only $n + 1$ ways. Given a guess of the set of functions such that $\mathrm{depth}(l_i, T) < t_i$, a subproblem is constructed by setting w_i's out of the set as zero and all t_i's as ∞. It is shown that if the guess is correct, an optimal solution to the subproblem is also optimal to the original problem.

References

[FJ14] H. Fujiwara and T. Jacobs. On the Huffman and alphabetic tree problem with general cost functions. *Algorithmica*, 69(3):582–604, 2014.

[FNF15] H. Fujiwara, T. Nakamura, and T. Fujito. The Huffman tree problem with unit step functions. *IEICE Trans. Fundamentals*, E98-A(6):1189–1196, 2015.

[Huf52] D. A. Huffman. A method for the construction of minimum-redundancy codes. In *Proc. the Institute of Radio Engineers*, volume 40, pages 1098–1101, 1952.

The Non-Existence of Convex Configuration for a Given Set of Radii in Two-Dimensional Space

Kirati Sriamorn[1], Sira Sriswasdi[2] and Supanut Chaidee[3]

[1] Department of Mathematics and Computer Science, Faculty of Science, Chulalongkorn University
254 Phayathai Rd, Wang Mai, Pathum Wan, Bangkok, 10330, Thailand, E-mail: kirati.s@chula.ac.th
[2] Research Affairs, Faculty of Medicine, Chulalongkorn University
1873 Rama IV Rd, Pathum Wan, Pathum Wan, Bangkok, 10330, Thailand, E-mail: sira.sr@chula.ac.th
[3] Department of Mathematics, Faculty of Science, Chiang Mai University
239, Huay Kaew Rd, Muang, Chiang Mai, 50200, Thailand, E-mail: supanut.c@cmu.ac.th

Abstract

Chaidee and Sugihara recently proposed a conjecture about the non-existence of two-dimensional convex polygon whose vertices are at given radii $\mathcal{R}$ from the origin. In this study, We prove the conjecture and provide some necessary and sufficient conditions on $\mathcal{R}$ for the existence of such convex configuration.

1 Introduction

A natural problem about the placement of n points on a plane is whether one could satisfy certain constraints while keeping such placement convex. In other words, the question is whether a *convex configuration* exists for a given set of constraints. A known example is the construction of convex polygon whose side lengths, also called linkages, are fixed [2, 3].

Recently, Chaidee and Sugihara [1] studied a different problem about convex configuration which asks for the existence of convex polygon (in the case of two-dimensional space) or convex polytope (in the case of three-dimensional space) whose vertices are at specified distances, also called radii, from the origin.

The answer to the above question is positive when one considers the case of three-dimensional space. However, it remained unclear whether a convex configuration exists for any given radii $\mathcal{R}$ in the case of two-dimensional space. Chaidee and Sugihara [1] proved that the answer is positive under some conditions on $\mathcal{R}$ and proposed the conjecture that the convex configuration does not always exist in the general case.

In this study, we prove the conjecture and provide some necessary and sufficient conditions on $\mathcal{R}$ for such convex configuration to exist.

2 Convex configurations for some $\mathcal{R}$

For some families of given radii $\mathcal{R}$, there are simple strategies to construct the convex configurations. Chaidee and Sugihara [1] have illustrated strategies when all of the radii are distinct (Figure 1a) and when none of the value of radii is repeated more than four times (Figure 1b).

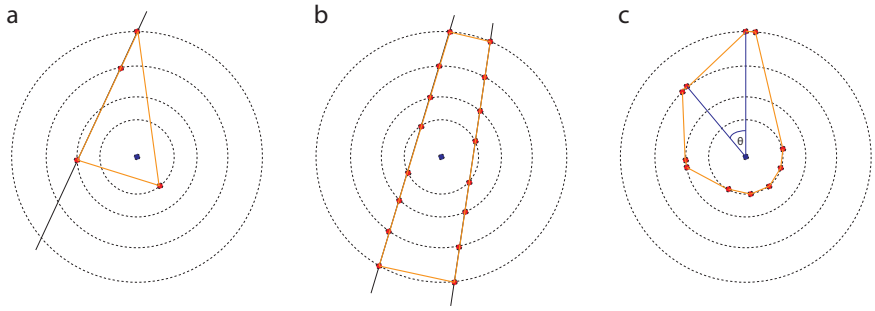

Figure 1: Strategies for constructing convex configurations for some $\mathcal{R}$

Here, we additionally observe that when there are no more than four distinct values of radii, i.e., $\mathcal{R} = \{r_1, ..., r_1, r_2, ..., r_2, ..., r_k, ..., r_k\}$ for $k \leq 4$ and $r_1 > r_2 > ... > r_k$, one can place points along the arc of circle with radius r_i followed by drawing a tangent line to the circle with radius $r_{i+1} < r_i$, as shown in Figure 1c, to obtain a convex configuration. This is always possible because the total angle around the origin covered by $k \leq 4$ tangent lines is less than $\frac{k\pi}{2} \leq 2\pi$ and the angle covered by each arc can be arbitrarily small.

3 A necessary and sufficient condition of $\mathcal{R}$ which has convex configuration

Definition 1. For a given finite set $\mathcal{R}$, a permutation $(r_i)_{i=1}^n$ of $\mathcal{R}$ is called a *initial sequence* of $\mathcal{R}$, if $r_1 = \max \mathcal{R}$.

To prove that the given set $\mathcal{R}$ cannot have a convex configuration, we need to prove that the convex polygon cannot be constructed for any initial sequence $(r_i)_{i=1}^n$.

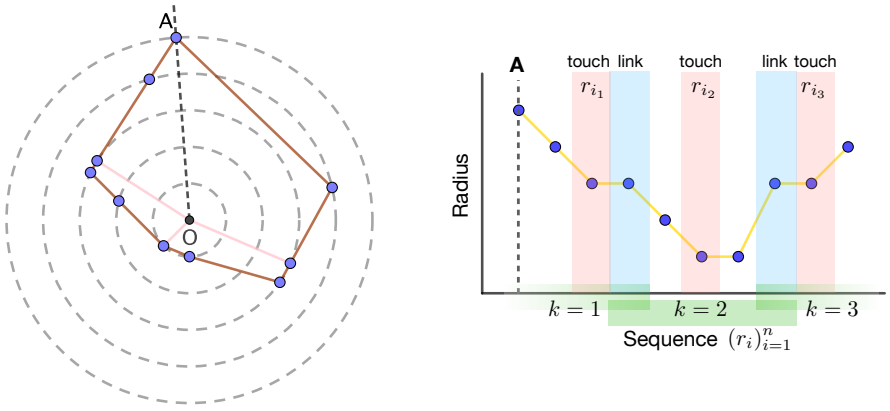

Figure 2: (Left) the points from an initial sequence $(r_i)_{i=1}^n$ of $\mathcal{R}$; (right) the plot of the radii where the sequence starts at the point A counterclockwise.

Definition 2. Let $S = (r_i)_{i=1}^n$ be an initial sequence of $\mathcal{R}$ and define $r_{n+m} = r_m$ for $m \geq 1$. Let $j_0 = 1$. For $k \geq 1$, let i_k be the smallest index such that $i_k > j_{k-1}$ and $r_{i_k} \leq r_{i_k+1}$. Let t_k be the index such that $t_k \geq i_k$, $r_{i_k} = ... = r_{t_k}$ and $r_{t_k} \neq r_{t_k+1}$. Let j_k be the smallest index such that $t_k \leq j_k$ and $r_{j_k} \geq r_{j_k+1}$. We call r_{i_k} a *touch* of S, and call r_{j_k} a *link* of S. Define

$$\alpha(S) = \sum_{k=1}^{l} \left(\arccos \frac{r_{i_k}}{r_{j_{k-1}}} + \arccos \frac{r_{i_k}}{r_{j_k}} \right)$$

where $j_l = n + 1$.

Definition 3. Let $S = (r_i)_{i=1}^n$ be an initial sequence of $\mathcal{R}$ and define $r_{n+m} = r_m$ for $m \geq 1$. We call S a *good sequence* of $\mathcal{R}$, if either $\alpha(S) < 2\pi$ or $\alpha(S) = 2\pi$ and $r_i \neq r_{i+1}$ for all $i \geq 1$. We call S a *perfect sequence* of $\mathcal{R}$, if $\alpha(S) < 2\pi$.

Theorem 1. For a given finite set $\mathcal{R}$,

1. $\mathcal{R}$ has a convex configuration if and only if there exists a good sequence $(r_i)_{i=1}^n$ of $\mathcal{R}$.
2. $\mathcal{R}$ has a strictly convex configuration if and only if there exists a perfect sequence $(r_i)_{i=1}^n$ of $\mathcal{R}$.

The theorem can imply Theorems 2 in [1], and obtain the following result.

Theorem 2. [1] For a given positive radii set $\mathcal{R} = \{r_{(1,1)}, ..., r_{(1,m_1)}, r_{(2,1)}, ..., r_{(2,m_2)}, ..., r_{(k,1)}, ..., r_{(k,m_k)}\}$ such that $r_{(i,1)} = ... = r_{(i,m_i)}$ for each $i = 1, ..., k$ and $1 \leq m_i \leq 4$. Then there exist a strictly convex configuration V with respect to the radii set $\mathcal{R}$.

Corollary 1. *If $\mathcal{R}$ consists of most four different radii such that each radius has finitely many points, then there exist a strictly convex configuration V with respect to the radii set $\mathcal{R}$.*

Theorem 3. There exists a set $\mathcal{R}$ such that $\mathcal{R}$ does not have a convex configuration.

The set $\mathcal{R} = \{r_1, ..., r_1, r_2, ...r_2, ..., r_k, ...r_k\}$ such that $r_1 > r_2 > ... > r_k$ for whom a convex configuration does not exist should meet the following conditions: $k \geq 5$, some r_i is repeated more than 5 times, and $\arccos\left(\frac{r_2}{r_1}\right) + \cdots + \arccos\left(\frac{r_k}{r_{k-1}}\right) + \arccos\left(\frac{r_k}{r_1}\right) > 2\pi$.

4 Acknowledgements

This work was done in the geometry research boot camp 2019 organized by the Department of Mathematics, Chiang Mai University on June 17-21, 2019. We would like to thank Wacharin Wichiramala and Chatchawan Panraksa for the discussions.

References

[1] Chaidee, S., Sugihara, K. Existence of a Convex Polyhedron with Respect to the Given Radii. submitted to Discrete and Computational geometry. https://arxiv.org/abs/1906.07919

[2] Everett, H., Lazard, S., Robbins, S., Schrder, H., & Whitesides, S.: Convexifying star-shaped polygons. In 10th Canadian Conference on Computational Geometry (CCCG'98) (pp. 10-12) (1998).

[3] Connelly, R., Demaine, E. D., & Rote, G: Blowing up polygonal linkages. Discrete Comput. Geom., 30(2), 205-239 (2003).

Delete Nim

Koki Suetsugu
National Institute of Informatics

Tomoaki Abuku
University of Tsukuba

1 Introduction

Combinatorial game theory is the mathematical study for strategy of perfect information games in which there are neither chance moves, nor hidden information. Among early results of combinatorial game theory there is a winning strategy for *Nim* by Bouton [1] in 1902. Nim is a two-player game with some heaps of stones in which the player to move chooses one of the heaps and takes away arbitrary numbers of stones from it. The upper part of Fig. 1 shows a game position of Nim. In the position, there are two heaps of stones: one has three stones and the other has two stones. Since each player can remove any number of stones from a single heap, the candidates for the next positions are shown in the lower part of the figure. The winner of Nim is the player who takes away the last stone. We express Nim positions by the number of stones in each heap like $(3, 2)$.

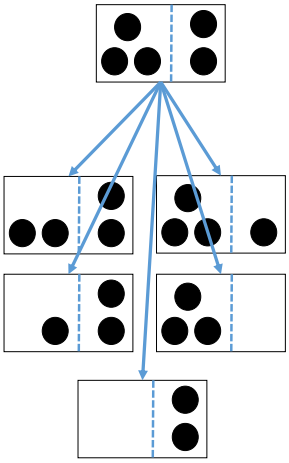

Figure 1: The Nim position $(3, 2)$

We say a game is in *normal play* if we define that the winner of the game is the player who moves last (like Nim). A game is called *impartial* if both players have the same set of options (like Nim). In this paper, we study only impartial games.

We say a player has a *winning strategy* if she can win regardless of her opponent's move. In an impartial game, we say that a game position is an $\mathcal{N}$*-position* or a $\mathcal{P}$*-position* if the next player (i.e. the current player) or the previous player (i.e. the other player) has a winning strategy, respectively. Clearly, a game position of an impartial two-player game is an $\mathcal{N}$-position or a $\mathcal{P}$-position.

In the following description, we assume that every game is impartial and in normal play, and will end in a finite number of moves.

We can analyze whether a Nim position is an $\mathcal{N}$-position or a $\mathcal{P}$-position in a simple way, by calculating modulo-2 sum without carry which is denoted by $\oplus$ (Nim sum).

Theorem 1 (Bouton [1])**.** *A Nim position $(n_1, n_2, \ldots, n_k)$ is a $\mathcal{P}$-position if and only if $n_1 \oplus n_2 \oplus \cdots \oplus n_k = 0$.*

Example 1. $2 \oplus 5 \oplus 7 = 10_2 \oplus 101_2 \oplus 111_2 = 0$*, therefore, Nim positon $(2, 5, 7)$ is a $\mathcal{P}$-postion.*

Example 2. $4 \oplus 5 \oplus 6 = 100_2 \oplus 101_2 \oplus 110_2 = 111_2 = 7$*, therefore, Nim positon $(4, 5, 6)$ is an $\mathcal{N}$-postion.*

1.1 Impartial game and $\mathcal{G}$-value

Sprague [5] and Grundy [4] extended Bouton's theorem for any impartial games in normal play.

Definition 1. *Let $\mathbb{N}$ be the set of all non-negative integers. For any proper subset S of $\mathbb{N}$, we define minimal excluded fuction $\mathrm{mex}(S)$ as follows:*

$$\mathrm{mex}(S) = \min(\mathbb{N} \setminus S).$$

Definition 2. *For any game position g, we define $\mathcal{G}$-value function $\mathcal{G}(g)$ as follows:*

$$\mathcal{G}(g) = \mathrm{mex}(\{\mathcal{G}(g') \mid g \to g'\}),$$

where $g \to g'$ means that g' is an option of g.

Theorem 2 (Sprague [5] and Grundy [4])**.** *For any game position g, g is a $\mathcal{P}$-position if and only if $\mathcal{G}(g) = 0$.*

Definition 3. *For any game positions g and h, we define the* disjoint sum *$g + h$ recursivey as the game whose options are $g + h'$ or $g' + h$ where g' ranges all options of g and h' ranges all options of h.*

Theorem 3 (Sprague [5] and Grundy [4])**.** *For any game positions g and h,*

$$\mathcal{G}(g + h) = \mathcal{G}(g) \oplus \mathcal{G}(h).$$

Therefore, people have been interested in $\mathcal{G}$-values of games and some of the early results show us various structures of $\mathcal{G}$-values in some games like Welter's game [7], cyclic Nimhoff [3], and Lim [2].

2 Delete Nim

Now we define a new impartial game called *Delete Nim*. In this game, there are two heaps of stones. The player chooses one of the heaps and delete it, and, she takes away 1 stone from the remaining heap and optionally splits it into two heaps. Fig. 2 shows a play of Delete Nim.

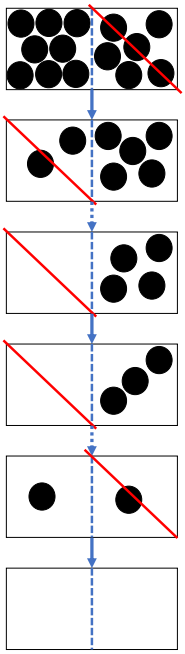

Figure 2: one game of Delete Nim

In this paper, we show how to compute the $\mathcal{G}$-value of Delete Nim.

To compute the $\mathcal{G}$-value of a position of the game, we need to prepare some defnitions and notations.

Definition 4. *We denote the usual OR operation of two numbers in binary notations by* $\vee$.

Example 3. $3 \vee 5 = 11_2 \vee 101_2 = 111_2 = 7$.

Example 4. $9 \vee 12 = 1001_2 \vee 1100_2 = 1101_2 = 13$.

Now we can compute the $\mathcal{G}$-value of a position of Delete Nim.

Theorem 4. *We denote the position of Delete Nim with two heaps of* x *stones and* y *stones by* (x, y). *Then,*

$$\mathcal{G}((x,y)) \quad = \quad v_2((x \vee y) + 1),$$

where $v_p(n)$ *is the p-adic valuation of* n, *that is,*

$$v_p(n) = \begin{cases} \max\{v \in \mathbb{N} : p^v \mid n\} & (n \neq 0) \\ \infty & (n = 0). \end{cases}$$

Proof. Refer to the full paper. □

A game similar to Delete Nim is introduced in [6]. There is an isomorphism $F(g)$ from the set of all positons of the game to that of Delete Nim:

$$F((x,y)) = (x-1, y-1).$$

In [6], the $\mathcal{P}$-positions of the game are shown but the $\mathcal{G}$-values of positions of the game are not discussed. By the isomorphism, now we can compute the $\mathcal{G}$-value of position (x, y) of the game as $v_2((x-1) \vee (y-1) + 1)$.

3 Conclusion

In this paper, we introduced a game for which one needs to use the OR operaion and 2-adic valuation $v_2(n)$ in order to compute the $\mathcal{G}$-value of a position. To the best of our knowledge, this is the only case we need the OR operation in order to calculate the $\mathcal{G}$-values. Therefore, we think that our results would contribute to the field of combinatorial game theory.

4 Aknowledgements

The authors would like to thank Dr. Kô Sakai for valuable discussions and comments.

References

[1] C. L. Bouton. Nim, a game with a complete mathematical theory. *Annals of Mathematics*, 3(1/4):35–39, 1901.

[2] Alex Fink, Aviezri S Fraenkel, and Carlos Santos. Lim is not slim. *International Journal of Game Theory*, 43(2):269–281, 2014.

[3] A. S. Fraenkel and M. Lorberbom. Nimhoff games. *Journal of Combinatorial Theory, Series A*, 58(1):1–25, 1991.

[4] Patrick M. Grundy. Mathematics and games. *Eureka*, 2:6–9, 1939.

[5] Roland P. Sprague. Über mathematische Kampfspiele. *Tôhoku Math. J.*, 41:438–444, 1935-36.

[6] Z. Stankova and T. Rike, editors. *A Decade of the Berkeley Math Circle*, volume 1, page 159. Mathematical Circles Library, 2008.

[7] Cornelius P Welter. The theory of a class of games on a sequence of squares, in terms of the advancing operation in a special group. *Indag. Math.*, 16:194–200, 1954.

Colored Finite Automata and de Bruijn Graphs

Yoshiaki TAKAHASHI, i003wc@yamaguchi-u.ac.jp, Faculty of Engineering, Yamaguchi University 2-16-1 Tokiwadai, Ube-shi, Yamaguchi, 755-8611 Japan,
and Akira ITO, akito@yamaguchi-u.ac.jp ditto

***Abstract*—We previously proved the structural equality of binary de Bruijn graph of order n and the state diagram for minimum state deterministic finite automaton which accepts regular language $(0+1)^*1(0+1)^{n-1}$. This paper extends this result to the both k-ary versions. That is, k-ary de Bruijn graph of order n and the state diagram for minimum state deterministic "colored" finite automaton which accepts the $(k-1)$-tuple of regular languages $(0+1+\cdots+k-1)^*1(0+1+\cdots+k-1)^{n-1}, \cdots$, and, $(0+1+\cdots+k-1)^*(k-1)(0+1+\cdots+k-1)^{n-1}$ are isomorphic for arbitrary k more than or equal to 2, where colored finite automata are generalization of ordinary finite automata whose accepting states are refined with two or more colors. We finally give some computational complexity results for decision problems concerning colored finite automata.**

***Index Terms*—keywords, de Bruijn graphs, finite automata, state-minimization, *NLOG*-completeness**

I. de Bruijn graph

Definition 1: Directed graph defined as follows is called k-ary order n de Bruijn graph and abbreviated $DB_{k,n}$.

$$\begin{cases} V &= \{\{0,1,\cdots,k-1\}^n\} = \{0,1,\cdots,k^n-1\}, \\ E &= \{(b_1b_2\cdots b_n, b'_1b'_2\cdots b'_n) \mid \\ & \quad b_i, b'_i \in \{0,1\}, i=1,\cdots,n, \\ & \quad b_2 = b'_1, b_3 = b'_2, \cdots, b_n = b'_{n-1}\}. \end{cases}$$

II. Colored Finite Automata

In this section, we introduce colored finite automata and investigate their fundamental properties.

Definition 2: If a language L is expressed with a direct sum $\sum_{i=1}^{k} L_i, k \geq 1$, L is called colored language of k colors.

Definition 3: A 5-tuple $M = (Q, \Sigma, \delta, q_0, \sum_{i=1}^{k} F_i)$ as follows is called nondeterministic colored finite automaton and abbreviated NCFA.

1) Q is a finite set of states,
2) Σ is a finite set of input symbols,
3) δ is the transition function from $Q \times \Sigma$ to 2^Q,
4) $q_0 \in Q$ is the initial state,
5) $\sum_{i=1}^{k} F_i \subseteq Q$ is the set of "colored accepting states".

If each $\delta(q,a)$ is a set with exactly one element, M is called deterministic and abbreviated DCFA.

We denote as $\hat{\delta}(q,x)$ the set of reachable states, when M starts from state q and finishes after it reads the input string x. If $\hat{\delta}(q_0,x) \cap F_i \neq \emptyset$, we say that M accepts x with ith color.

$$L_i(M) = \{x \in \Sigma^* \mid \hat{\delta}(q_0,x) \cap F_i \neq \emptyset\}$$

is called the language accepted by M with ith color and

$$L(M) = \bigcup_{i=1}^{k} L_i(M)$$

is called the language accepted by M. Especially, if it holds that

$$L(M) = \sum_{i=1}^{k} L_i(M),$$

we say that $L(M)$ is *unmixed* and that M *color-distinctly* accepts $L(M)$. Note that when M is deterministic, it is inherently unmixed.

For each $I \subseteq \{1,\cdots,k\}$, define

$$F'_I = \{S \subseteq Q \mid S \cap F_i \neq \emptyset, i \in I, S \cap F_j = \emptyset, j \notin I\}.$$

*Theorem 1 (*Subset construction method for NCFA): For an NCFA

$$M = (Q, \Sigma, \delta, q_0, \sum_{i=1}^{k} F_i),$$

let DCFA

$$M' = (2^Q, \Sigma, \delta', \{q_0\}, \sum_{I \subseteq \{1,\cdots,k\}, I \neq \emptyset} F'_I),$$

where

$$\delta'(S,a) = \bigcup_{p \in S} \delta(p,a) \text{ for each } S \subseteq Q, a \in \Sigma.$$

And define

$$L_I(M') = \bigcap_{i \in I} L_i(M) - \bigcup_{j \notin I} L_j(M) \text{ for each } I \subseteq \{1,\cdots,k\}$$

Then, we have the following.

(1) $L(M') = \sum_{I \subseteq \{1,\cdots,k\}, I \neq \emptyset} L_I(M') = L(M)$.

(2) $L(M)$ is unmixed $\Leftrightarrow \sum_{I \subseteq \{1,\cdots,k\}, I \neq \emptyset} F'_I = \sum_{i=1}^{k} F'_{\{i\}}$
$\Leftrightarrow L_i(M) = L_{\{i\}}(M')$ for each $i \in \{1,\cdots,k\}$.

(Proof) Proof is omitted here. □

III. Equivalence of $DB_{k,n}$ and State-Minimized Colored Finite Automaton $D_{k,n}$

In this section, we show that the graph structure of a certain deterministic colored finite automaton is isomorphic to k-ary de Bruijn graph of order n $DB_{k,n}$.

Define

$$N_{k,n} = (Q, \{0,1,\cdots,k-1\}, \delta, r_0, \sum_{i=1}^{k-1} F_i),$$

where

$$Q = \{r_0, r_{11}, \cdots, r_{1n}, \cdots, r_{(k-1)1}, \cdots, r_{(k-1)n}\},$$
$$\delta(r_0, 0) = \{r_0\},$$
$$\delta(r_0, a) = \{r_0, r_{1a}\} \text{ for each a } \in \{0, 1, \cdots, k-1\},$$
$$\delta(r_{ij}, a) = \{r_{ij+1}\} \text{ for each } i = 1, \cdots, k-1, a \in \{0, 1, \cdots, k-1\},$$
$$F_i = \{r_{in}\} \text{ for each } i = 1, \cdots, k-1.$$

It is clear that $N_{k,n}$ is unmixed and

$$\begin{aligned} L(N_{k,n}) &= \{x \in \{0,1,\cdots,k-1\}^* \mid \text{the } n\text{th symbol from the end of } x \text{ is either } 1, \cdots, \text{ or } k-1\} \\ &= (0+1+\cdots+k-1)^*(1+\cdots+k-1)(0+1+\cdots+k-1)^{n-1} \\ &= \textstyle\sum_{i=1}^{k-1} L_i(N_{k,n}), \end{aligned}$$

where

$$\begin{aligned} L_i(N_{k,n}) &= \{x \in \{0,1,\cdots,k-1\} \mid \text{the } n\text{th symbol from the end of } x \text{ is } i\} \\ &= (0+1+\cdots+k-1)^* i (0+1+\cdots+k-1)^{n-1}, \end{aligned}$$

for each $i = 1, \cdots, k-1$. In the following, we abbreviated

$$L_{k,n} = L(N_{k,n}) \text{ and } L_{k,n}^{(i)} = L_i(N_{k,n})$$

for each $i = 1, \cdots, k-1$.

Theorem 2: DCFA $D_{k,n}$ constructed from $N_{k,n}$ by using subset construction method for NCFA isomorphic to $DB_{k,n}$ for any $k \geq 2$, $n \geq 1$.

(Sketch of Proof) Applying the NCFA version of subset construction method to $N_{k,n}$, we get the following DCFA $D_{k,n}$.

$$D_{k,n} = (Q', \{0, 1, \cdots, k-1\}, \delta', q_0', \sum_{i=1}^{k-1} F'_{\{i\}}),$$

where

$$\begin{aligned} Q' &= \{[x_n \cdots x_1]_k \mid 0 \leq x_j < k, j = 1, \cdots, n\} \\ &= \{q_0, \cdots, q_{k^n-1}\}, \\ q_0' &= q_0 = [0 \cdots 0]_k. \end{aligned}$$

For each $i = 1, \cdots, k-1$,

$$\begin{aligned} F'_{\{i\}} &= \{q_{ik^{n-1}}, \cdots, q_{(i+1)k^{n-1}-1}\} \\ &= \{[ix_{n-1} \cdots x_1]_k \mid 0 \leq x_j < k, j = 1, \cdots, n-1\}. \end{aligned}$$

For each $i = 0, \cdots, k^n - 1, a \in \{0, 1, \cdots, k-1\}$,

$$\delta'(q_i, a) = \begin{cases} q_{k_i \bmod k^n}, & \text{if } a = 0, \\ q_{(k_i+1) \bmod k^n}, & \text{if } a = 1, \\ \quad \vdots & \\ q_{(ki+k-1) \bmod k^n}, & \text{if } a = k-1. \end{cases}$$

The above description of $D_{k,n}$ is identical to the description of $DB_{k,n}$ in Definition 1:

$$\begin{cases} V = \{0, 1, \cdots, k^n - 1\}, \\ E = \{(x, (kx+i) \bmod k^n) \mid x \in V, i = 0, \cdots, k-1\}. \end{cases}$$

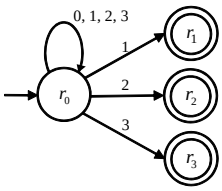

Fig. 1. NFA $N_{4,1}$ accepting $L_{4,1}$.

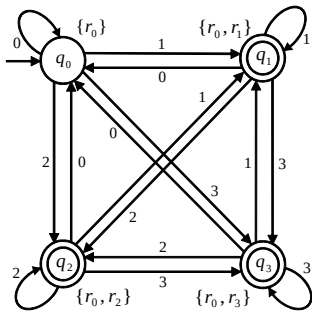

Fig. 2. DFA $D_{4,1}$ accepting $L_{4,1}$.

□

Fig 1 is the transition diagram of $N_{4,1}$. Furthermore, $D_{4,1}$ obtained from $N_{4,1}$ using subset construction method for NCFA is shown in Fig 2.

The following fact is a straightforward extension of binary case in to k-ary one.

Fact 1: Any DCFA which color-distinctly accepts the colored language $L_{k,n} = \sum_{i=1}^{k} L_{k,n}^{(i)}$ requires more than or equal to k^n states, where for each $i = 1, \cdots, k-1$,

$$L_{k,n}^{(i)} = \{x \in \{0,1,\cdots,k-1\}^* \mid \text{the } n\text{th symbol of } x \text{ from its right end is } i\}.$$

IV. Complexity Problems Concerning NCFA

In this section, we investigate computational complexities of some decision problems concerning the unmixedness of nondeterministic colored finite automaton NCFA.

$$\begin{cases} \text{Instance :} & \text{NCFA } M = (Q, \Sigma, \delta, q_0, \sum_{i=1}^{k} F_i), \\ \text{Question :} & \bigcup_{i=1}^{k} L_i(M) = \sum_{i=1}^{k} L_i(M)? \end{cases}$$

Theorem 3: The problem UM can be computed in polynomial time.

(Sketch of Proof) We can show that the complement $\overline{\text{UM}}$ of UM can be solved in nondeterministic logarithmic space by an off-line Turing machine. □

Reducing the nonemptiness problems of ordinary nondeterministic finite automata to $\overline{\text{UM}}$, we also get the following.

Corollary 1: The problem UM is *NLOG*-complete.

References

[1] Y. Takahashi and A. Ito, On Equivalence of de Bruijn Graphs and State-minimaized Finite Automata, $JCDCG^3$ 2017, p.143.

Linear-semiorders and their incomparability graphs

Asahi Takaoka*

Abstract

A linear-interval order is the intersection of a linear order and an interval order. For this class of orders, several structural results have been shown. In this paper, we study a natural subclass of linear-interval orders. We call a partial order a *linear-semiorder* if it is the intersection of a linear order and a semiorder. We show a characterization of linear-semiorders in terms of linear extensions. This gives a vertex ordering characterization of their incomparability graphs. We also show that being a linear-semiorder is a comparability invariant.

This is an extended abstract, and the full version can be found on arXiv.

Keywords: Comparability invariant, Linear-interval orders, PI graphs, Semiorders, Triangle orders, Vertex ordering characterization

1 Introduction

A graph is an *intersection graph* if there is a set of objects such that each vertex corresponds to an object and two vertices are adjacent if and only if the corresponding objects have a nonempty intersection. Intersection graphs of geometric objects have been widely investigated due to their interesting structures and their applications. See [3, 8, 14] for survey.

Well-known examples of intersection graphs are interval graphs and permutation graphs. An *interval graph* is the intersection graph of intervals on the real line. Let L_1 and L_2 be two horizontal lines in the xy-plane with L_1 above L_2. A *permutation graph* is the intersection graph of line segments joining a point on L_1 and a point on L_2. A common generalization of the two graph classes is trapezoid graphs [5, 6]. An interval on L_1 and an interval on L_2 define a trapezoid between L_1 and L_2. A *trapezoid graph* is the intersection graph of such trapezoids. The structure of trapezoid graphs are well investigated, and many recognition algorithms are provided. See [10, 12, 14].

There is a correspondence between partial orders and the intersection graphs of geometric objects between the two lines [9], [10, Theorem 1.11]. A partial order P on a set V is a *trapezoid order* if for each element $v \in V$, there is a trapezoid $T(v)$ between L_1 and L_2 so that for any two elements $u, v \in V$, we have $u \prec v$ in P if and only if $T(u)$ lies completely to the left of $T(v)$. The set of trapezoids $\{T(v)\colon v \in V\}$ is called a *trapezoid representation* of P. By restricting the trapezoids in the representation, many classes of orders have been introduced [1, 2, 13].

An *up-triangle order* [1] is a partial order representable by triangles spanned by a point on L_1 and an interval on L_2. An up-triangle order is also known as a *PI order* [3, 4, 5], where *PI* stands for *Point-Interval*, and as a *linear-interval order* [11] since it is the intersection of a linear order and an interval order.

*Department of Information Systems Creation, Kanagawa University, Rokkakubashi 3-27-1 Kanagawa-ku, Kanagawa, 221–8686, Japan E-mail: takaoka@jindai.jp

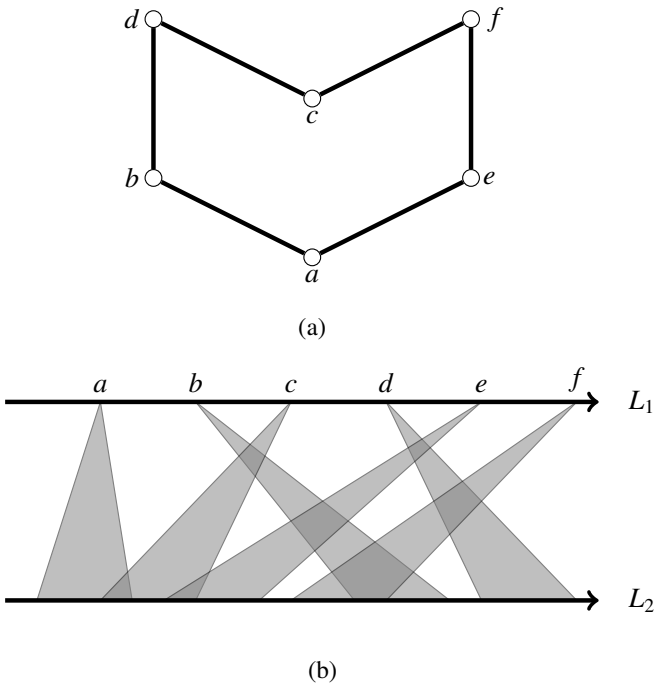

Figure 1: A partial order (the dual of chevron) with a triangle representation.

We use in this paper the term linear-interval orders to denote such orders. Several structural results, including polynomial-time recognition algorithms, are known for linear-interval orders [4, 5, 16, 11, 15].

In this paper, we study up-triangle orders representable by triangles spanned by a point on L_1 and a *unit-length* interval on L_2. See Fig. 1. Such an order is the intersection of a linear order and a semiorder; hence we call it a *linear-semiorder*.

This paper is an extended abstract, and a full version can be found in [17].

2 Preliminaries

A *partially ordered set* is a pair (V, P), where V is a set and P is a binary relation on V that is irreflexive, transitive, and therefore asymmetric. The set V is called the *ground set* while the relation P is called a *partial order* on V. In this paper, we will deal only with partial orders on finite sets.

We denote partial orders by $\prec$ instead of P, that is, we write $u \prec v$ in P if and only if $(u, v) \in P$. Two elements $u, v \in V$ are *comparable* in P if $u \prec v$ or $u \succ v$; otherwise u and v are *incomparable*, which we denote $u \parallel v$.

A partial order P on a set V is a *linear order* if any two elements of V are comparable in P. A partial order P on V is an *interval order* if for each element $v \in V$, there is a (closed) interval $I(v) = [l(v), r(v)]$ on the real line so that $u \prec v$ in P if and only if $r(u) < l(v)$ for any two elements $u, v \in V$. An interval order is a *semiorder* if every interval has unit length.

Let P_1 and P_2 be two partial orders on the same ground set V. The intersection of P_1 and P_2 is the partial order P on V such that $u \prec v$ in P if and only if $u \prec v$ in both P_1 and P_2. We call an order a *linear-semiorder* if it is the intersection of a linear order and a semiorder.

Let P be a partial order on a set V. The *comparability graph* of P is the graph $G = (V, E)$ such that $uv \in E$ if and only if u and v are comparable in P; the *incomparability graph* of P is the graph $G = (V, E)$ such that $uv \in E$ if and only if $u \parallel v$ in P.

3 Comparability invariance

A property of partial orders is a *comparability invariant* if either all orders with the same comparability graph have that property or none have that property. It is known that being a linear-interval order is a comparability invariant [4]. In this section, we will show the following.

Theorem 1. *Being a linear-semiorder is a comparability invariant.*

We use the proof technique developed in [7].

4 Characterization

Let P be a partial order on a set V. A linear order L on V is a *linear extension* of P if $u \prec v$ in L whenever $u \prec v$ in P. We define some properties of linear extensions.

The order $\mathbf{2+2}$ of P is the partial order consisting of four elements x, y, z, w of V such that $x \prec y$ and $z \prec w$ while $x \parallel w$ and $z \parallel y$ in P. Notice that $x \parallel z$ and $y \parallel w$ in P. We say that a linear extension L of P fulfills the $\mathbf{2+2}$ *rule* if $y \prec z$ or $w \prec x$ in L for each induced suborder $\mathbf{2+2}$ of P.

The order $\mathbf{3+1}$ of P is the partial order consisting of four elements x, y, z, w of V such that $x \prec y \prec z$ while $x \parallel w$ and $w \parallel z$ in P. Notice that $y \parallel w$ in P. We say that a linear extension L of P fulfills the $\mathbf{3+1}$ *rule* if $w \prec x$ or $z \prec w$ in L for each induced suborder $\mathbf{3+1}$ of P.

Our previous work [16] shows that a partial order is a linear-interval order if and only if it has a linear extension fulfilling the $\mathbf{2+2}$ rule. In this paper, we show a similar characterization for linear-semiorders.

Theorem 2. *A partial order is a linear-semiorder if and only if it has a linear extension fulfilling the* $\mathbf{2+2}$ *rule and* $\mathbf{3+1}$ *rule.*

Let $G = (V, E)$ be a graph. A *vertex ordering* of G is a linear order of the vertex set V. A *vertex ordering characterization* of a graph class is a characterization of the following type: a graph G is in that class if and only if G has a vertex ordering fulfilling some properties.

Incomparability graphs of linear-interval orders can be characterized so that a graph G is such a graph if and only if there is a vertex ordering of G that contains no suborderings in Figs. 2(a)–(c) [16]. For linear-semiorders, a similar characterization follows from Theorem 2.

Theorem 3. *A graph G is the incomparability graph of a linear-semiorder if and only if there is a vertex ordering of G that contains no suborderings in Figs. 2(a)–(e).*

The class of linear-interval orders contains interval orders and orders of dimension 2 as proper subclasses [5]. For linear-semiorders, we have the following hierarchical relationships between classes of orders.

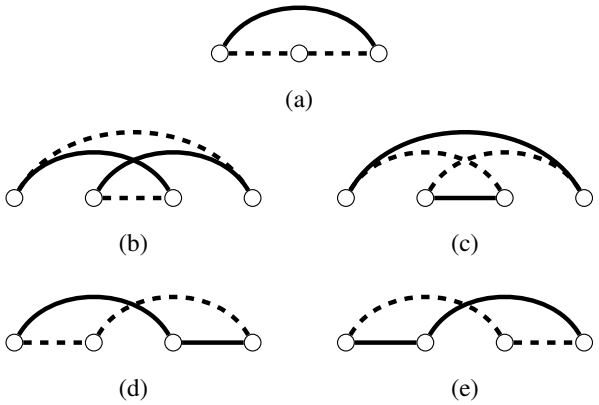

Figure 2: Forbidden patterns. Lines and dashed lines denote edges and non-edges, respectively. Edges that may or may not be present is not drawn.

Theorem 4. *The classes of linear-semiorders and interval orders are incomparable; therefore, the class of linear-semiorders is a proper subclass of linear-interval orders. The class of linear-semiorders contains semiorders and orders of dimension 2 as proper subclasses.*

References

[1] K. P. Bogart, J. D. Laison, and S. P. Ryan. Triangle, parallelogram, and trapezoid orders. *Order*, 27(2):163–175, 2010.

[2] K. P. Bogart, R. H. Möhring, and S. P. Ryan. Proper and unit trapezoid orders and graphs. *Order*, 15(4):325–340, 1998.

[3] A. Brandstädt, V. B. Le, and J. P. Spinrad. *Graph Classes: A Survey*. SIAM, Philadelphia, PA, USA, 1999.

[4] M. R. Cerioli, F. de S. Oliveira, and J. L. Szwarcfiter. Linear-interval dimension and PI orders. *Electron. Notes Discrete Math.*, 30:111–116, 2008.

[5] D. G. Corneil and P. A. Kamula. Extensions of permutation and interval graphs. *Congr. Numer.*, 58:267–275, 1987.

[6] I. Dagan, M. C. Golumbic, and R. Y. Pinter. Trapezoid graphs and their coloring. *Discrete Appl. Math.*, 21(1):35–46, 1988.

[7] S. Felsner and R. H. Möhring. Note: Semi-order dimension two is a comparability invariant. *Order*, 15(4):385–390, 1998.

[8] M. C. Golumbic. *Algorithmic Graph Theory and Perfect Graphs*, volume 57 of *Ann. Discrete Math.* Elsevier, 2 edition, 2004.

[9] M. C. Golumbic, D. Rotem, and J. Urrutia. Comparability graphs and intersection graphs. *Discrete Math.*, 43(1):37–46, 1983.

[10] M. C. Golumbic and A. N. Trenk. *Tolerance Graphs*. Cambridge Univ. Press, 2004.

[11] G. B. Mertzios. The recognition of simple-triangle graphs and of linear-interval orders is polynomial. *SIAM J. Discrete Math.*, 29(3):1150–1185, 2015.

[12] G. B. Mertzios and D. G. Corneil. Vertex splitting and the recognition of trapezoid graphs. *Discrete Appl. Math.*, 159(11):1131–1147, 2011.

[13] S. P. Ryan. Trapezoid order classification. *Order*, 15(4):341–354, 1998.

[14] J. P. Spinrad. *Efficient Graph Representations*, volume 19 of *Fields Institute Monographs*. AMS, Providence, RI, USA, 2003.

[15] A. Takaoka. Recognizing simple-triangle graphs by restricted 2-chain subgraph cover. In *porc. WALCOM*, volume 10167 of *LNCS*, pages 177–189, 2017.

[16] A. Takaoka. A vertex ordering characterization of simple-triangle graphs. *Discrete Math.*, 341(12):3281–3287, 2018.

[17] A. Takaoka. Linear-semiorders and their incomparability graphs. *CoRR*, abs/1907.07845, 2019.

Anti-Slide Placements of Pentominoes

extended abstract

Yasuhiko Takenaga (presenter), Xi Yang and Asuka Inada
Department of Computer and Network Engineering,
Graduate School of Informatics and Engineering,
The University of Electro-Communications

1 Introduction

An anti-slide puzzle is a puzzle to place the pieces into the frame so that no piece can move. This kind of puzzle was first proposed by Strijbos[1]. Fig.1 is an example of a solution for an anti-slide puzzle. As shown in the example, there may remain blank space in the frame where no piece is placed.

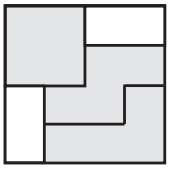

Figure 1: An example of an anti-slide puzzle.

In [2], Amano et al. solved three-dimensional anti-slide puzzles with $2 \times 2 \times 1$ pieces as in [1] using an IP solver. In this paper, we show how to check locally the condition to be an anti-slide placement and enumerate the number of anti-slide placements of pentomino pieces using ordered binary decision diagrams (OBDDs).

2 Ordered Binary Decision Diagrams

An OBDD is a directed acyclic graph representing a Boolean function. An OBDD has a source node and two sink nodes labeled by Boolean values 0 and 1 respectively. Each node except sinks is labeled by a variable and has two outgoing edges called a 0-edge and a 1-edge respectively.

On any path from the source to a sink, variables appear according to a total order of variables. Given an assignment to all the variables, the value of the function is computed by traversing from the source to a sink according to the values of the variables. Fig. 2 is an example of the OBDD, whose variable order is $x_1x_2x_3$.

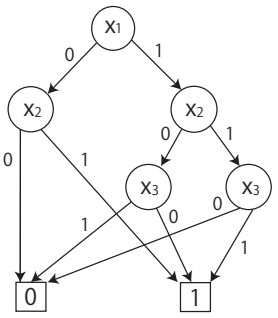

Figure 2: An example of an OBDD.

3 Enumeration of Placements

3.1 Condition to be Anti-Slide

In this section, we consider how to check if a placement of pieces satisfies the condition to be anti-slide.

In Fig.3(a), the cells with letter A (resp. B) are the cells adjacent to the left (resp. right) of a cell in piece U. Obviously, at least one of the cells with A (resp. B) must be occupied by another piece or the wall to prevent the piece to move to the left (resp. right). However, it is not sufficient as shown in Fig.3(b). In this figure, though both pieces satisfies the above condition, the pieces may move together to the right or left. To prevent the move to the left (resp. right), at least one of the cells with A' (resp. B') must be occupied by another piece or the wall. Thus, in the case that a piece is placed in the concave of piece U, we regard the pieces as a single piece and check the above condition. In the case of pentomino pieces, at most three pieces need to be considered as one piece. Note that the sets of pieces to consider as one piece for left-right moves and those for up-down moves are different.

In the following, we prove the correctness of the condition. When a piece includes cells (a, b) and $(a, b + c)$ and not a cell $(a, b + k)$ for some $1 \leq k \leq c-1$, the cell $(a, b+k)$ is called a horizontal concave. Similarly, if a piece includes cells (a, b) and $(a+c, b)$ and not a cell $(a + k, b)$ for some $1 \leq k \leq c - 1$, the cell $(a + k, b)$ is called a vertical concave.

Theorem 1. *Assume that no piece has a vertical concave. Then any piece on the board cannot move*

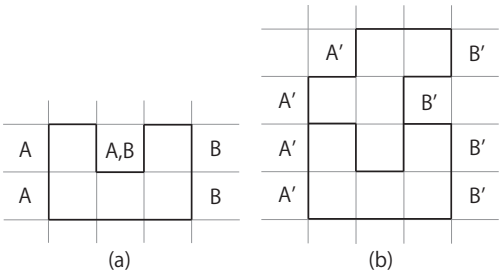

Figure 3: Condition for piece U.

to the left (resp. right) if and only if, for any piece on the board, there exists another piece or a wall on a cell adjacent to the left (resp. right) of the piece.

Clearly, the same result holds for the up and down moves of the pieces without horizontal concaves.

Proof. (only if) Obvious.

(if) Consider a directed graph G such that the set of vertices represents the pieces on the board and the left wall. There exists a directed edge from piece p to q when q is adjacent to the left of p. Then any vertex except the wall has at least one outgoing edge. Any piece from which there is a path to the sink (wall) in G cannot move to the left.

G has a vertex with no path to the sink only when G has a cycle from which there is no path to the sink. In the following, we show that G does not have a cycle. Assume to the contrary that there exists a cycle. Let p_i $(0 \leq i \leq k-1)$ be pieces on the cycle, such that there exists an edge from p_j to p_{j+1}, where the addition is under modulo k. We call a cell (s,t) in p_i to be a blocking cell when cell $(s+1,t)$ belongs to p_{i-1}. Let $b_i = (s_i, t_i)$ be a blocking cell in p_i and let $b'_{i-1} = (s_i + 1, t_i)$. Cell b_i can be arbitrary chosen except that the blocking cells with the largest and the smallest y-coordinates must be chosen. A path from b_i to b'_i can be made in p_i. Then a directed cycle C is formed by such paths and paths from b'_i to b_{i+1}.

We assume that cycle C is clockwise and lead a contradiction. Consider the blocking cell b_i with the largest y-coordinate. From b'_{i-1} to b_i, the cycle is going from right to left. As C is clockwise, the cycle must go from left to right above b'_{i-1} and b_i. As b_i is the blocking cell with the largest y-coordinate, there must exist a piece which includes cells on the left and right of b'_{i-1}. It means that the piece has a vertical concave.

Similarly, by considering the blocking cell with the smallest y-coordinate, we can see that C is not counter-clockwise. Thus, G does not include a cycle. □

3.2 Experimental Results

We have implemented the program to enumerate the number of anti-slide placements of pentominoes. A pentomino can be placed in at most eight ways by rotating and turning it over. We deal with them as different kinds of pieces. The implementation uses CUDD package[4] to manipulate OBDDs.

In the following experiments, we have assumed that only the kinds of pieces to be used are given and the number of pieces for each kind of piece is not limited. It is allowed that some kind of piece is not used at all. Experimental results are shown in Tables 1 and 2.

size of board	number of plecements
3×3	25
4×4	1,668
5×5	455,835
6×5	9,313,423
6×6	404,121,230

Table 1: Number of placements for all kinds of pieces.

size of board	number of placements
3×3	25
4×4	1,356
5×5	321,008
6×5	6,101,083
6×6	243,307,547

Table 2: Number of placements for pieces except U.

References

[1] Anti-Slide, https://johnrausch.com/PuzzleWorld/puz/anti_slide.htm (accessed June 2019).

[2] K.Amano, S.Nakano and K.Yamazaki, "Anti-Slide," Journal of Information Processing, Vol.23, No.3 pp.252-257, 2015.

[3] R.E.Bryant,"Graph-Based Algorithms for Boolean Function Manipulation," IEEE Transactions on Computers, Vol. C-35, No. 8, pp.6 77-691, 1986.

[4] The cudd package, http://web.mit.edu/sage/export/tmp/y/usr/share/doc/polybori/cudd/cuddExtDet.html (accessed June 2019).

Acknowledgement This work was supported by JSPS KAKENHI Grant Number 18K11601.

Graph Compression Through Bridge Coalescence and Ear Decomposition

Jose Enrico Tiongson*
Ateneo de Manila University
jose.tiongson@obf.ateneo.edu

Jude Buot
Ateneo de Manila University
jbuot@ateneo.edu

Let G be a simple, connected, undirected graph. A connected subgraph of G is called a *bridge component* of G if all its edges are bridges in G. A bridge component is said to be *maximal* if it is not a proper subgraph of any another bridge component of G. Denote the set of bridges of G by $B(G)$.

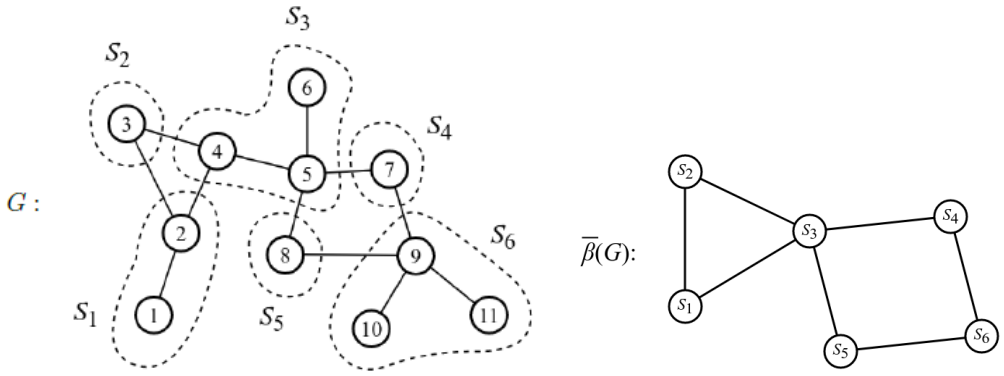

Figure 1: Graph G and it bridge coalescence graph $\bar{\beta}(G)$.

In Figure **??**, there are six maximal bridge components of G, labeled $S_1, S_2, \ldots, S_6$. We define the *bridge coalescence* of G, denoted by $\bar{\beta}(G)$, as the graph obtained if, for every bridge $\{u, v\}$ in G, we merge and identify u and v into a single vertex in $\bar{\beta}(G)$. Observe that the vertices of $\bar{\beta}(G)$ are labeled according to the maximal bridge components of G, that is, two vertices S_i and S_j in $\bar{\beta}(G)$ are adjacent if a vertex in S_i is adjacent to a vertex in S_j in G. Clearly, $\bar{\beta}(G)$ is a bridgeless graph.

On the other hand, an *ear decomposition* of a graph G is defined as the sequence of subgraphs of G, written as $(G_0; G_1; \ldots; G_k = G)$, where G_0 is a cycle (see Figure **??**(c)) and G_i is G_{i-1} but with an attached ear (see Figure **??**(a)). Robbins [1] proved that only bridgeless graphs have an ear decomposition.

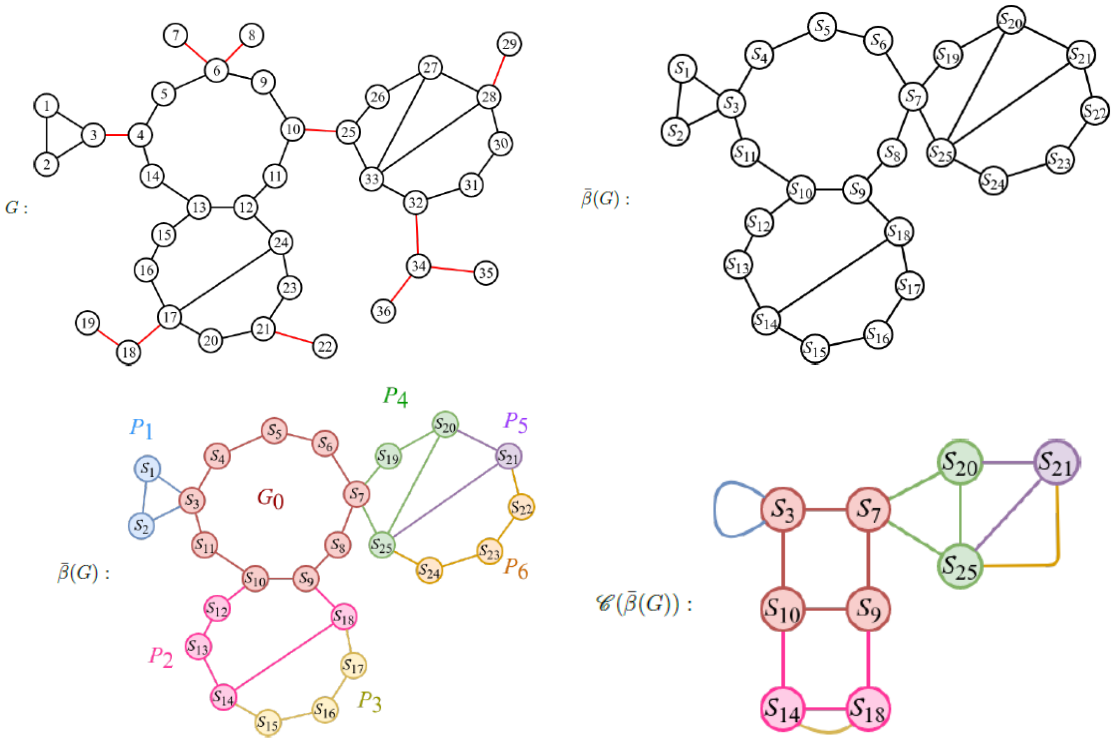

Figure 2: (a) A graph G, (b) its bridge coalescence $\bar{\beta}(G)$, (c) an ear decomposition of $\bar{\beta}(G)$, and (b) its graph compression $\mathscr{C}(\bar{\beta}(G))$.

In this paper, we begin with a graph G (see Figure **??**(a)) and then produce a bridgeless graph through bridge coalescence (see Figure **??**(b)). Next, we look into the ear decomposition of the latter (see Figure **??**(c)).

Finally, we introduce a two-fold compression scheme, denoted by $\mathscr{C}(\bar{\beta}(G))$ (see Figure **??**(d)). This procedure produces a minimal multigraph that preserves the cyclic structure of the original graph G. We claim that this two-fold compression can be used to categorize graphs based on their size-order difference. In this research, we computed the following bounds for the order and size of $\mathscr{C}(\bar{\beta}(G))$, namely,

$$|V(\mathscr{C}(\bar{\beta}(G)))| \leq \max\{1, 2(|E(G)| - |V(G)|)\}$$

$$|E(\mathscr{C}(\bar{\beta}(G)))| \leq \max\{1, 3(|E(G)| - |V(G)|)\}$$

If G is a tree, then $\mathscr{C}(\bar{\beta}(G))) \cong K_1$. If G is an almost-tree of order n and size m, then $m - n$ is small. With the order and size of $\mathscr{C}(\bar{\beta}(G)))$ being bounded by a factor of $m - n$, what this compression does is transform a cyclic graph G of order n and size m into a smaller graph with at most $\max\{1, 2(m - n)\}$ vertices and $\max\{1, 3(m - n)\}$ edges, thereby addressing the weakness of ear decomposition being only applicable to graphs with no bridges. With bridge coalescence, it is now possible to perform the same compression scheme even for graphs with bridges. Further, through $\mathscr{C}(\bar{\beta}(G)))$, it is now possible to objectively characterize the cyclic structure of graphs based on the circuit rank $r(G)$ (as in [2]).

This approach has potential in solving problems related to graph cycles more efficiently. For example, if a problem on a graph G is solvable in $O(f(n; m))$ complexity then, through $\mathscr{C}(\bar{\beta}(G)))$, the same problem can be reduced to $O(X + f(2(m - n); 3(m - n)))$ complexity, where X is the complexity of performing the two-fold compression. Thus, no matter how large m and n can become, as long as $m - n$ remains fixed, G remains solvable in $O(X + f(2(m-n); 3(m-n)))$ time. Finally, we proved that $O(X)$ is linear with respect to the order and size of the original graph G using a bridge finding algorithm [3], a linear ear decomposition step [4] and union-find algorithm [5].

References:

1. H.E. Robbins, "A theorem on graphs, with an application to a problem on traffic control," American Mathematical Monthly, 46:281-283, 1939.

2. H. Whitney, "Non-separable and planar graphs," Transactions of the American Mathematical Society, 34:339-362, 1932.

3. R. E. Tarjan, 11A note on finding the bridges of a graph," Information Processing Letters, 2 (6): 160-161, 1974.

4. S. Chakraborty, V. Raman, and S. R. Satti, "Biconnectivity, chain decomposition and st-numbering using O(n) bits," In 27th International Symposium on Algorithms and Computation (ISAAC 2016), Schloss Dagstuhl-Leibniz-Zentrum fuer Informatik, 22:1-13, 2016.

5. H. Zhang, "The union-find problem is linear," University of Iowa, 2008.

Sigma Coloring and Edge Deletions

Mark Anthony C. Tolentino, Agnes D. Garciano, Reginaldo M. Marcelo, Mari-Jo P. Ruiz
mtolentino@ateneo.edu,agarciano@ateneo.edu,rmarcelo@ateneo.edu,mruiz@ateneo.edu
Ateneo de Manila University

In [6], the authors considered the notion of critical edges (and vertices), defined as follows: An edge (or vertex) in a graph is *critical* if its deletion reduces the chromatic number of the graph by one. They studied the complexity of the problem of testing for the existence of critical vertices and edges in H-free graphs. They showed that an edge in a graph is critical if and only if its contraction reduces the chromatic number by one. The effect of edge deletion on the set chromatic number was also studied in [1], where it was shown that deleting an edge from a graph changes (increases/decreases) the set chromatic number by at most two.

In this work, we consider the notion of edge deletion with respect to a different kind of vertex coloring called sigma coloring. G. Chartrand, F. Okamoto, and P. Zhang [2] defined the concept of the *sigma chromatic number* of a graph as follows: For a non-trivial connected graph G, let $c : V(G) \to \mathbb{N}$ be a vertex coloring of G. For each $v \in V(G)$, let $N(v)$ denote the *neighborhood of* v, i.e., the set of vertices adjacent to v. Moreover, the *color sum* of v, denoted by $\sigma(v)$, is defined to be the sum of the colors of the vertices in $N(v)$. If $\sigma(u) \neq \sigma(v)$ for every two adjacent $u, v \in V(G)$, then c is called a *sigma coloring* of G. The minimum number of colors required in a sigma coloring of G is called its sigma chromatic number and is denoted by $\sigma(G)$.

It was shown in [3] that for each positive integer k, the problem of deciding whether the sigma chromatic number of a 3-regular graph equals k is **NP**-complete. Moreover, the sigma chromatic number of some families of graphs are discussed in [5, 4].

In this paper, we show the effect of edge deletion on the sigma chromatic number of a graph as follows:

Result 1. *Let G be a graph and e an edge of G. Denote by $G - e$ the graph obtained by deleting the edge e from G. then*

$$-1 \leq \sigma(G) - \sigma(G - e) \leq 2$$

Moreover, we show that for each $k = -1, 0, 1, 2$, there are infinitely many graphs G with an edge e for which $\sigma(G) - \sigma(G - e) = k$.

We also study the existence of sequences of edge deletions each of which decreases the sigma chromatic number by one. We consider this problem for path complements, which we define as follows:

Definition. *The **complement of a path** P_m, $m \geq 2$, in the complete graph $K_n, n \geq m$, is the graph obtained by deleting the edges of a subgraph of K_n that is isomorphic to P_m. This graph is denoted by $\overline{P}_{m,n}$.*

As an example, the graph $\overline{P}_{4,7}$ is shown in Figure 1 where the deleted edges are indicated using dashed segments.

It is easy to see that $\overline{P}_{2,n}$, $n \geq 3$, has sigma chromatic number $n - 2$; that is, deleting one edge from K_n decreases the sigma chromatic number by two. As a consequence of Proposition 3.1 in [2], it is worth noting that there is no sequence of edge deletions in K_n that will decrease the sigma chromatic number to $n - 1$.

We have the following result:

Result 2. *For $m = 2, 3, ..., \lceil n/2 \rceil$,*

$$\sigma\left(\overline{P}_{m,n}\right) = n - m.$$

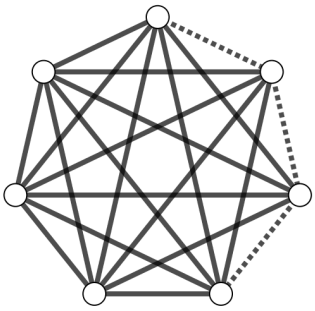

Figure 1: The path complement $\overline{P}_{4,7}$

The above result implies the following: Consider a subgraph of K_n isomorphic to a path $P_m : v_1 \to v_2 \to \cdots \to v_m$, where each v_i is a vertex of K_n. The deletion of edge v_1v_2 decreases the sigma chromatic number by two. Then in the sequence of deletions of edges v_iv_{i+1} where i runs from 2 to $m-1$, each edge deletion decreases the sigma chromatic number by one. This is illustrated for K_7 in Figure 2. For comparison, the same sequence of edge deletions in Figure 2 produce the following sequence of chromatic numbers: $\chi = 6, \chi = 6, \chi = 5$.

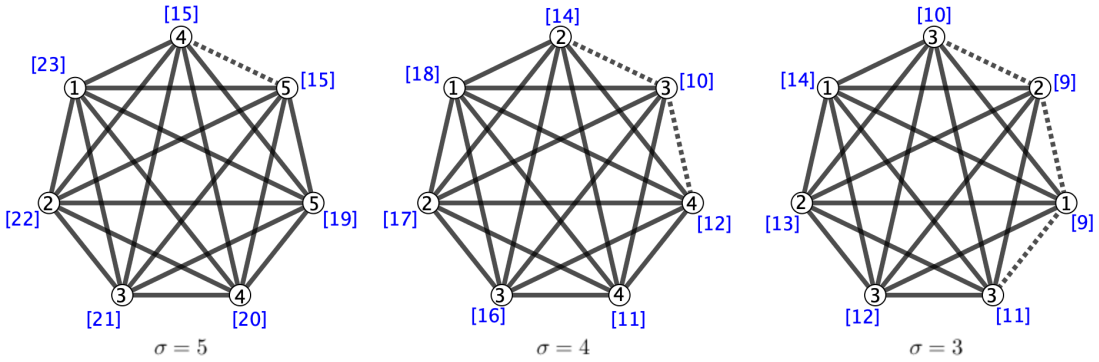

Figure 2: A sequence of edge deletions in K_7

References

[1] Gary Chartrand, Futaba Okamoto, Craig W. Rasmussen, and Ping Zhang. The set chromatic number of a graph. *Discussiones Mathematicae Graph Theory*, 29(3):545–561, 2009.

[2] Gary Chartrand, Futaba Okamoto, and Ping Zhang. The sigma chromatic number of a graph. *Graphs and Combinatorics*, 26:755–773, 2010.

[3] Ali Dehghan, Mohammad-Reza Sadeghi, and Arash Ahadi. The complexity of the sigma chromatic number of cubic graphs. arXiv:1403.6288v1 [math.CO], March 2014.

[4] Agnes D. Garciano, Reginaldo M. Marcelo, Mari-Jo P. Ruiz, and Mark Anthony C. Tolentino. The sigma chromatic number of the sierpiński gasket graphs and the hanoi graphs. Conference paper, JCDCGGG 2017, April 2018.

[5] Paul Adrian Luzon, Mari-Jo Ruiz, and Mark Anthony Tolentino. The sigma chromatic number of the circulant graphs $C_n(1,2)$, $C_n(1,3)$, and $C_{2n}(1,n)$. In Akiyama J., Ito H., Sakai T., and Uno Y., editors, *Discrete and Computational Geometry and Graphs. JCDCGG 2015.*, volume 9943 of *Lecture Notes in Computer Science*. Springer, Cham, 2016.

[6] Christophe Picouleau, Dani el Paulusma, and Bernard Ries. Reducing the chromatic number by vertex or edge deletions. *Electronic Notes in Discrete Mathematics*, 62(3):243–248, November 2017.

On cyclic decompositions of the complete graph into the generalized Petersen graph $P(6r, 3)$

Wannasiri Wannasit
Department of Mathematics
Chiang Mai University
Chiang Mai 50200, Thailand
e-mail: Wannasiri.w@cmu.ac.th

Saad El-Zanati
Department of Mathematics
Illinois State University
Normal, IL 61790-4520, USA
e-mail: Saad@ilstu.edu

Abstract

It is known that a uniformly-ordered ρ-labeling (also known as a ρ^{++}-labeling) of a bipartite graph G with m edges can be used to obtain a cyclic G-decomposition of K_{2mt+1} for every positive integer t. We show that the generalized Petersen graphs $P(6r, 3)$ admits a ρ^{++}-labeling for every positive integer r.

Keywords: Cyclic G-designs, Generalized Petersen Graphs, Uniformly-ordered ρ-labelings.

Dr. Mario Puzzle Generation: Theory, Practice, and History (Famicom/NES)

Aaron Williams*

1 Introduction

Dr. Mario (ドクターマリオ) was released by Nintendo on the Famicom/NES (Japan/USA) in 1990. It influenced countless matching games (see Juul [3]) and was one of the first games with randomly generated puzzles (see Parish [6]).
As **mathematicians** we ask the following question.

- *How are Dr. Mario puzzles defined combinatorially?*

As **computer scientists** we ask the following question.

- *How can puzzles be generated algorithmically?*

As **retroarcheologists** (Aycock [1]) we ask the following.

- *How did Nintendo's programmers generate puzzles?*

As **video game historians** we ask the following question.

- *Why do all NES puzzles have $v \leq 84$ viruses?*

Finally, as **retrogamers** we ask the following question.

- *Can we make the NES game more difficult (and fun)?*

This extended abstract briefly answers these questions. We assume the reader is familiar with the NES game.

2 Graph Coloring

A *Dr. Mario puzzle* fits v viruses in the bottom r rows of a grid. Each virus is red, yellow, or blue with most one per cell. All commercial releases have $c = 8$ columns and we assume this unless otherwise stated. For example, Figure 1a has several puzzles with viruses in the bottom $r = 13$ rows.

Remark 1. The hardest NES puzzles have difficulty level 20. These puzzles fit $v = 84$ viruses in the bottom $r = 13$ rows.

Nintendo never puts three consecutive same color viruses horizontally or vertically. In fact, they use a stronger constraint: Same color viruses are never two cells away horizontally or vertically. Thus, a virus in cell (a, b) forbids $(a+2, b)$, $(a-2, b)$, $(a, b+2)$, $(a, b-2)$ from having the same color of virus. If a puzzle satisfies this constraint, then it is *valid*.

For graph theorists a valid puzzle is simply a partially 3-colored r-by-c grid graph, except that edges connect vertices two rows/columns away. This graph has four connected components; each component is a standard grid graph containing vertices with the same pair of row and column parities (or *pairities*). Figure 2 illustrates the graphs associated with the puzzle in Figure 1a.

Remark 2. A Dr. Mario puzzle is valid if and only if its connected grid graphs receive proper partial 3-colorings.

2.1 Maximal and Balanced Puzzles

A color is *available* for an empty cell if adding that color of virus doesn't break Nintendo's constraint. A puzzle is *maximal* if no cells have available colors; equivalently, the grid graphs are maximally 3-colored. For example, Figure 1a is not maximal by Figure 2, but Figures 1b–1c are maximal.

A Dr. Mario puzzle is *balanced* if its three colors have (at most) two consecutive frequencies. Figure 1c is balanced since each color is used $\frac{60}{3} = 20$ times.

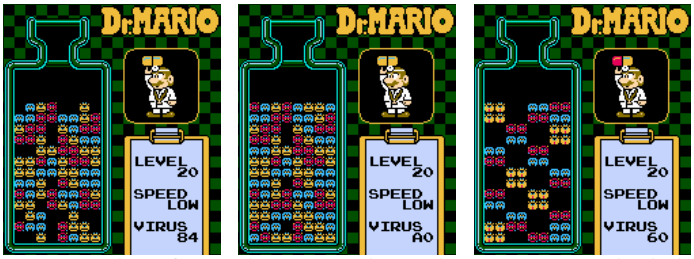

(a) Puzzle from seed 1394 with v=84 viruses in r=13 rows. (b) Maximal puzzle with seed 1394. It has 100 viruses. (c) Maximal balanced puzzle with only 60 viruses.

Figure 1: Puzzles from (a) NES game, (b) NES game with Game Genie code IANETZPA, with (c) a hypothetical puzzle.

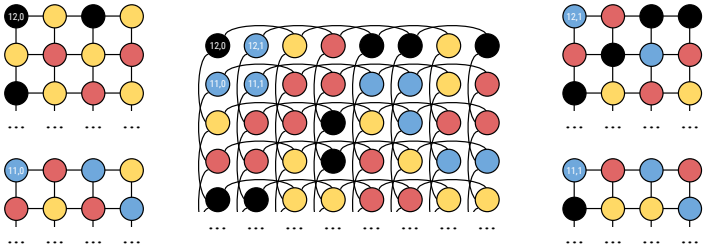

Figure 2: Figure 1a as graph coloring. Black denotes no color (i.e. no virus). The top-left grid graph has (even,even) pairity.

3 Algorithms

Now we design simple algorithms for generating random valid Dr. Mario puzzles with v viruses. We focus on algorithms that add one virus at a time and never backtrack.

Our first algorithm uses random positions and colors.

Algorithm 1. Choose a random cell and a random color until that color is available at that cell.

Our second algorithm also uses random positions, but it cycles through the colors to ensure the result is balanced.

Algorithm 2. Cycle through colors red, yellow, blue. Choose a random cell until that color is available.

Unfortunately, these algorithms do not safely generate NES puzzles. In particular, Figure 1c proves Remark 3.

Remark 3. Algorithms 1 & 2 can fail with 60 viruses in 13 rows.

Next we consider randomizing only the colors.

Algorithm 3. Visit the cells in row-major order. Choose a random available color or no color for the cell; reweight this probability[1] to ensure v are added in total.

Notice that Algorithm 3 always works. This is because each cell has ≤ 2 prior neighbors in row-major order, so every cell has at least one available color when it is visited.

Remark 4. Algorithms 3 always fits v viruses in an r-by-c grid, so long as the necessary condition $v \leq r \cdot c$ holds.

*Williams College, aaron.williams@williams.edu

[1] If there are x remaining viruses and y remaining cells, then the probability of choosing to color a cell is $\frac{x}{y}$.

4 NES Game

Next we consider how Nintendo programmer Takahiro Harada generated random levels in the NES game. The pioneering work of user `nightmareci` in disassembling the NES machine code was invaluable in this investigation (see [4, 5]).

4.1 Harada's Algorithm

Harada's approach is similar to Algorithm 2 in that it chooses random positions and attempts to cycle through the colors. However, when it fails with its preferred choice, it proceeds in a manner that is similar to Algorithm 3. For further details including pseudocode see [5].

Algorithm H. Choose a random cell. Add the highest-priority available color to this cell. If no colors are available, then repeat on the next cell in row-major order.

In theory, Algorithm H can generate any balanced puzzle, including Figure 1c. Therefore, Nintendo's algorithm is flawed—it does not safely generate NES puzzles!

Remark 5. Algorithms H can fail with 60 viruses in 13 rows.

If the NES game did generate Figure 1c, then it would *freeze* (i.e. infinite loop). Luckily, this never occurs in practice due to the limited form of randomization used in the game.

4.2 Nintendo's LFSR and Randomization

For randomization Harada used a 15-bit *linear feedback shift register* (see Golomb [2]) with primitive feedback polynomial $x^{15} + x^7 + 1$. Thus, bits 7 and 15 are tapped. So if the current state is $b_1 b_2 \cdots b_{15}$, then $x = (b_7 + b_{15}) \mod 2$ is the next random bit, and the next state is $x b_1 b_2 \cdots b_{14}$ (see Figure 3).

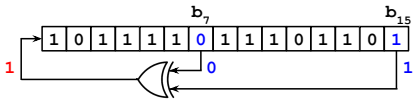

Figure 3: Nintendo's LFSR. For example, state 101111011101101 is followed by state 110111101110110.

Before generating a puzzle the NES game seeds the LFSR state to any non-zero value $b_1 b_2 \cdots b_{15}$. This gives an entry point into a cyclic stream of $2^{15} - 1 = 32{,}767$ pseudorandom bits. Algorithm H then proceeds deterministically.

Remark 6. Dr. Mario (NES) has at most 32,767 distinct puzzles per r-by-c grid. (Figure 1c isn't one of them.)

Note that the number of NES puzzles pales in comparison to the number of valid puzzles. For example, there are more than $\binom{104}{84} > 10^{21}$ puzzles with $r = 13$ rows and $v = 84$ viruses.

The use of a 15-bit LFSR instead of a 16-bit LFSR was likely due to efficiency. Maximal length 16-bit LFSRs require four taps [7] and hence more instructions. Due to the 8-bit architecture of the NES, the state is stored across two bytes with b_{16} ignored. Thus, state `0x5EED` and `0x5EEC` are equivalent.

4.3 Analyzing Algorithm H

A translation of Algorithm H (and its LFSR) into C is provided by `nightmareci` in [4]. By modifying this program, we can run Algorithm H until it generates a maximal puzzle, instead of quitting after the required number of viruses. The *failure point* (i.e. the virus number not added) for all 32,767 puzzles with 13 rows appears in Figure 4. For example, Figure 1b is one of the 5,247 different levels with a failure point of 101.

Notice that Algorithm H never fails before the 85th virus. Thus, it never freezes in the actual NES game.

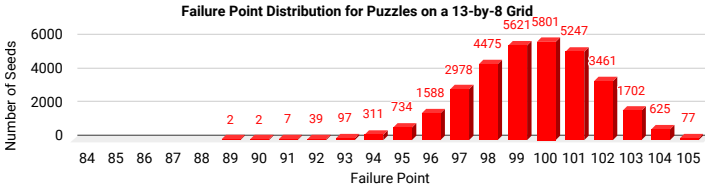

Figure 4: Distribution of Algorithm H failure points for level 20 puzzles using the Game Genie code `YANETZPA`.

5 Historical Signficance

Newer Dr. Mario titles have more viruses in the most difficult puzzles. For example, *Dr. Mario Online Rx* (Wii) fits $v = 99$ viruses in $r = 13$ rows. Our study has explained why the NES game only has $v = 84$ in these puzzles. Simply put, Harada's algorithm was not robust enough. In practice, Algorithm H begins to fail with more than $v = 88$ viruses.

Prototypes of Dr. Mario exist under the name *Virus* [8] and allow up to $v = 96$ viruses (although the three-in-a-row restriction is not followed). Thus, Nintendo likley wanted more viruses in the NES game, but were restricted by Algorithm H. Furthermore, parameters for the NES release were likely tuned to maximize viruses while avoiding game freezes.

6 Improving the NES Game with Game Genie Codes

In Section 4.3 we modified a simulation of the NES puzzle generation algorithm. Now we modify the actual game in order to create more difficult (and fun) puzzles.

The *Game Genie* is an NES peripheral that modifies memory values to alter gameplay. Table 1 has new codes for the number of viruses in all levels, and the rows in level 20.

Code	All Levels
AANETZPA	−4 viruses
ZANETZPA	+4 viruses
⚠ LANETZPA	+8 viruses
⚠ GANETZPA	+12 viruses
⚠ IANETZPA	+16 viruses
⚠ TANETZPA	+20 viruses
⚠ YANETZPA	+24 viruses
⚠ AANETZPE	+28 viruses
⚠ PANETZPE	+32 viruses

Code	Level 20
PENZZUGE	10 rows
⚠ ZENZZUGE	11 rows
⚠ LENZZUGE	12 rows
IENZZUGE	14 rows
TENZZUGE	15 rows
YENZZUGE	16 rows

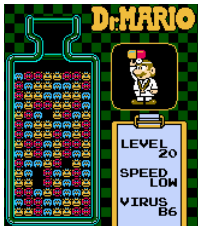

Table 1: New Game Genie codes for Dr. Mario (NES) and an impossibly hard puzzle.

Some codes can cause freezing during puzzle generation. For example, `TANETZPA` completely fills level 20 puzzles with viruses and its success rate is only $\frac{77}{32767} = 0.23\%$ by Figure 4.

References

[1] J. Aycock. *Retrogame Archeology: Exploring Old Computer Games*. Springer, 1st edition, 5 2016.

[2] S. W. Golomb. *Shift Register Sequences*. Aegean Park Press, 1981.

[3] J. Juul. Swap adjacent gems to make sets of three: A history of matching tile games. *Artifact*, 4(1):205–216, 2007.

[4] nightmareci. Dr. Mario virus placement. `https://tetrisconcept.net/threads/dr-mario-virus-placement.2037`, August 2012.

[5] nightmareci. Dr. Mario. `https://tetris.wiki/Dr._Mario`, March 2013.

[6] J. Parish. Dr. Mario retrospective: Heading for a malpractice suit | Game Boy Works 070. `https://www.youtube.com/watch?v=kGq1n9F1DFM`, July 2016.

[7] A. Partow. Primitive polynomial list. `https://www.partow.net/programming/polynomials/index.html`.

[8] Proto:Dr. Mario (NES). `https://tcrf.net/Proto:Dr._Mario_(NES)`.

On the Algorithm and Complexity of Motion Planning Problem of a Forklift (extended abstract)

Chao Yang
School of Mathematics and Statistics
Guangdong University of Foreign Studies, Guangzhou, 510006, China
sokoban2007@163.com, yangchao0710@gmail.com
http://sokoban.cn/yang

1 Introduction

The study of the robot motion planning problem, sometimes referred to as the geometric path planning problem, the generalized movers' problem or the piano movers' problem, dates back to the 1970s. We refer to [1] for a recent survey of this problem.

Definition 1 (Robot Motion Planning Problem)**.** *In a Euclidean space $\mathbb{R}^2$ or $\mathbb{R}^3$ (the workspace), guide a robot from one position to another, by avoiding the obstacles in the space.*

Note that in general, the robot may be consist of several parts, and each part may be moved independently. A standard way to study the problem is to define the *configuration space*. For example, let the robot be a long rectangle that can silde and rotate in the plane. Then a configuration of this rectangular robot can be exactly described by the coordinates (x, y) of one of its vertices, and the angle θ between its long edge and the x-axis. So the configuration space is the set of all points $(x, y, \theta) \in \mathbb{R} \times \mathbb{R} \times [0, 2\pi)$ which are collision-free with all obstacles. Usually the configuration space has a higher dimension than the workspace.

In general, the continous version of the robot motion planning problem is PSPACE-hard. Canny gave the first single exponential-time algorithm in the dimensionality of the configuration space in his doctoral thesis [2]. As a corollary, if we fix the dimension of the configuration space, then we will have a polynomial algortihm for the problem.

In real world application, there are lots of situation where the robot moves in a discrete manner. But the problem remains PSPACE-complete for the discrete case. The sliding block puzzles can be viewed as a discrete type of motion planning problem, and it is PSPACE-complete, even with blocks of size 1×2 and 2×1. If all blocks are of size 1×1, it becomes a generalization of the Fifteen Puzzle, and the problem is solvable in polynomial time.

In this paper, we study another discrete case of the motion planning problem, the motion planning for a forklift in a warehouse. Unlike the sliding block problem which has a workspace of dimesion 2, the motion planning problem of a forklift has a workspace of dimension 3. We apply the configuration space method to analyse the problem. As we shall see, the configuration space becomes a graph in the discrete case.

And we use a Japanese game called Zaikoban[1] developed by NetFarm in 2007 as a model for the forklift motion planning problem in a warehouse. The game was also available temporarily under the name *Soko Forklift - Zaikoban* for Android system at Google Play in 2014, and for iOS system in 2015. See Figure 1 for screenshots taken from the Android version.

[1] https://www.netfarm.ne.jp/island/release/070713_01.pdf

Figure 1: Screenshots of the game Zaikoban

2 Main results

In the game Zaikoban, a forklift has to transport one or more boxes from their initial positions to their respective goal positions. The warehouse is a 3-dimensional grid with walls. The forklift occupies 4 cubes of the grid, and it can move forwards or backwards, turn 90 degrees to the left or right, raise or lower the fork, and load or unload a box from the fork. There are a few addtional elements in the game of Zaikoban, such as fragile floors which the forklift can go through only without carring a box.

Definition 2 (Forklift Motion Planning Problem)**.** *Given a warehouse with walls, one forklift, one or more boxes with goal positions, and possibly a few addtional elements, decide whether the transportation of the boxes can be done by the forklift.*

If there is only one box to be transported, then the configuration space has dimension 4, and there exists a polynomial-time algorithm to find the shortest path.

Theorem 1. *The forklift motion planning problem can be solved in polynomial time for one box.*

If there is no limit on the number of boxes, which is equivalent to that there is no limit on the dimensionality of the configuration space, then we show the problem is PSPACE-complete, by an application of the NCL model [3] developed by Hearn and Demaine.

Theorem 2. *The forklift motion planning problem is PSPACE-complete in the general case.*

References

[1] L. E. Kavraki, S. M. LaValle, *Motion Planning.* In: B. Siciliano, O. Khatib (Eds.), Springer Handbook of Robotics, Springer, 2016

[2] J. F. Canny, *The Complexity of Robot Motion Planning*, MIT, Cambridge, 1988.

[3] R. A. Hearn, E. D. Demaine, *PSPACE-completeness of sliding-block puzzles and other problems through the nondeterministic constraint logic model of computation*, Theoretical Computer Science, (2005), **343**, 72-96.

Minimal forbidden graphs for widely generalized line graphs

Michitaka Furuya * Sho Kubota † Tetsuji Taniguchi ‡ Kiyoto Yoshino§

We consider only finite undirected graphs without loops or multiple edges. The eigenvalues of the adjacent matrix of a graph G are called the *eigenvalues* of G. Our motivation derives from the smallest eigenvalue of graphs. Hoffman [1] proved a celebrated theorem: For a graph G with the smallest eigenvalue greater than $-1-\sqrt{2}$, if the minimum degree is sufficiently large, then G is a generalized line graph. In addition, Woo and Neumaier [5] characterized graphs whose minimum degree is sufficiently large and the smallest eigenvalue is in the range $(-2.4812\cdots, -1-\sqrt{2}]$. To state it correctly, we need to introduce the concepts of so-called "Hoffman graph" and "slim $\mathfrak{H}$-line graph", which is defined in the next section. However, their characterization by using slim $\mathfrak{H}$-line graph are slightly complicated. We give a necessary condition of the minimal forbidden graphs for the slim $\mathfrak{H}$-line graphs for a set $\mathfrak{H}$ of Hoffman graphs satisfying a certain condition. In general, *minimal forbidden graph* G for a set $\mathcal{G}$ of graphs with hereditary property is a graph not in $\mathcal{G}$ and every proper induced subgraph of G is isomorphic to a graph in $\mathcal{G}$.

1 Hoffman graphs

In this section, we define Hoffman graphs and related concepts. A *Hoffman graph* $\mathfrak{h}$ is a pair (H,μ) of a graph H and a labeling map $\mu : V \to \{f,s\}$, where V denotes the vertex set of H, satisfying the following conditions:

1. every vertex with label f is adjacent to at least one vertex with label s; and
2. the vertices with label f are pairwise non-adjacent.

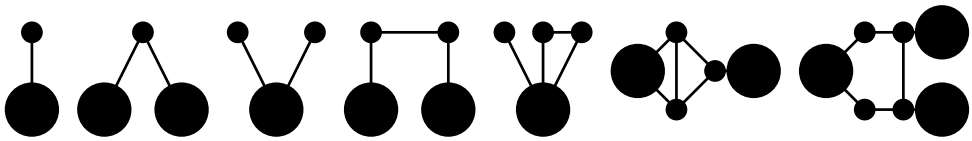

Figure 1: Hoffman graphs, whose slim (resp. fat) vertices are depicted as small (resp. large) filled circles

Let $\mathfrak{h}=(H,\mu)$ be a Hoffman graph. A vertex of H with label s (resp. label f) is called a *slim vertex* (resp. a *fat vertex*). We let $V_s(\mathfrak{h})$ (resp. $V_f(\mathfrak{h})$) denote the set of slim vertices (resp. fat vertices) of H, and let $V(\mathfrak{h}) = V_s(\mathfrak{h}) \cup V_f(\mathfrak{h})$. For a vertex x of $\mathfrak{h}$, we let $N^s_{\mathfrak{h}}(x)$ (resp. $N^f_{\mathfrak{h}}(x)$) denote the set of neighbors labeled s (resp. f) of x, and set $N_{\mathfrak{h}}(x) = N^s_{\mathfrak{h}}(x) \cup N^f_{\mathfrak{h}}(x)$. We regard (ordinary) graphs as Hoffman graphs with only slim vertices. A Hoffman graph $\mathfrak{h}'=(H',\mu')$ is called an *induced (Hoffman) subgraph* of $\mathfrak{h}$ if H' is an induced subgraph of H and $\mu|_{V(H')}=\mu'$. The *slim subgraph* of $\mathfrak{h}$ is the induced subgraph of $\mathfrak{h}$ whose vertices are the slim ones of $\mathfrak{h}$.

Definition (Sum of Hoffman graphs and slim $\mathfrak{H}$-line graphs). Let $\mathfrak{h}$ be a Hoffman graph, and let $\mathfrak{h}^1$ and $\mathfrak{h}^2$ be two non-empty induced Hoffman subgraphs of $\mathfrak{h}$. We say that $\mathfrak{h}$ is a *sum* of $\mathfrak{h}^1$ and $\mathfrak{h}^2$, denoted by $\mathfrak{h}=\mathfrak{h}^1\oplus\mathfrak{h}^2$, if the following conditions hold:

1. $V(\mathfrak{h})=V(\mathfrak{h}^1)\cup V(\mathfrak{h}^2)$, $V_s(\mathfrak{h})=V_s(\mathfrak{h}^1)\cup V_s(\mathfrak{h}^2)$ and $V_s(\mathfrak{h}^1)\cap V_s(\mathfrak{h}^2)=\emptyset$;
2. for $i\in\{1,2\}$ and a vertex $x\in V_s(\mathfrak{h}^i)$, $N^f_{\mathfrak{h}^i}(x)=N^f_{\mathfrak{h}}(x)\cap V_f(\mathfrak{h}^i)$; and

*M. F. was supported by JSPS KAKENHI; grant number: 18K13449
†S. K. was supported by JSPS KAKENHI; grant number: 18J10656
‡T. T. was supported by JSPS KAKENHI; grant number: 16K05263
§speaker

3. for vertices $x \in V_s(\mathfrak{h}^1)$ and $y \in V_s(\mathfrak{h}^2)$, $|N_{\mathfrak{h}}^f(x) \cap N_{\mathfrak{h}}^f(y)| \leq 1$ and $|N_{\mathfrak{h}}^f(x) \cap N_{\mathfrak{h}}^f(y)| = 1$ if and only if x and y are adjacent in $\mathfrak{h}$.

If $\mathfrak{h}$ is a sum of two Hoffman graphs, then it is said to be *decomposable*; otherwise, it is said to be *indecomposable*. Let $\mathfrak{H}$ be a family of Hoffman graphs. A graph G is called an *slim $\mathfrak{H}$-line graph* if it is an induced subgraph of $\mathfrak{h} = \bigoplus_{i=0}^{n} \mathfrak{h}^i$ where $\mathfrak{h}^i \in \mathfrak{H}$ for all i. In this case, $\mathfrak{h}$ is called a strict $\mathfrak{H}$-cover of G if $V_s(G) = V_s(\mathfrak{h})$. Moreover, for a strict $\mathfrak{H}$-cover $\mathfrak{g}$ of G, $\mathfrak{h}$ and $\mathfrak{g}$ is said to be *equivalent* if there exists graph isomorphism ϕ from the underlying graph of $\mathfrak{h}$ to that of $\mathfrak{g}$ preserving slimness and fatness such that $\phi|_{V(G)} = \mathrm{id}$.

2 Main results

Woo and Neumaier [5] proved that, for a graph G with the smallest eigenvalue in the range $(\alpha, -1-\sqrt{2}]$, if the minimum degree is sufficiently large, then G is a slim $\{\mathfrak{h}_2, \mathfrak{h}_5, \mathfrak{h}_7, \mathfrak{h}_9\}$-line graph, where α is the smallest root of the polynomial $x^3 + 2x^2 - 2x - 2$. Furthermore, they posed a problem to reveal the list of minimal forbidden graphs for the slim $\{\mathfrak{h}_2, \mathfrak{h}_5, \mathfrak{h}_7, \mathfrak{h}_9\}$-line graphs (see [5, Open Problem 3]). It is still open, however Taniguchi [4] partially solved the problem to give the minimal forbidden graph characterization of slim $\{\mathfrak{h}_2, \mathfrak{h}_5\}$-line graphs which is a subclass of slim $\{\mathfrak{h}_2, \mathfrak{h}_5, \mathfrak{h}_7, \mathfrak{h}_9\}$-line graphs. More specifically, he proved that there are precisely 38 minimal forbidden graphs for the slim $\{\mathfrak{h}_2, \mathfrak{h}_5\}$-line graphs and they have at most 8 vertices. Our result is a generalization of his result, and we give a short proof.

Let $\mathfrak{O}$ be the set of Hoffman graphs consisting of $\mathfrak{h}_2$ and the indecomposable Hoffman graphs $\mathfrak{h}$ such that $|V_s(\mathfrak{h})| \geq 2$, $|V_f(\mathfrak{h})| = 1$, and all slim vertices are adjacent to the unique fat vertex in $\mathfrak{h}$. For a set $\mathfrak{H} \subset \mathfrak{O}$, let $\bar{\mathfrak{H}} = \{\mathfrak{h}_2\} \cup \{\mathfrak{h} \in \mathfrak{O} : \mathfrak{h}$ is an induced Hoffman subgraph of a graph in $\mathfrak{H}\}$. The following is the first main result:

First main theorem. *Let $\mathfrak{H} = \bar{\mathfrak{H}} \subset \mathfrak{O}$. Let N be an integer at least 7. Suppose that every connected slim $\mathfrak{H}$-line graph of order N has exactly one strict $\mathfrak{H}$-cover up to equivalence. Then, so does every one of order at least N.*

In the above theorem, if there exists an integer N satisfying the assumption, we let $N_{\mathfrak{H}}$ be the smallest such integer N; otherwise, let $N_{\mathfrak{H}} = \infty$. Furthermore, we define $N_{\mathfrak{H}} := N_{\bar{\mathfrak{H}}}$ for any $\mathfrak{H} \subset \mathfrak{O}$. If $N_{\mathfrak{H}}$ is finite for $\mathfrak{H} \subset \mathfrak{O}$, then it can be found by using softwares such as MAGMA [3]. The following is the second main result:

Second main theorem. *Let $\mathfrak{H} = \bar{\mathfrak{H}} \subset \mathfrak{O}$. Let G be a minimal forbidden graph for the slim $\mathfrak{H}$-line graphs with $|V(G)| \geq N_{\mathfrak{H}} + 2$. Then, there exist $p \in V(G)$ and $\mathfrak{g} \in \mathfrak{H}$ such that $G - p$ is isomorphic to the slim subgraph of $\mathfrak{g}$.*

By applying two main theorems to $\{\mathfrak{h}_2, \mathfrak{h}_3, \mathfrak{h}_5\}$ and using computer, we derive Taniguchi's result. Finally, we introduce an application. The problem to classify the graphs with the smallest eigenvalue at least -3 was studied. Koolen, Yang and Yang [2] proved that if a graph with the smallest eigenvalue at least -3 has the sufficiently large minimum degree, then it is an induced subgraph of a Hoffman graph in $\mathcal{G}$, where $\mathcal{G}$ is the set of fat Hoffman graphs with the smallest eigenvalue at least -3 (in terms of Hoffman graph). By applying our main theorems, we derive that every minimal forbidden graph for the slim $\mathfrak{O} \cap \mathcal{G}$-line graphs has at most 13 vertices.

References

[1] A. Hoffman, On graphs whose least eigenvalue exceeds $-1-\sqrt{2}$, *Linear Algebra Appl.* **16** (1977), 153–165.

[2] J. H. Koolen, J. Y. Yang and Q. Yang, On graphs with smallest eigenvalue at least -3 and their lattices, *Adv. Math.* **338** (2018), 847–864.

[3] W. Bosma, J. Cannon and C. Playoust, The Magma algebra system. I. The user language, *J. Symbolic Comput.* **24** (1997), 235–265.

[4] T. Taniguchi, On graphs with the smallest eigenvalue at least $-1-\sqrt{2}$, part II, *Ars Math. Contemp.* **5** (2012), 239–254.

[5] R. Woo and A. Neumaier, On graphs whose smallest eigenvalue is at least $-1-\sqrt{2}$, *Linear Algebra Appl.* **226–228** (1995), 577–591.